Dissertation zur Erlangung des Doktorgrades (Dr. rer. nat.)

der Fakultät für Biologie

der Ludwig-Maximilians-Universität München

Innovations in rabies virus rescue –

positive approaches for a negative strand

RNA virus

Alexander Ghanem

aus Freiburg i. Br., Deutschland

2012

Erklärung

Diese Dissertation wurde im Sinne von §12 (3) der Promotionsordnung vom 27. November 1991 von Herrn Professor Dr. Conzelmann betreut und von Herrn Professor Dr. Grothe vor der Fakultät für Biologie vertreten.

Eidesstattliche Versicherung

Hiermit versichere ich ehrenwörtlich, dass meineDissertation selbständig und ohne Unerlaubte Hilfsmittel angefertigt worden ist. Die vorliegendeDissertation wurde weder ganz, noch teilweise bei einer anderen Prüfungskommission vorgelegt. Ich habe noch zu keinem früheren Zeitpunkt versucht, eine Dissertation einzureichen oder an einer Doktorprüfung teilzunehmen.
Teile der Dissertation wurden veröffentlicht in (Ghanem et al., 2012), die hier gezeigten Experimente wurden eigenständig von mir durchgeführt.

München, den ....

....
(Unterschrift des Autors)

Dissertation eingereicht am: 14.8.2012
Erstgutachter: Professor Dr. Benedikt Grothe
Zweitgutachter: Professor. Dr. Bettina Kempkes
Tag der mündlichen Prüfung: 26.11.2012

I Table of contents

II Summary

The neurotropic rabies virus (RABV) of the *Rhabdoviridae* family is the causative agent of rabies, a fatal zoonosis. The availability of a RABV reverse genetics system allowing the generation of recombinant viruses has greatly facilitated investigations on the molecular biology, neurotropism, and pathogenicity of RABV, as well as the establishment of specifically designed attenuated RABV vaccines, vectors, and neurotracers. Due to its neurotropism and strictly retrograde transmission via synapses, RABV has gained more and more attention as a valuable research tool in neural sciences.

A severe drawback of the classic RABV reverse genetics system is the poor efficiency of virus rescue from cDNA, which requires intracellular co-expression of a set of three viral "helper" proteins (N, P, and L) and of correctly (end-)processed T7 RNA polymerase-derived viral RNAs. The aim of this work was to facilitate and improve the RABV rescue system with respect to reliability, rescue efficiency, and time consumption. In addition, the potential of RABV vectors for expression of small interfering RNAs was addressed for the first time.

Following experiments revealing that RABV does not actively interfere with the cellular RNAi machinery, diverse RNAs were expressed from RABV mimicking natural miRNA or shRNA precursors. Notably, the 5'-capped and polyadenylated RABV mRNAs were not further processed in the cytoplasm to yield si/miRNA duplexes with knock-down activity, suggesting the requirement of nuclear processing by the Drosha/DCGR8 microprocessor complex. To generate RNAs directly cleavable by cytoplasmic Dicer, shRNAs flanked by hammerhead and hepatitis delta ribozymes were designed by thorough *in silico* analysis. Although ribozyme processing yielded the predicted shRNAs, these were not cleavable by Dicer, most probably because of the specific phosphate conformations at the RNA termini.

In contrast to providing suitable Dicer substrates, ribozymes tested here were highly efficient in generating correct viral RNA ends and could be used for significant improvement of the RABV rescue system. Specifically, generation of an exact viral 5'-end by a hammerhead ribozyme and highly efficient processing of the viral 3'-end by a hepatitis delta virus antigenomic ribozyme variant (SC1) resulted in a 100-fold more efficient and faster rescue of recombinant RABV from T7 RNA polymerase-derived RNA (Ghanem et al., 2012). This faster and more reliable system has become a standard technique in our lab and

enabled us to rescue severely attenuated RABVs as well as a variety of novel vectors for neurotracing.

The significant improvement of RABV rescue was a prerequisite for the following approach, namely, development of a single plasmid rescue system, generating a single infectious RABV cDNA. A completely new and unconventional system was established, which is based on the direct expression of "helper" proteins from the cDNA-encoded full-length antigenome-like RNA. To this end, picornaviral IRES elements and 2A-like sequences were integrated upstream of the respective ORFs in order to translate these directly from the antigenome-like RNA, thereby superseding extra "helper" protein plasmids. Unexpectedly, cis-active RABV sequences, which have not been described before, were identified in the course of the experiments at the leader-N junction and within the N coding region. Importantly, rescue of RABV was achieved with RNA polymerase II promoter-driven DNA, with reasonable efficiency. This opens the way to the development of animal models in which RABV is genetically encoded and an infectious cycle induced in certain cell types. Especially for neurotracing, but also pathogenicity studies, such systems benefit from the virtual infinite number of genetic e.g. mouse models available and contribute to a gain of specificity and accessibility in regard to target cells.

1 Introduction

1.1 Rabies virus

1.1.1 Taxonomy

Rabies virus (RABV) is a member of the family *Rhabdoviridae* which together with the *Paramyxoviridae*, the *Filoviridae* and the *Bornaviridae* constitute the order *Mononegavirales* also known as non-segmented negative strand RNA viruses (NNSV). The NNSV genome is tightly encapsidated by the nucleoprotein (N) into helical N-RNA structures. The N-RNA, or nucleocapsid (NC), is the template for genome replication and ordered transcription of sub-genomic mRNAs (reviewed in Whelan et al., 2004)

The family *Rhabdoviridae* is sub-divided into six genera: *Lyssavirus*, with RABV as the prototypical member, *Vesiculovirus*, *Ephemerovirus*, *Novirhabdovirus*, *Cytorhabdovirus* and *Nucleorhabdovirus.* Their virions have a typical bullet or rod shape in common. *Rhabdoviridae* are replicating in a broad spectrum of hosts, ranging from plants, insects, lower vertebrates to mammals and man (reviewed in Fu, 2005).

The *Lyssavirus* genus is divided further into 7 genotypes. RABV (genotype 2) is the causative agent of human rabies, as the result of a zoonosis. Natural infections occur in mammals, mostly carnivores. The other members of the *Lyssavirus* genus, Lagos Bat virus (genotype II), Mokola virus (genotype III), Duvenhage virus (genotype IV), European bat lyssavirus 1 and 2 (EBLV-1 and EBLV-2) (genotypes V and VI) and the Australian bat lyssavirus (ABLV) (genotype VII) are mostly found in bats and for some genotypes also deadly infections of humans have been observed.

Various strains of RABV exist. "Street" viruses are isolated directly from infected animals or humans whereas "fixed" strains are generated by serial passaging in cell culture or animals, which often goes together with attenuation of the virus.

The RABV SAD L16, the basis for all virus constructs in this thesis, originates from the first recovery of recombinant RABV from cDNA made from the fixed vaccine strain SAD B19 (Schnell et al., 1994). SAD B19 was generated by serial passaging in baby hamster kidney (BHK) cells of the "street" isolate "Street Alabama Dufferin" (SAD) from a rabid dog in Alabama 1935 (Schneider, 1995).

1.1.2 Epidemiology and pathogenicity

RABV infection of humans is a zoonosis, transmitted in the majority of cases by bites from rabid dogs. As RABV can replicate efficiently also in bats and most carnivore terrestrial mammals, exposure to wild life with endemic RABV cases entails a risk of infection with the virus.

Worldwide, more than 55,000 people die of rabies every year although effective vaccines and post-exposure treatments are available. More than 15 million people receive such post-exposure treatments, preventing more than 300,000 potential deaths each year (WHO, 2011). The majority of the fatal cases are reported in rural regions in Africa and South Asia where RABV infection is endemic in street dogs. Exposed humans, mostly due to economic reasons, do not have easy access to rapid medical treatment within the first few hours after the bite of an infected animal. In developed countries human rabies cases are relatively rare, which is due to the availability of post-exposure treatment and vaccination for individuals with higher exposure risks, like veterinarians, medical personnel and travelers on one hand, and vaccination programs to eradicate RABV in domestic dogs and wild-life populations of e.g. foxes, on the other hand. However, as RABV has a relative broad host range, and can replicate also in raccoons, skunks, or bats, a complete elimination seems not to be feasible. Additionally, rare cases of human rabies encephalitis cases after infections with bat lyssaviruses (EBLV-1, EBLV-2, or ABLV) have been reported (reviewed in Banyard et al., 2011).

After infection with RABV, at the site of the bite or scratch, and possibly an initial but symptomless replication, the virus enters the nervous system at the neuromuscular junction (NMJ). Once in a neuron, the virus is transported in an exclusively retrograde manner from the periphery towards the central nervous system (CNS) (Tang et al., 1999; Ugolini, 1995). The transport of viruses along the axons occurs within vesicles (Klingen et al., 2008) and cell-to cell spread is observed almost exclusively at synapses (Ugolini, 1995). One round of replication is required in each neuron on this way and each of these replication cycles takes between 1 and 2 days. The speed of retrograde transport along the axon was measured *in vitro* to be between 8 mm/d (Klingen et al., 2008) and 100 mm/d (Tsiang et al., 1991), however might be faster *in vivo* (Ugolini, 2011). Both factors contribute to the symptomless incubation time of the disease in dependence of the distance and neuronal connections

between the site of infection and the CNS. However, incubation periods up to five years have been reported that cannot be explained by these factors.

To reach the CNS, RABV has developed a stealth strategy in regard to the host immune system. Activation of innate immunity and inflammation is efficiently suppressed by the virus, and due to low cytotoxicity the neuronal network remains intact (reviewed in Finke and Conzelmann, 2005b; Rieder and Conzelmann, 2011).

As soon as RABV clinical symptoms appear, i.e. when the virus replicates in the CNS, the outcome of the disease is almost certainly (>99 %) fatal. First signs of RABV infection in human patients are fever and paresthesia at the wound site followed by paralysis, hyperactivity, hydrophobia, paranoia and coma.

RABV strains vary greatly in their virulence and neuroinvasiveness which is associated mainly with differences in their surface glycoproteins (G) and results in different pathogenicity *in vivo*. RABV G is essential for spread *in vitro* and *in vivo* (Etessami et al., 2000a; Mebatsion et al., 1996a) and the replacement of G in RABV SN-10, an SAD L16 variant, which is apathogenic in mice infected in the periphery, with the G from the pathogenic RABV Challenge Virus Strain (CVS) or from Silver Haired Bat rabies virus 18 (SHBRV-18) restores virulence and neuropathogenicity in these chimeras (Finke and Conzelmann, 2005b; Morimoto et al., 2000). These differences in neurotropism and pathogenicity for different G proteins can derive from the use of different receptors during RABV infection (Dietzschold et al., 2008). Also different abilities to activate or repress apoptosis in neurons may play significant roles (Lafon, 2008; Prehaud et al., 2010). Neutralizing antibodies to G are only made late in RABV infection.

Besides RABV G, also other protein functions of RABV are associated with pathogenicity. During RABV encephalitis little inflammation is observed and pathogenic RABV strains only cause a slight induction of innate immunity in mice whereas this is more pronounced for attenuated RABVs (Wang et al., 2005).

1.1.3   Genome organization and virion structure of RABV

RABV as a member of the order *Mononegavirales* or NNSV has an unsegmented genome of approximately 12 kb single stranded RNA and of negative sense. This genome comprises five genes in the order 3'-N-P-M-G-L-5'. From these genes the viral proteins, namely the

nucleoprotein (N), phosphoprotein (P), matrix protein (M), glycoprotein (G) and the large polymerase subunit (L) are expressed (figure 1A and 1B).
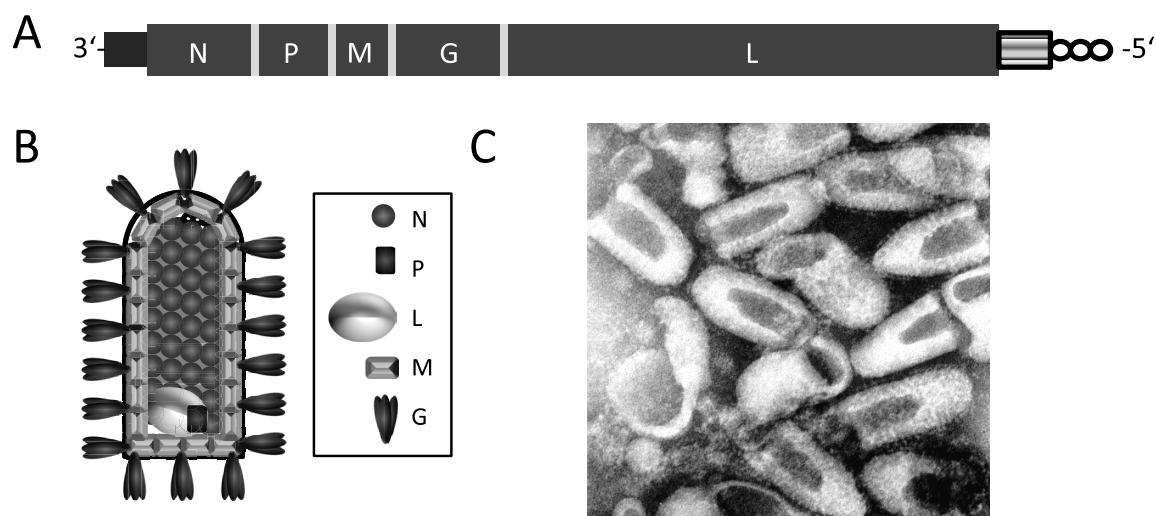
Figure 1: Rabies virus structure and genome organization.
(A) Schematic genome organization of RABV. The genome is arranged in the order 3'-le-N-P-M-G-L-tr-5' (adapted from Ghanem and Conzelmann, in press). (Black box = leader, striped box = trailer, white circles = 5'-triphosphate) (B) Schematic illustration of a bullet-shaped RABV particle (adapted from Ghanem and Conzelmann, in press) (C) Electron micrograph of RABV particles purified from cell culture (negative staining, approximately 70.000 fold magnification) (adapted from F. A. Murphy, University of Texas Medical Branch, Galveston, Texas).

The N protein encapsidates the viral genomes into helical N-RNA structures, also termed nucleocapsids (NCs). One N protomer covers 9 nucleotides of RNA (Iseni et al., 1998) and one helical turn of the N-RNA comprises 11 N protomers (Albertini et al., 2006; Green et al., 2006). N-RNA is the template for replication and transcription by the viral RNA-dependent RNA polymerase P-L. N-RNA together with P-L constitutes the viral ribonucleoprotein (vRNP) structure. The P protein has multiple functions. In P-L the highly phosphorylated P is a cofactor for the polymerase. P is also a chaperone for newly made soluble N protein (N^0) preventing its oligomerization and binding to cellular RNA and supporting the N^0 interaction with newly transcribed viral RNA (reviewed in Albertini et al., 2008). Moreover, P is a key player in modulating and repressing cellular innate immune responses to RABV replication (Brzózka et al., 2005; Rieder et al., 2011; Rieder and Conzelmann, 2011) and may also be involved in budding of progeny RABV (Kern, 2012).

The most prominent functions of the M protein are involved in assembly and budding of RABV (Mebatsion et al., 1999). M mediates the condensation of newly generated vRNPs and bridges these to the envelope by interaction with the G protein at the plasma membrane.

Further, it is responsible for budding of the progeny virus. Besides being involved in virus assembly, M also has a regulative influence on virus transcription and replication (Finke and Conzelmann, 2003; Finke et al., 2003; Schnellhammer, 2009).

The G protein, a type I transmembrane protein, is the only viral protein located in the RABV membrane envelope. It assembles at the plasma membrane into trimeric spikes (Gaudin et al., 1992) and although not being essential for budding, the release of RABV particles is significantly increased in the presence of G (Mebatsion et al., 1996a). G plays a crucial role for virus entry by interaction with cellular receptors and by mediating membrane fusion. Until today, the nicotinic acetylcholine receptor (nAChR) (Burrage et al., 1985; Castellanos et al., 1997), neuronal cell adhesion molecule (NCAM) (Thoulouze et al., 1998), and p75 neurotrophin receptor (p75NTR) (Tuffereau et al., 1998) have been described as RABV receptors. The G protein is essential for RABV transsynaptic spread in neurons (Etessami et al., 2000a).

Altogether, the five structural proteins and the negative sense vRNA genome are part of the typical bullet-shaped RABV virions with a length of about 180 nm and a diameter of about 80 nm (figure 1B / 1C).

1.1.4 RABV replication cycle

The RABV replication cycle can be roughly divided into 3 phases: entry, transcription and replication, and assembly and release of progeny virions. An overview is depicted in figure. 2A. RABV entry is dependent on the G protein. On the cellular site, the nAChR, NCAM and p75NTR have been described as receptors and also other components such as gangliosides might be involved in RABV entry (reviewed in Lafon, 2005). Since in cell culture RABV can infect virtually all mammalian cells, no clear read-out to identify receptors is available. *In vivo*, e.g. in mice, the different receptors are determinants of RABV cell tropism. The nAChR is thought to be important to mediate high concentrations of RABV at the NMJ. Directly after a bite or scratch from an infected animal this enrichment at the NMJ increases the probability of entry into the presynaptic neuron. The p75NTR is only found in neurons, and mainly after axonal injury, whereas it is not present in motorneurons of the spinal cord or at the NMJ (reviewed in Lafon, 2005). The same authors that proposed this protein as an entry receptor for RABV (Tuffereau et al., 1998) showed some years later, that *in vivo* p75NTR is not essential for RABV infection (Tuffereau et al., 2007). This indicates the presence of

further, yet unidentified, entry receptors for RABV. The RABV virions are taken up by endocytosis (Superti et al., 1984) and are transported in a retrograde manner inside vesicles from the entry side towards the cell body of the neurons (Klingen et al., 2008). This transport can be blocked by interference with the microtubule network (Ceccaldi et al., 1989).
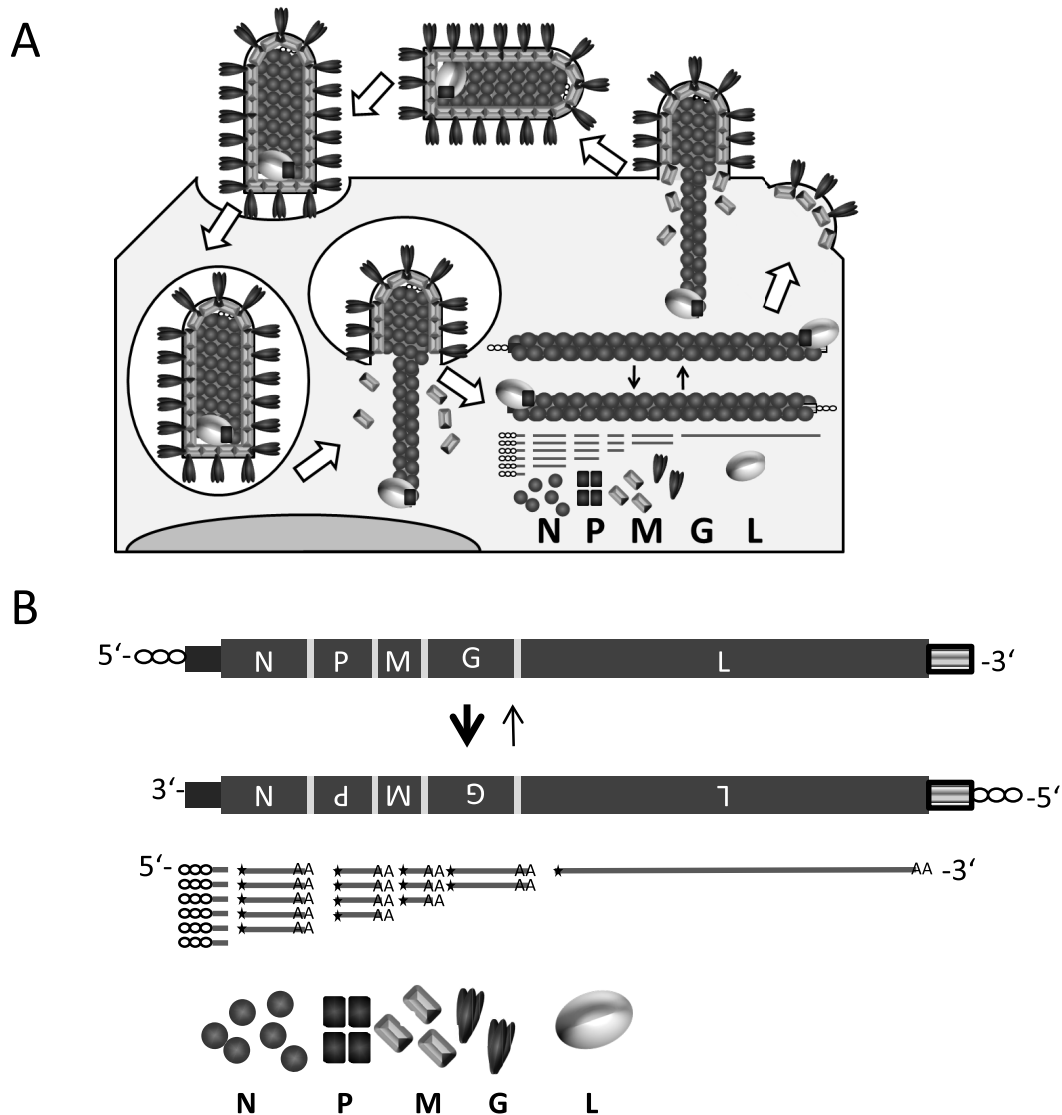
Figure 2: Rabies virus replication cycle.
(A) Schematic illustration of the RABV replication cycle. Attachment to the membrane is followed by endocytosis, membrane fusion, uncoating, replication and transcription. After gene expression and the production of progeny vRNPs, assembly and budding leads to the release of new RABV particles (adapted from Ghanem and Conzelmann, in press). (B) Schematic illustration of RABV transcription and replication (adapted from Ghanem and Conzelmann, in press). For replication, genomic NCs (middle) serve as a template to generate antigenomic NCs (above) which again are replicated into further genomic NCs. During transcription (below), a 5'-triphosphate comprising leader RNA is made and 5 monocistronic, capped and polyadenylated mRNAs for the 5 proteins N, P, M, G and L.

In the cell body, low pH triggers a conformational change of the G protein resulting in membrane fusion between the virus envelope and the endosomal membrane (Gaudin et al.,

1999). Following dissociation of the M protein, the tightly packaged and supercoiled vRNP is released into the cytoplasm and adopts a more relaxed structure so that viral gene expression and replication can take place.

An overview of RABV gene expression and replication is depicted in figure 2B. Once, the vRNP is released into the cytoplasm, the viral RNA-dependent RNA polymerase consisting of L and P starts RNA synthesis at the genomic promoter at the 3'-end of the genome, using the NC as a template. When RABV is recovered from cDNA a vRNP has to be reconstituted in the cell in order to allow expression of all viral genes ($\rightarrow$ 1.2: reverse genetics of RABV)

There are different models to explain how the polymerase gets access to the RNA genome which is tightly encapsidated into an NC structure. It was proposed that the P-L polymerase can only access the RNA at the genome termini. The N-terminal domain of N then would open up concurrently with the proceeding polymerase and allow partial access to the template RNA (reviewed in Albertini et al., 2008). How this is triggered, however, remains to be solved. Phosphorylation of the N protein has been proposed to be involved. For Sendai virus it was shown that an excess of P protein is needed for polymerase activity, indicating that P can induce conformational changes of the N-RNA structure (Curran, 1996).

Transcription always proceeds from 3' to 5'. Initially, a 58 nts long 5'-triphosphate (5'-ppp) containing RNA, the so called leader RNA (le) is made. The P-L polymerase (or transcriptase) can either reinitiate transcription at an N transcription restart site upstream of the N gene or enter from outside on an extra transcriptional promoter at the leader-N gene junction. These two possibilities are controversially discussed (see below).

The noncoding regions between the genes, which are arranged in the order 3'-le-N-P-M-G-L-5', comprise a transcription stop / polyadenylation signal for the upstream gene and a transcription restart signal for the downstream gene, separated by so called intergenic regions. Altogether these cis-active elements are also referred to as gene borders. Transcription stutters at the uridine stretch of the transcription stop / polyadenylation signal and a 3'-poly(A) tract is synthesized at the viral mRNA. With a certain probability the polymerase reinitiates transcription at the following transcription start site (reviewed in Whelan et al., 2004). The probability of reinitiation is dependent on the composition of the respective intergenic region (Finke et al., 2000). Thus, both the distance of a RABV gene towards the promoter, as well as the "strength" of its upstream gene border region, define

the amount of mRNA that is transcribed. This leads to a transcription gradient of the RABV subgenomic mRNAs. N mRNA is the most abundant RABV mRNA, whereas L mRNA is the least abundant. All five monocistronic RABV mRNAs are capped (Li et al., 2006; Ogino and Banerjee, 2007) and polyadenylated by functions of the viral polymerase, supporting the subsequent cap-dependent translation of viral proteins by the cellular translation machinery. Therefore the amounts of RABV proteins that are made is determined and regulated primarily at transcriptional levels. Translation initiation for the P protein occurs not only at the first AUG in the mRNA, but also to lower levels at in-frame downstream AUGs. Ribosomal leaky scanning results in shorter, N-terminally truncated, species of P, namely P2, P3 and P4 (and P5 and P6, respectively, dependent on the RABV strain) (Chenik et al., 1995).

In vesicular stomatitis virus (VSV), the synthesis of leader RNA seems not to be essential for transcription initiation to produce the subgenomic mRNAs (Whelan and Wertz, 2002). Studies with VSV (Qanungo et al., 2004) and Sendai virus (SeV) (Horikami et al., 1992) suggest the existence of two distinct polymerase complexes, a transcriptase, consisting of P-L and a replicase where N^0, unbound to RNA, is involved. In SeV, however, N^0 also contributes to transcription efficiency (Wiegand et al., 2007). In general, the suggested models for NNSV replication comprise two distinct mechanisms for N^0. In the first model, N^0 in a tripartite N-P-L replicase complex mediates replication initiation at the very 3'-end, in contrast to transcription initiation at the leader-N gene junction of P-L. In the second model, an excess of N^0 facilitates concurrent encapsidation of newly synthesized leader RNA thus triggering further elongation (reviewed in Banerjee, 2008; Curran and Kolakofsky, 2008; Whelan, 2008). Controversially discussed is also the stoichiometry of the respective transcriptase and replicase complexes.

Replication results in production of positive sense copy-RNAs (cRNAs), or antigenomes, which are encapsidated concurrently during RNA synthesis into antigenomic RNPs (cRNPs). The cRNPs then serve as a template for the production of further vRNPs, which can serve as further templates for secondary transcription and replication, or which can be assembled into progeny virions. The promoter for RNA synthesis from the antigenome, namely the antigenomic promoter, is located in the 3'-region of the antigenome (or the complement of the 5'-region of the genome) also termed trailer region (tr). Leader and trailer are complementary in the terminal 11 nts and can be partially replaced by their counterpart

although resulting in viruses or minigenomes with different features (Collins et al., 1991; Finke and Conzelmann, 1997).

Most importantly, newly synthesized vRNPs can be assembled into progeny virions. Assembly and budding of the progeny virions are the last steps during the replication cycle of RABV. The newly synthesized vRNPs are recruited by M to the cell membrane, where M interacts with the cytoplasmic domain of the membrane anchored G protein. The G protein is anchored co-translationally to the membrane of the endoplasmatic reticulum (ER) and transported via the Golgi network to the cytoplasm membrane. Upon accumulation of G protein in certain areas of the membranes, the sites of virus release are determined due to the recruitment of vRNP-M (Mebatsion et al., 1999). M is the key player in assembly and triggers the condensation of vRNPs into tightly packaged supercoiled structures. Furthermore, M is responsible for the formation of the typical bullet-shaped RABV particles and their release from the cytoplasm membrane, also termed as budding. Although G is not required for the budding process, its efficiency is increased in the presence of G (Mebatsion et al., 1996a). Also cellular proteins are involved in RABV budding and interact with the M (Harty et al., 1999) and P (Kern, 2012) proteins. Noteworthy, *in vivo* budding in neurons seems to occur only from postsynaptic areas of dendrites into the synaptic cleft such that only the presynaptic neurons are infected (Kelly and Strick, 2000; Ugolini, 1995; Ugolini, 2008). Different explanations for this observation are discussed. One possibility might be the strict retrograde transport of RABV in vesicles along the axons, thus that the assembling virus cannot reach the axon terminals for budding. Another possibility could be the enrichment of G protein at the dendritic site of the neurons which raises the possibility of assembly in proximity to the synaptic cleft. Also the ensheathment of axons by glia cells might contribute to the budding exclusively from postsynaptic dendrites (reviewed in Callaway, 2008; Ugolini, 2011). With budding of the progeny virions from the host cell, the RABV infection cycle is completed and a new cycle can proceed.

1.2 Reverse genetics of rabies virus

The bacteriophage Qβ was the first virus reported to be recovered completely from cDNA (Taniguchi et al., 1978). Amongst the first eukaryotic viruses were murine leukemia virus (MLV) (Lowy et al., 1980) and poliovirus (PV) (Racaniello and Baltimore, 1981), directly encoding for or representing an infectious positive sense RNA, respectively. Amongst all negative stranded RNA viruses, including viruses with segmented genomes like members of the *Orthomyxovirus* and *Arenavirus* as well as NNSV, or *Mononegavirales*, RABV was the first virus that was reconstituted completely from cDNA (Schnell et al., 1994).

The generation of recombinant RABV from cDNA allows the manipulation of the genome sequences, from point mutations to deletions of one or more genes. Reverse genetics facilitated research in terms of virus biology and pathogenicity and enables the production of designer virus vectors, e.g. for neuronal sciences or as vaccines. Detailed information about reverse genetics of NNSV can be found in several recent review articles (Conzelmann, 2004; Finke and Conzelmann, 2005a; Ghanem and Conzelmann, in press).

1.2.1 Intracellular reconstitution of the vRNP – minigenomes

For positive strand RNA viruses, like poliovirus, all proteins required to initiate an infectious cycle can be translated directly from the viral genomic RNA by the cellular machinery after transfection of a single RNA or cDNA.

In contrast, for negative strand RNA viruses the minimal infectious unit is the vRNP (or cRNP) complex, consisting of viral genomic (or antigenomic) RNA encapsidated by N protein into N-RNA together with the viral RNA-dependent RNA polymerase P-L (→1.1.4). A transcriptionally active RNP is required since the viral proteins cannot be expressed from full-length RNA. Thus, to recover RABV from cDNA all four components have to be expressed in the cell in order to reconstitute the vRNP (or cRNP). From this template viral replication as well as expression of all virus proteins, including M and G which are necessary for RABV assembly (→1.1.4), can occur.

First results to reconstitute a vRNP-like structure were described for VSV defective interfering particles (DIs). DIs are short viral RNA genome analogues, encapsidated into vRNPs, and can be used to study replication and transcription. However, as they do not comprise the genes coding for the components of the viral life cycle they are dependent on

"helper" proteins. Noteworthy, many naturally occurring DIs derive from copy-back replication of the virus polymerase, thus containing a trailer sequence at both ends.

DI-derived genomic RNA and proteins, purified from VSV-infected cells, were assembled successfully *in vitro* and the resulting vRNPs showed similar features like vRNPs purified directly from VSV infected cells (Mirakhur and Peluso, 1988).

Further success was reported for influenza A virus, a member of the *Orthomyxoviridae* with a segmented negative oriented genome (Luytjes et al., 1989). In this work a cDNA for the influenza virus NS segment, in which the NS coding region was replaced with a chloramphenicyl transferase (CAT) reporter gene was *in vitro*-transcribed and assembled *in vitro* with purified influenza polymerase PB1, PB2 and PA and with the influenza nucleoprotein NP. Exact ends of the virus segment-like RNA were achieved by linearization of the cDNA and run-off transcription with bacteriophage T7 RNA polymerase (T7-pol). This artificial vRNP segment was then transfected into cells co-infected with influenza "helper" virus. Indeed, the reporter segment was encapsidated, further amplified and CAT expression was observed not only in the transfected cells, but also after serial passaging of the supernatants.

For Sendai virus (SeV), a paramyxovirus, a minigenome containing the SeV genome ends and a CAT reporter gene was *in vitro* transcribed and transfected into SeV infected cells (Park et al., 1991). Again, exact genome ends were generated by linearization of the cDNA containing plasmid prior to the *in vitro* transcription. The CAT minigenome RNA was encapsidated intracellularly, amplified by the SeV polymerase, and packaged into progeny virions that could be passaged together with the full-length virus. The importance of the exact ends, especially the 3'-end was stressed by further similar studies with respiratory syncytial virus (RSV) (Collins et al., 1991) or human parainfluenza virus 3 (HPIV3) (De and Banerjee, 1993), both members of the *Paramyxoviridae*.

Following the *in vitro* assembled minigenomes, the next important step was to express the components in the cell. A vaccinia virus that expresses T7-pol (vTF7-3) (Fuerst et al., 1986) was first used to express the "helper" proteins, N, P, and L, of VSV from plasmids containing T7 promoters in cell culture (Pattnaik and Wertz, 1990). These "helper" proteins were able to support replication of virus-derived DIs. Not only the "helper" proteins, but also the M and G proteins, could be expressed with the vaccinia virus T7-pol (vv/T7) system (Pattnaik

and Wertz, 1991). The expression of all 5 VSV proteins, N, P, M, G, and L, from cDNA resulted in not only replication but also assembly and budding of virus-derived DIs.

For expression of plasmid-encoded virus-like RNAs, minigenomes or DIs, intracellularly in the vv/T7 system, new challenges appeared in regard to the genome ends, as plasmids no longer could be linearized before the transfection. The intracellularly transcribed RNA of a virus-like RNA could however be processed by a ribozyme. This was shown first for Flock House virus, a segmented positive strand RNA virus from the genus *Nodavirus* (Ball, 1992). This strategy also works for an NNSV, as demonstrated with VSV (Pattnaik et al., 1992). Notably, the ribozyme used in the work of Ball (Ball, 1992)was the self-cleaving ribozyme from tobacco ringspot virus (Prody et al., 1986) and due to cleavage at an internal position leaves 12 extra nts attached to the 3'-end of the virus RNA. Thus, this ribozyme would not be useful to create the exact end needed for an NNSV rescue. Therefore, Pattnaik and colleagues replaced this ribozyme by the hepatitis delta virus antigenomic ribozyme (HDVagRz) (Perrotta and Been, 1991). Cleavage of HDVagRz is not dependent on nts 5' to the ribozyme sequence, thus generating an exact viral 3'-end. Noteworthy, cyclic 2', 3'-monophosphate remains after ribozyme cleavage instead of the 3'-OH found in NNSV RNA (Sharmeen et al., 1988). This, however, is well accepted by the virus machinery.

To increase the efficiency of T7-pol dependent transcription, 3 extra G nts were included downstream of the T7 promoter (Pattnaik et al., 1992). These nts were removed from the 5'-end of the virus-like RNA following viral replication whereas the importance of an exact 3'-end was shown to be also true for rhabdoviruses.

1.2.2 Rescue of infectious RABV from cDNA

All the results obtained with minigenomes and DIs were steps that finally enabled the rescue of RABV completely from cDNA (Schnell et al., 1994). This RABV rescue system applied the vv/T7 system for expression of viral RNA as well as of the "helper" proteins N, P and L. Importantly, this system introduced the expression of positive strand RNA antigenome instead of negative strand RNA genome. Thus, not the vRNP was reconstituted as minimal infectious unit, but rather the cRNP.

In contrast to a negative oriented RNA genome, cRNA does not comprise long stretches which are complementary to the mRNAs of the "helper" proteins. Therefore, problems deriving from long dsRNA, as inducing RNAi or IFN responses, are avoided. In addition,

genome-like transcripts at the gene borders comprise stretches of several U residues, likely to result in premature termination of the T7-pol transcription. In the antigenome-like transcript these are represented by stretches of A residues. Indeed, for VSV (Lawson et al., 1995; Whelan et al., 1995) and measles virus (MeV) (Radecke et al., 1995) the use of a negative sense genome-like and a positive sense antigenome-like transcript were compared and the result was clear-cut in all cases. Only the positive approach successfully yielded recombinant virus.

A major bottleneck in rescue of recombinant RABV from cDNA seems to be the encapsidation of the newly transcribed naked RNA by the N protein. In contrast to the concurrent encapsidation during replication of viral NCs, *de novo* encapsidation, also termed "illegitimate" encapsidation, is rather inefficient (and might play a greater role in regard to the long antigenome-like RNA than with shorter minigenomes or DIs). The genome ends are expected to be important for this encapsidation, as shown for VSV DIs (Pattnaik et al., 1995).

1.2.3   Comparison of different rescue systems for RABV and other Mononegavirales

The initial RABV rescue was relying on the vv/T7 system which guaranteed high expression levels of proteins and antigenome-like RNA from plasmids comprising T7 promoters. This system was proven to be useful for rescue of numerous members within the *Mononegavirales*. The main difficulties in those systems arise from the presence of the vaccinia virus vTF7-3 together with the virus rescued.

To get rid of the vaccinia virus contamination, virus stocks were filtrated (Lawson et al., 1995; Schnell et al., 1994) or specific inhibitors of vaccinia virus replication like AraC or rifampicin were applied (Whelan et al., 1995). In other systems, following the rescue, cells were incubated at temperatures that do not allow vaccinia virus replication (Biacchesi et al., 2002; Biacchesi et al., 2000; Johnson et al., 2000) or supernatants were passaged to cell lines not permissive for vaccinia virus but for the rescued virus (Bridgen and Elliott, 1996). The latter was especially possible by the application of the Modified vaccinia virus Ankara (MVA) as a vector to deliver T7-pol (Sutter et al., 1995; Wyatt et al., 1995). Some examples for the application of this system are the rescue of MeV (Schneider et al., 1997), SeV (Leyrer et al., 1998), mumps virus (Clarke et al., 2000) and rinderpest virus (Baron and Barrett, 1997), all belonging to the *Paramyxoviridae*.

As an alternative to vv/T7 systems, expression systems dependent on nuclear Pol-II promoters have been described to deliver T7-pol (Elroy-Stein and Moss, 1990; Lieber et al., 1989). Based on these systems, cell lines, constitutively expressing T7-pol were generated. For rescue of RABV and other NNSV one of the most prominent cell lines is the BSR T7/5 clone derived from BHK cells (Buchholz et al., 1999). The major problem with vaccinia virus-free rescue systems dependent on T7-pol is that transcripts from this polymerase lack poly(A) tails and comprise a 5'-ppp instead of a 5'-cap structure. While this is useful to generation of virus antigenome-like RNAs, the lack of these elements is a problem with regard to efficient translation of the "helper" proteins. In vv/T7 systems enzymes of vaccinia virus indeed can cap and polyadenylate the T7 derived RNAs (Gershon et al., 1991). An encephalomyocarditis virus (EMCV) internal ribosome entry site (IRES) introduced upstream of the respective ORFs in the "helper" plasmids, however, can facilitate efficient cap-independent translation in vv-free rescue systems (Elroy-Stein and Moss, 1990). Notably, the BSR-T7/5 cell line has a defect in IRF-3 activation (unpublished data). Therefore no IFN response to 5'-ppp RNAs transcribed by T7-pol or to other pathogen-associated molecular patterns (PAMPs) is induced. This allows to rescue RABV that cannot interfere with innate immunity anymore (Rieder et al., 2011), particularly, in this cell line. Other examples for T7-pol expressing cell lines used for rescue of NNSV are BHK-T7-9 cells (Ito et al., 2003), the carp cell line EPC-T7 (Alonso et al., 2004) or the human embryonic kidney cell line HEK 293-3-46 (Radecke et al., 1995). The latter is used for the rescue of MeV and expresses not only the T7-pol but also MeV N and P protein.

Instead of generating a cell line stably expressing T7-pol it was also shown that the co-transfection of an expression plasmid encoding T7-pol can support virus rescue (Paterson et al., 2000; Witko et al., 2006; Wu and Rupprecht, 2008).

T7-pol dependent rescue systems have certain features in common that are of particular value for rescue of cytoplasmic NNSV. At first there is the mainly cytoplasmic localization of the T7-pol, thus the antigenome-like RNAs are synthesized already in the right compartment of the cell. Second is the production of uncapped and not polyadenylated RNAs, which in combination with ribozyme processing resemble the viral RNAs.

Nonetheless, also the cellular nuclear DNA dependent RNA polymerase II (Pol-II) has been described to successfully rescue cytoplasmic NNSV like RABV (Huang et al., 2010; Inoue et

al., 2003), the RABV-related EBLV-1 (Orbanz and Finke, 2010), the fish rhabdoviruses, infectious hematopoetic necrosis virus (IHNV) (Ammayappan et al., 2010b), and viral hemorrhagic septicemia virus (VHSV) (Ammayappan et al., 2010a) and various members of the *Mononegavirales* like Newcastle disease virus (NDV) (Li et al., 2011) MeV and Borna disease virus (BDV) (Martin et al., 2006) from cDNA. In regard to BDV it has to be mentioned that this virus in contrast to other NNSV replicates in the nucleus of the cell. The other rescue systems are compromised by nuclear delivery of the antigenome RNAs and the synthesis of 5'-capped and 3'-polyadenylated mRNAs by Pol-II. While the poly(A) tail again is cleaved off in all systems by different HDVagRz, elimination of the 5'-cap structures employs a hammerhead ribozyme (HHRz) (Blount and Uhlenbeck, 2002) inserted into the respective cDNAs upstream of the virus antigenome sequences. The exact 5'-ends, however, seem to be less critical, as MeV and BDV could be recovered successfully from Pol-II dependent cDNA constructs comprising defect mutants of the HHRz and 5'-cap structures and extra 5'-sequences were lost rapidly upon virus replication (Martin et al., 2006).

Another nuclear polymerase, the DNA dependent RNA polymerase I (Pol-I) was shown to be useful for rescue of especially viruses with a nuclear replication phase, like BDV (Perez et al., 2003) or influenza virus (Fodor et al., 1999; Neumann et al., 1999). Amongst negative strand RNA viruses with a strict cytoplasmic replication cycle that were rescued by Pol-I dependent systems are diverse members of the *Bunyaviridae* like Uukunemi virus (Flick and Pettersson, 2001), crimean-congo hemorrhagic fever virus (CCHFV) (Flick et al., 2003) and rift valley fever virus (RVFV) (Billecocq et al., 2008; Habjan et al., 2008) or the lymphocytic choriomeningitis virus (LCMV) from the *Arenaviridae* family (Flatz et al., 2006). All have segmented genomes and interestingly, for ebolavirus, a filovirus and member of the NNSV with a strict cytoplasmic replication cycle, Pol-I dependent minigenomes were described (Groseth et al., 2005), whereas the recovery of full-length ebolavirus (Theriault et al., 2004; Volchkov et al., 2001) or the related Marburg virus (Enterlein et al., 2006) until today is dependent on T7-pol.

For rhabdoviruses, no Pol-I system has been described. Although there are Pol-II dependent rescue systems available for the RABV strains HEP-Flury (Inoue et al., 2003) and CTN181 (Huang et al., 2010), the approaches to recover RABV from strain SAD L16 cDNA independently of T7-pol have failed so far (Osakada et al., 2011). State-of the art recovery

for RABV SAD L16 prior to this thesis employs BSR-T7-5 cells and "helper" plasmids containing T7 promoters and EMCV IRES elements (figure 3).
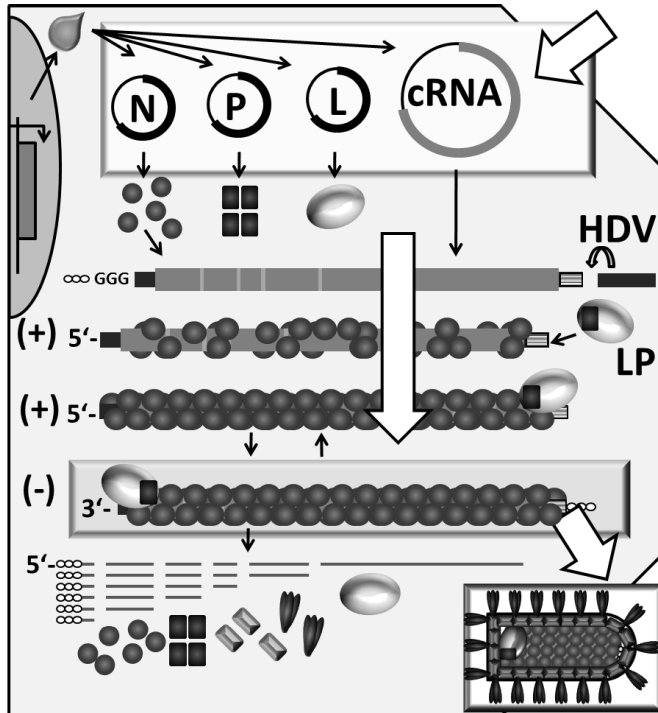
Figure 3: Reverse genetics of RABV – conventional system.
(A) Schematic illustration of RABV rescue from cDNA following the conventional standard protocol (adapted from Ghanem and Conzelmann, in press). 4 plasmids are introduced into BSR T7/5 cells. T7-pol directs transcription of a full-length cRNA and gene expression from the IRES comprising "helper" plasmids. "Illegitimate" encapsidation leads to a cRNP that can be replicated into a vRNP. From the vRNP, all RABV proteins can be expressed and recombinant virus is recovered.

1.3 Rhabdoviral vectors for neuronal tracing

While the strict neurotropism of RABV is one of the main reasons for the pathogenicity of the virus, for neuroscientists it is of particular interest. Years before the existence of a reverse genetic system to recover recombinant RABV, this virus was already proposed as a possible transneuronal tracer, however with little attention, compared to alpha-herpesviruses (Dolivo et al., 1982; Kuypers and Ugolini, 1990). However, the outstanding advantages of RABV as a transneuronal tracer were demonstrated in the following (Astic et al., 1993; Ugolini, 1995). The most important features of RABV (for detailed review see (Ugolini, 2010; Ugolini, 2011) are that it spreads *in vivo* exclusively via synapses, and in a strictly retrograde manner (Kelly and Strick, 2000; Prevosto et al., 2009). Virtually no infection of glia cells is observed *in vivo*, although in cell culture RABV can infect most mammalian cell lines. Thereby, as a replicating virus, unlike synthetic tracers, the self-amplifying signal is not diluted out. This allows the detection of connections over three or more synapses. Due to the neuroprotective features of RABV, the infected neuronal network remains intact for a long time (Tang et al., 1999; Ugolini, 1995).

The development of the reverse genetics system (Schnell et al., 1994) has made it possible to develop new tools and systems in the field of RABV mediated neuronal tracing. First it was possible now to express transgenes from RABV vectors and especially in neurons (Etessami et al., 2000b; Mebatsion et al., 1996b). G gene-deleted RABV mutants are still able to bud from the plasma membrane and a foreign type I transmembrane protein, provided *in trans* can redirect the RABV pseudotypes to different target cells (Mebatsion and Conzelmann, 1996; Mebatsion et al., 1997; Mebatsion et al., 1995). Successful pseudotyping of RABV requires the cytoplasmic C-terminal tail of the RABV G at the C-terminus of the heterologous transmembrane protein (Schnell et al., 1998). Infection of neurons with a G gene-deleted RABV *trans*-complemented with its own (RABV G) glycoprotein leads to a single-round infection and no spread to the presynaptic neuron can occur (Etessami et al., 2000a). This, in combination with e.g. fluorescent proteins expressed from the RABV vector, can be used to stain neurons with fine structures as dendrites or synaptic microstructures (Wickersham et al., 2007a).

If a neuron is infected with a single-round G gene-deleted RABV, and the RABV G is provided *in trans* in this cell, the *trans*-complemented RABV can retrogradely spread to the

presynaptic neurons that are connected to the infected cell. From the presynaptic cell no further spread can occur due to the lack of RABV G. This approach is known as "monosynaptic tracing" (Wickersham et al., 2007b). Further specificity is achieved in this system by pseudotyping the G gene-deleted RABV with a transmembrane protein like the envelope protein A (EnvA) from an avian retrovirus. The receptor for EnvA, tumor virus protein A (TVA), is in nature only present on avian cells and is provided in the neuron of interest. A combination of fluorescent proteins provided in the postsynaptic neuron, together with RABV G and TVA, and expressed from the RABV vector allows distinguishing between postsynaptic and presynaptic cells. Current approaches comprise RABV vectors not only expressing fluorescent proteins, but also calcium-indicators, photoreceptors or light-activated ion channels thus allowing monitoring and/or modulation of neuronal functions.

1.4 RNA interference

A small noncoding antisense RNA regulating a complementary gene was at first described for the *C. elegans* gene lin-4 playing an important role in timing of gene expression during development (Lee et al., 1993). Five years later, also in *C. elegans*, the principle of RNA interference (RNAi) was discovered (Fire et al., 1998). The introduction of long double-stranded RNAs (dsRNAs) was found to inhibit the expression of a complementary gene. Soon RNAi mechanisms were found to exist also in vertebrates like zebrafish *D. rerio* (Wargelius et al., 1999) and mammals like mice (Wianny and Zernicka-Goetz, 2000). The different cellular pathways related to RNAi were studied intensively and found to result in post-transcriptional gene regulation with different outcomes (reviewed in Carthew and Sontheimer, 2009; Grimm, 2009; Li and Liu, 2011; Liu and Paroo, 2010).

MicroRNAs (miRNAs) are encoded endogenously in distinct genomic clusters as single-stranded RNAs containing stem-loop structures as so-called primary miRNAs (pri-miRNAs) (reviewed in Bartel, 2004; Cullen, 2004; Li and Liu, 2011). These 80-100 nt long pri-miRNAs contain a 5'-cap and a 3'-poly(A) tail. They are processed by the Drosha/DGCR8 microprocessor complex into about 60 nt long precursor miRNAs (pre-miRNAs) comprising a duplex with a 3'-2 nt overhang at the cleavage site. Exported into the cytoplasm by Exportin 5 (Lund et al., 2004), they are further processed by Dicer, an enzyme of the RNase III family, into RNA duplexes. One strand, the passenger strand which has the same sequence as the target, is removed, whereas the so-called guide strand which is complementary to the target site, primarily in the 3'-UTR of mRNAs, is loaded into the RISC to repress translation from this mRNA. MiRNAs also have been found to be expressed by certain herpes viruses (Burnside et al., 2006; Pfeffer et al., 2004).

Short interfering RNAs (siRNAs) regulate the gene expression by mRNA degradation (Ngo et al., 1998). In the *D. melanogaster* RNAi pathway, dsRNA is cleaved by Dicer into shorter dsRNA fragments of about 22 nt (Bernstein et al., 2001). The possibility to trigger RNAi with 21 – 22 nts short RNA duplexes, or siRNAs, was demonstated first *in vitro* (Tuschl et al., 1999), later in *D. melanogaster* and in mammalian cell culture (Elbashir et al., 2001a; Elbashir et al., 2001b). SiRNAs, nowadays available commercially, have since become a common and valuable tool in life sciences to knock-down gene expression. Moreover, innumerable

approaches for the establishment of this technology for therapeutic purposes in humans exist (reviewed in Lares et al., 2010).

As an alternative to premade siRNAs, RNAi can be triggered by short hairpin RNAs (shRNAs) which have been shown to work with comparable efficiencies as siRNAs (Paddison et al., 2002). ShRNAs are either made synthetically (Paddison et al., 2004; Siolas et al., 2005), or expressed from Pol-II (Zhou et al., 2005) and Pol-III (Paddison et al., 2004) promoters. Depending on their origin they enter at different stages into the processing pathways. The Pol-II derived shRNAs for example have a 5'-cap structure and a 3'-poly(A) tail and therefore, like pri-miRNAs, must be cleaved by Drosha/DGCR8. Pol-III transcribed shRNAs however start with a 5'-ppp and are designed to terminate exactly in such a way that they have a 2 nt overhang at their 3'-end. Therefore they resemble already the Drosha/DGCR8 products that only differ in having a monophospate at their 5'-end, and only have to be exported by Exportin 5 from the nucleus. Synthetic shRNA have a 5'-monophosphate and are delivered i.e. by lipofection. Once in the cytoplasm, they can be processed directly by Dicer.

Further types of small noncoding RNAs have been described to play roles in the regulation of gene expression, like e.g. the Piwi-interacting RNAs (piRNAs) that are found only in the germline of multicellular organisms and thought to be involved in the protection from transposons (reviewed in Li and Liu, 2011).

The major difference between siRNAs and miRNAs is the perfect base pairing of siRNAs in contrast to the latter. While miRNAs lead to a translational repression upon base-pairing with their target in the 3'-UTR of an mRNA, shRNAs and siRNAs result in mRNA degradation, making them by far more potent and the knock-down effect lasts longer.

RNAi is an important cellular defense mechanism in insects and plants against viruses (reviewed in Haasnoot et al., 2007; Voinnet, 2005). Accordingly, numerous attempts are being made to apply this technology as an antiviral strategy in humans and life stock. On the other hand, viruses are being used as vectors to deliver RNAi triggers, in particular adeno-associated virus (AAV) vectors (Tomar et al., 2003) and lentiviruses (reviewed in Couto and High, 2010).

1.5 Aims of these studies

The aim of the first part of this thesis was to evaluate the possibilities to use RABV as a vector to deliver shRNAs in order to knock-down cellular target genes. Such a knock-down would be important especially for neurotracing and studies of brain function or virus-host interactions. Initial questions were whether RABV interferes with the RNAi machinery and whether RNAs made from a RABV vector can enter RNAi pathways. Several further attempts were made to achieve processing of RABV delivered shRNAs by ribozymes. Bottlenecks hampering either this pre-processing or more downstream steps in the RNAi pathway were identified.

The second part aimed at improving the conventional RABV rescue system by the application of better cleaving ribozymes processing the 5' and 3'-ends of the full-length antigenome-like RNA. Such improvement could ablate the obstacles related with poor recovery especially of attenuated RABVs. As genome ends have been described to be of special importance for RABV rescue, the idea was to enhance rescue efficiency by better and more efficiently processed ends. The better cleaving ribozymes used here were identified in part 1.

Purpose of the third part was to establish a single infectious RABV cDNA, opening the possibility to generate a genetically encoded RABV. This objective was based on the finding that it is possible to recover recombinant RABVs comprising an internal IRES element (Marschalek et al., 2009) and the idea that these IRES elements could be used to direct expression of RABV "helper" proteins from the full-length RNA transcribed during rescue. The improvement of the conventional rescue system established in part 2 (Ghanem et al., 2012) was a prerequisite for this part.

1.5 Aims of these studies

2 Materials and Methods

2.1 Materials

2.1.1 Chemicals

The chemicals used for this work were obtained from Invitrogen, Merck, New England Biolabs, Riedel-de-Häen, Roche, Roth, and Sigma-Aldrich. The radiochemicals ^{32}P-αCTP and ^{32}P-γATP were provided by Amersham Pharmacia and Hartmann Analytic.

2.1.2 Buffers and Solutions

Bacteria growth media			
LB	85	mM	NaCl
	0.5	% (w/v)	Bacto yeast extract
	1	% (w/v)	Bacto tryptone
	1	mM	$MgSO_4$
LB amp	1	x	LB
	25	mg/ml	Ampicillin
LB ++	1	x	LB
	20	mM	$MgSO_4$
	10	mM	KCl

Agarose gels			
10x TAE	2	M	Tris-HCl (pH 7.8)
	250	mM	Na-acetate-trihydrate
	250	mM	EDTA
1x TAE + EtBr	200	ml	10x TAE
	1800	ml	H_2O
	120	µl	Ethidium bromide solution 1 % (w/v)
OG loading buffer	50	% (v/v)	10x TAE
	15	% (w/v)	Ficoll 400
	0.125	% (w/v)	Orange G
10x TE	100	mM	Tris-HCl (pH 7.5)
	10	mM	EDTA
Blue juice	50	% (v/v)	10x TAE
	15	% (w/v)	Ficoll 400
	0.125	% (w/v)	Bromphenol blue
	0.125	% (w/v)	Xylenecyanol
	0.125	% (w/v)	Orange G
1 kb marker	380	µl	10x TE
	100	µl	Blue juice
	20	µl	1 kb DNA ladder (NEB)

Mini Preparation

Flexi I	100	mM	Tris-HCl (pH 7.5)	
	10	mM	EDTA	
	200	µg/ml	RNAse	
Flexi II	200	mM	NaOH	
	1	% (w/v)	SDS	
Flexi III	3	M	K-acetate	
	2	M	Acetic acid (pH 5.75)	

Western blots

10 % APS solution	10	% (w/v)	Ammoniumpersulfate
Jagow gel buffer	3	M	Tris-HCl (pH 8.45)
	0.3	% (w/v)	SDS
Jagow anode buffer	2	M	Tris-HCl (pH 8.9)
Jagow kathode buffer	1	M	Tris-HCl (pH 8.25)
	1	M	Tricine
	1	% (w/v)	SDS
Protein lysis buffer	62.5	mM	Tris-HCl (pH 6.8)
	2	% (w/v)	SDS
	10	% (v/v)	Glycerine
	6	M	Urea
	5	% (v/v)	β-Mercaptoethanol
	0.01	% (w/v)	Bromphenol blue
	0.01	% (w/v)	Phenol red
Staining solution	50	% (v/v)	Methanol
	10	% (v/v)	Acetic acid
	0.1	% (w/v)	Brilliant Blue
10x Semi dry buffer	480	mM	Tris-HCl (pH 8.6)
	390	mM	Glycine
	0.05	% (w/v)	SDS
1x Semi dry buffer	100	ml	10x Semi dry buffer
	180	ml	Methanol
	720	ml	H_2O
PBS	1.37	M	NaCl
	27	mM	KCl
	12	mM	KH_2PO_4
	65	mM	Na_2HPO_4 x 2 H_2O (pH 7.4)
PBS / Tween	1	x	PBS
	0.05	% (v/v)	Tween

Northern blots

50x Phosphate buffer	250	mM	Na_2HPO_4 x 2 H_2O (pH 6.8 - 7.0)
	250	mM	NaH_2PO_4 x H_2O
5x Phosphate buffer	10	% (v/v)	50x Phosphate buffer
	90	% (v/v)	H2O (ultra pure)
RNA agarose gel	2	g	Agarose (RNAse free)
	4	ml	50x phosphate buffer
	26,7	ml	Formaldehyde (37 %)
	167,3	ml	H_2O (ultra pure)
Glyoxal solution	8.8	M	Glyoxal
10x SSC	1.5	M	NaCl
	150	mM	Na-citrate x 2 H_2O (pH 7.0)
Zeta hybridizing buffer	250	mM	Na_2HPO_4 x 2 H_2O (pH 7.2)
	250	mM	NaH_2PO_4 x H_2O
	1	mM	EDTA
	7	% (w/v)	SDS
Zeta 5 % wash buffer	8	% (v/v)	50x phosphate buffer
	1	mM	EDTA
	5	% (w/v)	SDS
Zeta 1 % wash buffer	8	% (v/v)	50x phosphate buffer
	1	mM	EDTA
	1	% (w/v)	SDS

Small RNA Northern blots

2x Bromophenolblue loading buffer	8	M	Urea
	50	mM	EDTA
	0.3	mg/ml	Bromophenolblue
50x Denhardt's solution	1	%	Albumin fraction V
	1	%	Polyvinylpyrrolidon K30
	1	%	Ficoll 400
Hybridization solution	7.5	ml	20x SSC
	0.6	ml	1 M Na_2HPO_4 pH7.2
	21	ml	10% SDS
	0.6	ml	50x Denhardt's solution
	0.3	ml	Sonicated salmon sperm DNA (10 mg/ml)
Wash solution I			5x SSC
	0.1	%	SDS
Wash solution II			1x SSC
	0.1	%	SDS

Cell culture solutions and media

80 % Acetone	800	ml	Acetone p. a.
	200	ml	H$_2$O
PBS (5 mM EDTA)	1	x	PBS (Invitrogen)
	5	mM	EDTA
DMEM 3+	500	ml	DMEM (Invitrogen)
	50	ml	Fetal calf serum
	5	ml	L-Gluthamine (Invitrogen)
	2	ml	Pen-Strep (Invitrogen)
GMEM 4+	500	ml	GMEM (Invitrogen)
	50	ml	Fetal calf serum
	4.5	ml	Tryptose-phosphate (Invitrogen)
	10	ml	MEM amino acids (Invitrogen)
	2	ml	Pen-Strep (Invitrogen)

2.1.3 Kits

Plasmid preparation	Nucleobond Xtra Midi	Macherey-Nagel
DNA purification	QIAquick PCR Purification Kit	QIAGEN
	QIAquick Gel Extraction Kit	QIAGEN
RNA isolation	RNeasy Mini Kit	QIAGEN
Transfection	Mammalian Transfection Kit	Stratagene
	Lipofectamine 2000	Invitrogen
Luciferase assays	Dual-Luciferase® Reporter Assay System	Promega
Northern blot	Nick Translation Kit	GE Healthcare
In vitro-transcription	MEGAscript® T7 Kit	Ambion
	MEGAshortscript® T7 Kit	Ambion

2.1.4 Enzymes

Plasmid DNA cloning	Restriction enzymes	NEB, Fermentas
	DNA polymerase I, large fragment (Klenow)	NEB
	Calf intestine phosphatase	NEB
	T4 DNA Ligase	NEB
PCR	Biopfu DNA Polymerase	Biomaster
	Pfu DNA Polymerase	Fermentas
	Phusion High-Fidelity DNA Polymerase	Finnzymes
	Transcriptor Reverse Transcriptase	Roche
5'-labeling	T4 Polynucleotide Kinase	NEB

2.1.5 Antibodies

antibody	species	application (dilution)	source
anti-actin	rabbit	WB (1 : 10 000)	Sigma-Aldrich
anti-GAPDH	mouse	WB (1 : 1 000)	Abcam
anti-GFP	rabbit	WB (1 : 10 000)	Invitrogen
anti-RABV G (HCA05/1)	rabbit	WB (1 : 10 000)	custom-made, Metabion
anti-RABV N (S86)	rabbit	WB (1 : 10 000)	custom-made, J. Cox (BFAV, Tübingen)
anti-RABV N (FITC-labeled) Centocor^{TM}	mouse	IF (1 : 200)	FDI Fujirebio Diagnostics
anti-RABV P (FCA05/1)	rabbit	WB (1 : 10 000)	custom-made, Metabion
anti-RABV P (160-5)	rabbit	WB (1 : 50 000)	S. Finke (FLI, Riems)
anti-RABV RNP (S50)	rabbit	WB (1 : 25 000)	custom-made, J. Cox (BFAV, Tübingen)
anti-rabbit HRP	goat	WB (1 : 10 000)	Jackson ImmunoResearch Laboratories

2.1.6 Oligos

DNA oligos used in this work were ordered from Metabion. Sequences are listed in the appendix (→6.1).

2.1.7 Plasmids

Plasmids commercially available (alphabetical order)		
pCR3	Eucaryotic expression vector	Invitrogen
pEGFP-C3	CMV promoter-dependent eGFP expression	Clontech
pRL-CMV	CMV promoter-dependent *Renilla* luciferase	NEB
pSUPER	H1 Pol-III-driven shRNA vector (Brummelkamp et al., 2002)	Oligoengine
pTRE2hyg	Tet-inducible expression vector (TET-On)	Clontech

Plasmids kindly provided (alphabetical order)		
pCAGGS	Eukaryotic expression vector with chicken-β-actin promoter	(Niwa et al., 1991)
pCAGGS-P	RABV P in pCAGGS vector	K. Brzozka
pCMV-RL-FF-N/P	Expression plasmid for a bicistronic mRNA *Renilla*-N/P-firefly under control of a CMV promoter; RABV N/P gene border is inserted between the coding sequences for *Renilla* and firefly luciferase.	A. Marschalek
pCMV-FF-PV-RL	Like pCMV-RL-FF-N/P; N/P gene border replaced by poliovirus IRES sequence	A. Marschalek
pCR3-P	RABV P in pCR3 vector	K. Brzozka
pEGFP-miR23-2	Expression plasmid for eGFP with MCMV miR-23-2 sequence in the 3'-UTR.	L. Dölken
pSAD G_DsRed	DsRed cloned into extra transcription unit in pSAD L16 (N/P gene border)	(Klingen et al., 2008)
pSAD L16	Full-length cDNA of RABV SAD L16 cloned into pBluescript	(Schnell et al., 1994)
pSAD PVP(bi)	(or pSAD PVP) N/P gene border in pSAD L16 replaced by poliovirus IRES	(Marschalek et al., 2009)
pSC6 T7-neo	CMV promoter-dependent expression of T7-pol	(Radecke et al., 1995)
pSDI CNPL	RABV minigenome (negative sense); CAT and firefly luciferase reporter genes	(Finke et al., 2000)
pSDI(+)	(or pSDI-1plus) RABV minigenome positive sense	(Schnell et al., 1994)
pSDI-1	RABV minigenome (negative sense)	(Conzelmann and Schnell, 1994)
psiCHECK-23-2	Dual-luciferase Reporter construct to measure miRNA-dependent downregulation	L. Dölken (Dölken et al., 2010)
pTIT-L	T7-pol and EMCV IRES-dependent expression of RABV L	(Finke and Conzelmann, 1999)
pTIT-N	T7-pol and EMCV IRES-dependent expression of RABV N	(Finke and Conzelmann, 1999))
pTIT-P	T7-pol and EMCV IRES-dependent expression of RABV P	(Finke and Conzelmann, 1999)
pX8∂T	Plasmid comprising HDV and T7 terminator sequence	(Schnell et al., 1994)

The plasmids, cloned for this work, together with cloning strategies are listed in the appendix (→6.2)

2.1.8   Viruses

Viruses kindly provided (alphabetical order)	
SAD L16	Recombinant RABV, cDNA derived from strain SAD B19 (Schnell et al., 1994)
SAD PVP(bi)	(or SAD PVP) N/P gene border replaced by poliovirus IRES element (Marschalek et al., 2009)

Viruses rescued in this work (alphabetical order)	
SAD EL	EMCV IRES element in 5'-UTR of L gene (downstream G/L gene border)
SAD EP(mono)	EMCV IRES element in 5'-UTR of P gene (downstream N/P gene border)
SAD G_dHH-HSmm-SC	shRNA against GFP (guide strand and passenger strand are replaced in their positions) flanked by a defect 5'-HHRz and a 3'-SC1 ribozyme in extra transcription unit. Ribozymes in direct proximity to shGFP.
SAD G_dHH-SH-SC	shRNA against GFP flanked by a defect 5'-HHRz and a 3'-SC1 ribozyme in extra transcription unit. Ribozymes in direct proximity to shGFP.
SAD G_eGFP	eGFP in extra transcription unit between G gene and L gene, with N/P gene border
SAD G_eGFP-miR23-2	eGFP with MCMV miR23-2 in 3'-UTR in extra transcription unit
SAD G_HH-HSmm-SC	shRNA against GFP (guide strand and sense strand are replaced in their positions) flanked by a 5'-HHRz and a 3'-SC1 ribozyme in extra transcription unit. Ribozymes in direct proximity to shGFP.
SAD G_HH-shGFP-SC1	shRNA against GFP flanked by a 5'-HHRz and a 3'-SC1 ribozyme in extra transcription unit. Spacer nts between ribozymes and shGFP.
SAD G_HH-SH-SC	shRNA against GFP flanked by a 5'-HHRz and a 3'-SC1 ribozyme in extra transcription unit. Ribozymes in direct proximity to shGFP.
SAD G_shGFP	shRNA against GFP in extra transcription unit
SAD L16	Recombinant RABV, cDNA derived from strain SAD B19 (Schnell et al., 1994).
SAD N100(mut)EN G_eGFP	As SAD N100EN G_eGFP, but AUG at leader-N gene junction mutated to UUG.
SAD N100EN G_eGFP	First 100 nts of N gene and EMCV IRES inserted between leader-N gene junction and N gene (leader-N gene junction restored to wild-type). EGFP in extra transcription unit between G and L.
SAD N200(mut)EN G_eGFP	As SAD N200EN G_eGFP, but AUG at leader-N gene junction mutated to UUG.
SAD N200EN G_eGFP	First 200 nts of N gene and EMCV IRES inserted between leader-N gene junction and N gene (leader-N gene junction restored to wild-type). EGFP in extra transcription unit between G and L.
SAD N200EN(Fse)	First 200 nts of N gene and EMCV IRES inserted between leader-N gene junction and N gene (*FseI*-site at leader-N gene junction).
SAD N2AP	N/P gene border replaced by 2A-like sequence
SAD NEN	Second N gene and EMCV IRES inserted between leader-N gene junction and N gene (*FseI*-site at leader-N gene junction).

SAD NEN G_eGFP	Second N gene and EMCV IRES inserted between leader-N gene junction and N gene (leader-N gene junction restored to wild-type). EGFP in extra transcription unit between G and L.
SAD NEN_EL	Bicistronic N-EMCV IRES-N gene (with wild type-like leader-N gene junction) and monocistronic EMCV IRES-L gene.
SAD NEN2AP	Tricistronic N-EMCV IRES-N-2A-like-P gene (with wild type-like leader-N gene junction)
SAD NEN2APEL	Tricistronic N-EMCV IRES-N-2A-like-P gene and monocistronic EMCV IRES-L gene.
SAD NENEP	Bicistronic N-EMCV IRES-N gene (with wild type-like leader-N gene junction) and monocistronic EMCV IRES-P gene.
SAD NENEPEL	Bicistronic N-EMCV IRES-N gene, monocistronic EMCV IRES-P gene and monocistronic EMCV IRES-L gene.
SAD NEP(bi)EL	Derived from rescue of pCAGGS-T7_NEP(bi)_EL_SC: Bicistronic N-EMCV IRES-P gene and monocistronic EMCV IRES-L gene.
SAD NEP(bi)EL 1	Derived from rescue of pSAD T7-HH_NENEPEL_SC, rearranged variant: Bicistronic N-EMCV IRES-P gene and monocistronic EMCV IRES-L gene.
SAD NEP(mono)EL	Monocistronic EMCV IRES-P gene and monocistronic EMCV IRES-L gene.
SAD NPVN	Second N gene and poliovirus IRES inserted between leader-N gene junction and N gene (*FseI*-site at leader-N gene junction).
SAD PVP(bi)	(or SAD PVP) N/P gene border replaced by poliovirus IRES element (Marschalek et al., 2009).
SAD PVP(mono)	Poliovirus IRES element in 5'-UTR of P gene (downstream N/P gene border)

2.1.9 Cell lines

Cell line	Description	Medium	Source
A549	Human alveolar adenocarcinoma cell line	DMEM 3+	ATCC
A549-LR- siGFP	A549 cells stably transduced with a lentiviral vector to express shRNAs against GFP	DMEM 3+	L.Roux (Mottet-Osman et al., 2007)
A549-LR-siNGFR	A549 cells stably transduced with a lentiviral vector to express shRNAs against NGFR	DMEM 3+	L.Roux (Mottet-Osman et al., 2007)
BHK-21	Baby hamster kidney cells	GMEM 4+	ATCC
BSR T7/5	BHK-21-derived (baby hamster kidney) cells expressing T7-pol	GMEM 4+ + 1 M G418 sulfate every second passage	(Buchholz et al., 1999)
BSR-clone 13	BHK-21-derived (baby hamster kidney) cells	GMEM 4+	J. Cox (BFAV Tübingen)
HEK 293T	Human embryonic kidney cells expressing SV40 T-antigen	DMEM 3+	ATCC
HeLa	Human cervix carcinoma cells	DMEM 3+	ATCC
HEp-2	Human epidermoid (laryngeal squamous) carcinoma cells	DMEM 3+	ATCC
HEp-2-eGFP	HEp-2 cells stably expressing eGFP	DMEM 3+	This work
NA	Mouse neuroblastoma cell line	DMEM 3+	ATCC
U3A-LC3-GFP	U3A cell line (derived from human sarcoma cells HT1080) expressing an LC3-GFP fusion protein.	DMEM 3+	L. Fragnet
Vero	African green monkey kidney cells	DMEM 3+	ATCC

2.2 Methods

2.2.1   Polymerase Chain Reaction (PCR)

With the PCR DNA fragments can be amplified for either cloning or sequencing of reverse transcription derived cDNA. Template specific primers which flank the DNA of interest were used. For cloning these primers especially were designed in order to add extra nucleotides to the 5´- or 3´-ends of the amplified DNA (e.g. restriction sites, *de novo* sequences).

The standard PCR reaction was:

10 - 100	ng	Template DNA
10	µl	10x polymerase reaction buffer incl. $MgSO_4$
3 - 10	µl	DMSO
250	nM	Forward primer
250	nM	Reverse primer
1	µl	dNTPs (25 µmol each)
2.5	U	DNA polymerase
ad 100	µl	ddH_2O

Reactions were set up in a thermocycler with heated lid. The typical program was:

1.	30	s	95 °C	Enzyme activation	
2.	30	s	95 °C	Denaturing	
3.	30	s	50 °C	Primer annealing	30 x
4.	60	s / 500 bp	72 °C	Elongation	
5.	15	min	72 °C	Final elongation	
6.	∞		4 °C	Storage	

All PCR products were purified with the QIAquick PCR Purification Kit (QIAGEN) according to the supplier´s manual. DNA was eluted from the column using 35 µl ddH_2O.

A variation for some short fragments (<150 bp) was a PCR reaction lacking any template. In this case two long primers were designed to overlap in a reverse complement way in order to amplify the overlapping region together with specific overhangs.

2.2.2   Agarose gel electrophoresis of DNA fragments

The agarose gel electrophoresis was used to analyze the legth of PCR products or fragments derived from restriction digests. Gels contained 1 % agarose in 1x TAE or 2 % agarose for fragments <500 bp, respectively.

DNA samples were mixed at a ratio of 1:6 (v/v) with Orange G loading buffer, loaded onto the gels and subjected to electrophoresis at 120 – 140 V for 30 - 180 min, depending on the length of the fragments and the agarose concentration. The electrophoresis buffer was 1x TAE + EtBr. Gels were analyzed on a Biorad GelDoc System using UV light at λ=254 nm.

2.2.3   Purification of DNA from agarose gel

For cloning, the samples of preparative restriction digests were subjected to agarose gel electrophoresis. Visualized by long wavelength UV light the bands of the expected sizes were cut out of the gel. The QIAquick Gel Extraction Kit (QIAGEN) was used to isolate the DNA from the gel slice. The DNA was eluted from the column using 35 µl ddH$_2$O.

2.2.4   Restriction digest

DNA was digested with restriction endonucleases from New England Biolabs (NEB) or Fermentas according to the manufacturer's protocol.

Reactions of analytical digests were performed in 20 µl total volume containing <1 µg DNA with 1 - 5 U restriction enzyme(s). Reactions of preparative digests, used for cloning, were performed in 50 µl total volume containing 3 – 5 µg DNA with 10 – 20 U restriction enzyme(s).

The samples were subjected to agarose gel electrophoresis to observe the outcome of the digest and in the case of preparative digests to purify the fragments.

2.2.5   Dephosphorylation of DNA

To reduce the possibility of direct relegation, vector DNA was dephosphorylated at its 5'-ends directly after the restriction digest. The *Calf intestine phosphatase*(CIP) from New England Biolabs (NEB) was used following the manufacturer's instruction.

2.2.6   Klenow – fill-in or removal of overhangs

To generate blunt ends upon cloning *DNA polymerase I, large fragment (Klenow)* from NEB was used directly after the restriction digest. This enzyme fills in overhanging 5'-ends and degrades overhanging 3'-ends. The reaction accorded to the manufacturer's protocol.

2.2.7   Annealing of DNA oligos

For the creation of some inserts (<100 bp) two reverse complement DNA oligos were designed and synthesized in order to anneal to a double stranded fragment with single

stranded overhangs. Due to their sequence of these overhangs were compatible to "sticky ends" made from restriction digestions.

The standard reaction was as follows:

500	nM	Forward DNA oligo
500	nM	Reverse DNA oligo
2	µl	NEB buffer 3
ad 20	µl	ddH$_2$O

The reactions were heated for 2 min to 95 °C and allowed to cool down to RT. The fragments were purified using the QIAquick PCR Purification Kit (QIAGEN).

2.2.8 Ligation

Ligation of DNA fragments was performed with the T4 DNA Ligase (NEB). The fragment that contains the bacterial origin of replication and the antibiotics resistance gene is referred to as the vector. Any other fragment derived from either a restriction digest of a plasmid or PCR product, or from the annealing of two DNA oligos, is referred to as the insert. In the standard reaction an insert was ligated into a vector as follows:

1	µl	purified vector
7	µl	purified insert
1	µl	10 x T4 DNA Ligase buffer
1	µl	T4 DNA Ligase

Reactions were incubated either for 1 h at RT or overnight at 16 °C.

2.2.9 Transformation of plasmid DNA into competent bacteria

50 µl of chemical-competent *E.coli*, strain *XL1-Blue* were thawed on ice and either a total ligation mix or 100 ng of plasmid DNA were added. The mixture was incubated for 15 min in ice, followed by a heat shock (42 °C for 2 min) and 2 min further incubation on ice. Then 200 µl of LB++ medium were added and the bacteria were shaken at 37 °C and 800 rpm for another 45 min. The transformed bacteria were plated onto LB-agar plates containing 25 mg/ml of the appropriate antibiotic. Plates were incubated at 37 °C overnight.

2.2.10 Preparation of plasmid DNA from bacteria

a) Mini preparation (small scale):

Single colonies were picked from an LB-agar plate into 1 ml LB medium containing the appropriate antibiotic and incubated at 37 °C overnight while shaking at 800 rpm. The bacteria were pelleted (14,000 rpm, 30 s, RT) and the supernatant discarded. Pellets were resuspended in 200 µl Flexi I buffer. For cell lysis 200 µl Flexi II were added, tubes were mixed gently and incubated for 5 min at RT. Then 200 µl of Flexi III were added for neutralization and after mixing gently the reactions were incubated for another 5 min on ice. The resulting debris was pelleted by centrifugation (14,000 rpm, 7 min, RT) and the cleared supernatant was mixed thoroughly with 400 µl pure isopropanaol in order to precipitate the DNA. The plasmid DNA was pelleted by centrifugation (14,000 rpm, 7 min, RT), the supernatant was discarded and pellets air-dried and resolved in 50 µl ddH$_2$O.

b) Midi preparation (medium scale):

Single colonies were picked from an LB-agar plate into 50 - 100 ml LB medium containing the appropriate antibiotic and incubated at 37 °C overnight while shaking at 800 rpm.

50 ml of the bacterial overnight culture were used for DNA preparation with the NucleoBond® Xtra Midi/Maxi Kit (Machery & Nagel) according to the manufacturer's instructions.

2.2.11 Sequencing of DNA

Sequencing reactions were performed by MWG Eurofins (Martinsried, Germany) or GATC (Konstanz, Germany). DNA and sequencing primers were adjusted as requested by the respective company.

Sequencing results were analyzed using the software DNAMAN (version 6.0 or higher). If necessary, abi-files were examined using the Chromas software (version 1.45).

2.2.12 Isolation of RNA from eukaryotic cells

a) RNeasy Kit:

RNA from cells was isolated using the RNeasy Mini Kit (QIAGEN). 1 x 10^6 cells were lysed in 350 µl RLT buffer (included in the kit) containing 1 % β-mercaptoethanol and optionally stored at -80 °C. RNA was purified from these lysates following the manufacturer's protocol.

The RNA concentration was determined using the Nanodrop 1000 (Peqlab) and the extracted RNAs were stored at -80 °C.

b) Trizol extraction

To include also very short RNAs, e.g. miRNAs, RNA was isolated using Trizol The cells were detached using ice-cold PBS (5 mM EDTA) pelleted (5 min, 1500 rpm) washed in PBS and pelleted again. Supernatants were discarded and 4 ml Tri-reagent (Sigma-Aldrich) per g cell pellet were added. Optionally now the lysates were stored at – 80 °C.

To purify the RNA from these lysates, 1/5 volume of chloroform:isoamyl alcohol (24:1) (Ambion) and 1/20 volume of 2M sodium acetate (pH 4.2) were added and mixed by pipetting until the mix was turbid-white. The mixture was transferred to an Eppendorf tube/ Falcon tube (depending of the volume) and centrifuged. The upper (aqueous) phase was transferred to a new tube and 1 volume of acidic phenol:chloroform:isoamyl alcohol (25:24:1) (Ambion) was added followed by a centrifugation step. Extractions were repeated until the white interphase (DNA and proteins) almost disappeared and the aqueous phase was clear. The upper (aqueous) phase was transferred to a new tube and 1 volume of isopropanol was added. Precipitation was allowed to occur overnight at –20°C. The next day the tube was centrifuged (full speed at 4°C), the supernatant was removed and the pellet was washed once with 70 % ethanol. The pellet was resuspended in ddH2O (nuclease free) and stored at -80 °C. The RNA concentration was determined using the Nanodrop 1000 (peqlab).

2.2.13 Reverse transcription

Reverse transcription PCR was performed using the Roche Transcriptor RT (Roche). Therefore, 1 µg RNA was mixed with 0.3 M specific reverse primer, oligo dT or random hexamer primers in a final volume of 13 µl. After incubation at 65 °C for 10 min the reaction was chilled on ice to allow annealing of the primer. Then 4 µl RT buffer, 0.5 µl RNase inhibitor, 2 µl dNTPs and 0.5 µl Transcriptor RT were added and incubated at 55 °C for 30 min. The reaction was heated to 85 °C for 5 min in order to inactivate the enzyme.

2.2.14 *In vitro*-transcription

The MEGAscript Kit (RABV full-length cDNAs) or the MEGAshortscript Kit (pSDI constructs) (Ambion) were applied for *in vitro*-transcription as described in the manufacturer's

instructions. 10 μg of cDNA plasmids were linearized using adequate restriction enzymes and purified via agarose gel electrophoresis (→2.2.3). For the *in vitro*-transcription reaction 1 μg of linearized and purified DNA was used. Following the reaction (37 °C, 4 h) 1 μl of Turbo-DNase (Ambion) was added and further incubated (37 °C, 20 min) to get rid of the DNA template. The RNA was recovered using LiCl-precipitation (reagents provided within the kits).

2.2.15 Northern blot

The Northern blot was performed with either 2.7 μg RNA isolated from cells or 1 μg *in vitro*-transcribed RNA in a total volume of 7.2 μl RNase free ddH$_2$O. 1.8 μl glyoxal and 3 μl 5x phosphate buffer were added and the mix was incubated for 45 min at 56 °C.

Before loading of the samples to a denaturing agarose gel 3 μl Blue juice were added. For the gel 2 g of agarose (RNA grade) were dissolved in 167.3 ml of ddH$_2$O (ultrapure) and 4 ml of 50x phosphate buffer by heating and stirring. 26.7 ml of 37 % formaldehyde were added to the solution after cooling down to be lukewarm. A 24 cm x 20 cm gel was poured from the solution.

RNA probes were loaded to the gel and electrophoresis was performed using 1x phosphate buffer at 25 V overnight. RNA was stained using acridine orange solution and 1x phosphate buffer as washing solution to visualize prominent RNAs (e.g. rRNAs) under UV light.

To transfer the RNAs onto nylon membranes (Stratagene, GE Healthcare) the Vacu-Blot system (Biometra) was applied for 2 h at 100 mBar. The membrane was then air-dried and RNA UV-crosslinked (0.125 J). Probes were generated by radioactive labelling of specific PCR products (25 ng) with ^{32}P-α-CTP using the Ready prime II Kit (GE Healthcare) according to the manual followed by purification with the QIAquick Nucleotide Removal Kit (QIAGEN) and a denaturation step (5 min, 95 °C).

The nylon membranes were preincubated with Zeta hybridizing buffer for 10 min at 68 °C before the preincubation buffer was replaced by 8 ml fresh buffer containing the probe. Hybridising took place overnight at 68 °C. Membranes then were washed once with Zeta wash buffer 5 % and twice with Zeta wash buffer 1 % (in each case: 20 min, 68 °C) and allowed to air-dry. To detect the radioactively labeled RNAs the membranes were exposed

to a Phosphoscreen for 2 h up to 96 h depending on the strength of the signal. The screen was analyzed using a storm scanner (Molecular Dynamics; GE Healthcare).

2.2.16 Urea polyacrylamide gel (small RNAs)

The recipe to pour 8 M urea-PAA gels was:

component	10 % gel		15 % gel	
Urea	14.4	g	14.4	g
10 x TBE (Roth)	3	ml	3	ml
Acrylamide	6.8	g	10.2	ml
ddH$_2$O (nuclease free)	to 30	ml	to 30	ml
10 % APS	150	µl	150	µl
TEMED	30	µl	30	µl

The first four components were stirred at RT until the urea was completely dissolved, then APS and TEMED were added and the gel was casted immediately between two glass plates separated by plastic spacers (standard: 15 %, 15 x 10 cm; small gel for SDI IVT: 10 %,).

The RNA samples were mixed with an equal volume of 2X bromophenolblue loading buffer and heated for 3 min to 95 °C prior to loading.

Running Buffer was 1 x TBE and the gel was run for 4 h at 180 V.

RNA gels were either stained with a 1 % EtBr solution (1 x TBE) to directly detect bands of interest under UV light, or subjected to Small RNA Northern blot.

2.2.17 Small RNA Northern blot

For electrophoresis of small RNAs, 30 µg of total RNA together with an equal volume of 2X bromophenolblue loading buffer were loaded onto a 8 M urea and 15 % polyacrylamide gel (→2.2.16). The gel was run until the bromophenolblue reached the end of the gel.

For transfer to Hybond-N+ membranes (Amersham) 0.5 x TBE buffer was used and the semidry method was applied (peqlab) for 30 min at 400 mA wrapped in one layer of whatman paper.

Following the transfer the membrane was allowed to dry for about 20 min at RT. UV-crosslinking (1200 J, 30 s) and subsequent baking of the membrane for 1 h at 80 °C were

performed. The blotted membrane was then stored in a cylindrical glass bottle at 4 °C until hybridization was performed.

The hybridization solution was prepared fresh right before the experiment. Therefore the sonicated salmon sperm DNA was denatured at 100 °C for 5 min and added to the pre-heated (50 °C) solution.

Prior to hybridization, the membrane was pre-incubated with the hybridization solution at 50 °C for 1 h in a 100 ml cylindrical hybridization bottle under rotation. In the mean-time the probe was prepared.

The standard reaction for 5'-labelling of the probe was as follows:

1	µl	20 µM oligodeoxynucleotide (22 nts)
5	µl	^{32}P-γ-ATP (3000 Ci/mmol)
2	µl	10x T4 Polynucleotide Kinase buffer (NEB)
0.2	µl	T4 Polynucleotide Kinase (NEB)
11.8	µl	ddH$_2$O

The reactions were incubated for 15 min at 37 °C and stopped by adding 30 µl of 30 mM EDTA (pH 8.0) to the mix. The labeled oligos were purified using a Sephadex G25 spin column (Roche) according to the manufacturer's instructions and residual Polynucleotide Kinase was inactivated by heating to 95 °C for 1 min.

The probe was diluted in 15 ml of pre-heated hybridization solution and added to the membrane, replacing the pre-hybridization solution. Hybridization took place at 50 °C overnight under rotation.

The next day the hybridization solution was discarded and the membrane was washed twice for 10 min with 30 ml wash solution I and once for 10 min with 30 ml wash solution II (50 °C, under rotation). To avoid drying of the blot, the membrane was wrapped in saran and exposed to a phosphor-imager screen for 3 – 24 h.

2.2.18 Computer-based RNA secondary structure predictions

RNA secondary structure was predicted using the RNAfold software on the Vienna RNA server homepage (http://rna.tbi.univie.ac.at/cgi-bin/RNAfold.cgi). For comparison, predictions were simultaneously performed with the software DNAMAN 6.0.

2.2.19 Cell culture

Mammalian, adherent growing cell lines were kept in specific growth media (see 2.1.9) and cell culture flasks (T25 or T75) in incubators at 37 °C and 5 % CO_2. Cells were trypsinated using Trypsin/EDTA and split every 3-4 days at various ratios from 1:4 to 1:10 depending on the growth rate of each cell line. If necessary, selection drugs were added every other passage. All cell culture reagents were purchased from Invitrogen.

To seed the cells for experimental use, they were detached with Trypsin/EDTA and resuspended in growth medium. Cell numbers/ml were calculated based on estimated cell numbers/flask (T25: $3x10^6$; T75: $9.4x10^6$) or determined using a Neubauer counting chamber. And the appropriate number was given into dishes or wells.

2.2.20 Transfection

Cells were transfected with plasmid DNA or RNA using either $CaPO_4$ (*Stratagene Mammalian Transfection Kit*), Lipofectamine^{TM} 2000 (Invitrogen) or PEI as described by the manufacturers (PEI transfection followed the Lipofectamine 2000 protocol).

a) Transfection with Lipofectamine 2000

The standard protocol was to seed cells 12 – 16 h prior to the transfection into 6 wells (12 wells or 24 wells, respectively) to have them at a confluency of 50 %. 1 – 5 µg of plasmid DNA or RNA were diluted in 100 µl DMEM (accordingly downscaled for 12 wells and 24 wells). At the same time 2.5 µl Lipofectamine 2000 (Invitrogen) per µg of DNA or RNA were diluted in 100 µl DMEM. After 5 min the two dilutions were mixed incubated for another 20 min at RT and added drop-wise onto the cells.

A variation of this protocol was used for certain cell lines (e.g. BSR cells, BHK cells or Vero cells). The plasmids (1 – 5 µg / 6 well) and the Lipofectamine 2000 (2.5 µl per µg DNA) were diluted in 250 µl of Optimem each. After mixing both and incubation for 20 min at RT the growing medium of the cells was replaced by the transfection mix. The cells were incubated at standard conditions and 10 min after transfection 1.5 ml fresh medium was added.

b) Transfection with PEI

The Transfection with PEI was only suitable for the transfection of only one plasmid. The transfection followed the protocol for Lipofectamine 2000.

c) Transfection with CaPO$_4$

The standard protocol was to seed BSR or BSR-T7/5 cells 12 – 16 h prior to the transfection into 6 wells (12 wells or 24 wells, respectively) to have them at a confluency of 80 - 90 %. 1 h prior to the transfection the cells were washed with DMEM and 1 ml of fresh DMEM was given onto each well. Cells were incubated 1 h at standard conditions. During this time the transfection mixes were set up. 10 – 20 µg of plasmid DNA were diluted in 90 µl ddH$_2$O and chilled on ice. 10 µl solution #1 from the Mammalian Transfection CaPO$_4$ Kit (Stratagene) were added thoroughly mixed and chilled on ice again. Then 100 µl solution #2 were added and after mixing again thoroughly the mixture was incubated for 20 min at RT before it was added drop-wise onto the cells. Cells were returned to the incubator and washed 3.5 h post transfection with GMEM 4+ and 2 ml fresh GMEM 4+ was given into each well.

2.2.21 Fixation of cells with acetone

Cells were washed once with 1x PBS, once with cold 80 % acetone, fixed with cold 80% acetone for 20 min at 4°C and air dried.

2.2.22 Microscopy

For fluorescence microscopy of cells a fluorescence microscope (Olympus IX 71) was used, using UV- or transmission light.

2.2.23 Production of stable cell lines

To produce stable cell lines cells were seeded into 6 well dishes the day before the experiment. The cells were transfected with a plasmid encoding a selection marker together with the cDNA of interest. 24 h post transfection the appropriate drug was administered to the cells. After onset of selection (48 – 72 h post transfection) the cells were detached from the wells with Trypsin/EDTA re-suspended in medium and serial dilutions were seeded into 96 well plates together with the selection drug in order to generate single cell clones. Plates seeded with a dilution that resulted in less than 50 % of the wells containing cells were considered to contain these single clones in most cases. The clones were expanded and screened for the expression of the construct of interest.

2.2.24 Freezing of cells

For long-term needs and as a backup, cells were stored in liquid N_2. Cells were grown to confluence in T25 flasks, or T75 flasks, respectively. They were detached from the flasks using Trypsin/EDTA and re-suspended in medium (5 ml and 15 ml respectively). The cell containing medium was chilled on ice and 8 % (v/v) DMSO were added drop-wise. In cryotubes (Sarstedt), 1 ml at a time, the cell suspension was frozen to – 80 °C. Therefore the cryotubes were set into a NALGENE^{TM} Freezing container filled with isopropanol to ensure freezing rates of less than 1 K/min. After 24 h the cryotubes containing the frozen cells were transferred into an N_2-storage-tank. One aliquot was thawed the next day as a control.

2.2.25 Virus stock production

To generate virus stocks 7.5 x 10^5 BSR-T7/5 cells were seeded in 8 ml DMEM 4+ into a T25 flask. The cell suspension was directly infected with an MOI of 0.01. 72 h post infection the supernatants were collected and replaced by fresh GMEM 4+ to allow a second harvest after another 48 – 72 h. For viruses that were strongly attenuated compared to the wild type (SAD L16) cells were split 1:4 after the second harvest and 72 h later a third harvest could be obtained. Directly after the collection the supernatants were centrifuged (5 min, 4 °C, 1,600 rpm) to get rid of the cell debris. Aliquots of the supernatants of this centrifugation step were frozen at -80 °C.

2.2.26 Titration of virus

The amount of infectious particles in a virus supernatant was determined by titration. 1.2 x 10^4 BSR-T7/5 cells in 100 µl per well were seeded into 96 well plates and allowed to attach for at least 2 h. Frozen virus supernatants were thawed and seven serial 10-fold dilutions were prepared in GMEM. 100 µl of each dilution step and of the undiluted supernatant was added in duplicates onto the cells.

The infected cells were grown at standard conditions for 48 h (wild type like viruses) – 96 h (strongly attenuated viruses). After incubation the supernatants were discarded and the cells fixed in acetone (→2.2.21) and stained with a FITC-conjugated antibody against RABV-N (Centocor) for 2 h at 37 °C.

Foci were counted from each well using non-confocal UV microscopy (Olympus IX71) and focus forming units per ml (ffu/ml) were calculated from these results.

For strongly attenuated RABV infected cells were incubated up to 96 h before they were fixed and stained.

2.2.27 Generation of recombinant rabies virus (virus rescue)

The standard protocol to reconstitute a recombinant RABV from cDNA was to transfect 10 µg of the full-length cDNA together with 5 µg pTIT-N, 2.5 µg pTIT-P and 2.5 µg pTIT-L, into BSR-T7/5 cells. Therefore the CaPO$_4$ transfection (→2.2.20.3) was applied.

72 h post transfection the supernatants were collected cleared from the cell debris by centrifugation (5 min, 4 °C, 2,800 rpm) and passaged onto fresh BSR cells (supernatant passage #1A). The transfected cells were incubated for another 72 h with fresh GMEM 4+. After 72 h the cells of the supernatant passage 1A were fixed with acetone (→2.2.21) and stained with a FITC-conjugated antibody against RABV-N (Centocor) to check for the success of the rescue. Also 72 h after the first supernatant passage a second passage of the supernatants from the transfected cells was performed as described before (supernatant passage #1B) and the transfected cells were detached from the well using 1 ml Trypsin/EDTA. 250 µl were given into a new 6 well with 2 ml fresh GMEM 4+ (cell passage 1) and the remaining 750 µl into a T25 flask in 8 ml fresh GMEM 4+. After another 72 h the cells of the supernatant passage 1B and of the cell passage 1 were fixed with acetone and stained with Centocor. If RABV foci could be detected the supernatants from the T25 flasks were collected cleared from cell debris by centrifugation and aliquots were frozen at -80 °C (rescue harvest #1). Optionally the cells were incubated for another 72 h in fresh GMEM 4+ to collect the supernatants for a second harvest (rescue harvest #2). The harvests from the rescue were titrated (→2.2.26) and used as inoculums to produce virus stocks of the newly generated recombinant RABV.

For strongly attenuated RABV at the time point of the cell passage instead of splitting 750 µl into T25 flasks another 250 µl of the trypsinized transfected cells were given into a second 6 well (cell passage 1A and 1B). This allowed the fixation and staining of cell passage 1A as well as collecting and passaging supernatants from cell passage 1B for a third time (supernatant passage 1C). Also the cells of the supernatant passages were incubated up to 5 d before they were fixed and stained.

For cDNAs that were designed to express from one to all of the "helper" proteins the plasmids pTIT-N, pTIT-P or pTIT-L, were omitted in the transfection.

2.2.28 Infection of cells

According cell numbers were seeded in multi-well plates and directly infected in suspension with calculated MOIs of rapidly thawed virus stocks.

2.2.29 Growth curves

To determine the growth kinetics of recombinant viruses and compare it to wild type SAD L16 7.5×10^5 BSR-T7/5 cells were seeded into T25 flasks and allowed to attach while growing for at least 2 h at standard conditions. The cells then were infected with appropriate MOIs (0.01 for a multistep growth curve, 1 for a single step growth curve). 2 h post infection supernatants were discarded and replaced by 8 ml fresh GMEM 4+. After 30 min the first samples (t = 2.5 h post infection) were harvested in duplicates each 0.5 ml and stored at − 80 °C. 1 ml fresh GMEM 4+ was added to fill up the total volume of the cell medium again to 8 ml. Then at certain time points after the infection (from 24 h up to 144 h) samples were taken as described above in intervals of 24 h. The samples were titrated (→2.2.26) to determine the amount of infectious particles at each time point.

2.2.30 Minigenome assay

Minigenome assays are used in order to quantify transcription and replication of RV. 10 µg of the minigenome cDNA together with 5 µg pTIT-N, 2.5 µg pTIT-P and 2.5 µg pTIT-L, were transfected with $CaPO_4$ into BSR-T7/5 cells (→2.2.20.3). 10 ng of pRL-CMV were co-transfected for normalization and a negative control was the omission of one of the "helper" plasmids. 48 h post transfection the cells were harvested in passive lysis buffer (Promega). 20 µl of each lysate were transferred into a 96 well plate and firefly and *Renilla* luciferase activity were measured within a luminometer (Berthold Lumat LB 960) using the Dual-Luciferase® Reporter Assay System (Promega) according to the manufacturer's instruction.

2.2.31 Denaturing polyacrylamide gel electrophoresis (SDS-PAGE)

The recipe to pour the gels was:

	Separating gels			Stacking gel
component	8 %	10 %	12 %	4 %
H_2O	14.6 ml	12.9 ml	11.1 ml	9 ml
Jagow gel buffer	12 ml	12 ml	12 ml	3.5 ml
Glycerol	2 ml	2 ml	2 ml	-
Acrylamide	7.2 ml	9 ml	10.8 ml	1.4 ml
10 % APS	175 μl	175 μl	175 μl	116 μl
TEMED	17 μl	17 μl	17 μl	17 μl

The separating gel was casted between two glass plates separated by plastic spacers. Standard was a 10 % polyacrylamide concentration and a gel size of 15 x 10 cm (large: 20 x 20 cm). To exclude O_2 and allow the complete polymerization the separating gel was overlaid with isopropanol. Next, the isopropanol was discarded, the stacking gel was poured onto the polymerized separating gel and the comb (standard: 15 pockets) was inserted.

The gels were placed in an electrophoresis chamber (peqlab) and Jagow anode and cathode buffers were filled in. Protein lysates were incubated for 5 min at 95 °C and centrifuged shortly to pellet residual cell debris. 5 to 100 μl of protein lysates were loaded into each pocket. As a molecular weight marker 8 μL of Precision Plus Protein Standard (Biorad) were loaded directly into one pocket. Gels were run overnight at 30 – 65 V.

2.2.32 Western blot (Semi-dry)

After SDS-PAGE the proteins were transferred onto PVDF membranes (Millipore). First the stacking gel was removed and the separation gel was incubated for 5 min in 1 x semi-dry buffer. The PVDF membrane was to be activated in methanol. In a blotting chamber (peqlab) the Western blot was assembled in the following order. First 3 layers of Whatman paper (soaked in semi-dry buffer), above the membrane (activated) followed by the gel and 3 layers of Whatman paper (soaked) on top. Blotting was performed for 2 h at 400 mA.

The membranes then were blocked for 1 h at RT in PBS containing 5 % fat-free milk powder to reduce unspecific binding of antibodies during immunodetection.

2.2.33 Immunodetection

The membranes after performing the Western blot were taken out of the blocking solution and washed (3 x 10 min at RT) in PBS-Tween on a shaker. Specific primary antibodies against the proteins of interest were diluted in PBS (as indicated in 2.1.5) and the membranes were incubated in these antibody solutions overnight at 4 °C on a shaker or rolling incubator. Following again extensive washing (3 x 10 min at RT) in PBS-Tween the membranes were incubated for 2 h at RT with the appropriate secondary antibody. The HRP-conjugated secondary antibody was directed against the species of the primary antibody.

After washing the membranes in PBS (3 x 10 min at RT) 1 - 3 ml of Western Lightning® Plus-ECL substrate (PerkinElmer) were added directly onto the membrane. The chemiluminescence derived from the HRP and its substrate ECL immediately was detected either using Hyperfilm-ECL (GE Healthcare Amersham) or blots were directly scanned and light emission detected with the Fusion FX7 (Vilber Lourmat).

3 Results

3.1 Rabies virus vectors delivering RNAs

Cytoplasmic RNA viruses as RABV do not express siRNAs or shRNAs and some interfere with the siRNA machinery as observed for the p19 protein of tombusvirus that binds siRNA (Silhavy et al., 2002) and for many other viruses in plants and animals (reviewed in Haasnoot et al., 2007; Voinnet, 2005). The following work aimed at evaluating the possibility of RABV as a vector for the delivery of shRNAs.

3.1.1   Rabies virus infection does not interfere with shRNA mediated knock-down

To evaluate if a RABV vector is suitable for the delivery of shRNAs it was tested first if RABV infection interferes with short shRNA mediated knock-down or not.

Therefore, A549 cells, A549-LR-siGFP cells (Mottet-Osman et al., 2007), that stably express an shRNA against GFP (shGFP), or A549-LR-siNGFR cells (shRNA against NGFR) were transfected with pEGFP-C3 and 3 h p.t. either infected with RABV (MOI=3) or not, as indicated in figure 4. 48 h p.i. the cells were analyzed with a fluorescence microscope for GFP expression.
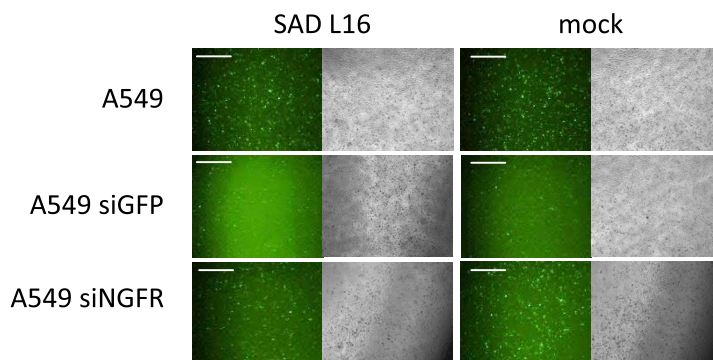

Figure 4: SiRNA expressing cells do not loose knock-down capacity upon infection with RABV.
A549 cells, A549-LR-siGFP cells or A549-LR-siNGFR cells in 6 well plates were transfected with 1 µg of pEGFP-C3. 3 h p.t. the cells were either infected with SAD L16 (MOI=3) or not. 48 h p.t. eGFP expression was monitored by fluorescence microscopy. In A549 siGFP cells significantly less eGFP was expressed independently of infection with RABV. Size bar = 200 µm.

In A549-LR-siGFP cells the expression of GFP was significantly reduced compared to A549 cells and to A549-LR-siNGFR cells. This reduction of the GFP expression was independent of RABV infection.

3.1.2 A miRNA transcribed from a RABV vector is not functional

To check if mRNAs from RABV which are transcribed exclusively in the cytoplasm can be processed either to functional miRNAs or to siRNAs, I created the recombinant RABV SAD G_eGFP-miR23-2 expressing eGFP in an extra ORF between the G and the L gene. The murine cytomegalovirus (MCMV) miRNA miR23-2 sequence is located in the 3'-UTR of the GFP-mRNA. To measure the efficiency of miR23-2 mediated translational inhibition the reporter construct psiCHECK-23-2 was used (Dölken et al., 2010). This construct expresses a firefly luciferase from a simian virus 40 (SV40) early promoter and a *Renilla* luciferase from a Herpes simplex virus (HSV) thymidine kinase (TK) promoter with the target sequence of miR-23-2 in the 3'-UTR of the firefly luciferase gene.

HEK 293T cells in 6 wells were transfected with 50 ng psiCHECK-23-2, and 450 ng pCAGGS. 4 h p.t. the cells were either infected with SAD G_eGFP-mir23-2 or with SAD G_eGFP at an MOI of 3.
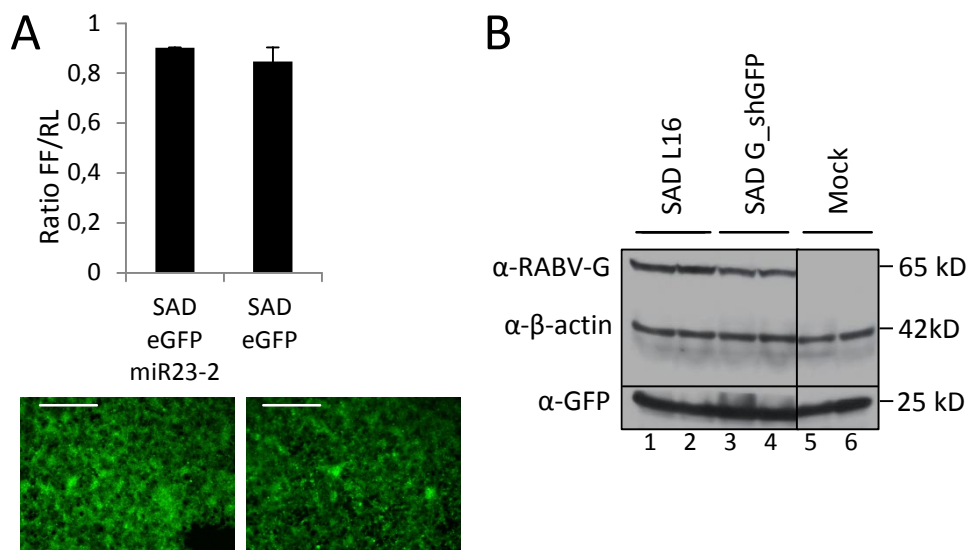

Figure 5: MiRNAs and shRNAs expressed from RABV mRNAs are not functional.
(A) HEK 293T cells in 6 well plates were transfected with 50 ng psiCHECK-23-2 together with 450 ng of pCAGGS. 4 h p.t. the cells were infected with either SAD G_eGFP-miR23-2 or SAD G_eGFP (MOI=3). 48 h p.t. the GFP expression was monitored by fluorescence microscopy. The cells were lysed and dual-luciferase assays were performed. No difference was observed for FF/RL ratios between infections with both viruses. Size bar = 500 µm. (B) HEK 293-GFP cells were infected (MOI=3) with SAD G_shGFP, SAD L16 or uninfected. 48 h p.i. the cells were lysed and Western blots with antibodies against RABV G, β-actin and GFP were performed.

48 h p.t. a dual-luciferase assay was performed to quantify the expression of firefly luciferase and to normalize using *Renilla* luciferase. The firefly luciferase values normalized to the *Renilla* luciferase values indicate the specific knock-down efficiency. As shown in figure 5A

no difference for the firefly luciferase / *Renilla* luciferase ratios was observed between the respective infections. This indicates that SAD G_eGFP-miR23-2 was not able to express functional miRNAs.

Analogously to the MCMV miRNA, the sequence coding for an shRNA against GFP (shGFP) was inserted into the RABV full-length cDNA into the extra transcription unit between the G and the L gene resulting in the construct pSAD G_shGFP. The sequence for the shGFP was the same that is expressed in A549-LR-siGFP cells. From pSAD G_shGFP the recombinant RABV SAD G_shGFP was recovered. HEK 293T-GFP cells, stably expressing eGFP (a kind gift from Dr. Armin Baiker) were infected at an MOI of 3 with SAD G_shGFP, SAD L16, or not infected. 48 h p.i. the cells were lysed and the lysates subjected to Western blot analysis (figure 5B). No difference in eGFP protein levels were detected upon infection with SAD G_shGFP compared to SAD L16 infection or to un-infected cells. Therefore it was concluded, that shGFP expressed as RABV mRNAs are not functional.

This outcome and the results obtained from the RABV encoded MCMV miRNA most likely are due to the cytosolic transcription of the RABV encoded RNAs.

3.1.3   *In vitro*-cleavage of a hammerhead ribozyme

As the cytoplasmic transcription of shGFP from a RABV vector failed to knock down GFP, further possibilities to express shRNAs were evaluated. It is possible, that the cytoplasmic RABV mRNAs cannot efficiently enter the nucleus and therefore are not processed by nucleic enzymes of the miRNA/shRNA pathway. In miRNAs transcribed by Pol-II in the nucleus, the Drosha/DGCR8 microprocessor complex cleaves off the 5'-cap structure and the 3'-poly(A) tail. To compensate this, one approach was to remove flanking sequences from the RABV encoded shRNA by adequate ribozymes.

To cleave off the cap-structure from the shGFP a hammerhead ribozyme (HHRz) sequence was inserted between the RABV transcription start signal and the shGFP. As a control a defect HHRz (dHH), lacking some nucleotides of its stem structure was inserted.

To test the cleavage activity of the HHRz *in vitro*, the RABV full-length cDNA constructs pSAD G_HH-shGFP, pSAD G_dHH-shGFP, and as further controls pSAD G_shGFP and pSAD G_DsRed, with an extra DsRed ORF instead of the hairpin structures in the extra transcription unit, were linearized by restriction with *AflII* and *in vitro*-transcribed.
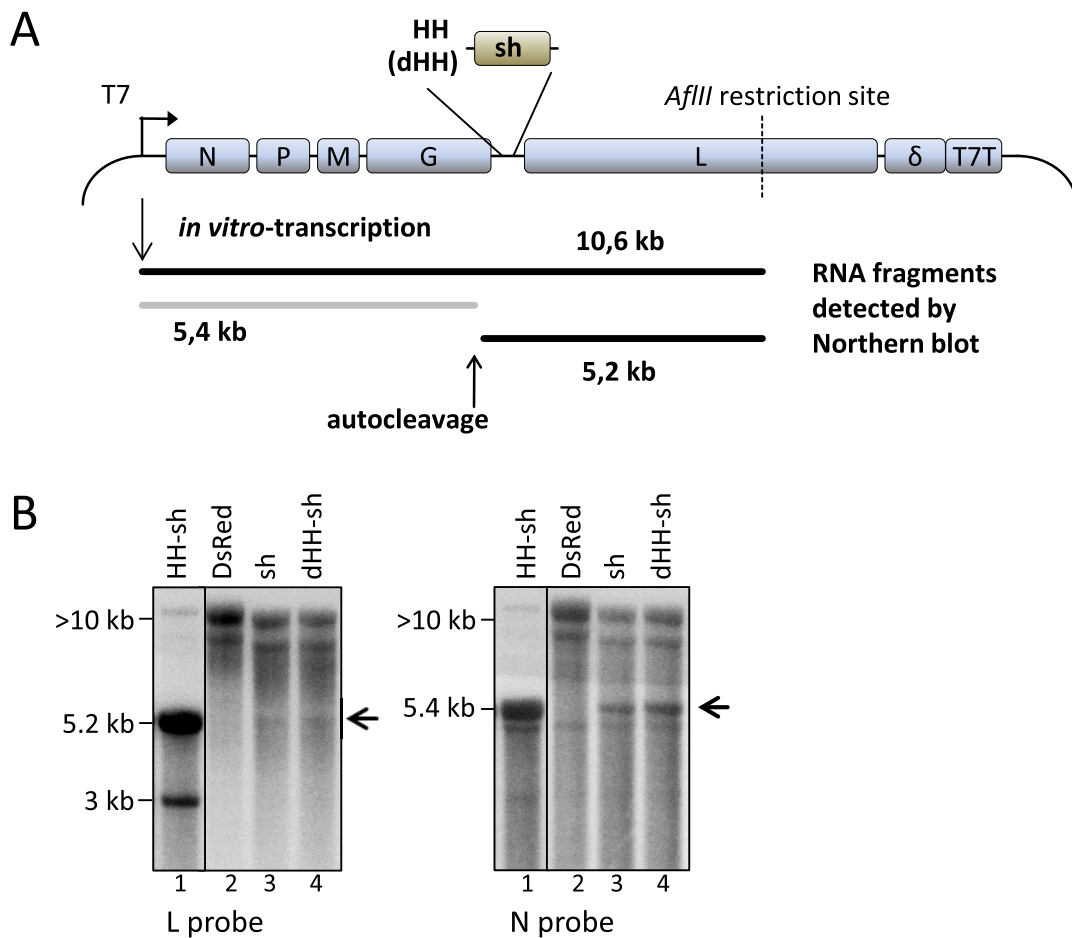
Figure 6: An HHRz in the RABV genome is active *in vitro*.
(A) Sequences coding for either shGFP, HH-shGFP, dHH-shGFP, or DsRed were cloned into an extra transcription unit between the RABV G and the L gene. Plasmids were linearized using the *AflII* restriction site and 1μg of each DNA was *in vitro* transcribed from the T7 promoter. Autocleavage site and resulting fragments are marked. (B) Northern blots of *in vitro*-transcribed RNAs: For each construct 1μg of RNA was loaded to Agarose gels. After transfer membranes were incubated either with an N probe (left side) or an L probe (right side). Arrows indicate expected size of cleavage products.

1 μg of the RNAs was subjected to Northern blot and radioactive labeled probes binding in the RABV N and L gene were used to detect the cleaved and un-cleaved products. As indicated in figure 6A the un-cleaved transcript from the *AflII* digested plasmids should run at 10.6 kb (long black line). If the HHRz cleaves the RNA, a 5.4 kb fragment should be detected with the N probe (short grey line) and a 5.2 kb fragment with the L probe (short black line). Figure 6B shows that the RNA transcribed from the construct pSAD G_HH-shGFP indeed is cleaved as the 5.4 kb fragment (N probe) and the 5.2 kb fragment (L probe), respectively, are detected. For the constructs pSAD G_shGFP and pSAD G_dHH-shGFP, but not for pSAD G_DsRed, a 5.4 kb fragment also is detected with the N probe, but no 5.2 kb

fragment with the L probe. This indicates this fragment to result from premature termination of the *in vitro*-transcription, probably caused by the stem-loop structure of the shGFP. For all full-length constructs a slight band occurs at about 8 kb and is detected with the N and the L probe. This minor product of *in vitro*-transcription can be detected for the cleaved RNA of pSAD G_HH-shGFP with the L probe at 3 kb indicating to originate from premature termination in the L gene. With the N probe the detected cleaved RNA from this minor product is identical to the cleaved major fragment.

3.1.4   *In vitro*-cleavage of HDVagRz

As the shGFP transcribed by RABV is assumed to contain a poly(A) stretch, an option to process the hairpin would be to cleave off unnecessary 3'-sequences by means of an autocatalytic Hepatitis Delta Virus antigenomic ribozyme (HDVagRz).

I inserted the 84 nt HDVagRz sequence (Perrotta and Been, 1991) between the shGFP sequence and the transcription stop signal of the additional shGFP RABV gene to generate the full-length plasmid pSAD G_shGFP-HDV. Analogously the construct pSAD G_HH-shGFP-HDV was generated containing an HHRz to cleave off the cap and an HDVagRz to cleave off the 3'-end from shGFP.

To test for the *in vitro*-cleavage activity, the constructs pSAD G_shGFP-HDV, pSAD G_HH-shGFP-HDV and as a control pSAD L16 were linearized with *MluI* and *in vitro*-transcribed. The RNAs were subjected to Northern blot and radioactively labeled probes were used to detect N, L, or shGFP sequences. Figure 7A shows the expected pattern of fragment sizes. The un-cleaved full-length RNA should run at 8.4 kb. Cleavage products from either the HHRz or the HDVagRz will be detected at 5.4 kb (N probe) or 3 kb (L probe), respectively.

The shGFP probe is a useful tool to distinguish between successful cleavage at the HHRz upstream of shGFP (3 kb) and cleavage at the HDVagRz downstream of shGFP (5.4 kb). If both ribozymes would cleave however, the product is too small for detection in this assay (< 0.1 kb).

The observed outcome of this experiment was that the HDVagRz applied in this construct cleaves RNA with a very poor efficiency (figure 7B). With the L probe, the 3 kb RNA only is detected for pSAD G_HH-shGFP-HDV (left panel - lane 1) but not for pSAD G_shGFP-HDV
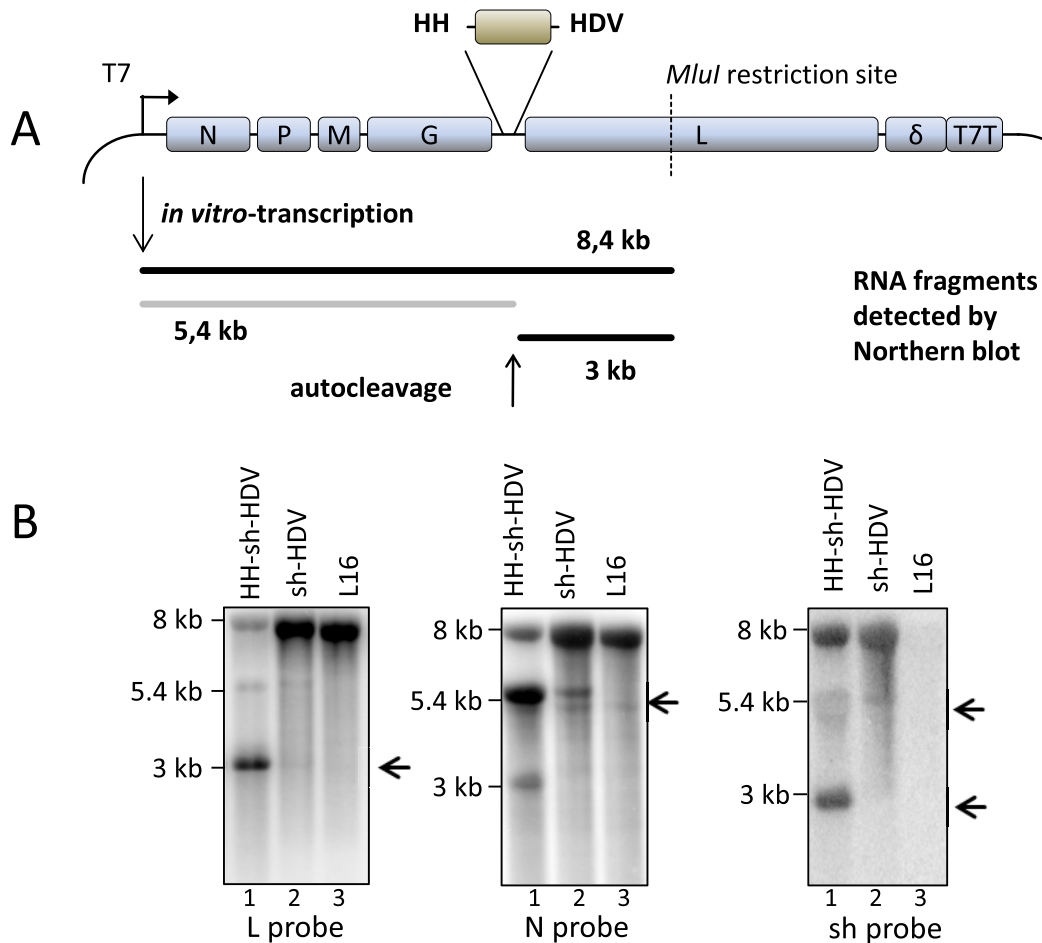
Figure 7: An HDVagRz in the RABV genome cleaves inefficiently *in vitro*.
(A) Sequences coding for either shGFP-HDV or HH-shGFP-HDV were cloned into an extra transcription unit between the G and the L gene. Plasmids were linearized using the *MluI* restriction site and 1µg of each DNA was *in vitro*-transcribed from the T7 promoter. Autocleavage site and resulting fragments are marked. (B) Northern blots of *in vitro*-transcribed RNAs: For each construct 1µg of RNA was loaded to Agarose gels. After transfer membranes were incubated either with an N probe (left side), an L probe (middle) or an shGFP probe(right side). Arrows indicate expected size of cleavage products.

(lane 2). This indicates that only the HHRz but not the HDVagRz was active. The N probe detects the cleaved product at 5.4 kb for pSAD G-HH-shGFP-HDV (middle panel – lane 1). A slight band runs at the same height for pSAD G_shGFP-HDV (lane 2). This may partially result from cleavage, however (as seen in figure 6B), may also result from premature termination of transcription at the shGFP hairpin structure. The shGFP probe at least detects a clear band at 3 kb for pSAD G_HH-shGFP-HDV (right panel – lane 1). This shows that the shGFP sequence is still attached to the HDVagRz and the downstream fragment of the L gene. For the construct pSAD G_shGFP-HDV (lane 2), however, at 5.4 kb only a slight band is visible over background, again showing poor cleavage.

3.1.5 HDVagRz sequences with improved cleavage activity

As the HDVagRz was shown to cleave with very poor efficiency, literature was searched for different ribozyme sequences. More recent publications showed that better cleaving HDVagRzs contained some bases more from the Hepatitis Delta Virus anti-genome than the initially prescribed HDVagRz. Also the exchange of certain nucleotides resulted in better cleavage. I picked two new sequences from the literature and labeled them as Supercut 1 (SC1) (from (Wadkins and Been, 2002)) and Supercut 2 (SC2) (from (Been and Wickham, 1997)). In contrast the "old" HDVagRz was labeled HDV. The sequences are shown in figure 8A.
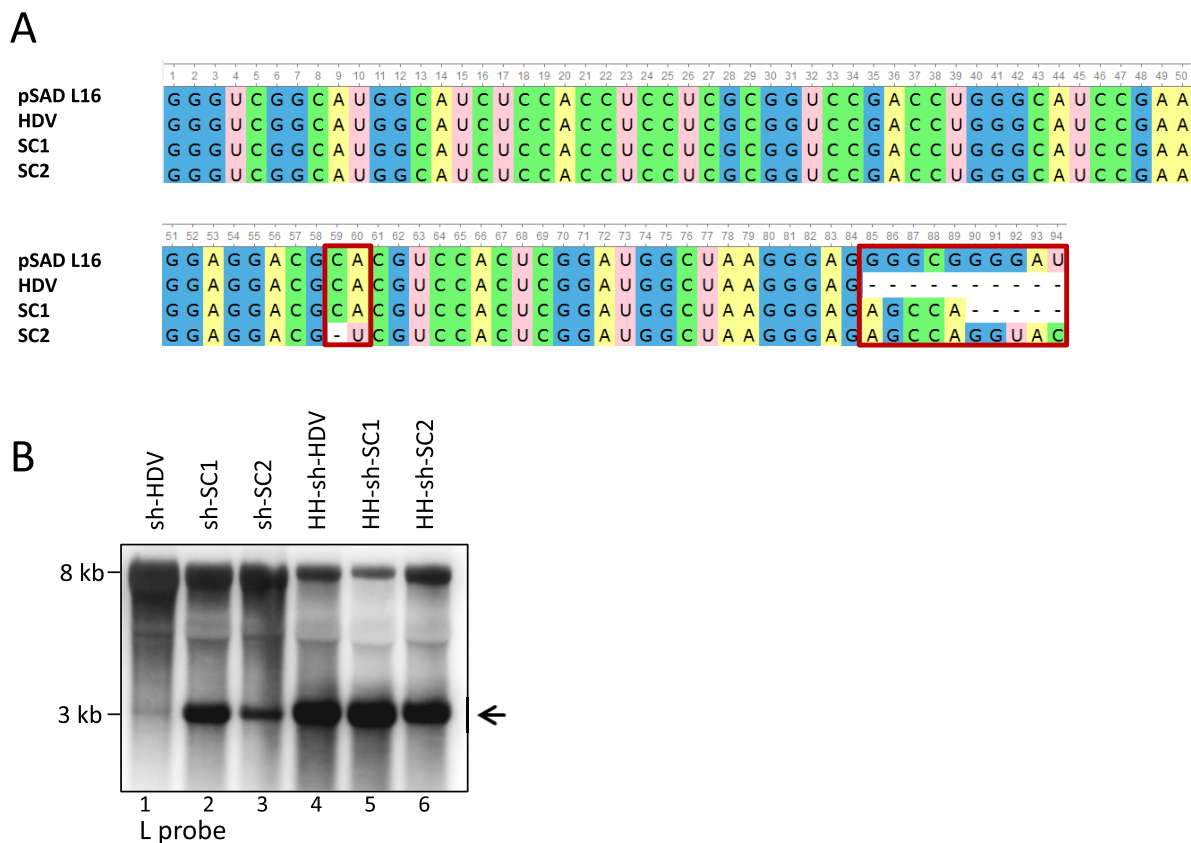
Figure 8: Alternative HDVagRzs with better cleavage activity.
(A) Alignment of different HDVagRz RNAs abbreviated as HDV, SC1 and SC2. pSAD L16 illustrates flanking sequences in full-length RABV constructs. Software: Ugene (Unipro) B) Plasmids pSAD sh-HDV, pSAD sh-SC1, pSAD sh-SC2, pSAD HH-sh-HDV, pSAD HH-sh-SC1 and pSAD HH-sh-SC2 were linearized with *MluI* and 1 µg of each DNA was used for *in vitro*-transcription. 1 µg *in vitro*-transcribed RNA was used for Northern blots and fragments detected with radioactively labeled probes against L. Arrow indicates expected size of cleavage products.

By inserting the new HDVagRz sequences into the full-length cDNA clones the constructs pSAD G_shGFP-SC1, pSAD G_shGFP-SC2 together with pSAD G_HH-shGFP-SC1 and pSAD G_HH-shGFP-SC2 were generated. Linearization of these four plasmids, together with pSAD

G_shGFP-HDV and pSAD G_HH-shGFP-HDV, was performed with *MluI* followed by a Northern blot. For detection of cleaved and un-cleaved RNAs an L probe was used. Again it is shown that the RNA derived from pSAD G_shGFP-HDV is not cleaved, or at least very inefficiently (figure 8B - lane 1). The new HDVagRzs, SC1 and SC2, however, cleave the RNA at significant higher rates (lanes 2 and 3). SC1 shows the most efficient cleavage pattern. They were not only functional alone, but also in combination with the HHRz (compare lanes 2 and 3 with 5 and 6).

3.1.6 No knock-down for virus derived shRNAs lacking 5'-cap and 3'-poly(A)

The HHRz and SC1 were shown to cleave efficiently *in vitro*. Initially, the virus SAD G_HH-shGFP-SC1, unlike SAD G_HH-shGFP, could not be rescued after numerous trials. This indicates a strong *in vivo*-activity of the SC1. In part 3.2 of this thesis a significantly improved rescue system of RABV is described (Ghanem et al., 2012). This improved method finally allowed the successful recovery of SAD G_HH-shGFP-SC1 from cDNA. This virus should transcribe an mRNA from which the 5'-cap and the 3'-poly(A) are cleaved off by auto-processive ribozymes.
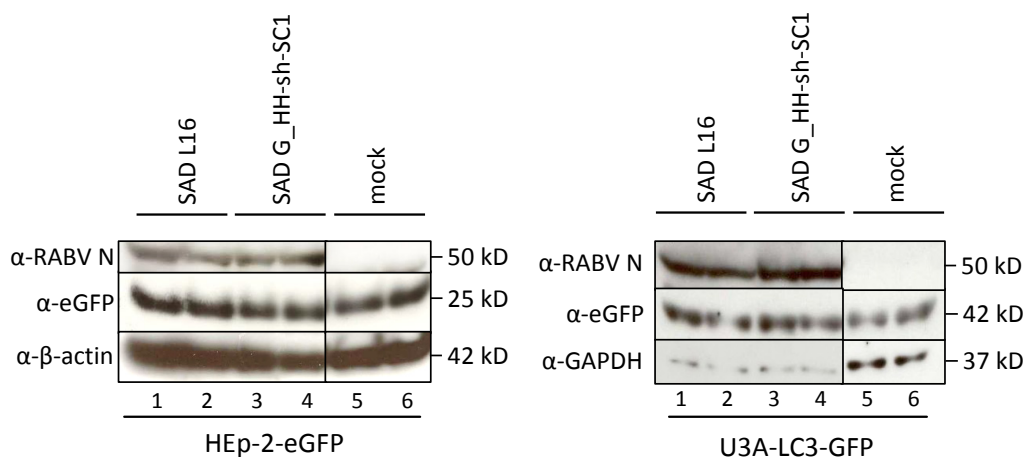
Figure 9: No knock-down of eGFP by SAD G_HH-shGFP-SC1.
Hep2-eGFP cells (left) or U3A LC3-GFP cells (right) were infected with SAD L16, SAD G_HH-shGFP-SC1 (MOI=3) or not infected. 60 h p.i. cells were lysed. Western blots with antibodies against RABV N, eGFP and β-actin (left) or GAPDH (right) were performed.

To check if SAD G_HH-shGFP-SC1 was able to knock-down eGFP expression SAD L16, SAD G_HH-shGFP-SC1 (MOI=3) or no virus were used to infect either HEp-2-GFP cells or U3A LC3-GFP cells. 60 h p.i. the cells were lysed and Western blots were performed. Using antibodies

against RABV N, eGFP and β-actin or GAPDH, respectively for normalization, protein levels could be compared.

No significant difference in eGFP or LC3-GFP expression levels was found between SAD L16 and SAD G_HH-shGFP-SC1 (figure 9). The same was true when eGFP expressing plasmids pEGFP-C3 or pCAGGS-GFP were transfected into different cell lines HEK 293T, NA or Huh7.5 prior to infection with SAD G_HH-shGFP-SC1 (data not shown).

3.1.7   *In silico*-design of the "perfectly processed" hairpin

In the virus SAD G_HH-shGFP-SC1 the HHRz and the SC1 were inserted with spacer sequences to reduce interference with the hairpin structure of shGFP. The RNAs expected to be made and processed were lacking 5'-cap and 3'-poly(A), however resemble more the pre-miRNAs that have to be processed by the Drosha/DCGR8 complex in the nucleus. In order to process a shGFP RNA resembling a direct Dicer substrate in the cytosol, these spacer sequences had to be removed. As RNA structures are present and functionally important in both ribozymes and in the shGFP sequence I wanted to evaluate the impact of these structures on each other. Therefore RNA secondary structure predictions were performed.

Sequences of interest were submitted to the RNAfold software on the Vienna RNA server homepage (http://rna.tbi.univie.ac.at/cgi-bin/RNAfold.cgi). The graphical output, as seen in figure 10, indicates the base pair probabiblity for each position. The results were crosschecked with the Software DNAMAN 6.0 (Lynnon Corporation) and the embedded function "secondary structure prediction", coming to similar results (data not shown).

Correct folding of the HHRz (figure 10A-I) is dependent on the stem loop formation. The secondary structure nicely indicates the special position of the C, after which the autocatalytic cleavage occurs (arrow). In order to process a correct 5'-end of the shGFP (figure 10A-II), the first four bases of the shGFP have to be identical with the four 3'-bases of the HHRz that are building the stem (blue line). However, upon direct linkage of the HHRz with the shGFP (figure 10A-III) the structure prediction shows that the stem and thereby the HHRz folding are impaired. Thermodynamic stability rather provides the folding of the longer stem within the shGFP than the four base pair stem of the HHRz. A two base pair mismatch at the 3'-end of the shGFP (figure 10A-IV), i.e. CC instead of GU (bold black circle), moves the equilibrium towards favoring the HHRz stem folding (thin black circle) over the shGFP

mismatch folding (V). This secondary structure prediction indicates a 2 base pair mismatch to restore correct folding and thereby cleavage activity of the HHRz.
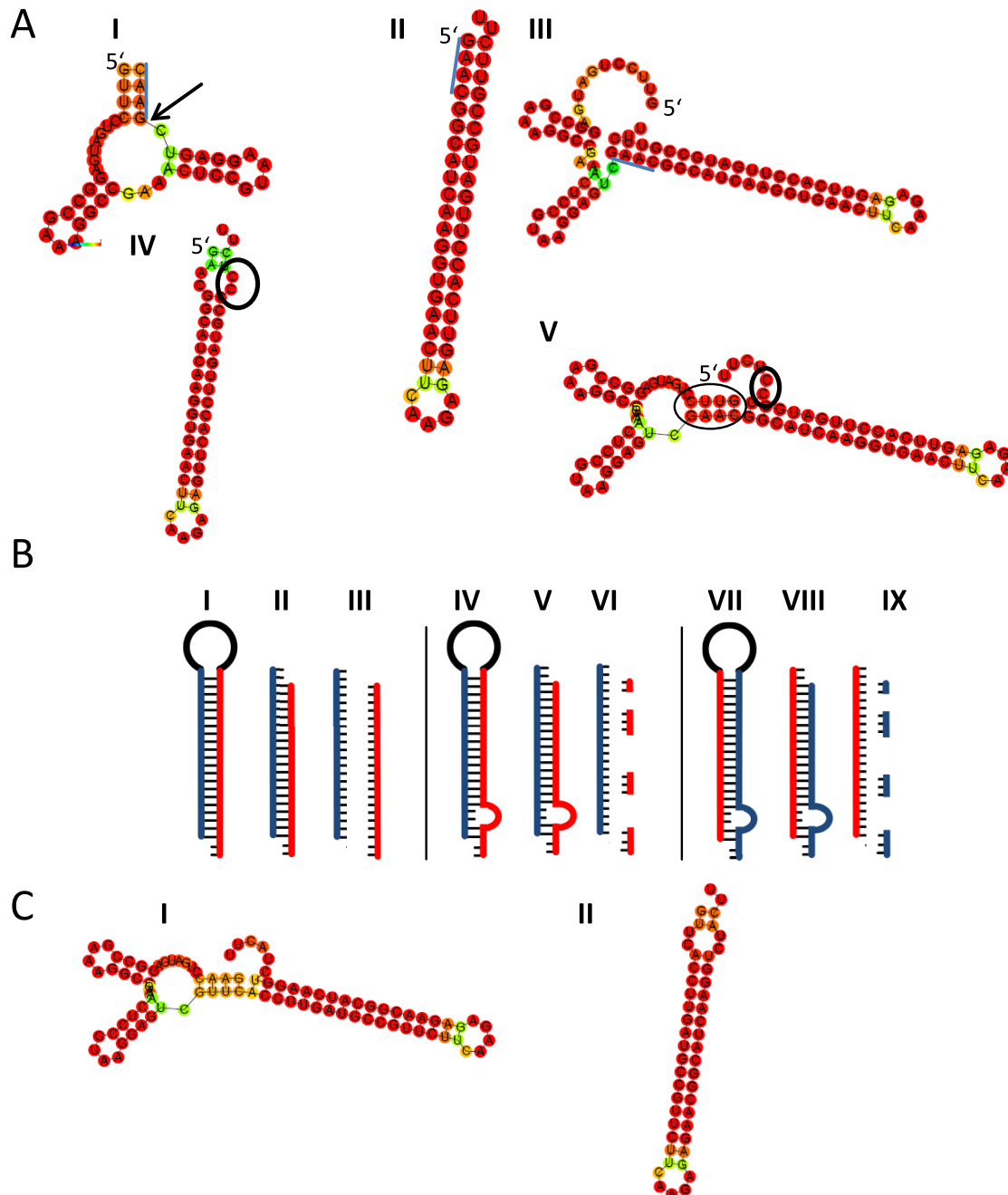
Figure 10: *In silico*-design of the "perfectly processed" hairpin.
(A) Secondary structure predictions by the Vienna RNA server. I: HHRz, II: SH, shGFP with "perfectly processed" ends, III: HH-SH without spacer, note that the HHRz does not fold correctly, IV: SHmm - shGFP with a CC mismatch, V: HH-SHmm, the mismatch rescues the correct fold of the HHRz. Arrow indicates cleavage site of HHRz. The blue line marks the sequence of the shGFP 5'-end that is part of the HHRz stem.(B) Theoretical thoughts on hairpin design according to Schwarz et al. (Cell, 2003). If a short hairpin RNA (I) is processed by Dicer into a dsRNA (II) one of the two strands (III) is preferably incorcoprated into RISC, the one that is unwinded more easily from its 5'-end. For SHmm the antisense strand would be degraded (IV-VI). For HSmm the antisense strand would be incorporated into RISC (VII-IX). (C)I: HH-HSmm, sense and antisense strand are interchanged, II: HSmm after processing by the HHRz.

If shGFP (figure 10B-I) now is the correct substrate for Dicer, the cleavage products would be two annealed complementary single stranded RNAs (figure 10B-II). One of these strands will be incorporated into the RISC complex and induce knock-down of the target gene (figure 10B-III). The antisense strand is shown in red here and if incorporated into RISC can base-pair with its target, the GFP mRNA.

In a work published by D. S. Schwarz et al. (Schwarz et al., 2003) it is shown that the strand that can be un-winded easier from its 5'-end will be incorporated into RISC whereas the other strand will be degraded.

The introduction of the 2 base mismatches at the 3'-end of the shGFP (SHmm) (figure 10B-IV-VI) would therefore lead to incorporation of the sense strand (blue) and the degradation of the antisense strand. The same outcome would result from introduction of the mismatches at the 5'-end of the shGFP.

To overcome this problem, I exchanged the sense and the antisense strand of the shGFP (figure 10B-VI). The new hairpin, labeled HSmm, in contrast to SHmm, has the mismatch at the 3'-end of the hairpin (and the 5'-end of the antisense strand after Dicer cleavage) and thus should allow the antisense strand to enter the RISC (figure 10B-VII-IX). Secondary structure prediction also indicates that the HHRz is processive in the construct HHRz-HSmm (figure 10C-I) and should release the "perfectly processed" hairpin HSmm (figure 10C-II).

3.1.8   *In vitro*-analysis of the "perfectly processed" hairpin

To test if the cleavage activities of the two ribozymes in close proximity to the hairpin correlate to their predicted secondary structures the *in vitro*-cleavage assay was applied again. I generated the construct pSAD G_HH-SH-SC1, for which the 2D structure predicted a wrong folding of the HHRz (compare figure 10A-III). To distinguish the cleavage of HHRz and SC1, also constructs with a defect HHRz (dHH), lacking the first 21 nt of the HHRz, a defect HDVagRz (dHDV), lacking 57 nt of the 3'-end, or with both dHH and dHDV were generated. Similarly, the plasmid pSAD G_HH-HSmm_SC1 together with the controls containing dHH, dHDV, or both, were constructed. The mismatches in HSmm were predicted to allow the correct folding of the HHRz (compare figure 10A-VI). The eight plasmids pSAD G_HH-SH-SC1, pSAD G_dHH-SH-SC1, pSAD G_HH-SH-dHDV, pSAD G_dHH-SH-dHDV, pSAD G_HH-HSmm-SC1, pSAD G_dHH-HSmm-SC1, pSAD G_HH-HSmm-dHDV, and pSAD G_dHH-HSmm-dHDV

were linearized with *MluI* and after *in vitro*-transcription a Northern blot with an L probe was performed.

The RNAs derived from pSAD G_dHH_SH_dHDV (figure 11 - lane 1) and from pSAD G_dHH-HSmm-dHDV (lane 5), were not cleaved, as they contained only defect ribozymes. RNAs from pSAD G_dHH-SH-SC1 (lane 3) and pSAD G_dHH-HSmm-SC1 (lane 7), showed the cleavage product at 3 kb. This indicates that the SC1 can cleave efficiently and seems not to be disturbed by either of the secondary hairpin structures. The RNA derived from pSAD G_HH-SH-dHDV (lane 2), however is not cleaved. This correlates with the prediction, in which the HHRz cannot fold correctly in close proximity to the SH hairpin. The two mismatches in the reverse complement hairpin however rescue the cleavage activity of the HHRz (lane 6). Again this is in accordance with the *in silico*-predictions.
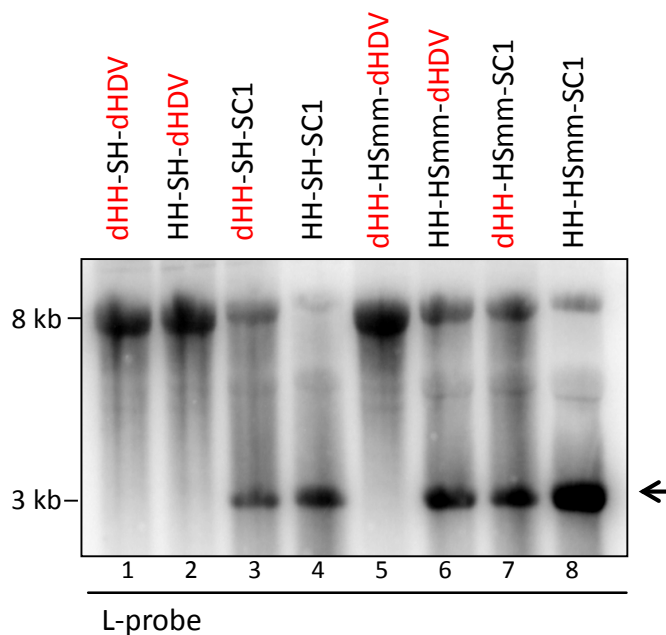
Figure 11: *In vitro*-verification of the secondary structure predictions.
Plasmids pSAD G_dHH-SH-dHDV, pSAD G_HH-SH-dHDV, pSAD G_dHH-SH-SC1, pSAD G_HH-SH-SC1, pSAD G_dHH-HSmm-dHDV, pSAD G_HH-HSmm-dHDV, pSAD G_dHH-HSmm-SC1 and pSAD G_HH-HSmm-SC1 were linearized with *MluI* and 1 µg of each DNA was used for *in vitro*-transcription. 1 µg *in vitro*-transcribed RNA was used for Northern blots and fragments detected with radioactively labeled probes against L. Arrow indicates expected size of cleavage products.

Noteworthy, the RNA from pSAD G_HH-SH-SC1 (lane 4) appears to be cleaved more efficient as the RNA from pSAD G_dHH-SH-SC1 (lane 3). While the same amount of cleaved fragment is detected for both, in lane 4 less un-cleaved fragment remains. In lane 8, the RNA derived from pSAD G_HH-HSmm-SC1 shows the strongest band for the cleaved product. Being about

twice as strong as in lane 7 where only the SC1 is functional, this indicates the activity of both ribozymes.

3.1.9 No knock-down effect for RABV vector delivered siRNAs

The full-length cDNAs tested in the *in vitro*-cleavage assay above were used to recover recombinant viruses. Again these viruses only could be rescued after significant improvement of the rescue system described in part 3.2 of this thesis.
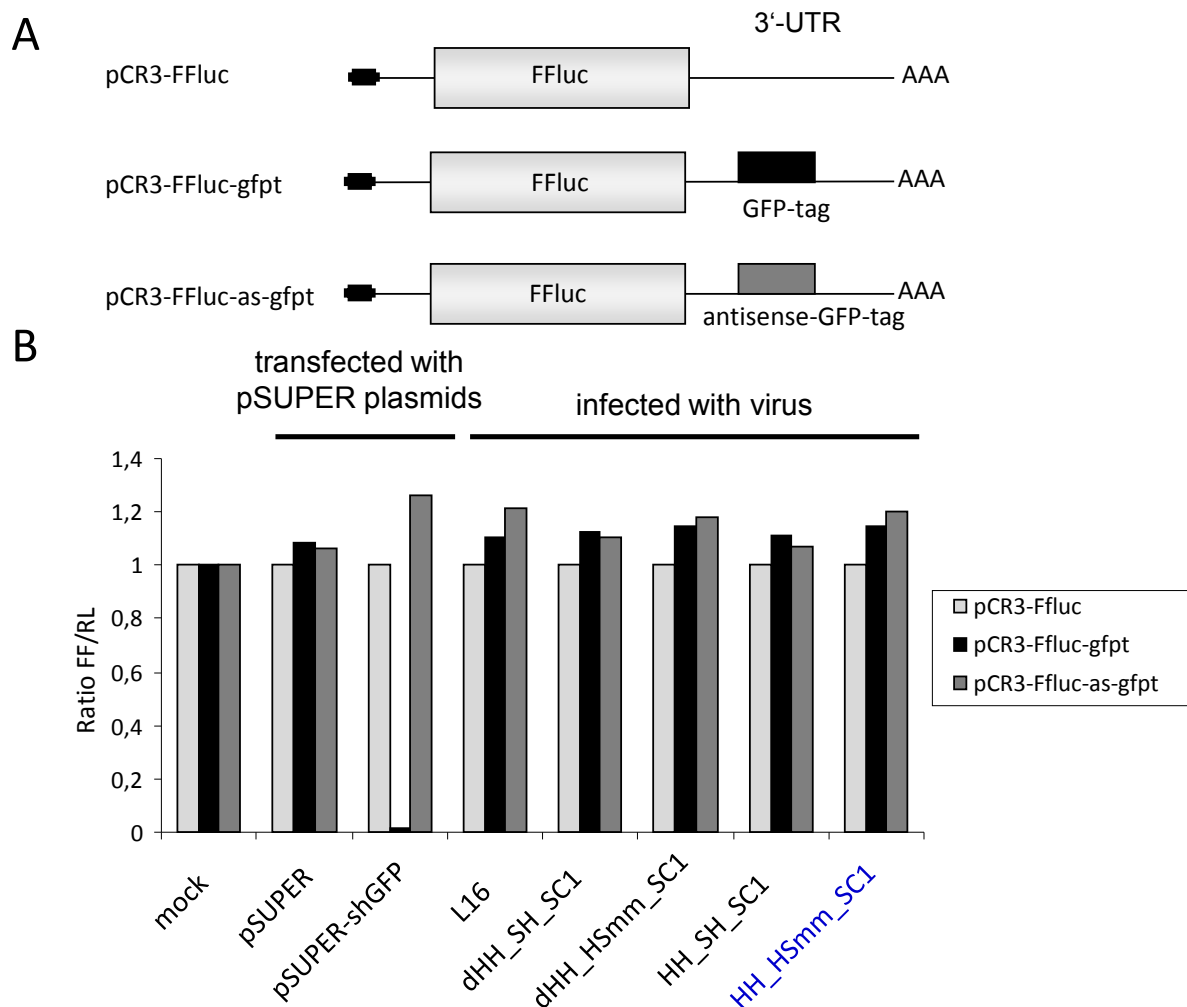
Figure 12: No knock-down effect for RABV vector delivered siRNAs.
(A) Reporter construct were either pCR3-FFluc coding for the firefly luciferase, pCR3-FFluc-gfpt, having the GFP sense target sequence of shGFP in the 3'-UTR or pCR3-FFluc-asgfpt having the reverse complement GFP target sequence in the 3'-UTR. (B) HEK 293T cells in 12 wells were transfected with 100 ng of either pCR3-FFluc, pCR3-FFluc-gfpt or pCR3-FFluc-asgfpt. 10 ng pRL-CMV for normalization and 90 ng pCAGGS were co-transfected. 4 h p.t. cells were either transfected with 250 ng pSUPER or pSUPER-shGFP, or infected with either SAD L16, SAD G_dHH-SH-SC1, SAD G_dHH-HSmm-SC1, SAD G_HH-SH-SC1 or SAD G_HH-HSmm-SC1 (MOI=2). 48 h p.i. dual luciferase assays were performed.

To test if the newly made viruses were able to knock down a target gene, and in order to quantify the knock-down effect, a luciferase based reporter system was developed. I

inserted either a GFP-tag or as a control an antisense GFP-tag into the 3'-UTR of the firefly luciferase expression unit in the CMV promoter-driven pCR3-FFluc. The GFP-tag contained the sequence of the sense strand of the hairpin and in sense orientation compared to the eGFP mRNA, enabling the correct hairpin to knock down firefly luciferase expression (figure 12A).

HEK 293T cells were transfected with 100 ng of pCR3-FFluc, pCR3-FFluc-gfpt or pCR3-FFluc-asgfpt. For normalization 10 ng of pRL-CMV were co-transfected. 4 h p.t. the cells were either transfected with 1 µg of pSUPER-shGFP or as a control pSUPER (Brummelkamp et al., 2002). The plasmid pSUPER allows Pol-III dependent transcription of the hairpin in the nucleus and the transcript can enter the miRNA microprocessor pathway (Drosha/DGCR8 dependent). In parallel other HEK 293T cells were infected with SAD L16, SAD G_HH-HSmm-SC or as controls with SAD G_dHH-HSmm-SC, SAD G_HH-SH-SC or SAD G_dHH-SH-SC (MOI = 3) 4 h p.t. with the respective luciferase reporter plasmids. 48 h p.t. the cells were lysed and dual-luciferase assays were performed in order to measure firefly and *Renilla* luciferase expression.

The plasmid pSUPER-shGFP that was used as a positive control was able to decrease the firefly luciferase expression from the construct with the sense GFP target region, by more than 95 % (figure 12B). In contrast, the viruses, including SAD G_HH-HSmm-SC, did not have any effects on the luciferase expression. No knock-down was observed.

3.1.10 Low amounts of RNA of shGFP

As no knock-down was observed in SAD G_HH-HSmm-SC infected cells it should be tested, if the HSmm hairpin is transcribed and processed upon virus infection.

Therefore at first, NA cells were infected with SAD G_HH-HSmm-SC, SAD G_shGFP, SAD L16 (MOI = 5) or mock-infected. Cells were lysed 48 h p.i. and RNA was isolated using Trizol. For comparison, 14.5 cm dishes of HEK 293T cells were transfected with 20 µg pSUPER-shGFP or pSUPER. In addition A549-LR-siGFP cells an as controls A549 cells were seeded into 14.5 cm dishes. The transfected HEK 293T cells together with un-treated A549 cells and A549-siGFP cells were lysed 48 h p.t or 60 h after seeded into dishes, respectively. A miRNA Northern blot was performed using a probe against shGFP.

In figure 13 the positive control pSUPER-shGFP shows two prominent bands (left panel - lane 1). The upper one most probably corresponds to the shRNA transcribed from the Pol-III promoter of pSUPER, whereas the lower band is the product after Dicer cleavage. The A549-siGFP cells as a stable cell line have much lower levels of the transcript (lane 4). Here only the lower band is detected as presumably all precursor (left thin circle) is cleaved by Dicer. In cells infected with SAD G_HH-HSmm-SC (left panel - lane 8), neither the precursor (right thin circle) nor the product is visible. However the precursor can be detected after longer exposure of the phosphor-screen with the radioactively labeled membrane (right panel - lane 8). Two larger bands are prominent for this construct which should be smaller than mRNAs that restricted by their size cannot enter the denaturing 8 M urea and 15 % PAA gel (compare left panel - lane 8 and lane 7). Most probably these bands reflect intermediate RNAs in which only one of the ribozymes was active.
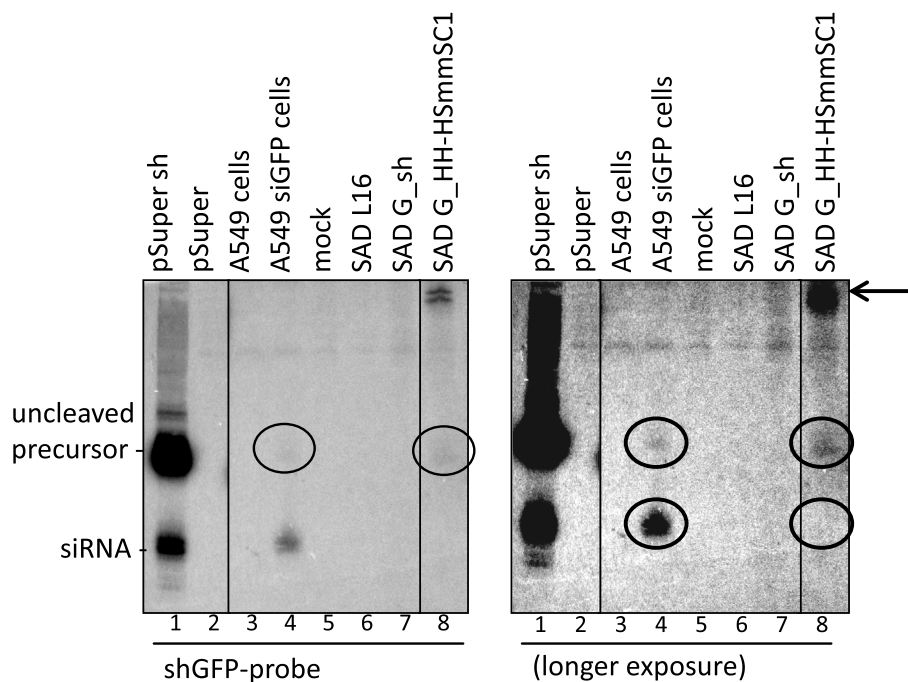
Figure 13: Northern blot reveals low amounts of RNA of shGFP.
MiRNA Northern blots: 15 % UREA-PAGE gels were loaded with 30 μg RNA from HEK 293T cells transfected with pSUPER-shGFP (lane 1) or untransfected (lane 2), A549 cells (lane 3), A549 siGFP cells (lane 4), NA cells (lane 5), or NA cells infected with SAD L16 (lane 6), SAD G_shGFP (lane 7) and SAD G_HH-HSmm-SC1 (lane 8) (MOI=5). DNA oligonucleotides with the shGFP target region were 5'-labeled using γ-ATP-32 and used to detect small RNA fragments after transfer to a nylon membrane. (right side: longer exposure).

3.2 Improved rescue for rabies virus

In the previous experiments a poor cleavage activity of HDV was observed. As this is also the ribozyme that is used during RABV rescue from recombinant cDNA to generate exact 3'-ends of the antigenome-like RNA, also rather inefficient cleavage can be assumed. Therefore, the aim was to evaluate if this indeed is the case and if so, to replace HDV with the better cleaving SC1.

The results shown in this part have been published in (Ghanem et al., 2012) and figures are adpted from the publication.

3.2.1 HDVagRz poorly processes the 3'-end of antigenome-like RNA

To test the cleavage activity of HDV downstream of the trailer of the full-length RABV RNA a smaller construct, pSDI-1 (Conzelmann and Schnell, 1994) was used.

In this construct (figure 14A) in contrast to the full-length RABV antigenome-like transcript, the trailer is at the 5'-end and the leader at the 3'-end. Due to the terminal complementary of RABV genomes, the 10 nts directly upstream of the HDV sequence, however, are identical.
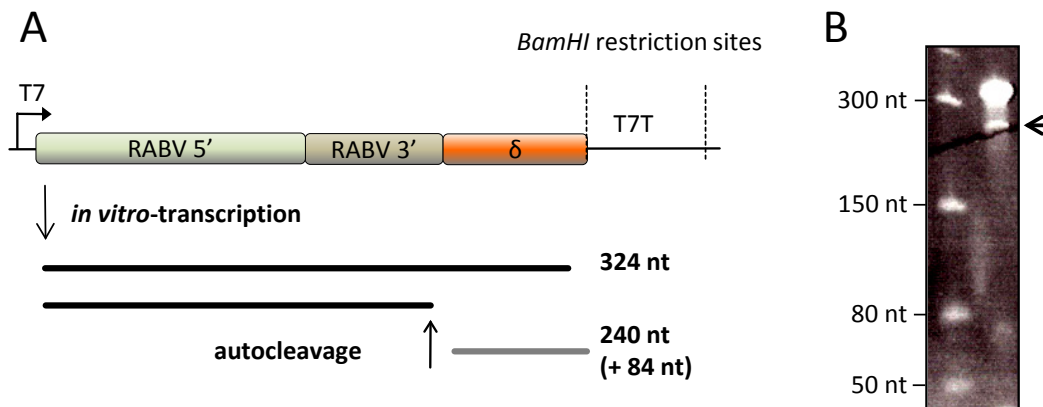
Figure 14: Poor cleavage of HDVagRz in processing the 3'-end of the RABV antigenome-like RNAs.
(adapted from Ghanem et al., 2012) (A) Plasmid pSDI-1 (Conzelmann and Schnell, JVI, 1994) was linearized using BamHI and *in vitro*-transcribed. Site of autocleavage and expected fragments are marked. (B) 1 µg RNA was loaded to a 10% UREA-PAA gel and stained using EtBr. Arrow indicates expected size of cleavage product.

The plasmid pSDI-1 was linearized with a *BamHI* digestion, cutting directly 3' of the HDV sequence. Following *in vitro*-transcription, the RNA was subjected to urea-PAA gel electrophoresis and bands were stained with EthBr (figure 14B). The un-cleaved RNA should run at about 320 nt and if the ribozyme cleaves off itself the band should run at 240 nt as indicated by the arrow. Only about 10 % of the RNA was cleaved. This result correlates with

the poor cleavage of the HDV located within the genomic RNA that was observed previously (→3.1.4).

3.2.2   Improved HDVagRz SC1 enhances rescue efficiency

A correctly processed 3'-end has been shown to be necessary for rescue of NNSV. As we found the ribozyme downstream of the trailer to cleave poorly, it was close at hand to replace the inefficient ribozyme by a better one.

I replaced the HDV sequence in the plasmid pSAD L16 with the SC1 sequence (→3.1.5). Thereby the construct pSAD L16_SC was generated (figure 15A).
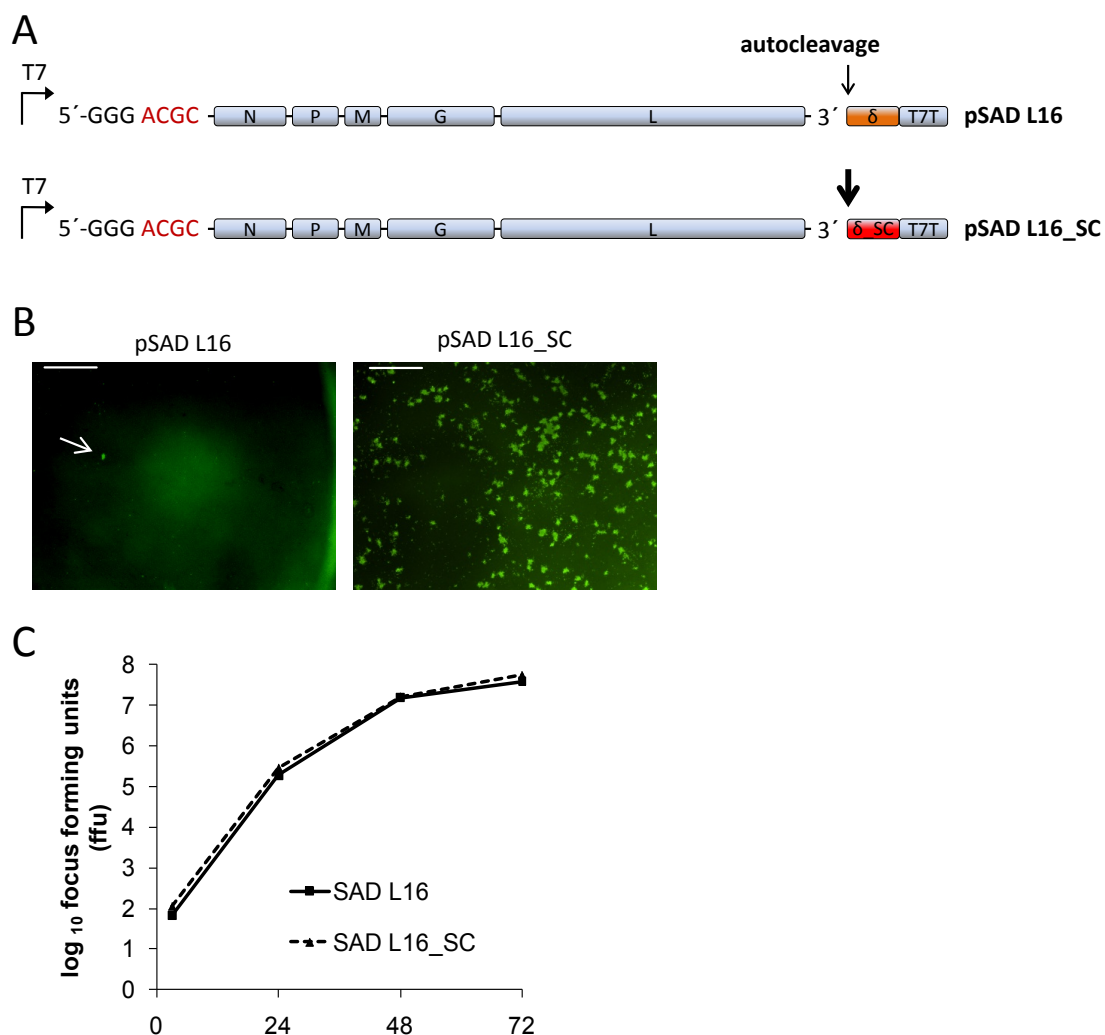
Figure 15: Replacement of HDV by SC1 enhances rescue efficiency.
(adapted from Ghanem et al., 2012) (A) Constructs pSAD L16 and pSAD L16_SC differ in their ribozymes processing the viral 3'-end. (B) FITC-α-RABV-N staining of BSR-T7/5 cells incubated for 3 d with supernatants taken 3 d after transfection of BSR-T7/5 cells with either 10 µg pSAD L16 or 10 µg pSAD L16_SC together with pTIT-N (5 µg), pTIT-P (2.5 µg) and pTIT-L (2.5 µg). Size bar = 1 mm. (C) Multistep growth curve with recombinant SAD L16 rescued from plasmid pSAD L16 or from plasmid pSAD L16_SC.

Rescue experiments were performed with both constructs pSAD L16 and pSAD L16_SC, in parallel and 3 d later the supernatants were passaged onto fresh cells. Following 3 d incubation at standard conditions, the cells of the supernatant passage were stained with a FITC-labeled RABV N antibody (figure 15B). While rescue of both constructs was successful, significantly more foci derived from infectious particles were detected in the passages from pSAD L16_SC.

To show, that the increase in rescue efficiency was not due to a difference within the virus genome, supernatants from both rescue attempts, with pSAD L16 and pSAD L16_SC, were used to inoculate fresh cells and virus stocks were prepared. Both virus stocks were subjected to multistep growth curve experiments (figure 15C). As the improved ribozyme SC1, as well as the standard HDV, cleave themselves off the 3'-end of the RABV antigenome-like RNA, the processed and rescued virus genomes are identical. Therefore it is not surprising that the 2 viruses are indistinguishable from their growth kinetics.

3.2.3 Significantly improved rescue with HHRz and HDVagRz SC1

The 5'-ends have been reported to be less critical for rescue of rhabdoviruses (Pattnaik et al., 1992), MeV and BDV (Martin et al., 2006). However, exact 5'-ends have been shown to improve rescue of measles virus, BDV (Martin et al., 2006) and RABV minigenomes (Le Mercier et al., 2002).

The standard full-length construct pSAD L16 contains three additional G residues upstream of the first nt of the RABV antigenome (figure 16A). As these Gs are important for efficient T7-pol transcription initiation, an HHRz was inserted between the three Gs and the RABV genome. As the HHRz cleaves itself off, 3' of a C residue, and releases part of its stem attached to downstream sequences, the first four bases of the RABV genome now have to be part of this stem and the 5'-end of the HHRz has to be changed accordingly (figure 16B).

Full-length constructs were made with or without the HHRz to process the virus 5'-end and with HDV or with the SC1 for improved processing of the 3'-end. For better quantification of the recue efficiencies a GFP gene was inserted as an extra transcription unit between the G and the L gene (figure 16A).

Standard rescue transfections were performed for the constructs pSAD GFP, pSAD GFP_SC, pSAD T7-HH_GFP and pSAD T7-HH_GFP_SC. The expression of GFP was followed live under

UV light microscopy. Every upcoming focus of eGFP-expressing cells was considered to be a positive rescue event. The SC1 improved the rescue efficiency as well as the speed of rescue significantly compared to the conventional HDV (figure 16C). The same was true for the HHRz that was processing the 5'-end in comparison to only the T7 promoter followed by the 3 G residues. Combining both, the HHRz and the SC1, resulted in synergistically increased rescue.
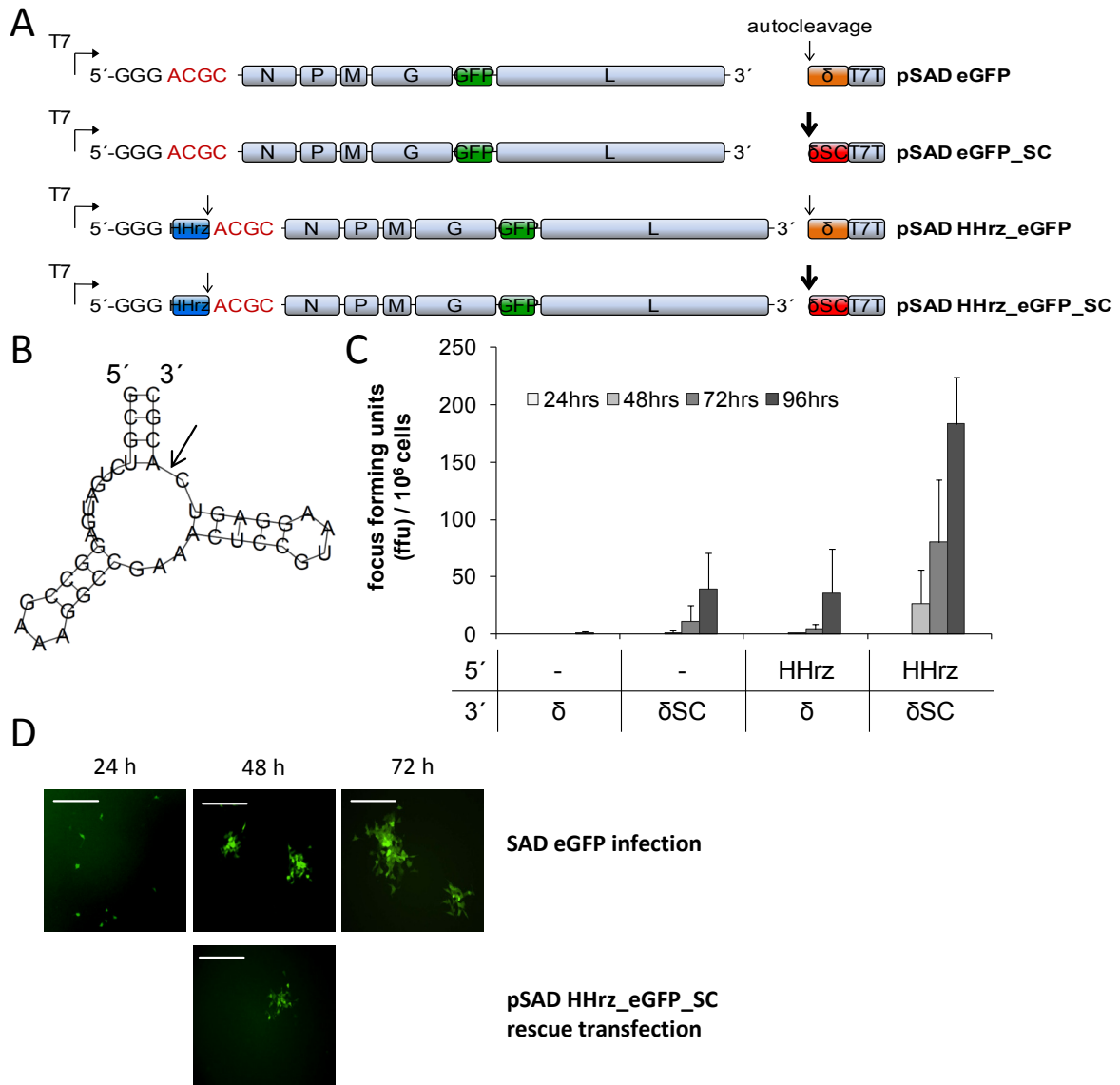
Figure 16: Significantly improved rescue with HHRz and HDVagRz_SC.
(adapted from Ghanem et al., 2012) (A) Constructs for quantification of rescue efficiency: pSAD eGFP, pSAD eGFP_SC, pSAD HHRz_eGFP and pSAD HHRz_eGFP_SC. (B) Design of HHRz with RABV starting nts ACGC as part of its stem. (C) BSR-T7/5 cells were transfected with 10 μg of either pSAD eGFP, pSAD eGFP_SC, pSAD HHRz_eGFP or pSAD HHRz_eGFP_SC together with 5 μg pTIT-N, 2.5 μg pTIT-P and 2.5 μg pTIT-L. Fluorescence microscopy was used to detect successful rescue events by means of eGFP expression in living cells. (D) upper row: GFP positive foci in BSR-T7/5 cells infected with SAD eGFP at different time points post infection. Lower: size of detected focus in rescue experiments with pSAD HHRz_eGFP_SC 48 h p.t. The same size as a focus 48 h p.i. indicates an immediate rescue event within the first few hours upon transfection. Size bar = 100 μm.

As by counting GFP positive foci each rescue event was detected only after a certain lag of time, because the first rescued virus already had to spread to the neighboring cells, an indirect method was applied to determine the time point of these rescue events. BSR T7/5 cells in BSR 6-well plates were infected with a low MOI (0.001) of SAD GFP virus. At 24, 48, and 72 h p.i. pictures of GFP positive cells were taken under UV light to set up a standard by which the size of a focus allowed to determine its age (figure 16D). The biggest foci detected in the positive rescues of pSAD T7-HH_GFP_SC at 48 h p.t. corresponded in their size to foci derived from infection with SAD GFP 48 h p.i. This indicates that the first rescue events must have happened almost instantly – or within a time frame of a few h – after transfection.

3.2.4   Increased minigenome activity due to ribozymes

Minigenomes of the RABV strain PV (Le Mercier et al., 2002) in an expression cassette between an HHRz and an HDVagRz were reported to have an increase in reporter gene expression compared to minigenomes with only the HDVagRz. To test if the same is true for SAD L16 derived minigenomes, we applied the previously described pSDI CNPL (Finke and Conzelmann, 1999). This bicistronic construct encodes a T7-pol-driven negative sense RNA. Within the 5'-end (trailer region) and the 3'-end (leader region) the minigenome contains two negative sense transcription units for CAT and firefly luciferase, separated by the RABV N/P gene border. Following transcription from the T7 promoter the 3'-end is processed by the HDV.

In analogy to the RABV full-length constructs, the HHRz was inserted between the 3 G residues downstream of the T7 promoter in order to cleave upstream of the first nt of the minigenome. The HDV was replaced by the better cleaving SC1.

Standard transfections for minigenome assays were performed with either the parental pSDI CNPL or pSDI T7-HH_CNPL_SC together with the N, P, and L "helper"-plasmids. For normalization of transfection pCMV-RL was co-transfected. As negative controls N was omitted. 48 h p.t. cells were lysed in PLB buffer (Promega) and a dual-luciferase assay was performed to determine the levels of firefly luciferase and *Renilla* luciferase. The values for firefly luciferase were normalized to their *Renilla* luciferase values and the ratios for transfections with N divided by the ratios for transfections without N were considered as 'fold induction'. The new minigenomes pSDI T7-HH_CNPL_SC were about five fold more efficient than the pSDI CNPL (figure 17).
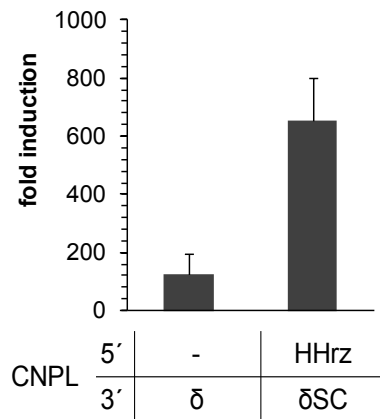
Figure 17: Increased minigenome reporter gene expression due to optimized ribozymes.
(adapted from Ghanem et al., 2012) BSR-T7/5 cells transfected with 4 µg pSDI CNPL or pSDI HHRz_CNPL_SC together with 5 µg pTIT-N, 2.5 µg pTIT-P, 2.5 µg pTIT-L and 10 ng pRL-CMV (negative control: without N). 48 h p.t. cells were lysed and dual-luciferase assays performed. Y-axis shows *Renilla* normalized values obtained with N divided by values without N as 'fold induction'.

The slighter increase in efficiency than observed for RABV rescue from full-length cDNA can be explained from the fact that from these negative sense minigenomes FFluc mRNAs can be made by transcription without further replication. Therefore these data indicate that for viral transcription in contrast to replication the genome ends are less important.

3.2.5 Application of the improved system to generate new recombinant RABV.

The new RABV rescue system has proven to be much more efficient and faster, than the previous system. Numerous recombinant RABV could be rescued. For instance several viruses used in Part 3.1 of this thesis (→3.1.6 →3.1.9) could only be rescued with the improved system whereas rescue failed with the "old" system. Many new attenuated viruses could be rescued easily for use in basic research about RABV biology as well as for use as neuronal tracers. Table 1 provides an overview about recombinant RABV that were recovered from cDNA with the new system. Almost all viruses that were generated in part 3 of this thesis, many of them also being strongly attenuated exclusively used the improved RABV cDNA vector (exceptions are specified).

Table 1: Novel recombinant RABV recovered with improved rescue system.

recombinant RABV	system		comments
	new	old	
SAD eGFP	+	+	eGFP in extra transcription unit
SAD ΔG eGFP	+	+	eGFP in extra transcription unit G gene deleted
SAD ΔG mcherry	+	+	mcherry in extra transcription unit G gene deleted
SAD ΔG GCamP3	+	n.d.	GCamP3 in extra transcription unit G gene deleted
SAD ΔG GCamP5	+	n.d.	GCamP5 in extra transcription unit G gene deleted
SAD ΔG ChR2	+	n.d.	ChR2 in extra transcription unit G gene deleted
SAD ΔG tm-tomato	+	n.d.	tm-tomato in extra transcription unit, G gene deleted
SAD ΔG mito-TurboGFP	+	n.d.	mito-TurboGFP in extra transcription unit, G gene deleted
SAD ΔM/ΔG mcherry	+	n.d.	mcherry in extra transcription unit M and G gene deleted
SAD ΔP G_eGFP	+	n.d.	eGFP in extra transcription unit P gene deleted
SAD ΔP N_eGFP	+	n.d.	P gene replaced by eGFP gene
SAD G_shGFP-SC1	+	-	viruses used in Part 3.1 of this thesis containing internal SC1
SAD G_shGFP-SC2	+	-	viruses used in Part 3.1 of this thesis containing internal SC2
SAD N2AP	+	n.d.	N/P gene border replaced by 2A-like sequence (see part 3.3)
SAD NENEPEL	+	-	RABV comprising 3 internal EMCV IRES elements (see part 3.3)

3.3 Single infectious cDNAs of rabies virus

A genetically encoded RABV, finally resulting in an inducible "RABV-on mouse" would open the wide field of mouse genetics, including knock-out mice and various tissue specific Cre recombinase expressing mouse lines, for new approaches in synaptic tracing with RABV vectors in neuronal sciences or for studies on RABV biology, spread and pathogenesis. The development of such a valuable research tool has been precluded so far by distinct features of RABV biology.

For all NNSV neither the genome nor the antigenome is infectious per se and to rescue RABV from cDNA the vRNP has to be reconstituted in the cell. Thus not only the RABV full-length antigenome-like RNA has to be provided, but also the RABV N protein, encapsidating this RNA into NCs and the RNA-dependent RNA polymerase P-L. Altogether 4 plasmids have to be present in the cell, hampering approaches of genetically encoded systems.

Although the RABV rescue system has been improved as described in part 3.2 of this thesis (Ghanem et al., 2012), it is still dependent on T7-pol. Pol-II dependent rescue systems have been reported for the RABV strains HEP-Flury (Inoue et al., 2003) and CTN181 (Huang et al., 2010). For the strain SAD L16, however, this has not been established so far.

In order to assess the possibility of generating a genetically encoded RABV the aim of the following studies was to develop rescue systems which depend on less than the conventional 4 plasmids, and with the final goal of ideally only one plasmid, a single-infectious RABV cDNA. Further, rescue from this infectious cDNA clone should be independent of T7-pol, allowing expression in various tissues and from different promoter systems.

3.3.1   SAD EP(mono) – P protein translated from full-length antigenomic RNA is sufficient for rescue without P "helper" plasmid.

For rescue of recombinant RABV in the conventional systems, the 3 "helper"-plasmids pTIT-N, pTIT-P and pTIT-L are necessary together with the full-length RABV cDNA. In these pTIT plasmids, T7-pol dependent transcription occurs from a T7 promoter. The transcripts are un-capped and for supporting translation initiation an EMCV IRES element is inserted upstream of the ORFs (Finke and Conzelmann, 1999).

Picornaviral IRES elements replacing the RABV N/P gene border have been shown not only to be tolerated within the RABV genome but also to facilitate translation of the P protein from a bicistronic N-IRES-P gene (Marschalek et al., 2009). With the aim of providing "helper" proteins directly translated from the RABV antigenome-like RNA instead of providing them *in trans*, the question arose whether these IRES elements sufficiently initiate translation of P protein from full-length antigenomic RNA, thus allowing to omit the P "helper" plasmid for recovery of recombinant RABV from cDNA. To address this question, rescue experiments were performed.

In the previously described virus SAD PVP the N/P gene border is replaced by a poliovirus IRES (figure 18A). Thus the virus instead of terminating transcription after the N gene, continues and transcribes a bicistronic mRNA. Translation of the P ORF is dependent on the PV IRES. A new cDNA, pSAD T7-HH_PVP(mono)_SC, was constructed analogously to the pSAD PVP (labeled pSAD PVP(bi) for differentiation) but with the PV IRES downstream of the N/P gene border. The idea behind this construct was to use the IRES element only for rescue of the antigenome RNA but to have the viral mRNA translated cap-dependently. As the "helper" proteins are translated dependent on an EMCV IRES, also this IRES element was tested, in the construct pSAD T7-HH_EP(mono)_SC. It was assumed that SAD PVP(mono) and SAD EP(mono) in contrast to SAD PVP(bi) would benefit from having the wild type-like transcriptional gradient regarding their N and P mRNAs. Notably, from now on all full-length RABV cDNA constructs were generated based on the improved cDNA pSAD T7-HH_L16_SC shown in part 3.2 of this work thus comprising the HHRz to process the 5'-end and the improved SC1 to process the 3'-end of the antigenome-like RNA (exceptions are mentioned individually).

First 10 µg of the 3 constructs pSAD T7-HH_PVP(bi)_SC, pSAD T7-HH_PVP(mono)_SC or pSAD T7-HH_EP(mono)_SC were transfected into BSR T7/5 cells using $CaPO_4$. As controls, un-transfected cells were infected with SAD L16 (MOI=1) or not. 48 h p.t. the cells were lysed and subjected to Western blot analysis. Whereas from constructs pSAD T7-HH_PVP(bi)_SC and pSAD T7-HH_PVP(mono)_SC only little P was made, the EMCV IRES in pSAD T7-HH_EP(mono)_SC was directing translation of significantly increased amounts of P protein from the full-length antigenomic RNA (figure 18B).
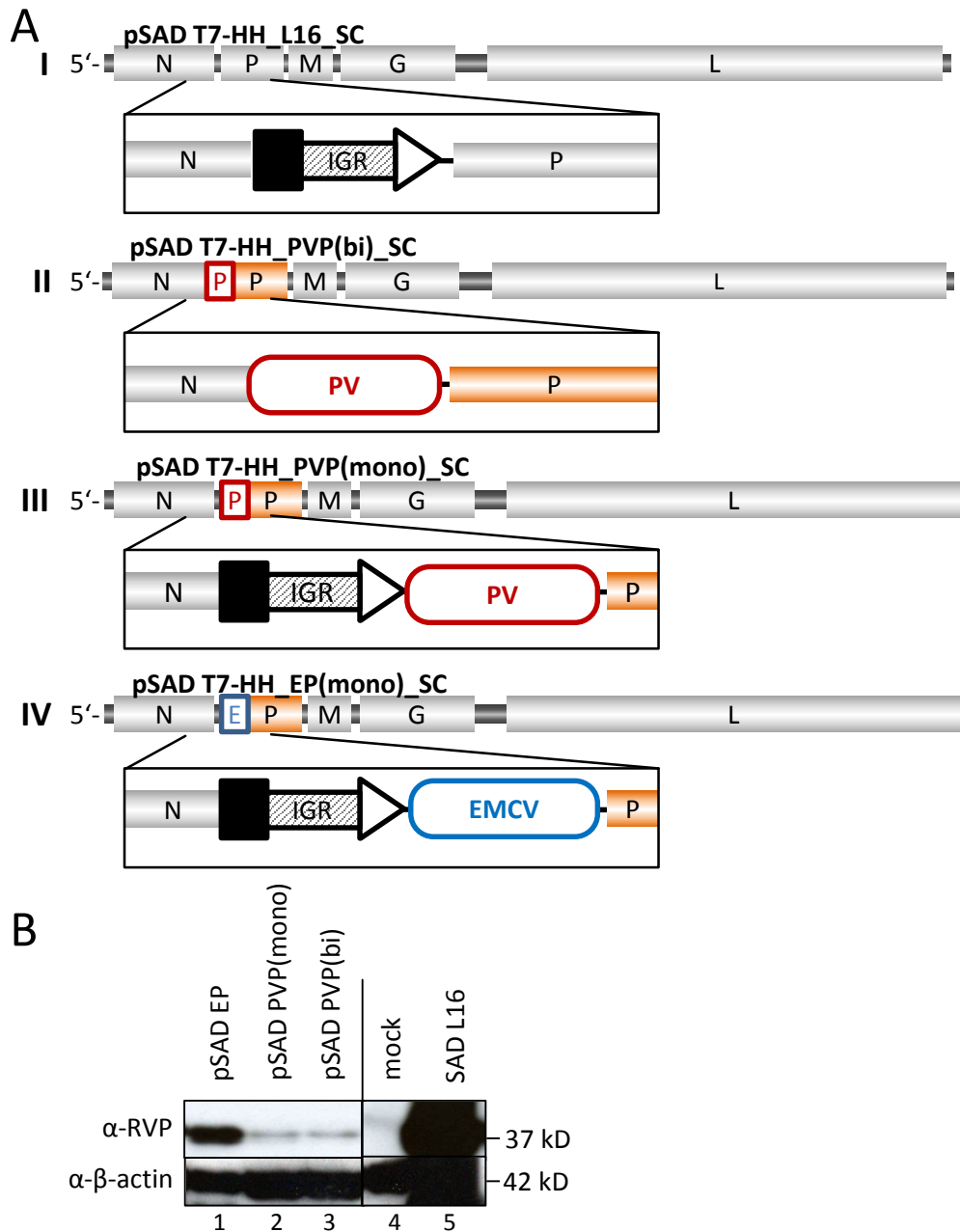
Figure 18: SAD PVP(bi), SAD PVP(mono) and SAD EP(mono) – different levels of P protein translated from full-length antigenomic RNA.

(A) In SAD L16 (I) all genes are separated by gene borders (V) containing the transcription stop signal (black box), an intergenic region (IGR – shaded box) and the transcription start signal (white arrow). In SAD PVP(bi) (II) the N/P gene border (VI) is replaced by the PV IRES. In SAD PVP(mono) (III) the PV IRES is inserted downstream of the N/P gene border (VII). In SAD EP(mono) (IV) the EMCV IRES is inserted downstream of the gene border (VIII). (B) Western blot of BSR-T7/5 cell lysates 48 h p.t. of 10 µg pSAD EP(mono), pSAD PVP(mono) or pSAD PVP(bi). Controls were BSR-T7/5 cells infected with SAD L16 (MOI=1) or uninfected. Boxes: P: poliovirus IRES, E: EMCV IRES, IGR: intergenic region.

To evaluate if the levels of P protein translated directly from the full-length RNA were sufficient to rescue the respective viruses, standard rescue experiments were performed with the new constructs. In this part of the thesis, all rescue experiments, referred to as "standard", were carried out by application of the improved rescue system, described in part

3.2 of this thesis (exceptions are mentioned individually). BSR T7/5 cells in 6-well plates were transfected with 10 µg of either pSAD T7-HH_PVP(bi)_SC, pSAD T7-HH_PVP(mono)_SC or pSAD T7-HH_EP(mono)_SC together with 5 µg pTIT-N and 2.5 µg pTIT-L using CaPO$_4$. 2.5 µg of pTIT-P were co-transfected or not. Although viruses could be rescued successfully from all constructs, only SAD EP(mono) could be rescued without additional P "helper" plasmid (table 2). This reflects the higher levels of P protein present in the cells upon transfection of pSAD T7-HH_EP(mono)_SC in contrast to the poliovirus IRES containing constructs.

Table 2: EMCV IRES allows rescue without P "helper" plasmid.

	+N	+P	+L	1. Pass. (3d)	2. Pass. (6d)	Transf. Cells (6d)
pSAD EP(mono)	+	+	+	3/8	5/8	8/8
	+	-	+	2/10	3/10	5/10
pSAD PVP(bi)	+	+	+	2/2	2/2	2/2
	+	-	+	0/4	0/4	0/4
pSAD PVP(mono)	+	+	+	4/6	5/6	6/6
	+	-	+	0/7	0/7	0/7

3.3.2 SAD N2AP – Expression of 2 proteins from 1 ORF.

By making use of picornavirus 2A-like elements, 2 proteins can be translated from a single ORF. The upstream protein carries the 2A-like sequence at its C-terminus whereas the downstream protein begins with an N-terminal proline. In contrast to an IRES element no *de novo*-translation initiation takes place at the 2A-like sequence.

The RABV N/P gene border together with the N 3'-UTR and the P 5'-UTR were replaced by a cDNA sequence from the picornavirus *Thosea asigna virus* coding for a 2A-like sequence resulting in pSAD N2AP (figure 19A). Standard rescue experiments were performed in BSR T7/5 cells with pSAD T7-HH_N2AP_SC and "helper" plasmids pTIT-N, pTIT-P and pTIT-L. Recombinant virus could be generated successfully from cDNA. Stocks were made from the

virus SAD N2AP. Multistep growth curves revealed the RABV SAD N2AP to be attenuated compared to the wild-type SAD L16 (figure 19B).
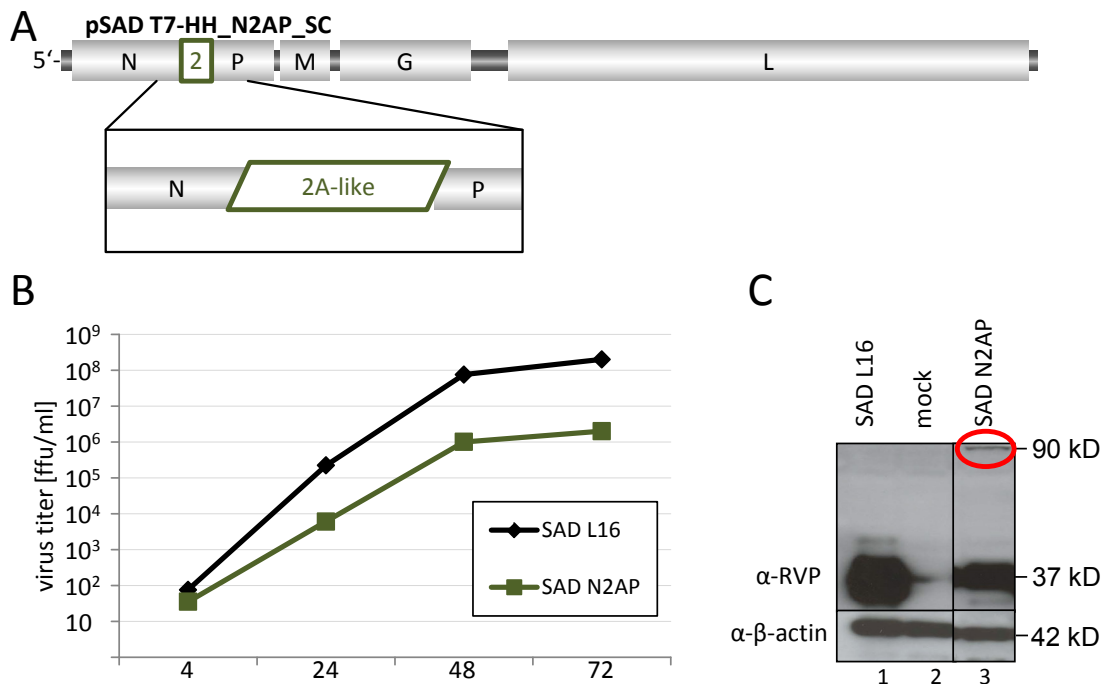
Figure 19: SAD N2AP – Expression of 2 proteins from 1 ORF.
(A) In SAD N2AP the 2A-like sequence was inserted in-frame between the N-ORF and the P-ORF, replacing the N/P gene border and untranscribed flanking sequences. Box 2: 2A-like sequence. (B) Multistep growth curve for SAD N2AP in comparison to SAD L16 indicates attenuation. (C) BSR-T7/5 cells were infected with either SAD L16, SAD N2AP (MOI=1) or uninfected. WB of cell lysates 48 h p.i. The red circle indicates residual read-through translation product.

To analyze the amounts of viral protein expression, BSR T7/5 cells were infected with either SAD L16, SAD N2AP (MOI = 1) or left un-infected. 48 h p.i. the cells were lysed and Western blots were performed using P160-5 antibody (α-RVP) or actin antibody (figure 19C). Reasonable amounts of P protein were detected after SAD N2AP infection (lane 3) and only a minute fraction of "read-trough" N2AP fusion protein was detected (lane 3, red circle). This indicates the 2A-like sequence to be very efficient in autoprocessing and generating two distinct proteins (N-2A and P) from one ORF. Nevertheless, compared to SAD L16 the expression of P was reduced.

3.3.3   SAD EL can be rescued without L "helper" plasmid

As it was shown to be possible to rescue the virus SAD EP from pSAD EP(mono) without adding the pTIT-P "helper" plasmid to the transfection mix, the same principle should be tested for the expression of other "helper" proteins. The construct pSAD T7-HH_EL_SC was

generated by inserting the cDNA sequences of the EMCV IRES downstream of the G/L gene border into the 5'-UTR of the L gene directly upstream of the L ORF (figure 20A).
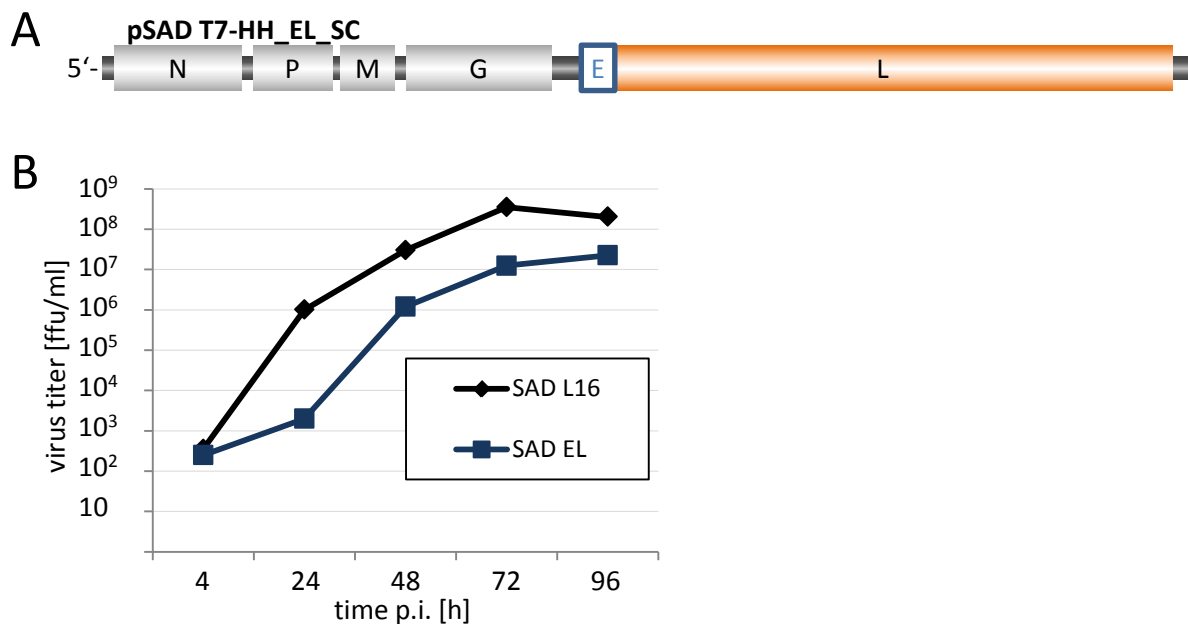
Figure 20: SAD EL – EMCV IRES upstream of the L gene.
(A) Genome organization of SAD EL: translation of L from primary transcript and monocistronic EL mRNA in virus life cycle. Box E: EMCV IRES. (B) Multistep growth curve for SAD EL in comparison to SAD L16. BSR-T7/5 cells in T25 flasks were infected with MOI=0.01.

Again standard rescue experiments were performed with pSAD T7-HH_EL_SC together with pTIT-N and pTIT-P. The "helper"-plasmid pTIT-L, coding for the L protein, was either co-transfected or not. The virus SAD EL could be rescued together with N, P and L and was viable. Noteworthy it could also be rescued when the pTIT-L was omitted (table 3) indicating the EMCV IRES to initiate the translation of L protein from the full-length RNA at sufficient levels.

Table 3: EMCV IRES allows rescue without L "helper" plasmid.

	+N	+P	+L	1. Pass. (3d)	2. Pass. (6d)	Transf.Cells (6d)
pSAD EL	+	+	+	0/4	3/4	4/4
	+	+	-	0/4	2/4	3/4

SAD EL was recovered from rescue experiments and virus stocks were produced. Multi-step growth curves were performed by infecting BSR T7/5 cells with either SAD L16 or SAD EL (MOI = 0.01). SAD EL was attenuated compared to SAD L16 most probably due to the additional IRES sequences (figure 20B) assumed to result in lower L levels than for SAD L16.

3.3.4   SAD EN: N expression but no rescue – double N gene catches on.

As demonstrated for the P and the L proteins, it was attempted to translate the RABV N protein directly from the full-length RNA by means of IRES elements. Directly downstream of the leader sequence and upstream of the AUG of the N ORF an *FseI* restriction site was created followed by insertion of either the EMCV IRES (SAD EN – figure 21A-I) or the PV IRES (SAD PVN – figure 21A-II). As the IRES elements with their extensive secondary structure were thought to possibly interfere with functions of the leader RNA, a GFP gene was inserted between the *FseI* site and the EMCV IRES as a Spacer (SAD GFPEN – figure 21A-III), thus, resulting in a bicistronic GFP-IRES-N gene. Several standard rescue experiments were performed in BSR T7/5 cells transfected with pSAD T7-HH_EN_SC, pSAD T7-HH_PVN_SC or pSAD T7-HH_GFPEN_SC together with pTIT-P, pTIT-L in the presence or absence of pTIT-N. However, none of these experiments resulted in rescue of a viable virus (table 4).

As it was demonstrated for the N-IRES-P RABVs (→3.3.1) that an IRES element downstream of the N gene is well tolerated a similar approach was applied for the N protein. By inserting a complete N ORF via the *FseI* site directly upstream of the EMCV IRES in pSAD T7-HH_EN_SC, or the PV IRES in pSAD T7-HH_PVN_SC respectively, the constructs pSAD T7-HH_NEN_SC or pSAD T7-HH_NPVN_SC were generated (figure. 21A-IV and V). These should result in viruses transcribing a bicistronic N-IRES-N mRNA. The first N ORF (N1) should be translated cap-dependently, whereas expression of the second (N2) should be dependent on the IRES element. The IRES dependent N2 should be translated directly from the naked full-length RNA during rescue.

Again standard rescue experiments were performed and together with pTIT-P, pTIT-L and pTIT-N both viruses SAD NEN and SAD NPVN could be recovered from their cDNA constructs. Most importantly, SAD NEN, but not SAD NPVN, could be rescued in the absence of the N "helper" plasmid (table 4) which is most likely due to the higher activity of the EMCV IRES.

To compare levels of N protein expressed from the different plasmid constructs, 5 µg of pTIT-N, pSAD T7-HH_EN_SC, pSAD T7-HH_PVN_SC, pSAD T7-HH_GFPEN_SC, pSAD T7-

HH_NEN_SC, pSAD T7-HH_NPVN_SC or as control pSAD T7-HH_L16_SC were transfected into BSR T7/5 cells in 6-wells using Lipofectamine 2000. 48 h p.t. the cells were lysed and Western blot was performed. N protein was detected using the S50 antibody (α-RVN, α-RVP) (figure 21B). Whereas the highest N levels were observed for pTIT-N (lane 1), reasonable amounts were made for all constructs containing the EMCV IRES, namely pSAD T7-HH_EN_SC (lane 3), pSAD T7-HH_GFPEN_SC (lane 5) and pSAD T7-HH_NEN_SC (lane 6). As it was observed for the P protein before (→ 3.3.1) the PV IRES was not able to translate substantial levels of N protein from the full-length construct (lane 4 and lane 7). Interestingly, a very tiny band of N protein was observed even for the construct pSAD T7-HH_L16_SC, deriving most probably from leaky ribosomal scanning and translation initiation at the N-AUG (lane 8). Noteworthy, the defect of the constructs pSAD EN and pSAD GFPEN to give rise to viable viruses is not due to defects in N expression.
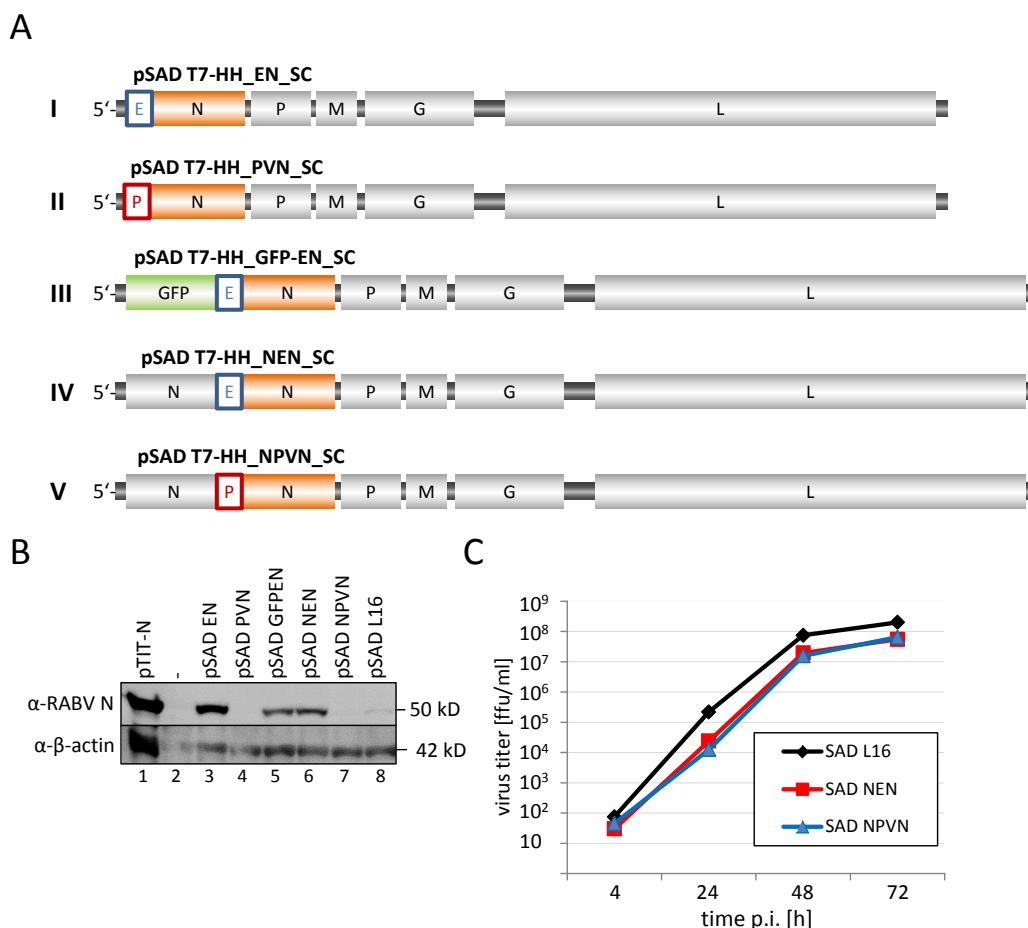
Figure 21: SAD EN sufficient N expression but no rescue – double N gene catches on.
(A)Constructs to translate N from an IRES: pSAD EN (I), pSAD PVN (II), pSAD GFPEN (III), pSAD NEN (IV), pSAD NPVN (V). Boxes: E: EMCV IRES, P: poliovirus IRES. (B) WB of BSR-T7/5 cells 48 h p.t. of 10 μg of either pSAD EN, 10 μg pSAD PVN, pSAD GFPN, pSAD NEN or pSAD NPVN. As controls 5 μg pTIT-N or cells were not transfected. (C) Multistep growth curve of SAD NEN and SAD NPVN in comparison with SAD L16. BSR-T7/5 cells were infected with MOI=0.01.

Stocks were grown from successful rescue approaches of SAD NEN and SAD NPVN. BSR T7/5 cells were infected with either of the two viruses or SAD L16 to determine growth kinetics in a multistep growth curve (figure 21C). SAD NEN and SAD NPVN were slightly attenuated compared to SAD L16. However, their growth kinetics was indistinguishable, indicating most N protein during virus life cycle to be made from the first N gene in both viruses, as the IRES element did not seem to have a major influence.

3.3.5 Significance of *cis*-active N sequences

Although all constructs were translating the same amount of N protein from their primary full-length transcript, only pSAD T7-HH_NEN_SC but not pSAD T7-HH_EN_SC or pSAD T7-HH_GFPEN_SC could be rescued. This indicated the existence of *cis*-active sequences within the N gene, important for RABV viability. To further analyze this I constructed the plasmids pSAD T7-HH_N100EN_SC(Fse) (figure 22A-I) and pSAD T7-HH_N200EN_SC(Fse) (figure 22A-II). Both had the *FseI* restriction site at the leader-N gene junction followed by either the 5'-100 nts or the 5'-200 nts of the N gene, again followed by the EMCV IRES and the second and full N gene. Rescue attempts revealed that only pSAD T7-HH_N200EN_SC(Fse) but not pSAD T7-HH_N100EN_SC(Fse) could be rescued (table 4).

Now multiple evidence indicated the importance of *cis*-active sequences within the N gene, although for RABV such sequences were described to occur only in the leader and trailer regions and in the intergenic regions. Therefore it was not unlikely that also the *FseI* restriction site at the leader-N gene junction might play a role and attenuates the RABV SAD N200EN(Fse).

To test this possibility, I removed these 8 nts restoring the wt sequence. Additionally I inserted an eGFP gene in an extra transcription unit between the G and the L gene. The resulting new constructs were pSAD T7-HH_N100EN G_eGFP_SC (figure 22A-III) and pSAD T7-HH_N200EN G_eGFP_SC (figure 22A-IV). Again standard rescue experiments were performed. Both viruses could be recovered from cDNA (table 4). SAD N100EN G_eGFP however was hard to detect in the supernatant and eGFP positive foci were only detected 6 d after passaging (figure 22B). When the plasmid pTIT-N was omitted in the rescue transfection, both constructs pSAD T7-HH_N100EN G_eGFP_SC as well as pSAD T7-HH_N200EN G_eGFP_SC lead to the successful rescue of viruses (table 4).

Table 4: EMCV IRES allows rescue without N "helper" plasmid.
(* Only single positive cells, no virus recovered)

	+N	+P	+L	1. Pass. (3d)	2. Pass. (6d)	Transf. Cells (6d)	3. Pass. (9d)	Transf. Cells (9d)
pSAD EN	+	+	+	0/8	0/8	(2)/8*	n.d.	n.d.
	-	+	+	0/5	0/5	0/5	n.d.	n.d.
pSAD PVN	+	+	+	0/12	0/12	0/12	n.d.	n.d.
	-	+	+	0/12	0/12	0/12	n.d.	n.d.
pSAD GFPEN	+	+	+	0/10	0/10	(4)/10*	n.d.	n.d.
	-	+	+	0/6	0/6	0/6	n.d.	n.d.
pSAD NEN	+	+	+	4/4	4/4	4/4	n.d.	n.d.
	-	+	+	2/5	2/5	2/5	n.d.	n.d.
pSAD NPVN	+	+	+	4/4	4/4	4/4	n.d.	n.d.
	-	+	+	0/4	0/4	0/4	n.d.	n.d.
pSAD N100EN(Fse)	+	+	+	0/11	0/11	0/11	n.d.	n.d.
	-	+	+	0/5	0/5	0/5	n.d.	n.d.
pSAD N200EN(Fse)	+	+	+	2/8	6/8	7/8	n.d.	n.d.
	-	+	+	0/4	0/4	0/4	0/4	1/4
pSAD N100EN G_eGFP	+	+	+	0/8	2/8	6/8	n.d.	n.d.
	-	+	+	0/5	0/5	6/9	n.d.	n.d.
pSAD N200EN G_eGFP	+	+	+	0/8	1/8	8/8	n.d.	n.d.
	-	+	+	0/5	0/5	6/9	n.d.	n.d.
pSAD NEN G_eGFP	+	+	+	2/3	3/3	3/3	n.d.	n.d.
	-	+	+	0/4	0/4	3/8	n.d.	n.d.
pSAD N100(mut)EN G_eGFP	+	+	+	n.d.	n.d.	2/4	n.d.	n.d.
	-	+	+	n.d.	n.d.	4/4	n.d.	n.d.
pSAD N200(mut)EN G_eGFP	+	+	+	n.d.	n.d.	4/4	n.d.	n.d.
	-	+	+	n.d.	n.d.	4/4	n.d.	n.d.

The differences in viability observed for SAD N100EN(Fse) and SAD N100EN G_eGFP, underline the importance of *cis*-active sequences at the leader-N gene junction for RABV viability. Moreover, the obvious difference in fitness between SAD N100EN G_eGFP and SAD N200EN G_eGFP further emphasized the importance of sequences within the N-coding region. To first exclude the possibility of small inhibitory N-peptides being expressed from the N100 or N200 sequence directly downstream the leader, the first AUG of N100 or N200, respectively, was mutated to UUG thereby constructing the plasmids pSAD T7-HH_N100(mut)EN G_eGFP_SC (figure 22A-V) and pSAD T7-HH_N200(mut)EN G_eGFP_SC (figure 22A-VI). Again standard rescue experiments as well as rescue experiments without pTIT-N were performed and from both constructs recombinant viruses could be recovered with or without pTIT-N (table 4). The virus SAD N100(mut)EN G_eGFP grew very slowly and made very small foci visible significantly later than others (figure 22B).

To compare the growth kinetics of the viruses with different sequences following the leader, a single-step growth experiment was performed. BSR T7/5 cells were infected with SAD N100EN G_eGFP, SAD N200EN G_eGFP or SAD NEN G_eGFP and in addition with SAD N100(mut) G_eGFP or SAD N200(mut) G_eGFP (MOI=1). Also SAD N200EN(Fse), the virus still containing the *FseI* sequence after the leader, SAD GFP and SAD L16 were included as controls. Cells infected with viruses expressing eGFP were monitored for eGFP expression 24 h and 48 h p.i. (figure 22D). 48 h p.i. the supernatants were collected and titrated (figure 22C). To compensate for the growth difference that was observed already for the foci size (figure 22B), titrations for SAD L16 were fixed after 2 d whereas titrations for SAD N200EN(Fse) were fixed after 4 d. Titrations for viruses expressing eGFP were monitored daywise for eGFP expression and fixed when foci were big enough for detection, but before the onset of secondary spread. For SAD N200EN G_eGFP a modest attenuation (about 1.5 log steps) in growth kinetics was observed in comparison to SAD eGFP and SAD NEN G_eGFP. Also the eGFP expression was reduced compared to the latter ones. Viruses comprising only 100 nts of the N gene were slightly more attenuated as indicated by comparison of SAD N100EN G_eGFP with SAD N200EN G_eGFP. SAD N100EN G_eGFP was growing lower titers and also significantly less eGFP was expressed 24 h p.i. The same was true for viruses with the UUG mutation as indicated by comparison of SAD N200(mut)EN G_eGFP with SAD N200EN G_eGFP. The combination of both attenuating factors, 100 instead of 200 nts of the

N gene following the leader and the UUG mutation, however, as observed for SAD N100(mut)EN G_eGFP lead to a severe
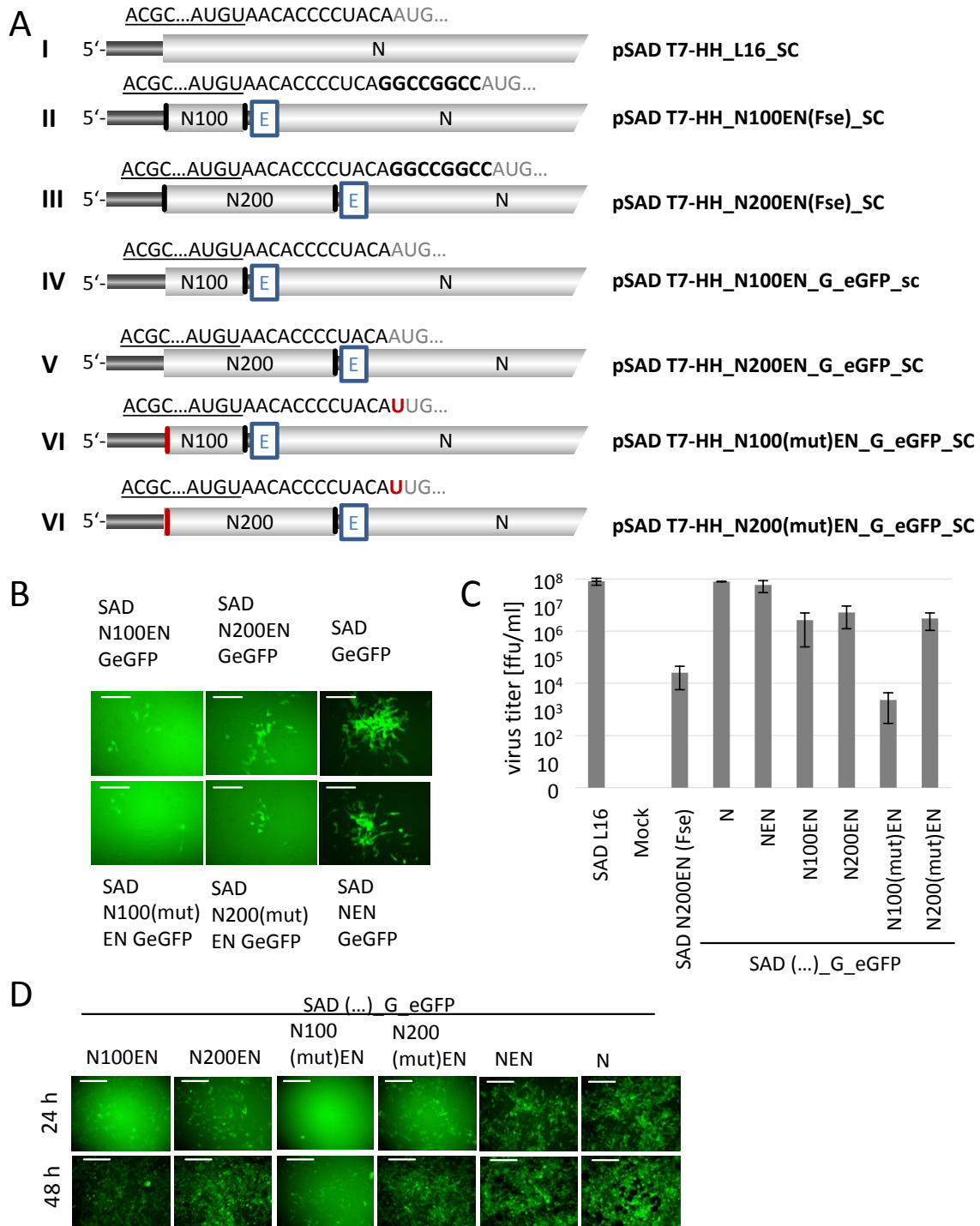
Figure 22: N sequences have a cis-active function.
(A) Genome organization of new constructs: (I) pSAD N100EN(Fse), (II) pSAD N200EN(Fse), (III) pSAD N100EN G_eGFP, (IV) pSAD N200EN G_eGFP, (V) pSAD N100(mut)EN G_eGFP, (VI) pSAD N200(mut)EN G_eGFP. Box E: EMCV IRES. (B) Comparison of foci after titration. The cells were photographed 48 h p.i. under UV-light. Size bar = 100 μm. (C) Single-step growth curve of different N-sequence mutants. BSR-T7/5 cells were infected with SAD N100EN G_eGFP, SAD N200EN G_eGFP, SAD NEN G_eGFP, SAD G_eGFP, SAD 100(mut)EN G_eGFP, SAD N200(mut)EN G_eGFP, SAD N200EN(Fse) or SAD L16 (MOI=1). 48 h p.i. supernatants were taken and titrated. (D) EGFP expression was monitored during infection for single-step growth curve 24 and 48 h p.i. under UV light. Size bar = 100 μm.

reduction in virus viability. This virus was found to have titers more than 10,000-fold reduced and no eGFP was observed 24 and 48 h p.i. These results correspond with the fact that we could not recover SAD N100EN(Fse). This RABV construct also has only 100 nts of the N gene and due to the FseI site a disruption at the leader-N gene junction.

Together these data indicate that *cis*-active sequences that have not been described yet are important for RABV viability. It can be concluded that parts of these sequences are located directly at the leader-N gene junction, and more downstream within the N gene.

3.3.6 Combining IRES elements and 2a-like sequences – towards an infectious RABV cDNA clone

As RABV constructs were already successfully created that could be rescued either without "helper" plasmids for P (→3.3.1), L (→3.3.3) or N (→3.3.4, 3.3.5), and virus constructs that express two proteins from one ORF, using 2A-like sequences (→3.3.2), the next step was to combine these approaches with the final goal to omit all "helper"-plasmids for the virus rescue. Namely, to generate a single infectious RABV cDNA clone.

The first step was to generate the construct pSAD T7-HH_NEN_EL_SC. This new construct was purposed to translate both N and L directly from the full-length RNA (figure 23-I). Importantly, in contrast to pSAD T7-HH_NEN_SC, pSAD T7-HH_NEN_EL_SC lacked the *FseI* site at the leader-N gene junction due to the cloning strategy applied (For details see Materials and Methods).
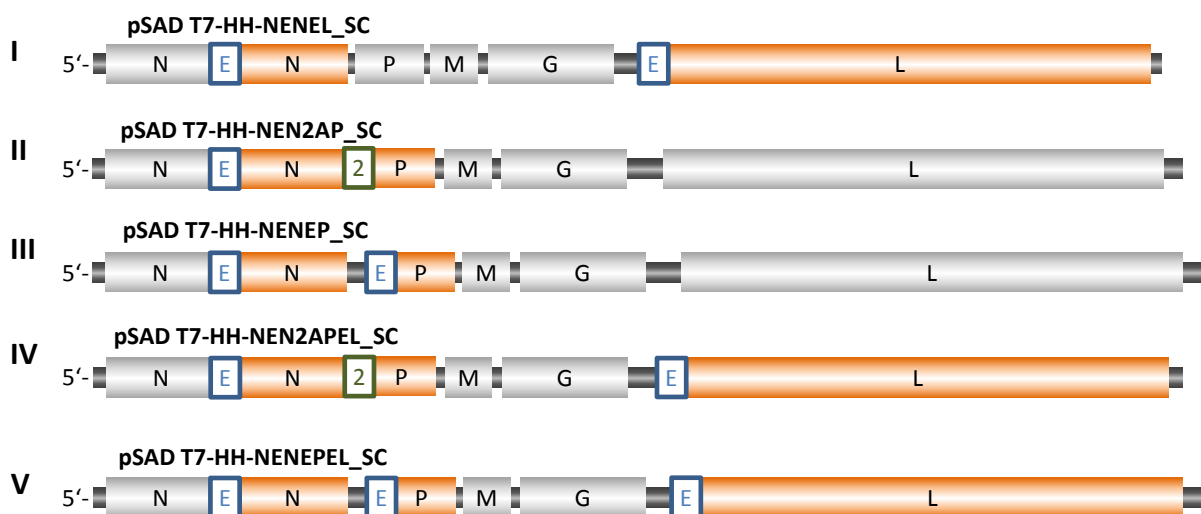

Figure 23: Combining IRES elements and 2A-like sequences – towards the infectious clone.
Genome organization of SAD NEN EL (I), SAD NEN2AP (II), SAD NENEP (III) and of the two single infectious clones SAD NEN2APEL (IV) and SAD NENEPEL (V). Boxes: E: EMCV IRES, 2: 2A-like sequence.

In standard rescue experiments, this construct yielded recombinant virus SAD NEN_EL either when co-transfected with pTIT-N, pTIT-P and pTIT-L, and also if only pTIT-P was co-transfected. This demonstrates the possibility to replace two "helper" plasmids (pTIT-N and pTIT-L) by the insertion of IRES elements upstream of the respective genes in the full-length RABV cDNA (table 5).

Table 5: Combination of IRES elements and 2A-like sequences – the infectious clone.

	+N	+P	+L	1. Pass. (3d)	2. Pass. (6d)	Transf. Cells (6d)	3. Pass. (9d)	Transf. Cells (9d)
pSAD NEN_EL (I)	+	+	+	2/2	2/2	2/2	n.d.	n.d.
	-	+	-	0/2	0/2	2/2	n.d.	n.d.
pSAD NEN2AP (II)	+	+	+	4/4	4/4	4/4	n.d.	n.d.
	-	-	+	3/4	4/4	4/4	n.d.	n.d.
pSAD NENEP (III)	+	+	+	2/4	3/4	3/4	n.d.	n.d.
	-	-	+	0/2	0/2	1/2	1/2	2/2
pSAD NEN2APEL (IV)	-	-	-	1/22	5/22	13/22	4/14	8/14
	+	-	-	2/7	2/7	2/7	2/7	3/7
	-	+	-	0/7	1/7	3/7	3/7	4/7
	-	-	+	1/7	1/7	5/7	4/7	5/7
	+	+	+	6/7	7/7	7/7	7/7	7/7
pSAD NENEPEL (V)	-	-	-	4/9	4/9	9/9	n.d.	n.d.
	+	-	-	0/3	2/3	3/3	3/3	3/3
	-	+	-	0/3	0/3	3/3	3/3	3/3
	-	-	+	0/3	0/3	0/3	0/3	1/3
	+	+	+	3/3	3/3	3/3	n.d.	n.d.

The next step was to equip the NEN approach together with IRES elements or a 2alike sequence in order to support the translation of N and P. The constructs pSAD T7-HH_NEN2AP_SC (figure 23–II) and pSAD T7-HH_NENEP_SC (figure 23-III), for viruses with a tricistronic NEN2AP mRNA or a bicistronic NEN mRNA together with a monocistronic EP mRNA, were generated. For pSAD T7-HH_NENEP_SC it was expected that the N protein and the P protein will be translated independently from their own upstream EMCV IRES elements. For pSAD T7-HH_NEN2AP_SC, however, only the IRES element upstream of the second N gene will provide translation initiation. As a single ORF, N2AP, will be translated and, directed by the 2A-like sequence, this translation will result in two distinct proteins: N2A and P. For both constructs during cloning the *FseI* site downstream of the leader was deleted and the sequence leader-N-AUG was restored to wild-type like.

The plasmids pSAD T7-HH_NENEP_SC and pSAD T7-HH_NEN2AP_SC were co-transfected with either all of the three "helper" plasmids or only pTIT-L into BSR T7/5 cells using $CaPO_4$. Together with the three "helper" plasmids all four constructs yielded recombinant viruses namely SAD NENEP and SAD NEN2AP (table 5), indicating their viability. Moreover, when pTIT-N and pTIT-P were omitted in the transfection mix and only pTIT-L was supplied, SAD NENEP and SAD NEN2AP could be successfully rescued. This demonstrates translation of the N and P protein directly from their full-length antigenome-like RNAs.

The ultimate step was to replace all three "helper" plasmids by *cis*-active sequences. The plasmids pSAD T7-HH_NEN2APEL_SC and pSAD T7-HH_NENEPEL_SC were constructed (figure 23-IV and V). Again the *FseI* site at the leader-N gene junction was restored to wild-type.

After transfection into BSR T7/5 cells using $CaPO_4$ both constructs resulted in the recovery of viable viruses. Most importantly, both constructs could be rescued without co-transfection of any "helper" plasmids (table 5). These constructs were the first single infectious cDNA clones of an NNSV demonstrating the successful replacement of all "helper" plasmids by introducing *cis*-active sequences into the viral cDNA (and genomes).

The rescue of SAD NENEPEL with about 50 % of experiments being positive after the first passage of supernatant was significantly more efficient than the rescue of SAD NEN2APEL where this ratio of positive rescues was only seen 6 d p.t. in the transfected cells and supernatants were tested positive at lower ratios (table 5). Co-transfection of either of the

"helper" plasmids had no significant impact on rescue efficiencies. However when all 3 "helper" plasmids were co-transfected the efficiency was increased for both, SAD NENEPEL and SAD NEN2APEL. This indicated that the ratio of "helper" proteins made from the infectious clones is not the cause of lower rescue efficiencies.

3.3.7 Infectious cDNA clones as "helper" plasmids

Rescue of recombinant RABV depends on production of "helper" proteins on one hand and the individual attenuation of the respective constructs, due to introduced changes to the viral genome, on the other hand. In regard to the rescue efficiencies of the single infectious RABV cDNA clones it was therefore necessary to distinguish between their respective expression of "helper" proteins during rescue and other attenuating factors that result in different growth kinetics and viability of the rescued viruses.

Therefore a standard RABV cDNA, pSAD T7-HH_GFP_SC, was rescued using either of the infectious cDNA clones or the standard pTIT-NPL-mix to supply the "helper" proteins. Rescue transfections were performed in BSR T7/5 cells using $CaPO_4$. 10 µg pSAD T7-HH_GFP_SC was co-transfected with either 5 µg pTIT-N, 2.5 µg pTIT-P and 2.5 µg pTIT-L, or with 10 µg pSAD T7-HH_NEN2APEL_SC or pSAD T7-HH_NENEPEL_SC, respectively.

UV microscopy allowed the monitoring of the GFP expression resulting from successful recovery of SAD GFP virus. The infectious cDNA clone pSAD T7-HH_NENEPEL_SC performed nearly as good as the pTIT-NPL-mix to rescue SAD GFP, whereas SAD GFP was recovered with a certain delay from its cDNA after transfection of pSAD T7-HH_NEN2APEL_SC as "helper" plasmid (table 6).

Table 6: Infectious clones as "helper" plasmids.

„helper" plasmid(s)	1d	2d	3d	4d	5d	6d	7d	8d	9d
pTIT-N/P/L	0/3	3/3	3/5	3/3	3/3	5/5	3/3	n.d.	2/2
pSAD NENEPEL	0/3	1/3	4/5	3/3	3/3	5/5	3/3	n.d.	2/2
pSAD NEN2APEL	0/3	0/3	0/5	1/3	3/3	4/5	3/3	n.d.	2/2

3.3.8 SAD NEN2APEL – a virus with a tricistronic mRNA

The viruses successfully recovered from the single infectious cDNA clones were used to produce virus stocks in order to analyze their growth behavior and to determine their degree of attenuation.

To determine the growth kinetics, BSR T7/5 cells were infected with either SAD NEN2APEL or SAD L16 (MOI = 0.01) and multistep growth experiments were performed resulting in growth curves. SAD NEN2APEL was strongly attenuated, only growing to titers reduced about 2 log steps in comparison to the wild-type virus (figure 24A). To look for sequence stability, SAD NEN2APEL was passaged on BSR T7/5 cells by transferring the supernatant every 4 – 5 days onto fresh cells. In total, the virus was passaged 17 times. The passaged virus (SAD NEN2APEL pass) together with the original SAD NEN2APEL was subjected to deeper analysis.

For Western blot analyses, BSR T7/5 cells were infected with SAD NEN2APEL, SAD NEN2APEL pass, SAD NEN2AP, SAD N2AP, SAD NEN, SAD EL, or SAD L16 (MOI = 0.05). 96 h p.i. the cells were lysed and WB was performed using antibodies against RABV N (S86), RABV P (FCA) or β-actin (figure 24B). For SAD L16, SAD NEN and SAD EL the N protein was detected at 50 kD (left panel – lanes 3, 6 and 7). In SAD N2AP the N protein is made by translation from the N2AP ORF. After release from the ribosome, the N protein therefore comprises the C-terminal 2A peptide sequence. It clearly runs higher than wild-type N (lane 4). SAD NEN2AP as well as SAD NEN2APEL expresses two different N proteins. From their first N gene normal N is made by cap-dependent translation. Translation of protein from the second N gene depends on the EMCV IRES. This product of the second gene again has the C-terminal 2A-tag. Therefore the two N products can be easily distinguished (lanes 1, 2 and 4).

The P gene of RABV from strain SAD L16 produces full length RABV P (P1), and minor amounts of P2, P3 and P4, truncated products that derive from translation initiation at the second, third and fourth in-frame AUG by ribosomal leaky scanning. For SAD L16, SAD NEN and SAD EL P2 can be detected being slightly smaller than P1 (right panel – lanes 3, 6 and 7). The P protein in SAD N2AP, SAD NEN2AP and SAD NEN2APEL (lanes 1, 2, 4 and 5) is translated from the N2AP or NEN2AP mRNA. Its translation starts with the AUG from the N gene. Therefore no P2 can be made and detected.
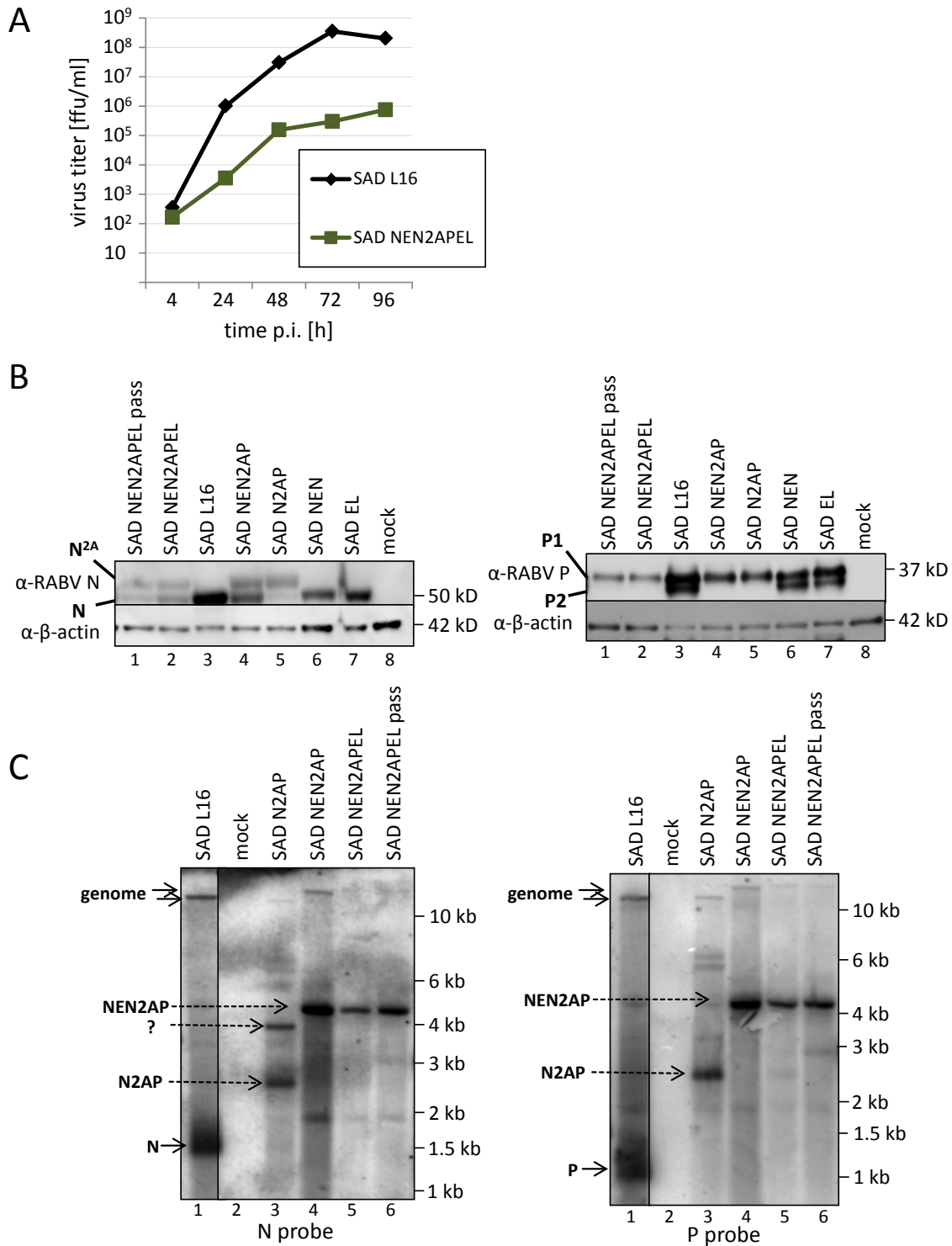
Figure 24: SAD NEN2APEL – a closer look.
(A)Multistep growth curve for SAD NEN2APEL in comparison to SAD L16.BSR-T7/5 cells in T25 flasks were infected with MOI=0.01. (B) BSR-T7/5 cells were infected with SAD NEN2APEL, SAD NEN2APEL(pass), that was passaged 17 times, SAD NEN2AP, SAD N2AP, SAD NEN, SAD EL SAD L16 (MOI=0.05) or uninfected. 96 h p.i. the cells were lysed and protein levels were detected by WB using anti-N and anti-P antibodies. (C)From 50 percent of the cells infected in (B) total RNA was isolated. Northern blot analysis using radioactively labeled probes against the N and P gene were used to detect genomic and subgenomic RNA fragments.

To analyze the RNA species made from SAD NEN2APEL, BSR T7/5 cells were infected with SAD L16, SAD N2AP, SAD NEN2AP, SAD NEN2APEL or the passaged SAD NEN2APEL pass (MOI = 0.05). 96 h p.i. the cells were lysed and total RNA was isolated. RNA was used for Northern blot analysis and radioactively labeled probes against the N gene or the P gene were generated and used to incubate the membranes. With the N probe for RNA from SAD L16 infected cells, the SAD NEN2APEL genome comprises >10 kb. The monocistronic N mRNA runs at about 1.5 kb (left panel – lane 1). This corresponds to the length of the N gene and about 300 nts of poly(A). With the P probe the P mRNA is detected at about 1.2 kb corresponding to 900 nts of the P gene together with 300 nts poly(A) (right panel – lane 1). For SAD N2AP (both panels – lane 3) neither of these mRNAs is detected with the N probe and P probe, however the N2AP mRNA is detected at about 2.5 kb reflecting 1.25 kb of the N gene, the small 2A-like sequence (60 nt), the P gene (0.9 kb) and the poly(A) tail. In addition, a second prominent band is detected with the N probe, running at 4 kb that however is not seen with the P probe.

SAD NEN2AP and SAD NEN2APEL express their N and P proteins from a tricistronic mRNA that is detected with the N and P probe at about 4.5 kb. The genomes of these viruses are clearly detected at a higher size due to the additional N gene (both panels – lanes 4, 5 and 6).

No rearrangements were detected for the passaged SAD NEN2APEL pass compared to the un-passaged virus.

3.3.9   SAD NENEPEL – recombination has occurred

SAD NENEPEL, one of the viruses generated from the single infectious cDNA clones, was also subjected to deeper analysis.

BSR T7/5 cells in 6-wells were infected with SAD NENEPEL, SAD NEN, SAD EP, SAD EL and SAD L16 (MOI = 0.5). As additional controls, SAD NEN2APEL, SAD NEN2AP and SAD N2AP were used for infection with the same MOI. 48 h p.i. the cells were lysed and total RNA was isolated. The RNAs were subjected to Northern blot analysis and RNA fragments were detected using an N probe (figure 25A).

For SAD NEN2APEL, as well as for SAD NEN2AP (lanes 1 and 7) again the 4.5 kb tricistronic NEN2AP mRNA was detected (→ compare to figure 24C). The bicistronic NEN mRNA could

be detected in SAD NEN infected cells at about 3.5 kb (figure 25A - lane 3) as it was expected from the design and sequence of the construct. However for this virus a shorter fragment of about 1.6 kb was also detected, corresponding in size to the monocistronic N mRNA that was seen for SAD EP, SAD EL and SAD L16 (lanes 4, 5 and 8). N mRNA of this size was not expected to be made by SAD NEN. Finally, for SAD NENEPEL, the pattern of fragments differed significantly from what was expected (lane 2). At first, the bicistronic NEN mRNA as in SAD NEN at about 3.5 kb was not present. In contrast, the most prominent band detected was an mRNA running slightly below 3 kb. Secondly, the genome of SAD NENEPEL appeared to be smaller than the one detected for SAD NEN2APEL. This again is in disagreement with the expectations.

As from the Northern blot analysis SAD NENEPEL appeared not to be what it should be, additional viruses were recovered from several independent rescue experiments with the single infectious cDNA pSAD T7-HH_NENEPEL_SC. The virus which was recovered originally and detected to have the "wrong" pattern of RNA fragments (→compare figure 25A – lane 2) was named SAD NENEPEL 1, the newly rescued viruses SAD NENEPEL 2 – 7. Stocks from all SAD NENEPEL viruses and SAD L16 were used to infect BSR T7/5 cells (MOI = 0.5). 48 h p.i. the cells were lysed and total RNA was isolated. The RNAs were subjected to Northern blot analysis and RNA fragments were detected using an N probe or a P probe (figure 25B).

SAD NENEPEL 1 in figure 25A was shown to transcribe an mRNA which is running at about 3 kb instead of the expected bicistronic NEN mRNA (3.5 kb). This product again was detected using the N probe (figure 25B - left panel, lane 6). The same was true for all the viruses except for SAD NENEPEL 2 (lane 1), which was the only one showing the correct pattern. For SAD NENEPEL 3, SAD NENPEL 6 and SAD NENEPEL 7 both bands were visible with the N probe, the correct 3.5 kb and the 3 kb mRNA (lanes 2, 4 and 5). Additionally all SAD NENEPEL independently on the correct size of the NEN mRNA made smaller RNA fragments, running slightly higher than the monocistronic N mRNA from SAD L16 (lane 7). One possibility is that they derive from premature termination in the EMCV sequences downstream the first N gene, during either transcription, or replication. To a lesser extent, they can also be detected in SAD NEN2APEL infected cells (→ compare figure 25A). For SAD NENEPEL 6 infected cells (figure 25B) - left panel, lane 4) also a fragment is detected, that corresponds in size to the monocistronic N mRNA.
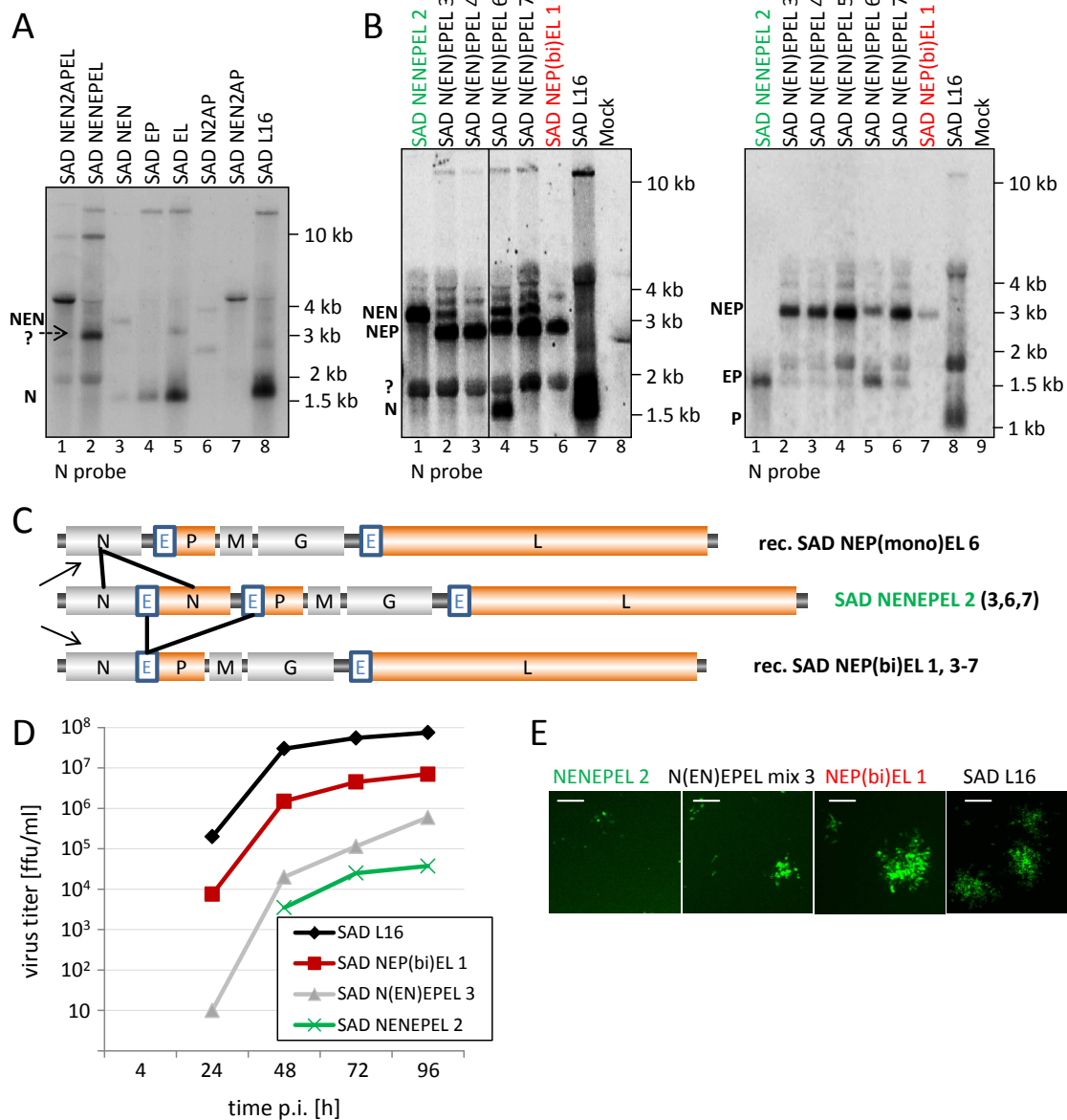
Figure 25: SAD NENEPEL – recombination observed.
(A)BSR-T7/5 cells were infected with SAD NENEPEL, SAD NEN, SAD EP, SAD EL, SAD NEN2APEL, SAD NEN2AP, SAD N2AP SAD L16 (MOI=0.05) or uninfected. 96 h p.i. the cells were lysed and total RNA was isolated. Northern blot analysis using radioactively labeled probes against the N and P gene were used to detect genomic and subgenomic RNA fragments. (B)SAD NENEPEL 2 – SAD NENEPEL 7 from 6 new rescues was used to infect BSR-T7/5 cells and total RNA was isolated. RNA in comparison to RNA from SAD NENEPEL 1 and SAD L16 was subjected to Northern blot analysis. Radioactively labeled probes against the N and P gene were used to detect genomic and subgenomic RNA fragments. (C) Possible recombination events coming from SAD NENEPEL (middle): recombination between the two N genes would lead to SAD NEP(mono)EL (upper row) recombination between the EMCV IRES would lead to SAD NEP(bi)EL (lower row). (D) Multistep growth curve for viruses from individual rescues with pSAD NENEPEL: SAD NENEPEL 1, 2 and 3 in comparison to SAD L16. BSR-T7/5 cells were infected with MOI=0.01. (E) Different phenotypes in foci size observed for titrations of (D). Size bar = 100 μm.

Using the P probe (figure 25B - right panel) for SAD NENEPEL 2, the virus with the correct size of the NEN mRNA, the monocistronic EP mRNA was detected at the correct size (lane 1). For SAD NENEPEL 6 and 7, that also had a prominent band for NEN at the correct size this

monocistronic EP mRNA was visible as well (lanes 5 and 6). For SAD NENEPEL 3, 4, and 5 (5 was excluded from the picture with the N probe due to RNAse contamination) only traces of the correct EP mRNA were detected, whereas SAD NENEPEL 1 did not show a signal at the correct size (lane 7). More interestingly, with the P probe also a band at 3 kb was detected for all viruses but for SAD NENEPEL 2. In combination with the pattern obtained with the N probe, this strongly indicates that some recombination events have occurred resulting in the viruses SAD NENEPEL 1, 3, 4, 5, 6, and 7. Especially the lack of monocistronic EP mRNA for SAD NENEPEL 1 hints to the expression of a bicistronic 3 kb NEP mRNA. This virus can result from a recombination event between the EMCV IRES upstream the second N gene and the EMCV IRES upstream the P gene (figure 25C – at bottom). Therefore SAD NENEPEL 1 appears rather to be SAD NEP(bi)EL 1. In principal also an additional recombination between the two N genes could have happened. This however would result in a monocistronic N mRNA and a monocistronic EP mRNA (figure 25C – at top). This might have happened in SAD NENEPEL 6, for which both of these fragments are detected (left panel – lane 4 and right panel – lane 5). Therefore this virus stock appears to be a mix of SAD NEP(mono)EL and SAD NEP(bi)EL. Also, in regard to the pattern observed for SAD NEN infected cells (figure 25A – lane 3), this possibility is likely, as together with the bicistronic NEN mRNA a shorter fragment is detected at the size of the monocistronic N mRNA.

Whereas SAD NENEPEL 2 seems to be the only un-recombined virus and SAD NEP(bi)EL 1 seems to be the prototype of a recombined virus all the other virus stocks seemed to consist rather of mixtures of the recombined and the un-recombined variant. SAD NEP(mono)EL was detected only in rescue No. 6 and only as part of a mixture.

To determine the influence of the recombined sequences on the growth kinetics, BSR T7/5 cells were infected with SAD NEP(bi)EL 1 (aka SAD NENEPEL 1), as the recombined prototype, SAD NENEPEL 2, as the un-recombined variant, SAD NE(NE)PEL 3, as a mixture of both viruses, or SAD L16 (MOI = 0.01) in order to do a multiple-step growth curve (figure 25D). The un-recombined SAD NENEPEL 2 was strongly attenuated in comparison with the wild type SAD L16. The recombined variant, SAD NEP(bi)EL 1 was growing significantly better, indicating a positive influence of the recombination event on the virus vitality. Figure 25E shows a detail from fixed cells after the titration of the growth curves. 48 h p.i. SAD NENEPEL 2 made significant smaller foci compared to SAD L16, whereas the recombination in SAD

NEP(bi)EL 1 seemed to rescue this phenotype. For SAD NE(NE)PEL 3, the assumed mixture of virus stocks, indeed two different types of foci were detected, small ones resembling SAD NENEPEL 2 and bigger ones, resembling SAD NEP(bi)EL 1.

3.3.10 SAD NENEPEL - recombination most probably on plasmid level

There are 3 possible explanations where and when the recombination for SAD NENEPEL has occurred, at plasmid level (before or after transfection into the cells), during T7 dependent transcription, or during replication of the rescued virus.

To address the latter possibility, the un-recombined virus, SAD NENEPEL 2, should be passaged multiple rounds and progeny virus checked for recombination events. Despite of displaying the correct pattern of RNA fragments (→figure 25B), the presence of already recombined sub-species in the virus stock could not be excluded so far. Therefore, single virus clones were isolated by serial dilution. Virus stocks were diluted to 20 ffu, 10 ffu or 5 ffu per 10 ml (figure 26A). For each dilution step, a complete 96 well plate containing BSR T7/5 seeded 24 h in advance was infected with 100 µl, resulting in calculated approximately 20, 10 or 5 infected wells per 96 well plate. 4 d p.i. in each single well the cells were detached using trypsin and 75 % from each well were transferred into 24 wells while the remaining 25 % were incubated for another 4 d in the 96 wells. Then the cells in the 96 well plates were fixed and stained using a FITC-conjugated anti-N antibody. In the 96 well plate infected with calculated 10 ffu / 10 ml, 5 wells were positive, in the plate infected with calculated 5 ffu / 10 ml 3 were positive. For differentiation they were labeled as clone 1 – clone 8, respectively. The corresponding 24 well cultures were expanded to 6 wells. Then after 3 d the supernatants were stored at – 80 °C and the cells were lysed and total RNA was extracted.

At the same time 1 ml of the supernatant from 5 of the single virus clones was used to infect fresh BSR T7 cells in 6 wells. These cells were referred to as passage 1 (P1). 5 d p.i. 1 ml of the supernatants from P1 was passaged to new cells (P2) the remaining was stored at – 80 °C. The cells from P1 were detached using PBS-EDTA and 75 % were pelleted and total RNA was isolated. 25 % were grown further 5 d (P1*). Then from P1* and P2 total RNA was isolated as well, whereas the supernatants from P2 were partially stored at – 80 °C and passaged further. The scheme of passaging is shown in figure 26B.
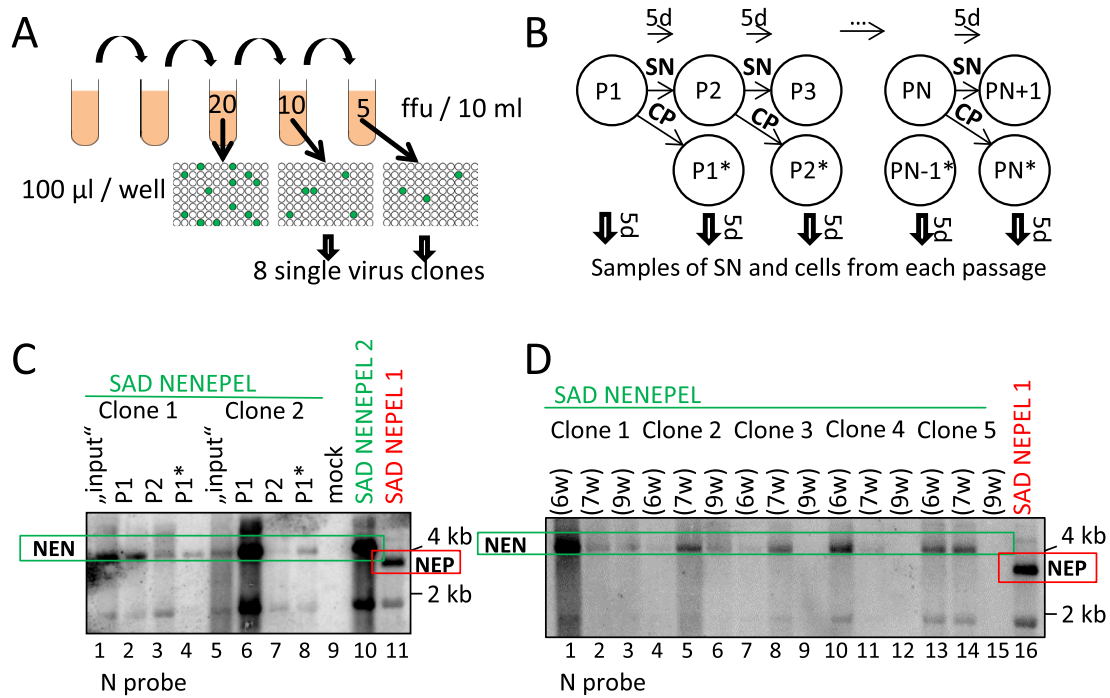
Figure 26: No recombination observed during passaging of SAD NENEPEL 2.
(A) Different clones of SAD NENEPEL 2 were isolated by serial dilution to calculated 20 ffu , 10 ffu and 5 ffu / 10 ml. 100 µl were seeded per 96 well. From the two highest dilutions 8 single virus clones were obtained. (B) Isolated clones were passaged during 9 weeks in cell culture. The passaging scheme is indicated. (SN = supernatant, CP = cell passage). (C) and (D) Northern blot analysis was performed with total RNA isolated at different time points after onset of passaging. RNA isolated from SAD NENEPEL 1 and SAD NENEPEL 2 served as negative and positive controls. A radioactively labeled probe against the N gene was used to detect the subgenomic fragments. Input and early passages are shown in (C), later passages in (D).

The RNAs from cells infected with the single virus clones and their passages were subjected to Northern blot analysis. As controls, RNAs isolated from cells infected with SAD NEP(bi)EL 1, SAD NENEPEL 2 or from un-infected cells were loaded. An N probe was used to detect sub-genomic RNA fragments. Figure 26C shows that clone 1 and clone 2 (P1) as well as the passages thereof (P2 and P1*) retain the un-recombined pattern of sub-genomic RNAs similar to SAD NENEPEL 2. The same was true for the other isolated clones (not shown). Further passaging for up to 9 weeks did not change this pattern (figure 26D). This strongly indicates the lack of recombination during RABV replication and suggested that recombination leading to the different SAD NENEPEL viruses has occurred rather in the cDNA plasmids before or after transfection or during T7 transcription in transfected cells.

3.3.11 SAD NENEPEL 2 – deeper analysis

As SAD NEP(bi)EL 1 happened to be the product of a recombination event, the un-recombined SAD NENEPEL 2 was subjected to deeper analysis. BSR T7/5 cells were infected

with SAD NENEPEL 2, one passaged SAD NENEPEL 2 single virus clone (SAD NENEPEL 2 pass), SAD NEP(bi)EL 1, SAD L16, SAD NEN, SAD EP and SAD EL, at an MOI of 0.05 or were left un-infected. 96 h p.i. the cells were detached using PBS-EDTA and the suspension was divided into 2 halves. One half was lysed in WB buffer for analysis of the protein expression and the other half was used to isolate total RNA.
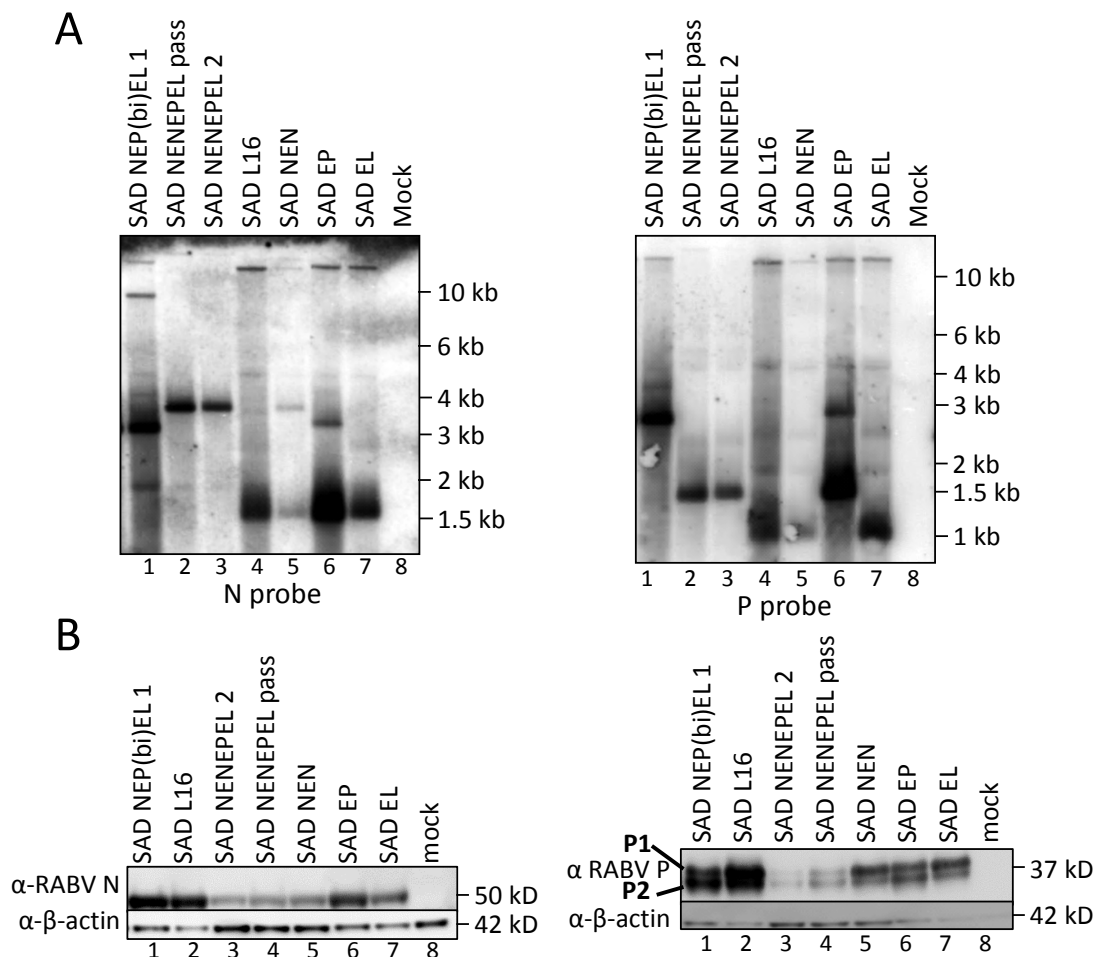

Figure 27: Unrecombined SAD NENEPEL – a closer look.
(A) BSR-T7/5 cells were infected with SAD NENEPEL 2(5.1) a single clone isolated from SAD NENEPEL 2 or SAD NENEPEL pass, virus passaged for 12 weeks at MOI=0.05. As controls the cells were infected with the same MOI with the recombined SAD NENEPEL 1, SAD NEN, SAD EP, SAD EL, SAD L16 or not infected.96 h p.i. total RNA was isolated. Northern blot analysis using radioactively labeled probes against the N and P gene were used to detect genomic and subgenomic RNA fragments. (B) 50 per cent of the infected cells from (A) were lysed and used for Western blot. Anti-P and anti-N antibodies were used to detect viral proteins.

1 µg of the RNAs was subjected to Northern blot analysis using N and P probes (figure 27A). With both probes, SAD NENEPEL 2 pass and the input virus SAD NENEPEL 2 were indistinguishable (left and right panel – lanes 2 and 3). As expected, their genomes were significantly larger than the genome of SAD NEP(bi)EL 1 (both panels – lane 1). The bi-

cistronic NEN mRNA was detected at the correct height analogously to SAD NEN (left panel – lane 5). SAD NEN itself also appeared to be a mixture of 2 viruses with a recombination event having occurred between the 2 N genes. In this virus the correct bi-cistronic NEN mRNA was detected in addition to a mono-cistronic N mRNA, corresponding in size to the N mRNA of SAD L16 (left panel – lane 4). With the N probe also 2 genome bands were detected for SAD NEN. The smaller one, likely to result from recombination, was running at the same height as the SAD L16 genome, whereas the un-recombined genome was running significantly higher due to its double N gene. With the P probe for the SAD NENEPEL 2 virus and for SAD NENEPEL 2 pass (lanes 2 and 3) but not for the recombined virus SAD NEP(bi)EL 1, the monocistronic EP mRNA was detected running at the correct height, as seen for SAD EP (lane 6). The virus SAD EP(mono) was transcribing significantly larger amounts of mRNA compared to SAD L16. An N-EP mRNA was detected with both probes for SAD EP(mono) infected cells. This is assumed to result from read-through of the virus polymerase during transcription and is often seen as well for SAD L16. Due to the high-transcription phenotype of SAD EP(mono), however it was more prominent. This N-EP read-through mRNA was running at the same position as the bicistronic NEP mRNA from the recombined virus SAD NEP(bi)EL 1.

Proteins expressed by the viruses were examined by Western blot analysis. Using the RABV N antibody (f 27B - left panel) it was observed that N protein levels varied between the viruses. SAD NENEPEL 2 and SAD NENEPEL 2 pass made significantly less protein (lanes 3 and 4) than SAD L16 (lane 2). The recombined variant SAD NEP(bi)EL 1 (lane 1) made levels of N protein comparable to the wild-type. Using the P antibody (right panel) a difference in ratio between P1 and P2 was observed for the viruses. While SAD L16 (lane 2), as well as the other viruses with a wild-type-like P gene (SAD NEN and SAD EL) make significantly more P1 than P2, for viruses translating their P from an EMCV virus this seems to be reversed. The recombined variant SAD NEP(bi)EL 1 was shown to transcribe only a bicistronic NEP mRNA and all the P protein must be translated from the EMCV IRES (lane 1). For SAD EP(mono) (lane 6), as well as the viruses SAD NENEPEL 2 and SAD NENEPEL 2 pass (lanes 3 and 4) this effect seems to be less prominent, but still the levels of P2 equal the P1 levels. The latter 3 viruses with their monocistronic EP mRNA therefore seem to initiate translation of P not only via the EMCV IRES, but also cap-dependently.

3.3.12 Failure of Pol-II dependent rescue of infectious RABV cDNA clones

The previous experiments were performed in BSR T7/5 cells and the transcripts from the infectious RABV cDNAs produced by the T7-pol in the cytoplasm. To try to recover the viruses SAD NENEPEL and SAD NEN2APEL in a Pol-II dependent manner the following different constructs were newly made (figure 28): pCAGGS-T7-HH_NEN2APEL_SC and pCAGGS-T7-HH_NENEPEL_SC (I), comprising the chicken β-actin promoter that is widely used for high level protein expression. pCR3-HH_NEN2APEL_SC and pCR3-T7-HH_NENEPEL_SC (II), comprise the immediate early CMV promoter. In pTre2hyg-T7-HH_NEN2APEL_SC and pTre2hyg-T7-HH_NENEPEL_SC (III), as TetOn constructs, the minimal CMV promoter was fused to a binding site of the Tet repressor. Due to cloning strategies or vector design all constructs initially have retained the T7 promoter between the Pol-II promoter and the HHRz processing the viral 5'-end. This allows control rescue experiments in BSR T7/5 cells to guarantee the integrity of the single infectious RABV cDNA clones. As a further control, pTre2hyg-HH_NEN2APEL_SC (IV) was constructed, lacking the T7 promoter.
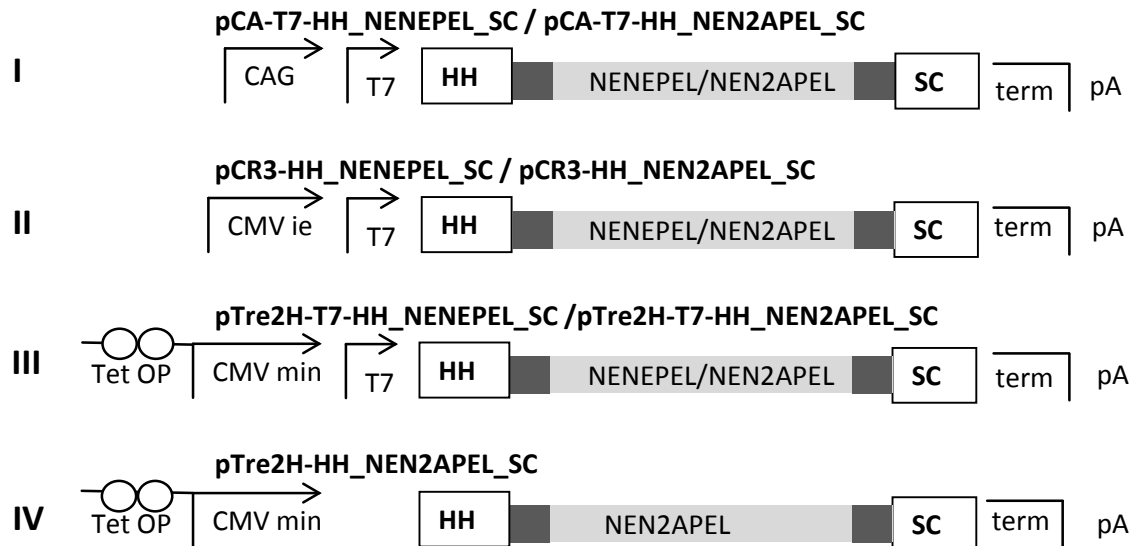
Figure 28: No Pol-II dependent rescue from infectious RABV cDNA clones.
(A) Constructs used to compare Pol-II and T7-pol dependent rescue: pCAGGS-T7-HH_NENEPEL_SC and pCAGGS-T7-HH_NEN2APEL_SC (I), pCR3-HH_NENEPEL_SC and pCR3-HH_NEN2APEL_SC (II), pTre2hyg-T7-HH_NENEPEL_SC and pTre2Hyg-T7-HH_NEN2APEL_SC (III), pTre2hyg-HH_NEN2APEL_SC (IV)

Rescue experiments with all constructs were first performed in BSR T7/5 cells. Recombinant viruses were successfully generated for all constructs, except for pTre2hyg-HH_NEN2APEL_SC (table 7). This showed that the cDNAs were intact, but indicated that

Table 7: Approaches for Pol-II dependent rescue of infectious clones.

	Cell line	Positive rescues
pCAGGS-T7-NEN2APEL	BSR-T7/5	15/19
	BSR	0/13
	HEK 293T	0/5
	Hep2	0/3
	Vero	0/3
pCAGGS-T7-NENEPEL	BSR-T7/5	8/13
	BSR	0/13
	HEK 293T	0/5
	Hep2	0/3
	Vero	0/3
pCR3-T7-NEN2APEL	BSR-T7/5	2/2
	BSR	0/2
	HEK 293T	0/2
pCR3-T7-NENEPEL	BSR-T7/5	4/4
	BSR	0/8
	HEK 293T	0/7
	HeLa	0/4
pTre2Hyg-NEN2APEL	BSR-T7/5	0/2
	BSR	0/2
pTre2Hyg-T7-NEN2APEL	BSR-T7/5	2/2
	BSR	0/2
pTre2Hyg-T7-NEN2APEL	BSR-T7/5	4/4
	BSR	0/4
pCAGGS-T7-NENEPEL + pSC6-T7neo	NA	2/4
	BHK-21	0/4

successful rescue into virus still was dependent on the T7 promoter. To determine the possibility of T7-pol independent rescue from the Pol-II promoters, various cell lines, BSR, BHK-21, HEK 293T, NA, Hep2 and Vero cells were transfected with the different constructs using either $CaPO_4$, Lipofectamine 2000, or PEI. None of the transfections led to the successful recovery of recombinant RABV (table 7).

Although RABV can grow on all of the used cell lines, cellular restriction factors like an intact IFN system may turn an already inefficient rescue into a rescue that is impossible. To determine if this is the case, 5 µg pCAGGS-T7-HH_NENEPEL_SC were co-transfected with 2 µg pSC6 T7-neo, a plasmid expressing the T7-pol, into NA cells using Lipofectamine 2000. SAD NENEPEL could be recovered from cDNA in the presence of T7-pol (table 7). These results indicated that the failure of virus rescue dependent on the Pol-II promoters is not due to the choice of cell lines but to the nuclear DNA promoters.

3.3.13 Failure of Pol-II dependent rescues due to lack of protein expression – convicting the ribozymes

To find out the reason for the inability of the infectious cDNA clones to be rescued via Pol-II promoters, the construct pCR3-HH_NENEPEL_SC and as controls pCR3-P or pCAGGS-P were transfected in either BSR T7/5 cells or HEK 293T cells using Lipofectamine 2000. As further controls cells were left untransfected. 48 h p.t. the cells were lysed and Western blots were performed. Using an antibody against RABV P it was obvious that P protein was made from pCR3-HH_NENEPEL_SC in BSR T7/5 cells, but not in HEK 293T cells (figure 29B - lane 3) and that the expression pattern was comparable to that of pTIT-P (lane 6) that has only the T7 promoter. This was not due to a defect of the CMV promoter in HEK 293T cells, as from pCR3-P the P protein was expressed even higher than in BSR T7/5 cells (lane 4). Similar results were obtained when transfecting pCAGGS-T7-HH_NENEPEL_SC or pTre2Hyg-T7-HH_NENEPEL_SC (not shown). Substantial amounts of proteins were only detected when the respective RNAs were transcribed by T7-pol, but not when transcribed from Pol-II promoters.

To narrow down the reason for the lack of protein expression, two new smaller constructs were made, pCR3-HH_NEP(mono) and pCR3-HH_NPVP(bi) (figure 29A-IV). Both contain the CMV immediate early promoter followed by the T7 promoter. Downstream of the T7 promoter there is the cDNA coding for an HHRz and about one third of the RABV antigenome

until the end of the P gene. The gene border between N and P is replaced by an EMCV IRES or PV IRES, respectively. Both constructs were transfected into BSR T7/5 cells and HEK 293T cells. As observed before, the EMCV IRES but not the PV IRES was able to translate sufficient protein in BSR T7/5 cells. In HEK 293T cells, however, none of the constructs was expressed at detectable levels (figure 29B – lanes 1 and 2).
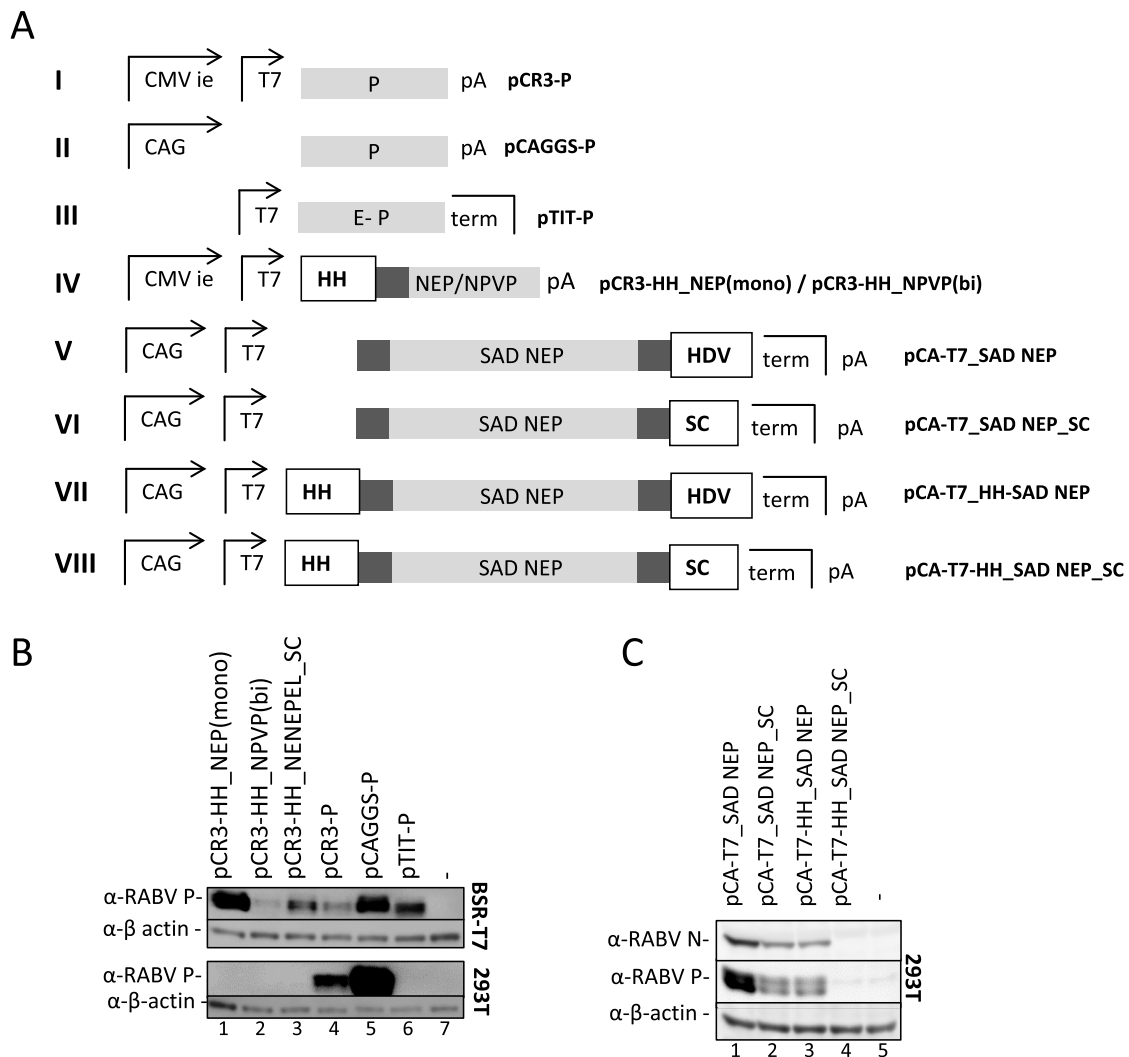

Figure 29: Failure of Pol-II dependent rescue from infectious RABV cDNA clones due to lack of protein expression.
(A) Constructs used to examine T7-pol and Pol-II dependent protein expression: pCR3-P (I) pCAGGS-P (II), pTIT-P (III), pCR3-HH_NEP(mono) and pCR3-HH_NPVP(bi) (IV), pCA-T7_SAD NEP (V), pCA-T7_SAD NEP_SC (VI), pCA-T7_HH_SAD NEP (VII), pCA-T7_HH_SAD NEP_SC (VIII). (B) BSR-T7/5 cells and HEK 293T cells were transfected with 2 µg of pCR3-HH_NEP(mono), pCR3-HH_NPVP(bi), pCR3-T7-HH_NENEPEL_SC, pCR3-P, pCAGGS-P, pTIT-P using Lipofectamine 2000 or not transfected. 48 h p.t. the cells were lysed and Western blots were performed using anti-P and anti-actin antibodies to compare levels of P protein. (C) 5 µg of pCA-T7_SAD EP, pCA-T7_SAD EP_SC, pCA-T7-HH_SAD EP or pCA-T7_SAD EP_SC were transfected into HEK 293T cells using PEI. As control cells were left untransfected. 48 h p.t. the cells were lysed and Western blots were performed using anti-RABV-P, anti-RABV-N and anti-actin antibodies to compare levels of protein expression.

The discrepancy between cytoplasmic T7-pol dependent expression and nuclear Pol-II dependent expression observed for pCR3-HH_NEP(mono) let us come to the possibility that

either the transcribed RNA is degraded, or not exported adequately from the nucleus. In Pol-II dependent cellular mRNAs the 5'-cap structure and the 3'-poly(A) tail are responsible for RNA stability, as well as for export into the cytoplasm. In the full-length constructs, however, due to processing of the RABV genomic RNA ends by ribozymes, both are cleaved off. To test the influence of ribozymatic end-processing on protein expression from RABV full-length cDNAs 4 new constructs were generated, all based on the pCAGGS plasmid and all consisting of the RABV cDNA for SAD EP(mono). They differed in regard to the ribozyme sequences at the 5' and 3'-end of the RABV cDNA. The first construct, pCAGGS-T7-SAD NEP(mono) (figure 29A-V) comprises the T7 promoter, followed by three G residues followed by the SAD EP(mono) cDNA and the HDV ribozyme, shown to cleave poorly *in vitro* (→3.1.4). pCAGGS-T7_SAD NEP(mono)_SC (VI) containes the SC1 ribozyme instead of HDV. pCAGGS-T7-HH_SAD NEP(mono) (VII) comprises the T7 promoter followed by an HHRz processing the antigenomic 5'-end. pCAGGS-T7-HH_SAD NEP(mono)_SC (VIII), in analogy to the Pol-II full-length RABV constructs tested so far, comprises both the HHRz and SC1. HEK 293T cells were transfected with 5 µg of either pCAGGS-T7_SAD NEP(mono), pCAGGS-T7_SAD NEP(mono)_SC, pCAGGS-T7-HH_SAD NEP(mono) or pCAGGS-T7-HH_SAD NEP(mono)_SC, using PEI, or were left untransfected. 48 h p.i. the cells were lysed and subjected to Western blot analysis. Antibodies against RABV P, RABV N and β-actin were used to detect levels of the respective proteins. The construct without a 5'-HHRz and with the poor cleaving HDV at the 3'-end, pCAGGS-T7_SAD NEP(mono) was expressing substantial amounts of P protein (figure 29C – at top - lane 1). When, however, either the 5'-cap or the 3'-poly(A) tail were cleaved off due to an HHRz (lane 3) or the better cleaving SC1 (lane 2), levels of RABV P translated from the respective full-length RNAs were significantly reduced. The combination of both ribozymes (lane 4), completely abolished expression of RABV P. Interestingly, due to the Pol-II promoter upstream of the RABV sequences, the N protein was translated cap-dependently from these constructs (figure 29C – middle) as could be seen with the anti-RABV N antibody. As for the P protein, the N expression pattern depended on the 5' and 3'-end processing ribozymes.

3.3.14 Pol-II dependent infectious RABV cDNA clones - deconstructing the construction

The construct pCAGGS-T7_SAD NEP(mono), lacking a 5'-processing HHRz and containing only the inefficiently cleaving HDV sequence to process the 3'-end resulted in substantial amounts of P protein expression upon transfection and nuclear Pol-II dependent transcription. Due to the Pol-II mediated capping of the transcripts also N protein was made.

In order to express also the L protein from that construct, the EMCV IRES sequence was inserted downstream of the G/L gene border and upstream of the RABV L gene AUG. Thereby the construct pCAGGS-T7_NEP(mono)EL was generated (figure 30-I). The same was done for pCAGGS-T7_SAD NEP(mono)_SC, resulting in pCAGGS-T7_NEP(mono)EL_SC (II). The latter construct was expected to result in significantly less N, P and L proteins expressed from the full-length RNA due to the better cleaving SC1. However, more antigenome-like RNAs having the correct 3'-ends were anticipated.
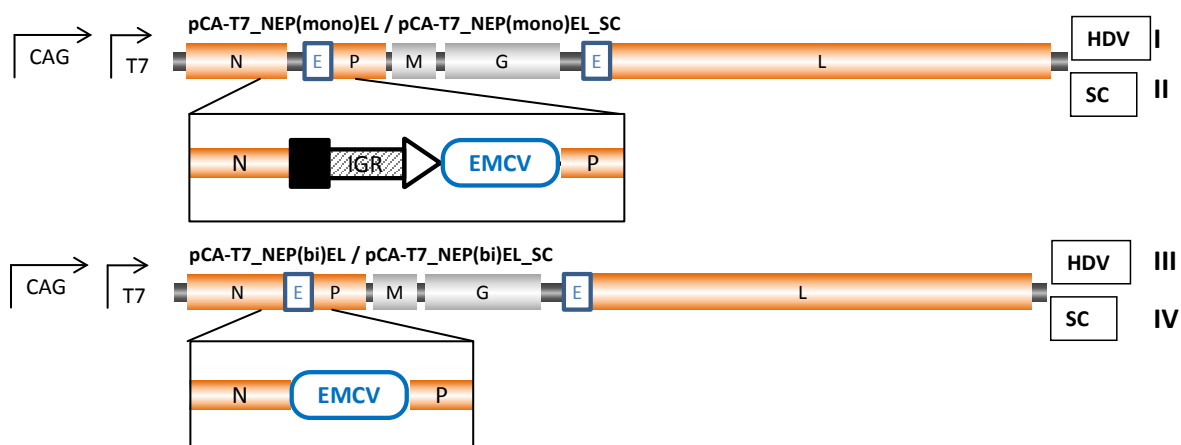

Figure 30: Pol-II-dependent single infectious cDNAs.
Genome organization of pCAGGS-T7_NEP(mono)EL (I), pCAGGS-T7_NEP(mono)EL_SC (II), pCAGGS-T7_NEP(bi)EL (III) and pCAGGS-T7_NEP(bi)EL_SC (IV). Note that all constructs comprise neither a 5'-HHRz nor an IRES element upstream of the N ORF. E: EMCV IRES, IGR: intergenic region.

To test if recombinant virus could be recovered from these constructs, dependent on the cellular Pol-II, 5 µg of either pCAGGS-T7_NEP(mono)EL or pCAGGS-T7_NEP(mono)EL_SC were transfected into HEK 293T cells or into BHK-21 cells. From pCAGGS-T7_NEP(mono)EL, one single rescue experiment out of 12 was successful in HEK 293T cells (table 8). For pCAGGS-T7_NEP(mono)EL_SC all rescue attempts failed. In BHK-21 cells also no virus could be recovered from any construct. Most probably this was due to the lower transfection efficiency that was observed for this cell line with the reporter construct pCAGGS-eGFP (not shown). These results show that it is indeed possible to recover recombinant RABV from a

single infectious cDNA clone dependent on Pol-II transcription. However, this system appears to be very inefficient.

SAD NEP(mono)EL the virus recovered from pCAGGS-T7_NEP(mono)EL should resemble the virus SAD NENEPEL 2 (→3.3.6 →3.3.9) in all features but the second N gene and thus a slightly smaller genome. Therefore, like SAD NENEPEL 2, SAD NEP(mono)EL is assumed to be attenuated. As the recombined SAD NEP(bi)EL 1 was found to grow significantly better (→3.3.9) constructs that could give rise to such a virus were generated. The plasmids pCAGGS-T7_NEP(bi)EL (figure 30-III) and pCAGGS-T7_NEP(bi)EL_SC (IV), with the better cleaving SC1, were made by replacing the N/P gene border by an EMCV IRES sequence. Therefore these viruses should transcribe a bicistronic NEP mRNA. In order to translate the L protein from full-length RNAs, again the EMCV IRES sequence was inserted downstream of the G/L gene border and upstream of the L gene AUG.

Table 8: Pol-II dependent rescue of infectious clones.

	Cell line	1.Pass (3d)	2.Pass (7d)	3.Pass (11d)
pCA-T7-NEP(mono)EL	293T	0/12	1/12	1/12
	BHK-21	0/12	0/12	0/12
pCA-T7-NEP(mono)EL_SC	293T	0/12	0/12	0/12
	BHK-21	0/12	0/12	0/12
pCA-T7-NEP(bi)EL	293T	0/12	2/12	2/12
	BHK-21	0/12	0/12	0/12
pCA-T7-NEP(bi)EL_SC	293T	0/6	7/12	6/12
	BHK-21	0/12	0/12	0/12

Both constructs pCAGGS-T7_NEP(bi)EL and pCAGGS-T7_NEP(bi)EL_SC were transfected into either HEK 293T or BHK-21 cells. In BHK-21 cells again all rescue attempts failed. With pCAGGS-T7_NEP(bi)EL, 2 out of 12 rescue experiments in HEK 293T cells resulted in successful recovery of SAD NEP(bi)EL (table 8). With pCAGGS-T7_NEP(bi)EL_SC, however,

more than 50 per cent of the rescue approaches in HEK 293T were positive. This again demonstrates the importance of the precise 3'-end for RABV RNAs. The benefits from better processed 3'-ends seem to overweigh the disadvantages of lower protein expression in this case.

Northern blot and Western blot analyses with SAD NEP(bi)EL and SAD NEP(mono)EL revealed, that indeed the former virus translates the N and P proteins from a bicistronic NEP mRNA, whereas the latter virus expresses both proteins from monocistronic mRNAs, respectively (data not shown). Also the better growth kinetics of SAD NEP(bi)EL, in comparison with SAD NEP(mono)EL, was again confirmed experimentally (not shown).

3.3.15 Pol-II dependent rescue of SAD L16 – a 2-plasmid system

The rescue of RABV from a single infectious cDNA clone apparently faces the dilemma that either large amounts of proteins are made from primary transcripts with mainly in-precise RNA ends or that most of the ends are precise, on the expense of significantly lower expression of "helper" proteins. To solve this, a 2-plasmid system could be the method of choice. The cDNA to be rescued can be optimized for this purpose, thus having the wild type or wild type-like genome sequence (e.g. SAD L16) and more importantly, efficiently processed genome ends. The second plasmid, expressing the "helper" proteins, on the other hand, can lack 5' and 3'-ribozyme sequences.

To check the feasibility of such a 2-plasmid system, RABV full-length cDNA constructs pCAGGS-T7_L16 (lacking the 5'-HHRz and with HDV to process the 3'-end), pCAGGS-T7_L16_SC (lacking the 5'-HHRz but with SC1 to process the 3'-end) and pCAGGS-T7-HH_L16_SC (comprising the 5'-HHRz and the 3'-SC1) were made comprising all the cDNA sequence of RABV SAD L16 and differing only in the flanking ribozyme sequences. To test for different promoters, also pCR3-HH_L16_SC (comprising the 5'-HHRz and the 3'-SC1) was constructed.

5 µg of either of the 4 plasmids pCAGGS-T7_L16, pCAGGS-T7_L16_SC, pCAGGS-T7-HH_L16_SC or pCR3-HH_L16_SC were co-transfected together with 5 µg pCAGGS-T7_NEP(mono)EL into HEK 293T cells or BHK-21 cells, using the CaPO4 based ProFection® mammalian transfection system (Promega). Supernatants were passaged onto fresh cells after 3 d, 7 d and 11 d to identify positive rescue events. Indeed RABV could be rescued from virtually all transfections (table 9). Thus the efficiency of Pol-II dependent RABV rescue from

cDNA could be increased by the application of the 2-plasmid system. Notably, constructs with a 5'-HHRz sequence and a 3'-SC1 sequence appeared to be the most efficient, whereas pCAGGS-T7_L16, lacking the 5'-HHRz and only comprising the poorly cleaving 3'-HDV showed a reduced rescue efficiency. Noteworthy, the size of the foci after passaging of the supernatants and staining by a FITC-labeled anti-RABV N antibody indicated that the vast majority of the rescued virus indeed was SAD L16 (not shown). However, the presence of contaminating residual SAD NEP(mono)EL, derived from the "helper" construct cannot be excluded.

Table 9: Pol-II dependent rescue of SAD L16 – 2-plasmid system.

pCA-SAD NEP(mono)EL +		1.Pass (3d)	2.Pass (7d)	3.Pass (11d)
pCA-T7_L16	293T	0/2	0/2	1/2
	BHK-21	0/2	0/2	0/2
pCA-T7_L16_SC	293T	0/4	3/4	3/4
	BHK-21	0/4	0/4	0/4
pCA-T7-HH_L16_SC	293T	2/4	3/4	4/4
	BHK-21	0/4	0/4	0/4
pCR3-HH_L16_SC	293T	0/2	2/2	2/2
	BHK-21	0/2	0/2	0/2

In summary, these experiments provided proof-of-principle that RABV can be rescued from single infectious cDNA clones. Moreover, recovery was possible utilizing the endogenous cellular Pol-II for transcription of RABV. These achievements provide the basis for further development and improvement of constructs that can be used for generating animal models with genetically encoded RABV expression.

4 Discussion

4.1 Rabies virus vectors delivering RNAs

The aim of these studies was to evaluate the possibilities to use RABV, a cytoplasmic RNA virus, as a vector to deliver shRNAs for gene knock down.

In brief, although it was not possible in this work to knock-down specific genes by RABV delivered shRNAs, bottlenecks of the RABV system that are responsible could be determined experimentally. Moreover, it was possible to recover viable recombinant RABV containing an internal ribozyme cassette which was shown to process an shRNA of interest *in vitro* and *in vivo*. Indeed, knowledge gained from ribozyme cleavage assays in this part was a prerequisite for the improvement of the RABV rescue system described in the second part of this thesis. The main reasons for the failure of RABV–encoded and ribozymatically processed shRNAs to knock down genes are most likely the low levels of the processed product, mismatches that had to be introduced to allow cleavage by the ribozymes, and the chemistry of 5' and 3'-ends generated by the ribozymes. This will be discussed in the following chapters.

4.1.1 Biological limitations of RABV vectors for the delivery of shRNAs.

Retroviruses (Barton and Medzhitov, 2002), lentiviruses (An et al., 2003), baculoviruses (Ong et al., 2005) adenoviruses (Krom et al., 2006) and AAV (Tomar et al., 2003) have been used as vectors to deliver shRNAs in cell culture and *in vivo* so far. RABV as an NNSV has certain disadvantages in terms of siRNA or miRNA delivery. For RNA viruses, with the exception of retroviruses, the application as a vector to deliver shRNAs has not been demonstrated so far and no RNA virus at all has been described to encode any miRNAs.

Importantly, RNAi is a major cellular defense mechanism in insects and plants against different viruses and many viruses have evolved anti-RNAi functions (reviewed in Haasnoot et al., 2007; Voinnet, 2005). Also for mammalian viruses mechanisms to block RNAi are known, examples are the HIV Tat protein (Bennasser et al., 2005) or Vaccinia virus E3L and influenza A virus NS1 (Delgadillo et al., 2004; Li et al., 2004), the latter two however were tested only in insect and plant systems. Most recently, Ebola virus VP30, VP35 and VP40

have been described to interfere with the RNAi machinery (Fabozzi et al., 2011) as the first anti-RNAi function in a mammalian NNSV.

For RABV no such inhibition of RNAi is known and neither did we observe an anti-RNAi function experimentally. The A549-LR-siGFP cells, expressing an shRNA against eGFP, in our hands, were still able to knock-down eGFP significantly when infected with RABV. In addition, it has been shown that siRNAs can be used to inhibit RABV replication in cell culture and *in vivo* in mice (Brandao et al., 2007; Gupta et al., 2012; Halbach, unpublished results; Israsena et al., 2009; Sonwane et al., 2011). This is true for many NNSV members. The first human pathogenic virus that was inhibited with siRNAs was RSV (Bitko and Barik, 2001). For morbilliviruses very recently the upcoming of escape mutations upon treatment with siRNAs was detected and analyzed. This indicates that a rather weak or no viral function against the RNAi machinery is present (Holz et al., 2012).

The second obstacle of RABV as an NNSV is its RNA genome together with the fact that it only replicates in the cytoplasm. During replication the genome is transcribed into antigenome and vice versa. Both RNAs are encapsidated into helical NC structures during replication, thus inhibiting any formation of secondary structures as hairpins. This is underlined by our findings that it is possible to generate RABV containing intra-genomic ribozymes. Although some of these viruses were difficult to rescue and could only be generated by the improved rescue system, once their genomes were packaged accurately, the ribozymes did not impair growth and viability. Most likely this is because in an NC structure these ribozymes could not fold any more.

RABV mRNAs have, similar to Pol-II transcripts, a 5'-cap structure and a 3'-poly(A) tail. For Pol-II derived miRNAs or shRNAs both are cleaved off by Drosha/DGCR8. This, however, takes place in the nucleus and therefore cannot be expected for RABV mRNAs. Indeed, as shown in this thesis, RABV transcribing an eGFP mRNA with the miRNA 23-2 from MCMV in the 3'-UTR could not produce functional miRNAs as revealed by a reporter system. The same was true for an shGFP hairpin transcribed from an extra gene in a RABV vector. No knock-down activity of GFP was observed for this verified sequence when it was delivered by RABV. Most probably this is due to the inaccessibility of the Drosha/DGCR8 complex for the cytoplasmic virus derived mRNA and vice versa. Several approaches to target the RABV RNAs to the nucleus failed and are not shown in this work.

Unlike for cellular (or retrovirus) and DNA virus derived miRNAs and shRNAs, the possibility to transcribe RABV RNAs from different promoters is not given. RABV has only two mechanism of RNA synthesis, one mechanism to make 5'-capped and 3'-polyadenylated mRNAs from transcription start sites in the RABV intergenic regions and one mechanism to replicate the genome and antigenome starting from the genomic or antigenomic promoter in the genome termini, respectively. Transcripts from the latter two start with a 5'-ppp and terminate with a 3'-OH, however the genome ends are essential for the viability and manipulation like introducing hairpins would destroy the promoters and not be tolerated.

In summary, although having an RNA genome no miRNAs so far have been reported to be made by any RNA virus. RABV was not observed to interfere with the RNAi machinery, as is reported for several other viruses. However, the major disadvantage of RABV as a cytoplasmic RNA virus for shRNA or miRNA delivery seems to be the lack of processing by nuclear enzymes. Therefore the next approach was to deliver shRNAs that resemble cytoplasmic intermediates of the miRNA or shRNA pathway.

4.1.2 Approaches to deliver Dicer substrates by RABV vectors – ribozymes

As RABV delivered shRNA precursors could not be processed by nuclear enzymes of the miRNA or shRNA pathway we aimed at producing RABV transcripts resembling Dicer substrates. In the miRNA pathway, mostly Pol-II transcribed pri-miRNAs are processed by the nuclear Drosha/DGCR8 complex into about 60 nts long pre-miRNA hairpins that contain now a 3'- 2 nts overhang at the cleavage site. Exported into the cytoplasm by Exportin 5 (Lund et al., 2004), they are further processed by Dicer into RNA duplexes from which one strand, the passenger strand, that has the same sequence as the target, is removed, whereas the so-called guide strand being antisense to the target site (which is located primarily in the 3'-UTR of mRNAs) is loaded into the RISC to repress translation from this mRNA (reviewed in Bartel, 2004; Cullen, 2004; Li and Liu, 2011).

Short hairpin RNAs have either been made synthetically (Paddison et al., 2004; Siolas et al., 2005) or expressed from Pol-II (Zhou et al., 2005) and Pol-III (Paddison et al., 2004) promoters. Depending on their origin they enter into the processing pathways at different stages. The Pol-II derived shRNAs for example have a 5'-cap structure and a 3'-poly(A) tail and therefore, like pri-miRNAs, must be cleaved by Drosha/DGCR8. Pol-III transcribed shRNAs however start with a 5'-ppp and are designed to terminate exactly in such a way that

they have a 2 nt overhang at their 3'-end upon hairpin formation. Therefore, they resemble already the Drosha/DGCR8 products that only differ in having a monophospate at their 5'-end, and only have to be exported by Exportin 5 from the nucleus. Synthetic shRNA have a 5'-monophosphate and are delivered i.e. by lipofection. They, once in the cytoplasm, directly can be processed by Dicer.

The first approach to achieve RABV delivered Dicer substrates was to cleave off the 5'-cap and the 3'-poly(A) tail by *cis*-active ribozymes. For removal of the 5'-cap an HHRz was chosen that has been shown to produce an exact 5'-end for rescue of measles virus and BDV (Martin et al., 2006). HHRzs were first described as autocatalytic RNAs in plant viroids (Buzayan et al., 1986; Hutchins et al., 1986; Prody et al., 1986). All HHRz share structural similarities like the presence of three stems and a catalytic pocket. Cleavage produces a cyclic 2', 3'-monophosphate at the cleaved off ribozyme end and a 5'-OH at the processed RNA (Birikh et al., 1997; Uhlenbeck, 1987; van Tol et al., 1990).

In vitro-tests conducted in this work with the HHRz revealed its functionality and efficiency as we observed about 90 % of the RNA to be processed. The HHRz was placed in an orientation that allowed its correct folding and cleavage in RABV mRNAs (or in the antigenome). Although during rescue of the virus the antigenome-like RNA transcribed by T7-pol initially lies naked in the cytoplasm before its encapsidation by N protein, it was possible to generate recombinant RABV containing the HHRz sequence. The rescue of this critical virus did not seem to be impaired significantly in comparison with wild-type virus. This might indicate a lower *in vivo*-activity of the ribozyme. However in the second part of this thesis, it is shown that an HHRz processing the 5'-end of the antigenome-like RNA *in vivo* significantly increases the rescue efficiency and minigenome activity (Ghanem et al., 2012). Also as shown in part 3 of this thesis, IRES mediated translation from a Pol-II transcript decreased significantly, dependent on the ribozymes. These findings emphasize the *in vivo*-activity of the ribozyme although not allowing a direct quantitative comparison with the *in vitro*-activity.

Analogously to the 5'-cap structure the 3'-poly(A) tail should be cleaved off from the RABV derived mRNA by a ribozyme. Therefore an HDVagRz was applied. The HDVagRz was discovered as a self-cleaving RNA sequence in the Hepatitis Delta virus antigenome. The

cleavage reaction it produces a cyclic 2', 3'-monophosphate at the processed RNA and a 5'-OH at the cleaved off ribozyme end (Sharmeen et al., 1988).

The HDVagRz I tested first was the 84 nt "core" sequence that has been used to process the 3'-end of the antigenome-like RNA in the first rescue system for RABV developed in our lab (Schnell et al., 1994). This "core" sequence initially was reported to be the HDVagRz (Perrotta and Been, 1991), however in more recent publications longer sequences are considered to constitute the HDVagRz (Perrotta and Been, 1998; Perrotta et al., 1999). The initial "core" sequence was abbreviated in this work as HDV and the two newer versions we chose, "supercut 1" (SC1) and "supercut 2" (SC2) as we found both to cleave significantly better *in vitro*.

The HDVagRzs again were inserted in an orientation that allowed cleavage to occur (either in the antigenome or) in the viral mRNAs generated from the extra transcription unit between the G and the L gene. Interestingly, RABV containing internal SC1 or SC2 could only be rescued after the significant improvement of the rescue system (Ghanem et al., 2012) shown in the second part of this thesis. This strongly indicated the *in vivo*-activity of SC1 and SC2. A further proof was the significantly increased rescue efficiency itself, which depended on the replacement of HDV with SC1 to process the 3'-end of the RABV antigenome-like RNA.

In summary, evidence was provided that it is possible to generate recombinant RABV containing diverse ribozymes within their genome. These ribozymes may interfere with virus rescue, when they cleave the naked full-length RABV RNA. Once the full-length RNAs are encapsidated by N protein and rescued into virus, however, the ribozymes can only fold in the virally transcribed mRNAs, but not in the tightly packaged RABV N-RNA genome or antigenome.

4.1.3   Limits derived from the ribozyme cassette – the perfectly processed hairpin

For initial studies evaluating the HHRz cleavage properties spacer sequences were introduced between the HHRz and the shRNA. To become Dicer substrates, however, the shRNAs have to be processed with an exact 5'-end. This was also confirmed experimentally. RABV transcribed shRNAs containing spacer sequences between the HHRz and the shGFP failed to induce RNAi.

To produce an exact end, the 5'-end of the sequence of interest has to be inserted immediately downstream of the cleavage site of the HHRz. The sequence following the cleavage site (the 5'-end of interest) also has to build a duplex with the 5'-end of the ribozyme, forming one of the ribozyme's stem structures. Therefore, the 5'-end of the HHRz has to be manipulated to allow this base pairing. The same HHRz core sequence was chosen and the shGFP sequence introduced directly downstream the cleavage site. The 5'-end of the HHRz was changed to allow base pairing with the 4 nts downstream of the cleavage site. RNA secondary structure predictions, however indicated, that despite of the antiparallel design of the HHRz 5'-end, the sequence downstream the cleavage site (being at the same time the 5'-end of the shGFP) would rather base pair with its counterpart at the 3'-end of the shGFP. Therefore, the HHRz was predicted not to fold correctly in this construct. *In vitro-*cleavage assays confirmed these predictions and the respective RABV transcribing this construct, SAD G_HH-SH-SC1, was not able to induce gene knock-down *in vivo*.

Knowing now that the HHRz could not process the 5'-end of shGFP due to the direct proximity to the hairpin on one hand and the need for exact processing on the other hand, not many possibilities remained. One option was the introduction of mismatches into the hairpin close to its end. Computational analyses predicted a correct folding for the HHRz if, at positions 3 and 4 from the 5'-end of the shGFP, mismatches were introduced. The HHRz should cleave and release a shGFP containing 2 mismatches. These mismatches, however give rise to two new major problems.

First, the HSmm due to its mismatches will most likely, after Dicer cleavage, enter the fate of miRNAs that often contain mismatches instead of siRNAs with their perfect complementary. Regarding RNAi it has been shown in *D. melanogaster* and in *C. elegans* that only a few molecules of dsRNA are sufficient for a significant knock-down of a target gene (Fire et al., 1998; Kennerdell and Carthew, 1998). This self-amplification of the RNAi trigger, due to mRNA degradation makes siRNAs by far more potent than miRNAs (and the knock-down effect lasts longer). In contrast, miRNAs only lead to a translational repression upon base-pairing with their target in the 3'-UTR of an mRNA.

The second critical point is that, assuming Dicer will cleave the hairpin, the resulting RNA duplex will now thermodynamically be more unstable at the 5'-end of the progenitor hairpin. For miRNAs a functional asymmetry has been described, in a way that the strand of

the duplex, that is un-winded easier from its 5'-end will be incorporated into RISC, while the other strand is degraded (Khvorova et al., 2003; Krol et al., 2004; Schwarz et al., 2003). Therefore the strand derived from the 5'-end of the hairpin would be incorporated into RISC. This strand, however, is the passenger strand having the sense GFP sequence and not the desired guide strand with the antisense GFP sequence.

The first drawback of generating rather a miRNA instead of siRNA due to the mismatches has to be accepted as otherwise no efficient processing by the HHRz can be achieved. The latter problem, in regard to the thermodynamic stability, I intended to overcome by a little trick. The sense and antisense strand of the shGFP simply were exchanged in their position in the hairpin. In the new construct the antisense strand was now positioned at the 5'-end of the hairpin whereas the sense strand was located at the 3'-end. Again mismatches were introduced. Now, however, not the nts 3 and 4, counted from the 5'-end, were mutated, but their counterparts at the 3'-end of the hairpin (the sense strand). Again the correct folding of the HHRz was predicted due to the mismatches. The hairpin set free after processing by the ribozymes now has the antisense strand at the 5'-end and 2 mismatches. A hypothetic RNA duplex after Dicer cleavage will now be more unstable and easier to unwind from the 5'-end of the antisense strand. Therefore this strand now would be incorporated into RISC. ShRNAs usually have the sense strand (passenger strand) at their 5'-end and the antisense strand (guide strand) at their 3'-end. This is also labeled as "R-type" shRNA, as the loop is at the right hand side. It has been shown, however, that "L-type" shRNAs (left handed loop), where sense and antisense strand are interchanged, have similar knock-down efficiencies (Harborth et al., 2003). The new hairpin design in contrast to "SH", because of its complementary and the mismatches was labeled "HSmm". *In silico* secondary structure predictions indicated correct folding of the HHRz in this construct and were confirmed by *in vitro*-cleavage assays with mutated and un-mutated HHRz and SC1.

For the 3'-end no such structure predictions were possible with the applied software algorithms. The HDVagRz is by far more complex and tertiary structures like pseudoknots play a role for its activity (Perrotta and Been, 1991; Wadkins et al., 1999). However *in vitro*-experiments demonstrated efficient cleavage of SC1 when fused directly downstream to the shGFP in constructs with (HSmm) or without (SH) mismatches. This might be facilitated by

the fact that the shGFP in order to be a Drosha/DGCR8 product or a Dicer substrate was designed with a 2 nts 3'-overhang.

Briefly, by a combination of theoretical thoughts on design, secondary structure predictions and *in vitro*-cleavage analysis solutions were found to overcome the natural limits of RABV in delivery of shRNAs. Initially, the HHRz was not able to cleave due to incorrect folding. This was solved by introducing mismatches into the hairpin. Those mismatches resulted in predicted incorporation of the wrong strand into RISC. To overcome this problem, sense and antisense strand of the hairpin were exchanged (from SH to HSmm).

4.1.4 The "perfectly processed" hairpin fails to knock-down its target gene *in vivo* – possible reasons

Recombinant RABV SAD G_HH-HSmm-SC1 transcribing the ribozyme cassette with the "perfectly processed" hairpin containing two mismatches (HSmm) could be recovered from cDNA. However, this virus, like all constructs tested before, failed to knock down its target gene. Neither in a dual luciferase system with a firefly luciferase reporter, comprising a GFP-sequence-tag in the 3'-UTR, nor in infected GFP expressing cells (not shown), any reduction of reporter gene expression upon virus infection was observed. The positive control, pSUPER-shGFP, where shGFP is transcribed from a nuclear Pol-III promoter, showed that the reporter system was susceptible to silencing.

To find possible reasons for the lack of knock-down activity, a miRNA-Northern blot was performed and showed that significantly less small RNAs were made from SAD G_HH-HSmm-SC1 than from pSUPER-shGFP. For pSUPER-shGFP two bands were detected, the band for the transcribed hairpin and a lower one that should reflect the products of Dicer cleavage. With the high transcription rate from pSUPER, obviously more RNA is made than can be processed by the RNAi machinery. In A549-LR-siGFP cells, that make the same hairpin as pSUPER-shGFP, but at lower levels, most of the RNA is processed by Dicer. For the RABV transcribed RNA it is obvious, that only very low levels of "perfectly processed" RNA hairpins are made by the ribozyme cassette. Visible bands running at a higher level reflect most probably RNA species where only one or none of the ribozymes were active. The ribozyme-processed bands however are only detected at the length of the hairpin state, indicating that this hairpin is not further processed by Dicer.

In summary this shows that the "perfectly processed" hairpin is indeed processed by ribozymes *in vivo*, although at very low levels. However, this ribozymatically processed hairpin is not further cleaved by Dicer. Together these two observations, low levels of product processed by the ribozymes and lack of further processing by Dicer, seem to be the main cause for the failure of the RABV SAD G_HH-HSmm-SC1 to knock down genes.

4.1.5 Low levels of the "perfectly processed" hairpin – A question of transcription efficiency?

There are several possible explanations for the presence of too low amounts of the "perfectly processed" hairpin, HSmm,. Either the overall levels of the RABV mRNA HH-HSmm-SC1 are too low due to inefficient transcription or degradation, or the HH-HSmm-SC1 containing mRNA is not processed at efficient rates into HSmm. There are some hints that incomplete processing of HH-HSmm-SC1 into HSmm indeed plays a role. In the miRNA Northern blot for SAD G_HH-HSmm-SC1 infected cells, fragments were detected running significantly higher than HSmm. These fragments however can be excluded to be mRNAs that cannot enter the gel because of their large size and therefore were neither detected in SAD G_shGFP infected cells. It is possible, that these higher bands represent RNA fragments in which only one of the ribozymes was active. This problem will be difficult to address, reasons might be a difference between the observed *in vitro*-cleavage and the *in vivo*-activity of the ribozymes. For ribozymes transcribed by T7-pol (mainly "naked" RNA) it has been shown that *in vitro* and *in vivo*-cleavage efficiencies are comparable (Chowrira et al., 1994). This was also confirmed in this thesis, as discussed above (→4.1.2). Poor *in vivo*-cleavage as suggested by the miRNA Northern blot could, however, derive from proteins associated with the RABV mRNAs. Cellular mRNAs transcribed by Pol-II are rather tightly packaged into cellular RNPs by proteins responsible for many steps, from splicing, nuclear export, protection against RNases to translation and degradation. Although the RABV transcription machinery is more simple and splicing, or nuclear export, do not play a role, it is most likely that cellular proteins will be attached to the viral mRNAs. However, the protein composition interacting with the virus transcripts is completely unknown. Therefore cellular proteins might bind the RABV mRNA and thereby interfere, at least partially, with correct folding of the ribozymes.

Low ratios of processed HSmm may at least partially derive from low levels of the RABV transcribed mRNA HH-HSmm-SC1. RABV transcription starts at the 3'-end of the genome and proceeds to the 5'-end by transcribing a 5'-ppp leader RNA and 5'-capped and polyadenylated mRNAs in the order 3'-leader-N-P-M-G-L-5'. After each gene that is transcribed, the polymerase stalls and reinitiates with a certain probability. The efficiency of reinitiation is dependent on the sequence and length of intergenic regions and the respective transcription start signals (Finke et al., 2000).

The HH-HSmm-SC1 construct is transcribed from an extra gene located between the G and the L gene of the RABV vector. The N/P gene border was introduced upstream of this extra gene to guarantee efficient re-initiation of transcription downstream of the G gene. This transcription start signal was shown to be very efficient (Finke et al., 2000) and the transcription unit between G and L is widely used for high level gene expression. For VSV it has been shown, however, that introducing genes more proximal or distal to the virus genome promoter increases or decreases gene expression, respectively (Wertz et al., 1998). This reflects a steep transcription gradient in which most transcripts are made from genes at the most proximal position.

Therefore more transcripts of HH-HSmm-SC1 should be expected if the extra gene would be introduced more upstream in the RABV genome. One possibility would be to introduce it downstream of the P gene. Theoretically even more transcripts could be expected if the extra gene would be inserted directly downstream of the leader. In part 3 of this thesis, however, it was shown, that extra sequences at the RABV leader-N gene junction and within the N coding region influence RABV viability (→3.3.5). As RABVs with mutations in this region were severely attenuated, it can be excluded that a shRNA located downstream of the leader will be tolerated. This problem could be addressed by RABV constructs similar to SAD N200EN described in part 3.

Low transcription rates of RABV mRNA HH-HSmm-SC1 may not only result from the relative downstream position between the G and the L gene within the RABV genome, but also from the hairpin structures within the ribozymes and the shGFP itself. During RABV replication these sequences seem to be tolerated well due to the direct encapsidation into N-RNA structures. However during RABV mRNA transcription the folding might interfere with the virus polymerase function and lead to premature termination of transcription. This was

observed during *in vitro*-transcription which, however, cannot be compared to RABV transcription. As growth kinetics and final titers of the shRNA containing RABV were similar to wild-type SAD L16 (not shown), transcription attenuation by the hairpin (which should affect expression of the downstream L) is unlikely. Also degradation is likely to occur, when 5'-cap structures and 3'-poly(A) tail are cleaved off from the transcripts.

4.1.6   The "perfectly processed" hairpin – not so perfect to be a Dicer substrate?

Not only were the shRNAs made from the RABV vector at low levels, there also appeared to be a block in further processing by Dicer. Whereas in A549-LR-siGFP cells also the levels of shGFP were relatively low, it was obvious that most of these Pol-III transcribed hairpins were further processed by Dicer. In cells infected with SAD G_HH-HSmm-SC1, this was not the case. To find possible explanations for this lack of Dicer cleavage one has to compare the features of the shGFP derived from Pol-III transcription in A549-LR-siGFP cells and the "perfectly processed" hairpin HSmm.

In A549-LR-siGFP cells the shGFP is transcribed from the human class III Pol-III promoter H1 (Mottet-Osman et al., 2007). Class III Pol-III promoters like H1 or U6 are widely used for the intracellular delivery of shRNAs as they have the advantage of an exact transcription start and termination at 5 thymidines in a row (Brummelkamp et al., 2002; Paddison et al., 2002). Also some endogenous miRNAs are made from Pol-III promoters (Borchert et al., 2006). These transcripts in contrast to Pol-II derived miRNAs have no flanking sequences and therefore will not depend on processing by Drosha/DGCR8 (Zeng and Cullen, 2005). Short hairpin RNAs, like miRNAs, are exported from the nucleus by Exportin 5 (Yi et al., 2003). For Exportin 5, direct interaction with Dicer has been shown (Bennasser et al., 2011; Lund et al., 2004). It is conceivable that this interaction also plays a role in the direct loading of the miRNA/shRNA to Dicer. The RABV derived HSmm is made in the cytoplasm and does not utilize the Exportin 5 pathway.

Another difference between shGFP and HSmm are the 2 mismatches, introduced to facilitate the ribozyme folding. They are thought to play a role in the further fate of the duplex after processing by Dicer as discussed above (→4.1.3).

The most important differences however, are the 5'- and 3'- ends of HSmm generated by the ribozymes. The HHRz after processing leaves a 5'-OH and the HDVagRz a cyclic 2', 3'-monophosphate at the hairpin RNA. Today it becomes inceasingly clear that the ends play a

crucial role in binding to shRNAs/miRNAs and in determining the cleavage site. The current model, derived from *in vitro*-assays and the crystal structure of *Giardia* Dicer, was that the 3'- end of shRNAs/miRNAs, a 2 nt overhang ending with a hydroxyl group, is recognized by the PAZ-domain of Dicer and fixed to measure 22 nt, the distance between the PAZ domain and the cleavage site (Macrae et al., 2006; Starega-Roslan et al., 2011; Vermeulen et al., 2005). A more recent work (Park et al., 2011) has shown with both, using recombinant human Dicer and in *D. melanogaster*, that the RNAs 5'-end, a monophosphate for cellular miRNAs or synthetic shRNAs, is important to the same extent for recognition and processing by Dicer. A 5'-pocket was identified, that is highly conserved in all analyzed species, but *Giardia* Dicer. For Pol-III derived shRNAs, comprising 5'-ppp, it is still unclear whether they can bind to the 5'-pocket, or if the triphosphate has to be hydrolized to monophosphate. Anyway, they are being processed by Dicer and are effective in knock-down.

Altogether, most probably the 5'-OH, and the cyclic 2', 3'-monophosphate are structurally not compatible with Dicer requirements for a 5'-monophosphate and 3'-OH. Furthermore, the mismatches that had to be introduced to allow the ribozymatic processing of HSmm might constitute an additional impairment in regard to the induction of knock-down. Therefore processing by ribozymes, as described here, does not seem to be the strategy of choice in order to produce Dicer substrate-like RNAs.

4.1.7 Future approaches - circumventing Dicer?

It becomes more and more clear that it is not feasible to deliver a Dicer substrate by a ribozyme cassette. The data obtained in this thesis therefore are in agreement with recent findings in the RNAi field. Future approaches thus have to apply completely new strategies.

One remaining option could be the direct processing of two antiparallel short RNAs, resulting in an siRNA duplex. Of course there will be major difficulties with this strategy. First, to generate two short RNAs instead of one hairpin, 4 internal ribozymes instead of 2 have to be introduced into the RABV genome. The two internal ribozymes were already challenging with respect to the recovery of recombinant RABV. Second, the transcription efficiency most likely will be impaired as well by four ribozymes. The relatively low amounts of the "perfectly processed" hairpin HSmm are considered to be due to factors such as premature termination of RABV transcription, degradation of cleaved products and partially malfunction of the ribozymes in context of a RABV mRNA, as discussed above. In a construct

with 4 ribozymes instead of 2, all these problems most probably will accumulate. An option to deal with this could be the delivery of the two strands required for an siRNA duplex by 2 separate RABV vectors, each transcribing and processing one strand by 2 ribozymes. This system will then depend on coinfection with these two RABV vectors.

For both systems delivering siRNA duplexes, by either one or two RABV vectors, it is an important question, weather the ribozyme derived ends will allow the strands to enter RISC. What has been studied so far with modified ends in siRNA is partially controversial. It was shown that conjugated Alexa-488 was tolerated in the sense strand at both ends and in the antisense strand at the 5'-end, but not at the 3'-end (Harborth et al., 2003). In another work, amino-modifications of siRNA ends were tolerated at all positions, but the antisense 5'-end (Chiu and Rana, 2002). A clear advantage arising from the siRNA duplex strategy is that it allows the duplexes with a perfect match, as no mismatches have to be introduced in order to allow processing by the ribozymes.

A variation of the "perfectly processed" hairpin, HSmm might also be an option to circumvent Dicer. The shRNAs I used contain a stem of 21 nt, the sequence of the anti-GFP shRNAs that were approved to function in the stably transduced A549-LR-siGFP cells, as well as with transient transfection the pSUPER-shGFP plasmid. The use of hairpins longer or shorter than 21 nts has been proposed by different groups.

Synthetically synthesized hairpins with a 29-mer stem have been shown to be slightly more efficient than hairpins with a 19-mer stem (Siolas et al., 2005). They are dependent on Dicer cleavage and therefore could not be delivered adequately from our ribozyme cassette. In the same work it was shown that the 19-mers are not cleaved effectively by recombinant human Dicer *in vitro*. Although being less potent than 29-mers they show a knockdown phenotype and therefore must be incorporated into RISC. In a more recent study this was analyzed further and the existence of a certain group of short shRNAs (sshRNAs) is proposed (Ge et al., 2010b). They find ssRNAs with stems shortened to a minimum of 16 or 17 nts and minimal loops of 2 – 4 nts (dependent on base pairing of the adjacent 5' and 3'- nt) also not to be processed by Dicer *in vitro,* but to be as potent as comparable siRNAs in cell culture. The main difference to the 19-mers from the Siolas study, an R-type shRNA, is that Ge et al. also interchanged the position of sense and antisense strand. By comparison of conventional R-type and exchanged L-type sshRNAs the L-type appears to be more efficient. If indeed no

Dicer cleavage is involved, this would make sense, because the hairpin still has to be un-wound and if the antisense strand is at the 5'-end, the only end that can be un-winded, it is more likely to enter RISC. Notably, the *in vivo*-Dicer activity or the presence of another duplex-specific endonuclease cannot be excluded. Also did they observe that certain sshRNAs could dimerize and these dimers then were cleaved by Dicer. This dimerization however was not a prerequisite for knock-down activity. Interestingly they also analyzed diverse modifications of their L-type sshRNAs. Modifications of the phosphate-backbone were tolerated at the 5'-end of the antisense strand as well as the 3'-end of the sense strand. Longer disulfide-containing groups conjugated to the 3'-end of the hairpin were accepted as well, whereas they abolished the knock-down function, when conjugated to the 5'-end (Ge et al., 2010a).

As it was possible to recover recombinant RABV expressing ribozyme-comprising mRNAs in this thesis, another interesting idea is to directly use the ribozymes in order to cleave and thereby destroy target mRNAs. Trans-splicing as the first ribozymatic reaction has been observed for the *T. thermophilae* group I intron (Been and Cech, 1986; Inoue et al., 1985) and was shown to be useful to specifically repair defect mRNAs (Sullenger and Cech, 1994). For a trans-cleaving HHRz it is in principle possible to target any RNA sequence by Watson-Crick base pairing of flanking sequences (Haseloff and Gerlach, 1988). The same is true for HDVagRz and other ribozymes. Numerous applications *in vitro* and *in vivo* have been proposed for ribozymes targeting mostly mRNAs (reviewed in Mastroyiannopoulos et al., 2010; Scherer and Rossi, 2003). Although established more than 10 years before RNAi, the ribozyme technique never gained the similar impact. Reasons might be that the target sites are more dependent on mRNA structure and that no algorithm is available allowing the prediction of a good target sequence. For their identification empirical screens have to be done that are time-consuming, whereas for siRNAs this is not necessary. Also effects on their target genes seem to be rather moderate compared to the potency of RNAi.

In conclusion, whatever construct will be considered to get a new try, *in vitro*-analyses of Dicer cleavage or ribozyme processing with synthetic RNAs or *in vivo*-tests for knock-down, after microinjection into the cytoplasm, can be of advantage to evaluate the probability of success.

4.2 Improved rescue for rabies virus

Efficient rescue of RABV from cDNA is dependent on the formation of correct genome ends of the T7-pol derived antigenome-like RABV full-length RNA. As we found the 3'-terminal HDV ribozyme to cleave very inefficiently in the first part of this work, the aim was to replace the HDV sequence by the better cleaving SC1 sequence and thereby improving the rescue efficiency. Since SC1 indeed improved the rescue system significantly, we also applied an HHRz to process the 5'-end of the RABV cRNA. Together, the HHRz and the better cleaving SC1 improved the efficiency of RABV rescue by more than 100-fold and made it a faster and more reliable system (Ghanem et al., 2012).

4.2.1   Ends are important

The initial RABV rescue system already was dependent on an HDVagRz to process the 3'-end of the T7-pol transcribed RABV cRNA (Schnell et al., 1994). The sequence applied in this system was labeled HDV in the first part of this thesis and found to have a poor cleavage activity *in vitro*. As flanking sequences may play an important role in the activity of the ribozyme, *in vitro*-cleavage assays were performed with the HDV sequence at its position downstream of the 3'-end of the RABV cDNA. For these experiments the minigenome construct pSDI-1 (Conzelmann and Schnell, 1994) was applied as it was easier with this shorter construct than with a full-length RABV cDNA to distinguish between cleaved and un-cleaved RNAs. The results, correlating with the cleavage activity of HDV inserted artificially between the G and the L gene, indicated poor cleavage activity for HDV also when it was located downstream of the RABV sequences.

The importance of the genome ends during rescue of NNSV from cDNA has been demonstrated initially for VSV DIs (Pattnaik et al., 1992). Constructs with diverse 3'-ends were tested and although those with incorrect 3'-ends could be encapsidated into N-RNA, no rescue was possible. Therefore it is very likely that RABV cRNAs with incorrect ends compete with those being correctly processed for encapsidation by N protein. The increased rescue efficiency from pSAD L16_SC compared to pSAD L16 underlines this hypothesis.

Studies with a ribozyme cassette comprising negative oriented RABV minigenomes indicated also an influence of the 5'-end, although this seems to be less important than the 3'-end (Le Mercier et al., 2002). The classical RABV rescue system contains, like various other systems dependent on T7-pol, three extra G residues directly downstream of the T7 promoter and

upstream of the 5'-end of the RABV antigenome. These G residues are important for efficient transcription initiation from the T7 promoter. Their beneficial effect in regard to transcription seems to overweigh their negative effect in regard to a precise 5'-end. Upon viral replication the extra G residues were shown to be removed (not copied) by the viral polymerase (Martin et al., 2006; Pattnaik et al., 1992). Indeed, was it also possible in the third part of this work ($\rightarrow$3.3.13, $\rightarrow$3.3.13) to rescue RABV from Pol-II dependent constructs lacking HHRz sequences for processing the 5'-ends.

However, the importance of a correct RABV cRNA 5'-end was supported by the results obtained in this thesis, as the insertion of an HHRz significantly improved the rescue from pSAD T7-HH_L16 compared to pSAD L16. Generation of a correctly processed 5'-end by HHRz resulted in a 10-fold increase in recue efficiency and the impact is therefore as strong as the application of SC1 in comparison to HDV for the 3'-end. In the work of Le Mercier et al. (Le Mercier et al., 2002) only a 3-fold increase in luciferase activity was observed when correct 5'-ends were generated with an HHRz. This difference can be explained by the fact that the majority of the luciferase activity obtained for the negative oriented minigenome depends rather on viral transcription than on viral minigenome replication. And the promoter for this viral transcription is located in the leader at the 3'-end (whereas the incorrect 5'-end only plays a role during replication, when the viral polymerase terminates there by a yet unknown mechanism at either the correctly or incorrectly processed end).

The negative orientated minigenome pSDI HH_CNPL_SC, in comparison to pSDI CNPL also showed an increase in firefly luciferase activity by only about 5-fold. This is a much smaller difference than the significant improvement of more than 100-fold observed for pSAD T7-HH_L16_SC compared to pSAD L16. As mentioned above, it was shown for VSV DIs, that they can be encapsidated by N protein although they do not replicate. Additionally, it might be the case that for RABV transcription of subgenomic mRNAs the requirement of exact ends is not as strict as for replication of viral genomes (or minigenomes).

4.2.2 Significantly improved rescue with HHRz and HDVagRz_SC

The new rescue system developed in this part, allowed the recovery of recombinant RABV that were severely attenuated. Some examples are SAD G_HH-HSmm-SC1 and other RABV containing 2 internal ribozymes, that were used in part one of this thesis. These constructs are severely attenuated during rescue, as the internal ribozymes can cleave the naked cRNA

transcript. They could only be rescued in the improved system, whereas several rescue experiments with the classical rescue system failed. RABV containing IRES elements or 2A-like sequences from part 3 of this work are attenuated in their growth kinetics and therefore of course also difficult to rescue. Some of these viruses, although being attenuated could be generated also with the classical rescue system (Marschalek et al., 2009), however, these rescue experiments were more time consuming and less reproducible. The new rescue system has allowed us not only to recover severely attenuated RABV constructs, moreover, it gains substantial time while recovering new recombinant RABV. Some examples are G gene deleted RABV clones (SAD ΔG) expressing fluorophores like eGFP or mCherry and which can be used for example for mono- or polysynaptic neuronal tracing. Derivatives of these fluorescent proteins contain specific tags, relocalizing them to distinct intracellular compartments, like turbo-mito-GFP (mitochondria) or mem-tomato (plasma membrane). Also proteins that can be used for functional assays could be successfully expressed from the new RABV vectors. G deleted RABV expressing calcium-indicators (GCamp3 and GCamp5) and channelrhodopsin 2 (ChR2c) were readily recovered. Although many of these recombinant RABV might have been rescued with the classical system, their recovery has been facilitated considerably by the improvements shown here.

As numerous rescue systems for NNSV that are used today go back to the initial RABV system, the poor cleaving HDV "core" ribozyme is still widely used. Therefore also rescue systems for other members of the *Mononegavirales* might benefit from the improved rescue system.

4.3 Single infectious RABV cDNA clones

RABV is being rescued from cDNA clones since almost 20 years (Schnell et al., 1994) and the system has been improved significantly (Ghanem et al., 2012) as described here. The availability of a highly efficient system allowed the addressing of the question if it is possible to generate cells genetically encoding RABV. Such cells could represent a basis for the development of mouse lines conditionally expressing infectious RABV.

4.3.1 RABV rescue dependent on IRES elements

For the recovery of recombinant RABV from cDNA, one has to provide the full-length cDNA from which antigenome-like RNA is transcribed into the cytoplasm. This newly made RNA is, however, not infectious per se. Since neither plus-sense nor minus-sense RNA of RABV can be translated to provide the "helper" proteins N, P and L, extra expression plasmids are necessary. Only upon encapsidation by the N protein into NCs and association of these NCs with the RABV polymerase P-L into a vRNP is the viral RNA infectious. Therefore at least 4 plasmids have to be introduced into the cell. Transcription of all 4 plasmids is usually dependent on T7-pol that can be either transiently provided by an additional plasmid or viral vectors like vaccinia virus, or be stably expressed by certain cell lines (for review see (Ghanem and Conzelmann, in press)). As a first step towards a genetically encoded RABV this work addressed the possibility of simplifying the rescue system by reducing the numbers of plasmids needed for rescue.

For influenza virus, a segmented negative stranded RNA virus from the family *Orthomyxoviridae* such a simplification in terms of a single plasmid system recently has been demonstrated (Zhang et al., 2009). To reconstitute an infectious influenza virus cycle, the 8 genome segments have to be delivered together with 4 proteins of the vRNP, the nucleoprotein NP and the tripartite polymerase PB1, PB2 and PA. In the initial rescue systems this was achieved by simultaneous delivery of 12 plasmids, 4 expressing the proteins and 8 delivering the segmented genome RNA (Fodor et al., 1999; Neumann et al., 1999). By using ambisense strategies, where a Pol-I promoter transcribes the negative orientated genome segment and a Pol-II promoter from the other direction transcribes an mRNA to generate the proteins, this was reduced to 8 plasmids (Hoffmann et al., 2000; Hoffmann and Webster, 2000). Zhang et al. fused these 8 plasmids to a single plasmid of approximately 24 kb from which they were able to rescue recombinant influenza virus.

For RABV rescue, the antigenome must be transcribed as naked RNA to reconstitute the virus together with N, P and L. This means the antigenome-like RNA has already the orientation of mRNAs, thus an ambisense strategy is not helpful. The fusion of the three "helper" plasmids, coding for N, P and L, in one plasmid together with the cDNA for the full-length RNA would result in a single plasmid of at least 24 kb, the same size as the influenza single rescue plasmid. The genome comprises about 12 kb, the L gene about 6.5 kb, the N gene about 1.5 kb and the P gene about 1 kb. Additionally promoter and termination sequences together with sequences for amplification and selection in bacteria would be necessary. The major difficulty, however, would not be the size, but rather the duplication of about 75 % of the sequences, as there would be two N genes, two P genes and two L genes, one of each as part of the genome and the other as expression unit for the "helper" proteins. This is expected to result in extensive recombination between the plasmid sequences in bacteria. Therefore, another approach using regulative elements on RNA basis, the IRES element was explored to overcome this problem.

Recently, the successful replacement of RABV gene borders by diverse picornaviral IRES elements has been demonstrated (Marschalek et al., 2009). There it was shown first that these internal IRES elements were tolerated in the viral genome. Further, as the gene border and thereby the transcriptional stop/restart signals were replaced by IRES elements, the translation of the downstream gene was dependent on the respective IRES element. Different IRES elements could therefore direct the relative levels of protein translated from the downstream ORF. In regard to expression of "helper" proteins these IRES elements were expected to also translate proteins from the downstream ORF from the naked full-length antigenome-like RNA directly after transcription, as this RNA has the same orientation as mRNAs. Once the genome is packaged into helical N-RNA, this should not be the case anymore, due to the loss of IRES secondary structures.

The translation of protein from an ORF with the support of an upstream IRES element indeed was confirmed. Transfection of only pSAD T7-HH_PVP(bi)_SC, the full-length cDNA for a RABV in which the NP gene border is replaced by the poliovirus IRES, resulted in expression of low levels of P protein as indicated in Western blot experiments. The replacement of the NP gene border in RABV results in translational regulation of gene expression instead of transcriptional regulation. As we did not aim primarily to influence the natural transcription

gradient, the construct pSAD T7-HH_PVP(mono)_SC was created. In contrast to pSAD T7-HH_PVP(bi)_SC, in this construct, the poliovirus IRES does not replace the NP gene border but is located in the 5'-UTR of the P gene. As this does not lead to a bicistronic N-PV-P mRNA but to a monocistronic PV-P mRNA, the abbreviations "bi" or "mono" were chosen. Like pSAD T7-HH_PVP(bi)_SC, pSAD T7-HH_PVP(mono)_SC was able to translate P protein at low levels when transfected into BSR-T7/5 cells. As the P levels still were low, other IRES elements were tested. The EMCV IRES was found to result in the highest levels of P protein translated directly from the full-length transcript.

More interesting in regard to a simpler rescue system was the question if these P levels were sufficient to rescue the virus. And indeed they were. Transfection of pSAD T7-HH_EP(mono)_SC, together with only pTIT-N and pTIT-L, but omitting pTIT-P was sufficient to rescue the RABV SAD EP(mono) from cDNA. This demonstrated that a *cis*-active sequence, namely the EMCV IRES, can direct the translation of P protein in amounts sufficient for rescue and therefore supersedes the use of an extra P plasmid. The full-length plasmids pSAD T7-HH_PVP(bi)_SC and pSAD T7-HH_PVP(mono)_SC, however, comprising the poliovirus IRES, did not provide similar amounts of P protein and therefore could not be rescued without pTIT-P. When pTIT-P was co-transfected, recombinant RABV successfully could be recovered from these cDNAs.

The next step was to transfer this principle to the other two genes of RABV that need to be expressed during rescue, N and L. For the L gene this was working readily, by introducing an EMCV IRES downstream of the GL gene border into the 5'-UTR of L. The resulting cDNA construct, pSAD T7-HH_EL(mono)_SC could be rescued by co-transfection of only pTIT-N and pTIT-P, but without pTIT-L. Due to a lack of L antibodies, the levels of L protein translated directly from the full-length RNA could not be determined. As L is at the most promoter distal (5'-end) position in the NNSV context, the least mRNA is made. Moreover, viruses have been made containing two additional transcription units between the G and the L gene, probably reducing the already low amounts of L mRNA, without significantly attenuating the virus (unpublished data). Thus it is thought that already low amounts of L protein are sufficient for supporting virus replication and transcription.

When an EMCV IRES element was introduced upstream of the N gene, directly between the RABV antigenome leader and the AUG of the N gene (pSAD T7-HH_EN_SC), it was able to

mediate translation of significant amounts of N protein from the full-length RNA. Strikingly, however, no RABV could be rescued from pSAD T7-HH_EN_SC. In pSAD T7-HH_EN_SC the EMCV IRES with its intensive secondary structure is in close proximity to the antigenomic leader sequence at the 5'-end of the newly transcribed RNA. To exclude that the leader-proximal IRES has a negative effect on virus replication, an eGFP ORF was inserted as a spacer between the leader and the EMCV IRES. As no gene border was inserted, this would result in a bicistronic GFP-IRES-N mRNA transcribed by the virus. The construct pSAD T7-HH_GFPEN_SC still was able to provide sufficient amounts of N protein translated from the N-ORF on the full-length RNA, but again could not be rescued, neither with nor without providing N *in trans*. The same was true when instead of the eGFP, an extra RABV P ORF was inserted (data not shown). As indicated by these results and confirmed by later experiments, *cis*-active sequences at the leader-N gene junction, as well as within the N coding region play a critical role for virus viablitiy. This is discussed below (→4.3.5). In order to retain an authentic leader-N gene junction, a virus with a bicistronic N-IRES-N gene (SAD NEN) was constructed. This construct has the first N gene (N1) directly downstream of the leader, followed by the EMCV IRES and a second N gene (N2). In contrast to pSAD T7-HH_EN_SC, pSAD T7-HH_NEN_SC could be rescued readily into viable virus. Moreover, this rescue was possible by co-transfecting only pTIT-P and pTIT-L.

The major implication from these results is that it was demonstrated that each "helper" protein can be omitted by the use of *cis*-active sequences in the antigenome-like RNAs.

4.3.2 RABV dependent on 2A-like sequences

Another regulatory element allowing protein expression from bicistronic or multicistronic mRNAs is the 2A-like sequence. 2A-like sequences have been found in many genera of the *Picornaviridae* (Luke et al., 2008). They are *cis*-active hydrolase elements and their mechanism is the co-translational separation of the upstream peptide chain together with the C-terminal 2A-like peptide and the downstream peptide chain together with an N-terminal proline derived from the 2A-like sequence. By a ribosomal skipping mechanism the peptide bond is not made, while translation goes on (Donnelly et al., 2001a; Donnelly et al., 2001b). In some picornaviruses this mechanism is present instead of the classical 2A-protease to separate the viral proteins 2A and 2B.

In the present work the RABV NP gene border was replaced by the *Thosea asigna* virus 2A-like sequence (Donnelly et al., 2001a). During construction, an *XmaI* restriction site, coding for amino acids proline and glycine, was created at the N C-terminus upstream of the 2A-like sequence. SAD N2AP could be rescued from cDNA, representing the first RABV whose replication is dependent on a 2A-like sequence. This virus (SAD N2AP) made a bicistronic N2AP mRNA as observed in Northern blots and from this mRNA the proteins N-2A and P are made during translation. As mentioned before, the majority of the 2A-like sequence remains at the C-terminus of the N protein (N-2A). The P protein translated from N2AP starts with an N-terminal proline. N-2A could be clearly distinguished from N in Western blot by its MW, for proline-P that was not the case.

Most probably, the 2A-tag at the C-terminus of the N protein is the main reason for the attenuation observed for SAD N2AP in comparison with SAD L16. There are reports on the failure to recover a RABV with an N-GFP fusion protein (C-terminal GFP fusion) (Koser et al., 2004) and although the 2A-like tag is significantly smaller, it might be only due to the improved rescue system that SAD N2AP could be rescued successfully. In principle, however, it was demonstrated that C-terminal tags of N are tolerated, although attenuating the virus. The N-terminal proline of P might also play a minor role for the attenuated phenotype observed. However, recombinant RABV with N-terminal GFP fusions have been generated and shown to be viable (Brzózka et al., 2005). It is worth to mention that this N-terminally GFP-tagged P-protein was not able any more to prevent the induction of IFN. Shorter N-terminal tags to the P-protein, however, do not impede this important function since a Flag-P can still abolish the induction of IFN (Martina Rieder, personal communication). Additionally, BSR-T7/5 cells, in which SAD N2AP was rescued and tested for growth kinetics, have a defect in IFN induction, therefore this cannot play a role.

In wild-type RABV (SAD L16) not only the full-length P protein is expressed from the P gene (P1), but, due to a ribosomal leaky scanning mechanism and translation initiation at more downstream in-frame AUGs, also minor amounts of N-terminally truncated P proteins (P2, P3, P4) are made. Although some of these minor P proteins have been described to interact with promyelytic leukemia (PML) protein (Blondel et al., 2002) or to interfere with IFN induction (Marschalek et al., 2012), their overall impact and function in the RABV life cycle is not clear. As translation of the bicistronic N2AP-mRNA of SAD N2AP exclusively starts at the

N-AUG, these smaller P products cannot be made and are not detected in Western blot experiments (→3.3.8). Their lack might also contribute to the attenuated phenotype of SAD N2AP compared to SAD L16.

A negative effect on the virus fitness may also result from the fact that in SAD N2AP the N and P protein are synthesized in equimolar amounts from a single mRNA. The transcriptional gradient observed by NNSV as RABV is thought to be the only possibility for the virus to regulate relative expression levels of viral proteins. For BDV it was shown that a distinct ratio of N to P protein is important (Schneider et al., 2003).

In terms of providing "helper" proteins from the antigenome-like RNA, the 2A-like sequence alone is not useful, as it allows two proteins to be made from one ORF, but not internal translation initiation like an IRES element. If however, the 2A-like sequence is combined with an upstream IRES element, it has the advantage of translating two proteins dependent on only one IRES element.

4.3.3 Combination of IRES elements and 2A-like sequences – single infectious cDNA clones

To provide all "helper" proteins through *cis*-active sequences in the genome instead of co-transfecting plasmids and to achieve the goal of a single infectious cDNA, many combinations of IRES elements and 2A-like sequences were tested during my work. Two cDNA constructs, pSAD T7-HH_NEN2APEL_SC and pSAD T7-HH_NENEPEL_SC fulfilled the criteria, namely to allow rescue from a single cDNA clone. From both plasmids, when transfected alone into BSR-T7/5 cells, recombinant RABV could be recovered without providing any "helper" plasmids *in trans*. In the following chapter, the features of both approaches and a comparison of their advantages and disadvantages are provided.

SAD NENEPEL was a combination of SAD NEN, SAD EP, and SAD EL. The N protein was made from a bicistronic NEN mRNA in which the N1 ORF was followed by an EMCV IRES and the N2 ORF. P and L were made from monocistronic EP and EL mRNAs. Altogether, three EMCV IRES elements were applied to translate sufficient amounts of N, P and L protein from the primary full-length transcript in order to rescue this virus. From pSAD T7-HH_NENEPEL_SC, virus was found to be rescued fast, compared to pSAD T7-HH_NEN2APEL_SC, however, a significant percentage of rescued viruses possessed re-arranged genomes. The origin of these recombinations will be discussed in an extra chapter (→ 4.3.4). The un-recombined viruses

rescued from pSAD T7-HH_NENEPEL_SC, like SAD NENEPEL 2, were found to be severely attenuated. This attenuation may contribute to the swift emergence of the recombined (and fitter) virus variants.

One attenuating factor could be the genome length of SAD NENEPEL. The sequences of the extra N gene and the three additional EMCV IRES elements sum up to about 2.5 kb. However, this cannot be the major cause of attenuation, as RABV vectors have been generated containing additional genes of similar size without significant attenuation. Strikingly, SAD NEP(bi)EL 1, the virus rescued from pSAD T7-HH_NENEPEL_SC after a recombination event was found to be less attenuated than SAD NENEPEL 2, the unrecombined variant. The second N gene of SAD NENEPEL 2, which is not present in SAD NEP(bi)EL 1, is, however, not considered to be a major cause of the attenuation observed. SAD NEN, with the bicistronic N-IRES-N mRNA was not attenuated significantly. Most likely, this is because the bulk of N protein was made from the N1 gene, as observed for SAD NEN2AP (where both N genes can be distinguished by their size, due to the N-2A made from the second N gene). The second major difference between both viruses is that SAD NEP(bi)EL transcribes a bicistronic N-IRES-P mRNA whereas SAD NENEPEL 2 transcribes a monocistronic IRES-P mRNA. Therefore, the IRES elements upstream of the respective monocistronic genes are a possible explanation for the severe attenuation. SAD EL, transcribing a monocistronic IRES-L mRNA was already attenuated by about 2 log steps. The same was true for SAD EP(mono) with the monocistronic IRES-P mRNA (data not shown). Differences observed in growth kinetics between the slightly attenuated SAD NEP(bi)EL and the severely attenuated SAD NEP(mono)EL (compared to SAD L16), which both were rescued from Pol-II dependent single infectious RABV cDNA clones (→3.3.14 →3.3.15), support this hypothesis. Whether the secondary structure of the EMCV IRES interferes with cap-dependent translation from the monocistronic mRNAs, or yet unknown, but impotant, *cis*-acting sequences in the 5'-UTR of the respective mRNAs were disrupted, remains unclear. Further studies are required to pinpoint the reason for these phenotypic differences. It is easy to imagine, however, that attenuating factors of e.g. SAD EP(mono) and SAD EL accumulate in SAD NENEPEL 2.

SAD NEN2APEL was a combination of the bicistronic NEN approach with the N2AP approach and from the virus thus a tricistronic NEN2AP mRNA was made. From this mRNA three

proteins N, N-2A, and P are made. L is made from a monocistronic EL mRNA. During rescue from pSAD T7-HH_NEN2APEL_SC by translation from the full-length RNA, almost exclusively N-2A is made but only background levels of N. This indicates that N-2A is also able to support rescue similar to untagged N. Background levels of untagged N protein may derive from translation initiation at the AUG of N1 and are also observed upon transfection of pSAD T7-HH_L16_SC. as neither a 5'-cap structure nor an IRES element is present upstream of N1, these background levels, however, appear not sufficient to rescue SAD L16 without providing pTIT-N in *trans* or, in our case, providing N-2A from the EMCV IRES.

Rescue from pSAD T7-HH_NEN2APEL_SC was less efficient and delayed not only in comparison with rescue from pSAD-L16 but also with rescue from pSAD T7-HH_NENEPEL_SC. Recombinant variants of SAD NEN2APEL were not found. The virus SAD NEN2APEL was also attenuated significantly if compared to SAD L16, although growing slightly better than the un-recombined SAD NENEPEL 2. Reasons responsible for this attenuation most likely resemble the reasons found to be responsible for SAD EL (discussed above) and SAD N2AP (→4.3.2). Regarding factors discussed to be responsible for the attenuation of SAD N2AP, however, only the lack of minor P products (P2, P3, P4) and the proline at the N-terminus of P are expected to play a major role. Authentic N protein is made from the N1 ORF at substantial amounts and significantly less is found to be made from the N2 ORF as N-2A. Noteworthy, the distinct N products allow a direct comparison of the efficiencies of cap-dependent translation and EMCV IRES dependent translation. Not only derive both N products from the same mRNA, moreover, they are detected with the same antibody.

Rescue efficiencies from both single infectious RABV cDNAs pSAD T7-HH_NENEPEL_SC and pSAD T7-HH_NEN2APEL_SC were found to be reduced compared to the standard rescue system. For pSAD T7-HH_NENEPEL_SC, however, only about 50 % of rescue experiments were positive, and at significantly later time points compared to standard SAD L16 rescue. Rescue experiments with pSAD T7-HH_NEN2APEL_SC failed even more often. As discussed above, both viruses were attenuated in their growth kinetics compared with SAD L16. Rescue efficiency of the single infectious cDNA clones does, however, not only depends on the growth kinetics of the recombinant RABV recovered, but also on the quality, amount, and ratio of "helper" proteins directly expressed from these cDNAs.

To determine the ability of the single infectious cDNA clones to serve as "helper" plasmids, a standard RABV cDNA pSAD T7-HH_GFP_SC was co-transfected with either of the infectious cDNA clones or with the standard mix of pTIT-N, pTIT-P, and pTIT-L "helper" plasmids (NPL-mix). The GFP positive foci of SAD GFP allowed the detection of rescue elements in live cells. Using pSAD T7-HH_NENEPEL_SC as a "helper" plasmid, rescues were almost as efficient as with the NPL-mix. This relatively efficient rescue is not surprising, as for both pSAD T7-HH_NENEPEL_SC and the pTIT "helper" plasmids all proteins are translated via the EMCV IRES. In standard rescue experiments, the NPL-mix contains pTIT-N, pTIT-P and pTIT-L in a ratio of 2:1:1 (see Materials and Methods) and a different ratio of proteins expressed from pSAD T7-HH_NENEPEL_SC may account for the slight decrease in efficiency observed (compared to the NPL-mix).

Using pSAD T7-HH_NENE2APEL_SC as "helper" plasmid, also all rescue experiments resulted in successful recovery of recombinant SAD GFP, however, a delay of several day was observed. This indicates that from this plasmid the composition of "helper" proteins expressed is less efficient. Reasons therefore might be as well the N-2A protein or the proline-P.

4.3.4 SAD NENEPEL - recombination on plasmid level or during rescue

Rescue experiments with the RABV single infectious cDNA pSAD T7-HH_NENEPEL_SC often resulted in a mixture of genetically different viruses. While only from one experiment (SAD NENEPEL 2) exclusively the un-recombined virus corresponding to the cDNA construct was recovered, most virus stocks contained minor fractions of SAD NENEPEL together with recombined variants. The most prominent rearrangement could be seen in SAD NEP(bi)EL 1. For this virus, in Northern blot experiments, neither the bicistronic N-IRES-N mRNA nor the monocistronic IRES-P mRNA were detected. Instead of that, a bicistronic N-IRES-P mRNA was made. Therefore it was concluded that a recombination between the EMCV IRES separating the two N genes and the EMCV IRES upstream of the P gene had occurred. A recombination between the two N sequences (N1 and N2) would result in SAD NEP(mono)EL, a virus transcribing a monocistronic N mRNA and a monocistronic IRES-P mRNA. Indeed, this virus could be detected as well in the virus stock SAD N(EN)EPEL 6, however only in a mixture with SAD NENEPEL (the brackets indicate the presence of either of the two viruses in the stock). Upon several repetitions of the rescue experiments with pSAD T7-HH_NENEPEL_SC, it came

out that SAD NEP(bi)EL was detected at the highest rates. Most probably, this is due to the increased growth kinetics of this virus (final titers only reduced about 1 log(10) compared to SAD L16), allowing it to outgrow the severely attenuated SAD NENEPEL (titers reduced by about 3 log(10)).

There are theoretically 3 possible explanations where and when the recombination for SAD NENEPEL has occurred. The first possibility would be during replication of the virus. For RABV as a member of the *Mononegavirales* this is not very likely to occur and was for a long time excluded in the text books. So far only one publication has indicated the possibility of recombination events in wild type RABV (Liu et al., 2011). For some other members of the *Mononegavirales* recombination has been described (Chare et al., 2003; Schierup et al., 2005) but most of these publications rely on sequencing data. A more recent work suggested that many recombined sequences in databases could be artificially generated by template switching during PCR (Song et al., 2011). However, in rare cases, e.g. for RSV, recombination has been demonstrated to occur experimentally (Spann et al., 2003).

The critical point in addressing the question of recombination during RABV replication was to isolate only un-recombined virus clones and exclude a contamination with recombined virus (below detection levels of the radioactive probes). To address this, single virus clones were isolated by serial dilutions down to titers that were only able to infect a few (5 -10) wells from a 96-well dish. Briefly, none of the SAD NENEPEL single virus clones (isolated from SAD NENEPEL 2) showed any recombination. Therefore contamination of the inoculating virus stock with recombined virus could be excluded. When a mixed virus stock (e.g. SAD N(EN)EPEL 3) was chosen as an inoculum for the isolation of single virus clones, the outcome was always a distinct progeny virus of either one or the other type (data not shown). This also confirms the usability of the approach. More interestingly, when single virus clones isolated from SAD NENEPEL 2 were passaged over several weeks, no recombination was observed to occur. This strongly indicates that the genomic rearrangements have happened prior to virus rescue. Formally, these experiments do not exclude the possibility of recombination during RABV replication. However, it is very unlikely that the high frequency of recombination observed in rescue experiments derives from recombining viruses.

A second possible cause for the genomic rearrangements is a recombination event on RNA level in the cell, directly during the rescue, or prior to it. Template switching, or copy-choice

recombination, is a common mechanism of RNA recombination, where the transcribing polymerase during transcription "jumps" from one template to another. Thereby, an RNA, comprising information from both templates, is transcribed, as observed for many positive stranded RNA viruses (Arnold and Cameron, 1999; Cheng and Nagy, 2003; Kim and Kao, 2001) but also during reverse transcription of retroviruses (Huber et al., 1989). Most importantly, the ability of template switching has been demonstrated *in vitro* for T7-pol (Rong et al., 1998). During transcription of RABV antigenome-like RNAs from the cDNA construct pSAD T7-HH_NENEPEL_SC, the double N gene and the EMCV IRES repeats might have an influence on the fidelity of T7-pol. Interestingly, for retroviral vectors expressing proteins from artificial multicistronic RNAs it was observed that the EMCV IRES was a recombinational hot-spot (Duch et al., 2004). Although the retroviral template switching during reverse transcription cannot be compared to T7-pol transcription, IRES structures seem to be prone to recombination in various systems. Another mechanism of RNA recombination was described for poliovirus as non-replicative recombination (Gmyl et al., 1999). This mechanism was not dependent on transcription by the poliovirus polymerase, but rather on cleavage and re-ligation by unknown proteins or RNA structures. Notably, the poliovirus IRES with its intensive secondary structures was again detected as a hot-spot for the observed rearrangements.

The third and most plausible explanation for the rearrangements observed, is recombination at plasmid level in bacteria. Due to the long repetitive sequences, as N1 and N2 or the 3 EMCV IRES elements, recombinations are likely to occur during amplification of the plasmids in bacteria. For some full-length constructs during cloning more than 98 per cent of the bacterial plasmid minipreps were recombined as observed in restriction digestions. Although all cDNA constructs used for transfections were checked by adequate restriction digestion and sequencing, the presence of a small fraction of recombined plasmid (below the detection levels by agarose gel electrophoresis) cannot be excluded. It is clear that the un-recombined virus SAD NENEPEL 2 is strongly attenuated and the recombination resulting in SAD NEP(bi)EL 1 enhances the viral fitness by magnitudes. Threrefore, even after a small contamination, due to the better fitness, viral replication will rapidly result in higher amounts of the recombined variant.

The latter two possibilities, recombination on RNA or DNA level, prior to the rescue would imply the presence of significant amounts of un-recombined pSAD T7-HH_NENEPEL_SC, as from the recombined pSAD T7-HH_NEPEL_SC plasmids (or from its RNA transcript) no N protein could be made. Therefore in contrast to the rescue of un-recombined virus this rescue per definition would be not from a single infectious cDNA clone but from 2 cDNAs or RNAs.

Genomic rearrangements were also observed for SAD NEN. Here, in Northern blot experiments, together with the correct genome, a smaller genome was detected and together with the expected bicistronic mRNA a smaller monocistronic mRNA was found. This indicates a recombination event between the two N ORFs. The same recombination event was detected also in some rescue experiments of SAD NENEPEL.

Interestingly, for SAD NEN2APEL none of such drastic rearrangements were detected although two EMCV IRES elements and two complete N genes were present as well. This can be explained by the fact that a recombination between the two N ORFs would rather attenuate the virus than contribute to its fitness. SAD NEN2APEL can produce the wild type N from the N1 ORF whereas SAD N2APEL would only encode the N-2A protein. The possible gain of fitness of the shorter genome thus seems not to compensate for the loss of the untagged wild-type N protein.

4.3.5 *Cis*-active signals in the N gene.

While RABV SAD NEN was recovered successfully from cDNA (→3.3.4), the cDNA constructs pSAD T7-HH_EN_SC and pSAD T7-HH_GFPEN_SC failed to be rescued into virus. These results strongly suggested the presence of *cis*-active sequences at the RABV leader-N gene junction or within the N gene which are important for viability. Interestingly, it was shown for the closely related VSV, that the N gene could be transferred to more distal positions of the genome (Wertz et al., 1998). For RABV, however, no such rearranged viruses have been described yet. Moreover, and in correlation with these results, serious attempts to generate a RABV with an N-terminally tagged N protein failed (Stefan Finke, personal communication).

To identify important *cis*-active sequences, I truncated the N1 gene in pSAD T7-HH_NEN_SC to retain the first 100 or 200 nts of the N sequence. Thereby the constructs pSAD T7-HH_N100EN_SC(Fse) and pSAD T7-HH_N200EN_SC(Fse), respectively, were generated with short N-fragments downstream of the leader followed by the EMCV IRES and the complete

N2 gene. Noteworthy, these initial constructs, like pSAD T7-HH_NEN_SC or pSAD T7-HH_EN_SC, comprised an *FseI* restriction site as an artifact from cloning directly at the leader-N gene junction. SAD N200EN(Fse) but not SAD N100EN(Fse) could be rescued from the respective cDNA, indicating that essential *cis*-acting sequences are located between nts 100 and 200 of the N gene. New reporter constructs were generated with an additional GFP gene inserted between the G and the L gene and most importantly, in which the *FseI* site at the leader-N gene junction was restored to wild type. Strikingly, from both new constructs, pSAD T7-HH_N100EN G_eGFP_SC and pSAD T7-HH_N200EN G_eGFP_SC, recombinant RABV could be rescued. This indicates that not only the sequences between nts 100 and 200 of the N gene are important for RABV viability, but also sequences located directly at the leader-N gene junction. However, also the importance of sequences between N100 and N200 was emphasized by (1) the slight difference in growth kinetics between SAD N100EN G_eGFP and to SAD N200EN G_eGFP, (2) significantly smaller foci and (3) reduced eGFP expression in the former virus.

As all mutants tested so far comprised a functional AUG at the authentic position of either the N100 or N200 sequence, the production of small peptides was possible from this N1 position. As no stop-codon was included at the end of the N100 or N200 fragment, termination should occur in the EMCV IRES sequence. Thus, hypothetically, peptides were made from the respective viruses with the same N-terminal sequences, but different length and C-termini. To evaluate an influence of such peptides on the virus the N1 AUG at the leader-N gene junction, was mutated to UUG in order to exclude the production of any peptides from these mini-ORFs. The constructs pSAD T7-HH_N100(mut)EN G_eGFP_SC and pSAD T7-HH_N200(mut)EN G_eGFP_SC differed from pSAD T7-HH_N100EN G_eGFP_SC and pSAD T7-HH_N200EN G_eGFP_SC in only a single nucleotide. Both viruses were, however, growing slower than their respective (AUG comprising) variants. This indicates that peptides are not the cause for the attenuated growth kinetics observed for N100 comprising viruses compared to N200 comprising viruses. SAD N100(mut)EN G_eGFP, the virus with the mutation at the leader-N gene junction and only 100 instead of 200 nts of N, was found to be severely attenuated (10.000-fold). In comparison, RABV with only 100 nts of N, but an un-mutated leader-N gene junction (SAD N100EN G_eGFP) or RABV with 200 nts of N, but the UUG mutation downstream of the leader (SAD N200(mut)EN G_eGFP), had a milder growth defect. These data correlated with the failure of pSAD T7-HH_N100EN_SC(Fse) to be rescued

into viable virus. This construct also comprises only 100 nts of the N coding region upstream of the EMCV IRES and due to the *FseI* site has a disrupted leader-N gene junction. These results all together strongly suggest that two distinct *cis*-active functions, one at the leader-N gene junction, and one within the N coding region (N100 – N200) are important for RABV viability.

The infections with high MOIs and the monitoring of eGFP expression indicate rather a defect in gene expression for SAD N100(mut)EN G_eGFP virus but also, less prominent, for SAD N200(mut)EN G_eGFP. Indeed, at the leader-N gene junction, the RABV polymerase is discussed to initiate transcription of subgenomic mRNAs. RABV minigenomes, only comprising the terminal leader and trailer sequences and an internal reporter gene (but lacking the correct leader-N gene junction or N-internal sequences), do not show severe defects in reporter gene expression upon co-transfection with the "helper" plasmids expressing N, P and L. If, however, these minigenomes are passaged onto fresh cells (by co-transfection of expression plasmids for RABV M and G), they are rapidly lost upon coinfection with SAD L16 (Finke and Conzelmann, 1999). This indicates that these artificial minigenomes (unlike defective interfering particles (DIs) from other NNSV) do not perform all steps of the RABV life cycle in an optimal way. Initial experiments with RABV minigenomes comprising an intact leader-N gene junction together with N sequences indicate that this defect can be rescued partially. Additionally, the negative influence of the FseI restriction site, disrupting the leader-N gene junction, could be confirmed (not shown).

Why these sequences are important and which functions of the virus life cycle are impaired in their absence remains unclear and has to be studied further.

4.3.6   Pol-II dependent rescue – single infectious cDNA clones vs 2-plasmid systems

In this work, evidence was provided, that pSAD T7-HH_NENEPEL_SC and pSAD T7-HH_NEN2APEL_SC, indeed were single infectious RABV cDNA clones. Their expression is, however, still dependent on T7-pol.

As we aimed at generating a genetically encoded RABV, other promoters than T7 were tested. Therefore the full-length RABV cDNAs for SAD NENEPEL and SAD NEN2APEL were cloned together with flanking ribozyme sequences into either of the Pol-II expression vectors pCAGGS, pCR3 or pTre2hyg. The pCAGGS plasmid with the chicken-β-actin promoter (Niwa et al., 1991) is commonly being used for high level protein expression. The pCR3 plasmid

(Invitrogen) contains the immediate early CMV promoter and the plasmid pTre2hyg (Clontech) contains a minimal CMV promoter together with an upstream binding site for the Tet-repressor. In cell lines stably expressing the Tet repressor, e.g. TetOn cells, transcription from this plasmid is inhibited. Upon the addition of doxycycline, which sequesters the Tet-repressor, transcription will start. For all these constructs Pol-II dependent RABV rescue failed. Different cell lines were tested, namely, BSR cells, BHK-21 cells, HEK 293T cells, NA cells, and Vero cells, but in all cell lines the outcome remained the same. It has to be mentioned that all constructs except for pTre2Hyg-HH_NEN2APEL_SC contained a T7 promoter and thus could be tested in T7 cells for their integrity. As in T7 cells recombinant RABV could be recovered from all constructs but pTre2Hyg-HH_NEN2APEL_SC, we could exclude rearrangements of the plasmids to be the reason for the failure of rescue. Also was it possible to recover recombinant RABV from pCAGGS-T7-HH_NENEPEL_SC in NA cells, when the T7 polymerase was provided by co-transfection of the plasmid pSC6-T7neo.

Western blot experiments, after transfection of the infectious RABV cDNA clones into different cell lines, revealed that proteins were only expressed from these constructs when they were transcribed by the cytoplasmic T7-pol, but not by the Pol-II promoters present in all these constructs. Most likely this contributes the reason for the failure of Pol-II dependent RABV rescue from these cDNAs.

To identify the reason for this lack of Pol-II dependent protein expression, and to exclude e.g. incorrect splicing of the transcripts, various shorter constructs were tested in diverse cell lines. The plasmids pCR3-HH_NEP(mono) and pCR3-HH_NPVP(bi) comprise both the CMV promoter and the T7 promoter, followed by the HHRz sequence and the cDNA coding for the first part of the RABV antigenome (from leader until the end of the P gene). In pCR3-HH_NEP(mono) an EMCV IRES is inserted between the P transcription start signal and the P ORF. In pCR3-HH_NPVP(bi) the NP gene border is replaced by the poliovirus IRES. In BSR-T7 cells transfected with these plasmids, substantial amounts of RABV P protein were made from pCR3-HH_NEP(mono) and significantly less from pCR3-HH_NPVP(bi). In HEK 293T cells however, and in BSR cells (not shown) for none of the transfected constructs expression of RABV P was observed. The results obtained with these shorter cDNA constructs excluded incorrect splicing to be the reason for the lack of Pol-II expression, as RABV P and N (not shown) both can be expressed from Pol-II promoters. The intention behind the bicistronic

construct was to examine the influence of the RABV transcription stop and start signals on Pol-II dependent expression. Due to the lower activity of the PV IRES compared to the EMCV IRES, however, already in BSR-T7/5 cells, P expression levels were found to be low.

Another major difference between e.g. pCR3-P and pCR3-HH_NEP(mono) is the HHRz, processing the 5'-end of the mRNA made from the latter. Therefore the influence of the HHRz and of the HDVagRz on Pol-II dependent protein expression from RABV cDNA clones was tested. Therefore 4 new cDNA constructs were made, all based on the pCAGGS vector, as pCAGGS-P was found to express significant higher levels of RABV P than pCR3-P. The full-length cDNA for SAD_EP(mono) (→3.3.1) was inserted into the vector with 4 different combinations of ribozymes, namely either an HHRz at the 5'-end or not and either a 3'-HDV (poorly cleaving) or a 3'-SC1 (better cleaving). Strikingly, from pCAGGS-T7_SAD NEP(mono), lacking the 5'-HHRz and comprising the 3'-HDV, substantial amounts of RABV P were made upon transfection into HEK 293T cells. Moreover, as the transcripts now comprised a 5'-cap, RABV N was directly translated (superseding an IRES element). When, however, either the 5' or the 3'-end were processed efficiently by the respective ribozymes, expression levels decreased significantly. The processing of both ends, as seen for pCAGGS-T7-HH_SAD NEP(mono)_SC, resulted in a complete block of protein expression.

The export of mRNAs from the nucleus into the cytoplasm is one of the major steps in mRNA surveillance. Starting co-transcriptionally the pre-mRNA is 5'-capped, spliced, processed at the 3'-end and polyadenylated. Numerous proteins, amongst these also factors involved in nuclear export, assemble with the mRNA during the biogenesis (reviewed in Kohler and Hurt, 2007). Quality control occurs during all steps of this complex mRNP formation (reviewed in Fasken and Corbett, 2005). MRNAs lacking a poly(A) tail are not exported into the cytoplasm (Hilleren et al., 2001). Also the 5'-cap structure is essential for mRNA export (Cheng et al., 2006). As both ends of the transcripts are reported to be essential for mRNA export from the nucleus, most likely, the residual protein expression observed upon transfection of either pCAGGS-T7_SAD NEP(mono)_SC or pCAGGS-T7-HH_SAD NEP(mono), where only one ribozyme is present, does rather represent the percentage of incomplete ribozymatic cleavage *in vivo*, than residual export of processed RNAs. This hypothesis is strengthened by the fact that for pCAGGS-T7-HH_SAD NEP(mono) residual amounts of N protein are

detected. Efficient translation of N protein from this construct can only occur if a 5'-cap is present (and not cleaved off).

As from pCAGGS-T7_SAD NEP(mono) substantial amounts of RABV N and P protein were made upon transfection into HEK 293T cells (Pol-II dependent), the intent was also to directly express the L protein from this construct. Therefore, analogously to SAD EL (→3.3.3), an EMCV IRES sequence was inserted upstream of the L ORF in pCAGGS-T7_SAD NEP(mono) and pCAGGS-T7_SAD NEP(mono)_SC resulting in pCAGGS-T7_NEP(mono)EL and pCAGGS-T7_NEP(mono)EL_SC, respectively. Although from the latter less protein was expected to be made, the idea was that this disadvantage was compensated by the better processed 3'-end.

Rescue experiments were performed with both plasmids and the recombinant RABV SAD NEP(mono)EL could be recovered after transfection of pCAGGS-T7_NEP(mono)EL into HEK 293T cells. This provides evidence, that indeed Pol-II dependent rescue from a single infectious RABV cDNA is possible.

The efficiency of this rescue system was, however, found to be low. Only 1 out of 12 transfection experiments with pCAGGS-T7_NEP(mono)EL was successful. For pCAGGS-T7_NEP(mono)EL_SC, all approaches failed, most likely due to the lower amounts of "helper" proteins translated directly from the full-length RNA. In BHK-21 cells neither of the constructs could be rescued, probably because the transfection efficiency (as determined by a pCAGGS-eGFP reporter construct) was reduced significantly (not shown).

Pol-II dependent rescue from single infectious RABV cDNA clones in this work was found to have two distinct requirements which seem to be diametrically opposed. One requirement is the expression of sufficient amounts of "helper" proteins, translated either cap-dependent (RABV N from pCAGGS-constructs) or IRES-dependent (N-IRES-N, IRES-P and IRES-L). The second important point is the delivery of an antigenome-like RNA, comprising precise 3' and 5'-ends, which can be efficiently encapsidated into viral NCs.

To distinguish between these two demands, a 2-plasmid rescue system was developed. In this system, the "helper" proteins were expressed by pCAGGS-T7_NEP(mono)EL. As the second plasmid (the cDNA that should be rescued), the cDNA of RABV SAD L16 was cloned into the pCAGGS vector comprising different ribozymes to process the 5' and 3'-ends of the full-length transcripts. Additionally, to test different Pol-II promoters, pCR3-HH_L16_SC was made comprising the SAD L16 full-length cDNA with the flanking 5'-HHRz and the 3'-SC1, in

the vector pCR3. For rescue, equal amounts of pCAGGS-T7_NEP(mono)EL and either of the SAD L16 cDNAs were transfected into HEK 293T cells or BHK-21 cells. Strikingly, almost all transfections resulted in successful recovery of recombinant SAD L16. Formally, the simultaneous rescue of SAD NEP(mono)EL cannot be excluded, and the existence of virus mixtures in supernatants was not followed further. However, the significant differences in efficiency compared to transfections of only pCAGGS-T7_NEP(mono)EL, together with phenotypes of the foci upon staining with FITC-labeled RABV N-antibodies, indicate that almost exclusively SAD L16 was recovered from these experiments. The fastest and most efficient rescue was achieved with pCAGGS-T7-HH_L16_SC, comprising the HHRz and SC1. From pCAGGS-T7_L16, lacking the 5'-HHRz and comprising the 3'-HDV, rescues were delayed and only partially successful. This emphasizes the need of the RABV RNAs for precise ends also in Pol-II dependent systems. Rescue attempts in the inefficiently transfected BHK-21 cells failed and rescues with the weaker CMV promoter were slightly delayed, indicating the importance of sufficient transcription of antigenome-like RNA. It was discussed above, in regard to the cap-dependent translation of the RABV N protein, that rather the unprocessed full-length RNAs are exported to the cytoplasm. Therefore it might be the case that full-length transcripts with precise ends (which can be rescued far better) are only *trans*-located to the cytoplasm due to eventual failure of mRNA quality control mechanisms, (or e.g. during cell division). This however remains to be analyzed further. Noteworthy, this was the first rescue of RABV from strain SAD L16 in a Pol-II dependent manner. Numerous attempts to rescue this virus from Pol-II promoters together with Pol-II dependent "helper" proteins failed, as seen in our hands (not shown) and by others (Osakada et al., 2011; Stefan Finke, personal communication).

Alltogether, the 2-plasmid rescue system has the advantage, that one plasmid can be optimized for efficient delivery of "helper" proteins, whereas the second construct can deliver the best RABV antigenome-like RNA. The higher efficiency of this system, compared to the 1-plasmid system, derives, however, not only from the precise genome ends of the SAD L16 constructs. SAD L16, importantly, can replicate and grow significantly better than SAD NEP(mono)EL. Thus, I intended to rescue a RABV with better growth kinetics (than SAD NEP(mono)EL) also from a 1-plasmid system. As such a virus, that still had to comprise IRES elements to translate the P and L protein from the RNA transcript, SAD NEP(bi)EL was chosen. This RABV, identified as the outcome of a recombination event upon rescue from

pSAD T7-HH_NENEPEL_SC, was found to grow significantly better and was only attenuated about 1 log(10) in titer compared to SAD L16 (→3.3.9 →4.3.4). Therefore the plasmids pCAGGS-T7_NEP(bi)EL (3'-HDV) and pCAGGS-T7_NEP(bi)EL_SC (3'-SC1) were made, both comprising a bicistronic N-IRES-P gene. Indeed, this resulted in significantly increased rescue efficiencies (compared to the monocistronic IRES-P constructs).

Remarkably, for pCAGGS-T7_NEP(bi)EL_SC about 50 % of rescue experiments resulted in successful recovery of recombinant RABV in HEK 293T cells. For pCAGGS-T7_NEP(bi)EL, the efficiency was lower, indicating that between these constructs, the advantage of more RNAs comprising a precise 3'-end overweighs the disadvantage of lower levels of "helper" proteins expressed.

To summarize, in this work, evidence was provided, that it is indeed possible to rescue RABV from single infectious cDNAs. A prerequisite was the significant improvement of the RABV rescue system by generating precise 5' and 3'-ends (figure 31A). T7-pol dependent single infectious cDNAs, expressing the RABV N, P and L proteins directly from the antigenome-like transcripts (by supporting IRES elements or 2A-like sequences) were the next step (figure 31B). For T7-pol-independent rescue, as a further bottleneck, (most likely) the export of Pol-II transcribed antigenome-like RNAs from the nucleus was impaired upon ribozymatic procession. To achieve efficient and reproducible RABV rescue two different strategies were applied. To rescue RABV from a Pol-II-dependent single infectious RNA, only the 3'-end but not the 5'-end was processed to allow a minimum of "helper" protein expression. Secondly, a RABV with better growth kinetics than the first generation infectious clones was used (figure 31C). As an alternative to Pol-II dependent single infectious cDNA clones, a 2-plasmid rescue system was developed, allowing the simultaneous improvement of both plasmids, one for "helper" protein expression and one to be rescued, to their respective needs (figure 31D).
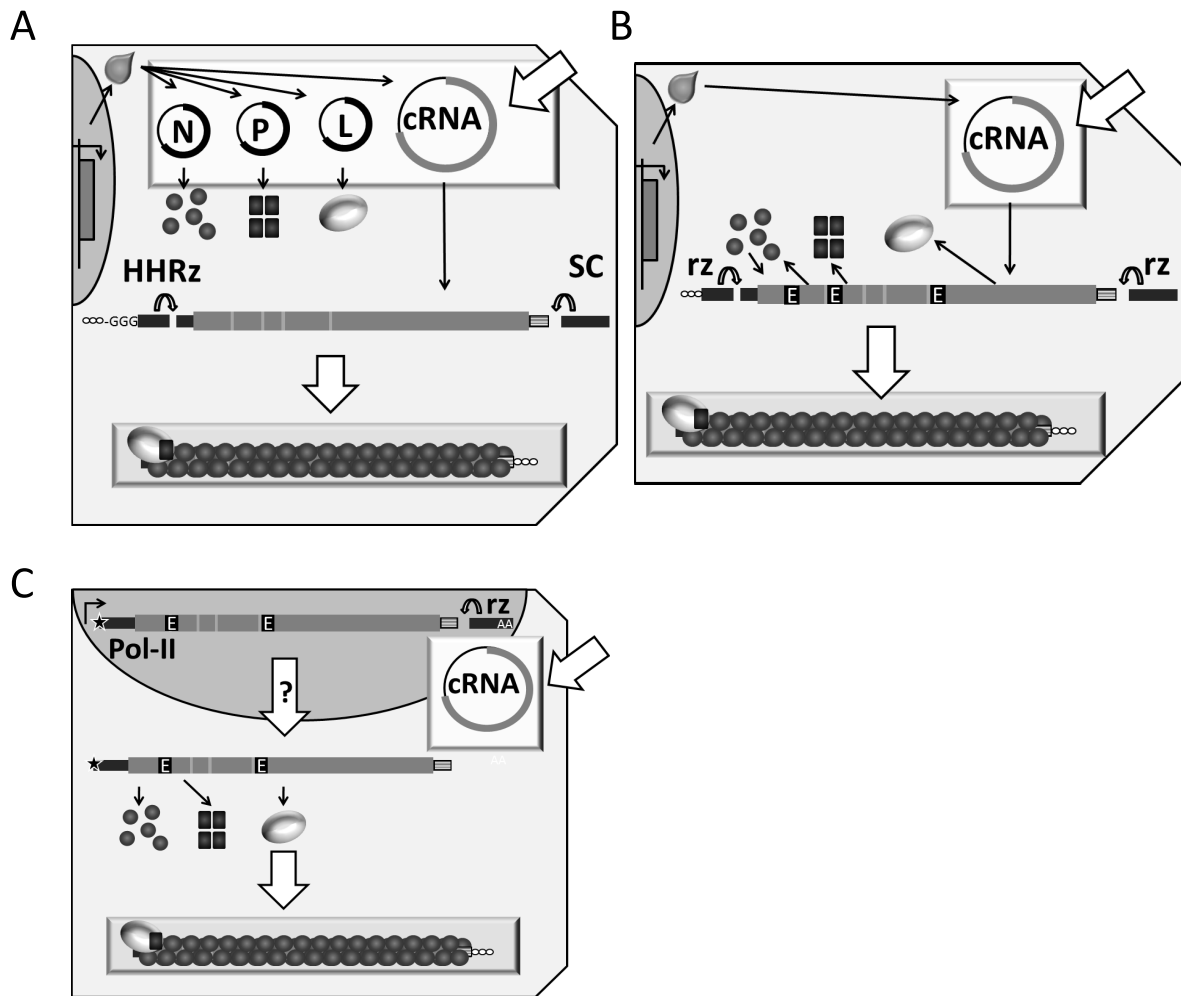
Figure 31: Comparison of reverse genetics systems for RABV.
(adapted from Ghanem and Conzelmann, in press). (A) significantly improved rescue system due to better processing of 3'- and 5'-ends by ribozymes (as described in (Ghanem et al., 2012)) (B) Single infectious cDNA clones. IRES elements (or 2A-like sequences) allow translation of "helper" proteins directly from the cRNA. Noteworthy this system is still dependent on T7-pol. (C) Pol-II-dependent single infectious cDNAs. Nuclear export of ribozymatically processed cRNAs is a critical step. N protein can be expressed cap-dependently.

4.3.7 Future outlook

The completely new and unconventional ways to recover recombinant RABV, from either single infectious cDNA clones or the 2-plasmid rescue system, developed in this work, provide an excellent basis for the further development of a genetically encoded RABV.

The most straight-forward approach would be to replace the chicken-β-actin promoter used e.g. in pCAGGS-T7_NEP(bi)EL_SC, by an inducible promoter (e.g. Tet-On) and to use this new construct for the generation of an inducible RABV-On cell line. In principle, this should also be feasible with a 2-plasmid system.

The success of these attempts depends on the expression levels achieved with the genetically encoded systems, and it is unclear so far, whether these are sufficient in regard to "helper" protein expression and antigenome-like RNA transcription.

A more knowledge-based approach therefore would be to further optimize the systems developed in this work before they are brought to the next step. To do so, different procedures are conceivable, dependent on the systems. Within the 2-plasmid system, one would expect that the plasmid expressing the "helper" proteins can be optimized the most. As only RABV N, P, and L have to be provided, additional RABV sequences could be deleted, thus shortening the plasmid. Additionally, one could integrate an optimal Kozac sequence (instead of the leader-N gene junction) upstream of the N-ORF to increase expression of this protein. Furthermore it could be an option to test IRES elements others than used in this work, thereby varying the ratios between the provided "helper" proteins. In doing so, no influence on the viability of the recombinant RABV has to be considered, as the virus RNA is made from the second plasmid.

For the single infectious cDNAs other possibilities of improvement exist. It was found that SAD NEP(bi)EL grows significantly better than SAD NEP(mono)EL. This indicates that for RABV, the monocistronic IRES-P mRNA is problematic. Therefore, one could try to construct a RABV transcribing a bicistronic G-IRES-L mRNA (e.g. SAD GEL(bi)) and compare its growth kinetics with that of SAD EL. Alternatively, spacer sequences could be inserted into the 5'-UTRs of IRES comprising monocistronic mRNAs. In regard to these 5'-UTRs, another option could be the restoration of wild-type-like RABV sequences, upstream of the respective IRES elements, as these were partially disrupted during cloning. A more time-consuming approach is the serial passaging of e.g. SAD NEP(bi)EL in the cell line in which it is intended to encode a RABV genetically (e.g. MEFs, NA cells). One could expect the emergence of adaptive mutations, specifically increasing the virus viability in the respective cell line. Identification (and characterization) of these mutations is conceivable to contribute also to the rescue efficiency. The balance between the demands for precise ends on one hand and the efficient expression of "helper" proteins on the other hand is another important task to adjust the system. For the 3'-end an HDVagRz with an intermediate cleavage activity, such as SC2 (→3.1.5) could improve the system. Additionally, for generation of an exact 5'-end the use of an inducible HHRz, or riboswitch, should be examined. Such inducible ribozymes have

been reported to cleave dependent on a ligand drug, like theophylline or flavin mononucleotide (Soukup and Breaker, 1999). Also in mammalian cells some of these are reported to be functional (Auslander et al., 2010; Kumar et al., 2009).

In summary, new working single and double plasmid Pol-II dependent RABV rescue systems have been developed in this work, which pave the way for genetically encoded RABV animal model systems, and which provide promising options for optimization.

5 References

Albertini, A.A., G. Schoehn, W. Weissenhorn, and R.W. Ruigrok. 2008. Structural aspects of rabies virus replication. *Cell Mol Life Sci*. 65:282-294.

Albertini, A.A., A.K. Wernimont, T. Muziol, R.B. Ravelli, C.R. Clapier, G. Schoehn, W. Weissenhorn, and R.W. Ruigrok. 2006. Crystal structure of the rabies virus nucleoprotein-RNA complex. *Science*. 313:360-363.

Alonso, M., C.H. Kim, M.C. Johnson, M. Pressley, and J.A. Leong. 2004. The NV gene of snakehead rhabdovirus (SHRV) is not required for pathogenesis, and a heterologous glycoprotein can be incorporated into the SHRV envelope. *J Virol*. 78:5875-5882.

Ammayappan, A., G. Kurath, T.M. Thompson, and V.N. Vakharia. 2010a. A Reverse Genetics System for the Great Lakes Strain of Viral Hemorrhagic Septicemia Virus: the NV Gene is Required for Pathogenicity. *Mar Biotechnol (NY)*.

Ammayappan, A., S.E. Lapatra, and V.N. Vakharia. 2010b. A vaccinia-virus-free reverse genetics system for infectious hematopoietic necrosis virus. *J Virol Methods*. 167:132-139.

An, D.S., Y. Xie, S.H. Mao, K. Morizono, S.K. Kung, and I.S. Chen. 2003. Efficient lentiviral vectors for short hairpin RNA delivery into human cells. *Hum Gene Ther*. 14:1207-1212.

Arnold, J.J., and C.E. Cameron. 1999. Poliovirus RNA-dependent RNA polymerase (3Dpol) is sufficient for template switching in vitro. *J Biol Chem*. 274:2706-2716.

Astic, L., D. Saucier, P. Coulon, F. Lafay, and A. Flamand. 1993. The CVS strain of rabies virus as transneuronal tracer in the olfactory system of mice. *Brain Res*. 619:146-156.

Auslander, S., P. Ketzer, and J.S. Hartig. 2010. A ligand-dependent hammerhead ribozyme switch for controlling mammalian gene expression. *Mol Biosyst*. 6:807-814.

Ball, L.A. 1992. Cellular expression of a functional nodavirus RNA replicon from vaccinia virus vectors. *J Virol*. 66:2335-2345.

Banerjee, A.K. 2008. Response to "Non-segmented negative-strand RNA virus RNA synthesis in vivo". *Virology*. 371:231-233.

Banyard, A.C., D. Hayman, N. Johnson, L. McElhinney, and A.R. Fooks. 2011. Bats and lyssaviruses. *Adv Virus Res*. 79:239-289.

Baron, M.D., and T. Barrett. 1997. Rescue of rinderpest virus from cloned cDNA. *J Virol*. 71:1265-1271.

Bartel, D.P. 2004. MicroRNAs: genomics, biogenesis, mechanism, and function. *Cell*. 116:281-297.

Barton, G.M., and R. Medzhitov. 2002. Retroviral delivery of small interfering RNA into primary cells. *Proc Natl Acad Sci U S A*. 99:14943-14945.

Been, M.D., and T.R. Cech. 1986. One binding site determines sequence specificity of Tetrahymena pre-rRNA self-splicing, trans-splicing, and RNA enzyme activity. *Cell*. 47:207-216.

Been, M.D., and G.S. Wickham. 1997. Self-cleaving ribozymes of hepatitis delta virus RNA. *Eur J Biochem*. 247:741-753.

Bennasser, Y., C. Chable-Bessia, R. Triboulet, D. Gibbings, C. Gwizdek, C. Dargemont, E.J. Kremer, O. Voinnet, and M. Benkirane. 2011. Competition for XPO5 binding between Dicer mRNA, pre-miRNA and viral RNA regulates human Dicer levels. *Nat Struct Mol Biol*. 18:323-327.

Bennasser, Y., S.Y. Le, M. Benkirane, and K.T. Jeang. 2005. Evidence that HIV-1 encodes an siRNA and a suppressor of RNA silencing. *Immunity*. 22:607-619.

Bernstein, E., A.A. Caudy, S.M. Hammond, and G.J. Hannon. 2001. Role for a bidentate ribonuclease in the initiation step of RNA interference. *Nature*. 409:363-366.

Biacchesi, S., M. Bearzotti, E. Bouguyon, and M. Bremont. 2002. Heterologous exchanges of the glycoprotein and the matrix protein in a Novirhabdovirus. *J Virol*. 76:2881-2889.

Biacchesi, S., M.I. Thoulouze, M. Bearzotti, Y.X. Yu, and M. Bremont. 2000. Recovery of NV knockout infectious hematopoietic necrosis virus expressing foreign genes. *J Virol*. 74:11247-11253.

Billecocq, A., N. Gauliard, N. Le May, R.M. Elliott, R. Flick, and M. Bouloy. 2008. RNA polymerase I-mediated expression of viral RNA for the rescue of infectious virulent and avirulent Rift Valley fever viruses. *Virology*. 378:377-384.

Birikh, K.R., P.A. Heaton, and F. Eckstein. 1997. The structure, function and application of the hammerhead ribozyme. *Eur J Biochem*. 245:1-16.

Bitko, V., and S. Barik. 2001. Phenotypic silencing of cytoplasmic genes using sequence-specific double-stranded short interfering RNA and its application in the reverse genetics of wild type negative-strand RNA viruses. *BMC Microbiol*. 1:34.

Blondel, D., T. Regad, N. Poisson, B. Pavie, F. Harper, P.P. Pandolfi, H. De The, and M.K. Chelbi-Alix. 2002. Rabies virus P and small P products interact directly with PML and reorganize PML nuclear bodies. *Oncogene*. 21:7957-7970.

Blount, K.F., and O.C. Uhlenbeck. 2002. The hammerhead ribozyme. *Biochem Soc Trans*. 30:1119-1122.

Borchert, G.M., W. Lanier, and B.L. Davidson. 2006. RNA polymerase III transcribes human microRNAs. *Nat Struct Mol Biol*. 13:1097-1101.

Brandao, P.E., J.G. Castilho, W. Fahl, P. Carnieli, Jr., N. Oliveira Rde, C.I. Macedo, M.L. Carrieri, and I. Kotait. 2007. Short-interfering RNAs as antivirals against rabies. *Braz J Infect Dis*. 11:224-225.

Bridgen, A., and R.M. Elliott. 1996. Rescue of a segmented negative-strand RNA virus entirely from cloned complementary DNAs. *Proc Natl Acad Sci U S A*. 93:15400-15404.

Brummelkamp, T.R., R. Bernards, and R. Agami. 2002. A system for stable expression of short interfering RNAs in mammalian cells. *Science*. 296:550-553.

Brzózka, K., S. Finke, and K.K. Conzelmann. 2005. Identification of the rabies virus alpha/beta interferon antagonist: phosphoprotein P interferes with phosphorylation of interferon regulatory factor 3. *J Virol*. 79:7673-7681.

Buchholz, U.J., S. Finke, and K.K. Conzelmann. 1999. Generation of bovine respiratory syncytial virus (BRSV) from cDNA: BRSV NS2 is not essential for virus replication in tissue culture, and the human RSV leader region acts as a functional BRSV genome promoter. *J Virol*. 73:251-259.

Burnside, J., E. Bernberg, A. Anderson, C. Lu, B.C. Meyers, P.J. Green, N. Jain, G. Isaacs, and R.W. Morgan. 2006. Marek's disease virus encodes MicroRNAs that map to meq and the latency-associated transcript. *J Virol*. 80:8778-8786.

Burrage, T.G., G.H. Tignor, and A.L. Smith. 1985. Rabies virus binding at neuromuscular junctions. *Virus Res*. 2:273-289.

Buzayan, J.M., W.L. Gerlach, and G. Bruening. 1986. Satellite tobacco ringspot virus RNA: A subset of the RNA sequence is sufficient for autolytic processing. *Proc Natl Acad Sci U S A*. 83:8859-8862.

Callaway, E.M. 2008. Transneuronal circuit tracing with neurotropic viruses. *Curr Opin Neurobiol*. 18:617-623.

Carthew, R.W., and E.J. Sontheimer. 2009. Origins and Mechanisms of miRNAs and siRNAs. *Cell*. 136:642-655.

Castellanos, J.E., D.R. Castaneda, A.E. Velandia, and H. Hurtado. 1997. Partial inhibition of the in vitro infection of adult mouse dorsal root ganglion neurons by rabies virus using nicotinic antagonists. *Neurosci Lett*. 229:198-200.

Ceccaldi, P.E., J.P. Gillet, and H. Tsiang. 1989. Inhibition of the transport of rabies virus in the central nervous system. *J Neuropathol Exp Neurol*. 48:620-630.

Chare, E.R., E.A. Gould, and E.C. Holmes. 2003. Phylogenetic analysis reveals a low rate of homologous recombination in negative-sense RNA viruses. *J Gen Virol*. 84:2691-2703.

Cheng, C.P., and P.D. Nagy. 2003. Mechanism of RNA recombination in carmo- and tombusviruses: evidence for template switching by the RNA-dependent RNA polymerase in vitro. *J Virol*. 77:12033-12047.

Cheng, H., K. Dufu, C.S. Lee, J.L. Hsu, A. Dias, and R. Reed. 2006. Human mRNA export machinery recruited to the 5' end of mRNA. *Cell*. 127:1389-1400.

Chenik, M., K. Chebli, and D. Blondel. 1995. Translation initiation at alternate in-frame AUG codons in the rabies virus phosphoprotein mRNA is mediated by a ribosomal leaky scanning mechanism. *J Virol*. 69:707-712.

Chiu, Y.L., and T.M. Rana. 2002. RNAi in human cells: basic structural and functional features of small interfering RNA. *Mol Cell*. 10:549-561.

Chowrira, B.M., P.A. Pavco, and J.A. McSwiggen. 1994. In vitro and in vivo comparison of hammerhead, hairpin, and hepatitis delta virus self-processing ribozyme cassettes. *J Biol Chem*. 269:25856-25864.

Clarke, D.K., M.S. Sidhu, J.E. Johnson, and S.A. Udem. 2000. Rescue of mumps virus from cDNA. *J Virol*. 74:4831-4838.

Collins, P.L., M.A. Mink, and D.S. Stec. 1991. Rescue of synthetic analogs of respiratory syncytial virus genomic RNA and effect of truncations and mutations on the expression of a foreign reporter gene. *Proc Natl Acad Sci U S A*. 88:9663-9667.

Conzelmann, K.K. 2004. Reverse genetics of mononegavirales. *Curr Top Microbiol Immunol*. 283:1-41.

Conzelmann, K.K., and M. Schnell. 1994. Rescue of synthetic genomic RNA analogs of rabies virus by plasmid-encoded proteins. *J Virol*. 68:713-719.

Couto, L.B., and K.A. High. 2010. Viral vector-mediated RNA interference. *Curr Opin Pharmacol*. 10:534-542.

Cullen, B.R. 2004. Transcription and processing of human microRNA precursors. *Mol Cell*. 16:861-865.

Curran, J. 1996. Reexamination of the Sendai virus P protein domains required for RNA synthesis: a possible supplemental role for the P protein. *Virology*. 221:130-140.

Curran, J., and D. Kolakofsky. 2008. Nonsegmented negative-strand RNA virus RNA synthesis in vivo. *Virology*. 371:227-230.

De, B.P., and A.K. Banerjee. 1993. Rescue of synthetic analogs of genome RNA of human parainfluenza virus type 3. *Virology*. 196:344-348.

Delgadillo, M.O., P. Saenz, B. Salvador, J.A. Garcia, and C. Simon-Mateo. 2004. Human influenza virus NS1 protein enhances viral pathogenicity and acts as an RNA silencing suppressor in plants. *J Gen Virol*. 85:993-999.

Dietzschold, B., J. Li, M. Faber, and M. Schnell. 2008. Concepts in the pathogenesis of rabies. *Future Virol*. 3:481-490.

Dolivo, M., P. Kucera, and W. Bommeli. 1982. [Progression of the rabies virus in the visual system of the rat]. *Comp Immunol Microbiol Infect Dis*. 5:67-69.

Dölken, L., A. Krmpotic, S. Kothe, L. Tuddenham, M. Tanguy, L. Marcinowski, Z. Ruzsics, N. Elefant, Y. Altuvia, H. Margalit, U.H. Koszinowski, S. Jonjic, and S. Pfeffer. 2010. Cytomegalovirus microRNAs facilitate persistent virus infection in salivary glands. *PLoS Pathog*. 6:e1001150.

Donnelly, M.L., L.E. Hughes, G. Luke, H. Mendoza, E. ten Dam, D. Gani, and M.D. Ryan. 2001a. The 'cleavage' activities of foot-and-mouth disease virus 2A site-directed mutants and naturally occurring '2A-like' sequences. *J Gen Virol*. 82:1027-1041.

Donnelly, M.L., G. Luke, A. Mehrotra, X. Li, L.E. Hughes, D. Gani, and M.D. Ryan. 2001b. Analysis of the aphthovirus 2A/2B polyprotein 'cleavage' mechanism indicates not a proteolytic reaction, but a novel translational effect: a putative ribosomal 'skip'. *J Gen Virol*. 82:1013-1025.

Duch, M., M.L. Carrasco, T. Jespersen, L. Aagaard, and F.S. Pedersen. 2004. An RNA secondary structure bias for non-homologous reverse transcriptase-mediated deletions in vivo. *Nucleic Acids Res*. 32:2039-2048.

Elbashir, S.M., J. Harborth, W. Lendeckel, A. Yalcin, K. Weber, and T. Tuschl. 2001a. Duplexes of 21-nucleotide RNAs mediate RNA interference in cultured mammalian cells. *Nature*. 411:494-498.

Elbashir, S.M., W. Lendeckel, and T. Tuschl. 2001b. RNA interference is mediated by 21- and 22-nucleotide RNAs. *Genes Dev*. 15:188-200.

Elroy-Stein, O., and B. Moss. 1990. Cytoplasmic expression system based on constitutive synthesis of bacteriophage T7 RNA polymerase in mammalian cells. *Proc Natl Acad Sci U S A*. 87:6743-6747.

Enterlein, S., V. Volchkov, M. Weik, L. Kolesnikova, V. Volchkova, H.D. Klenk, and E. Muhlberger. 2006. Rescue of recombinant Marburg virus from cDNA is dependent on nucleocapsid protein VP30. *J Virol*. 80:1038-1043.

Etessami, R., K.K. Conzelmann, B. Fadai-Ghotbi, B. Natelson, H. Tsiang, and P.E. Ceccaldi. 2000a. Spread and pathogenic characteristics of a G-deficient rabies virus recombinant: an in vitro and in vivo study. *J Gen Virol*. 81:2147-2153.

Etessami, R., K.K. Conzelmann, R. Marion, H. Tsiang, and P.E. Ceccaldi. 2000b. [Neuronal expression of foreign genes with recombinant rabies virus variants]. *Rev Neurol (Paris)*. 156:236-241.

Fabozzi, G., C.S. Nabel, M.A. Dolan, and N.J. Sullivan. 2011. Ebolavirus proteins suppress the effects of small interfering RNA by direct interaction with the mammalian RNA interference pathway. *J Virol*. 85:2512-2523.

Fasken, M.B., and A.H. Corbett. 2005. Process or perish: quality control in mRNA biogenesis. *Nat Struct Mol Biol*. 12:482-488.

Finke, S., and K.K. Conzelmann. 1997. Ambisense gene expression from recombinant rabies virus: random packaging of positive- and negative-strand ribonucleoprotein complexes into rabies virions. *J Virol*. 71:7281-7288.

Finke, S., and K.K. Conzelmann. 1999. Virus promoters determine interference by defective RNAs: selective amplification of mini-RNA vectors and rescue from cDNA by a 3' copy-back ambisense rabies virus. *J Virol*. 73:3818-3825.

Finke, S., and K.K. Conzelmann. 2003. Dissociation of rabies virus matrix protein functions in regulation of viral RNA synthesis and virus assembly. *J Virol*. 77:12074-12082.

Finke, S., and K.K. Conzelmann. 2005a. Recombinant rhabdoviruses: vectors for vaccine development and gene therapy. *Curr Top Microbiol Immunol*. 292:165-200.

Finke, S., and K.K. Conzelmann. 2005b. Replication strategies of rabies virus. *Virus Res*. 111:120-131.

Finke, S., J.H. Cox, and K.K. Conzelmann. 2000. Differential transcription attenuation of rabies virus genes by intergenic regions: generation of recombinant viruses overexpressing the polymerase gene. *J Virol*. 74:7261-7269.

Finke, S., R. Mueller-Waldeck, and K.K. Conzelmann. 2003. Rabies virus matrix protein regulates the balance of virus transcription and replication. *J Gen Virol*. 84:1613-1621.

Fire, A., S. Xu, M.K. Montgomery, S.A. Kostas, S.E. Driver, and C.C. Mello. 1998. Potent and specific genetic interference by double-stranded RNA in Caenorhabditis elegans. *Nature*. 391:806-811.

Flatz, L., A. Bergthaler, J.C. de la Torre, and D.D. Pinschewer. 2006. Recovery of an arenavirus entirely from RNA polymerase I/II-driven cDNA. *Proc Natl Acad Sci U S A*. 103:4663-4668.

Flick, R., K. Flick, H. Feldmann, and F. Elgh. 2003. Reverse genetics for crimean-congo hemorrhagic fever virus. *J Virol*. 77:5997-6006.

Flick, R., and R.F. Pettersson. 2001. Reverse genetics system for Uukuniemi virus (Bunyaviridae): RNA polymerase I-catalyzed expression of chimeric viral RNAs. *J Virol*. 75:1643-1655.

Fodor, E., L. Devenish, O.G. Engelhardt, P. Palese, G.G. Brownlee, and A. Garcia-Sastre. 1999. Rescue of influenza A virus from recombinant DNA. *J Virol*. 73:9679-9682.

Fu, Z.F. 2005. Genetic comparison of the rhabdoviruses from animals and plants. *Curr Top Microbiol Immunol*. 292:1-24.

Fuerst, T.R., E.G. Niles, F.W. Studier, and B. Moss. 1986. Eukaryotic transient-expression system based on recombinant vaccinia virus that synthesizes bacteriophage T7 RNA polymerase. *Proc Natl Acad Sci U S A*. 83:8122-8126.

Gaudin, Y., R.W. Ruigrok, C. Tuffereau, M. Knossow, and A. Flamand. 1992. Rabies virus glycoprotein is a trimer. *Virology*. 187:627-632.

Gaudin, Y., C. Tuffereau, P. Durrer, J. Brunner, A. Flamand, and R. Ruigrok. 1999. Rabies virus-induced membrane fusion. *Mol Membr Biol*. 16:21-31.

Ge, Q., A. Dallas, H. Ilves, J. Shorenstein, M.A. Behlke, and B.H. Johnston. 2010a. Effects of chemical modification on the potency, serum stability, and immunostimulatory properties of short shRNAs. *RNA*. 16:118-130.

Ge, Q., H. Ilves, A. Dallas, P. Kumar, J. Shorenstein, S.A. Kazakov, and B.H. Johnston. 2010b. Minimal-length short hairpin RNAs: the relationship of structure and RNAi activity. *RNA*. 16:106-117.

Gershon, P.D., B.Y. Ahn, M. Garfield, and B. Moss. 1991. Poly(A) polymerase and a dissociable polyadenylation stimulatory factor encoded by vaccinia virus. *Cell*. 66:1269-1278.

Ghanem, A., and K.K. Conzelmann. in press. Reverse genetics of rhabdoviruses. *In* Reverse Genetics of RNA Viruses: Applications and Perspectives. A. Bridgen, editor. Chichester, West Sussex : John Wiley & Sons, 2012.

Ghanem, A., A. Kern, and K.K. Conzelmann. 2012. Significantly improved rescue of rabies virus from cDNA plasmids. *Eur J Cell Biol*. 91:10-16.

Gmyl, A.P., E.V. Belousov, S.V. Maslova, E.V. Khitrina, A.B. Chetverin, and V.I. Agol. 1999. Nonreplicative RNA recombination in poliovirus. *J Virol*. 73:8958-8965.

Green, T.J., X. Zhang, G.W. Wertz, and M. Luo. 2006. Structure of the vesicular stomatitis virus nucleoprotein-RNA complex. *Science*. 313:357-360.

Grimm, D. 2009. Small silencing RNAs: state-of-the-art. *Adv Drug Deliv Rev*. 61:672-703.

Groseth, A., H. Feldmann, S. Theriault, G. Mehmetoglu, and R. Flick. 2005. RNA polymerase I-driven minigenome system for Ebola viruses. *J Virol*. 79:4425-4433.

Gupta, P.K., A.A. Sonwane, N.K. Singh, C.D. Meshram, S.S. Dahiya, S.S. Pawar, S.P. Gupta, V.K. Chaturvedi, and M. Saini. 2012. Intracerebral delivery of small interfering RNAs (siRNAs) using adenoviral vector protects mice against lethal peripheral rabies challenge. *Virus Res*. 163:11-18.

Haasnoot, J., E.M. Westerhout, and B. Berkhout. 2007. RNA interference against viruses: strike and counterstrike. *Nat Biotechnol*. 25:1435-1443.

Habjan, M., N. Penski, M. Spiegel, and F. Weber. 2008. T7 RNA polymerase-dependent and -independent systems for cDNA-based rescue of Rift Valley fever virus. *J Gen Virol*. 89:2157-2166.

Harborth, J., S.M. Elbashir, K. Vandenburgh, H. Manninga, S.A. Scaringe, K. Weber, and T. Tuschl. 2003. Sequence, chemical, and structural variation of small interfering RNAs and short hairpin RNAs and the effect on mammalian gene silencing. *Antisense Nucleic Acid Drug Dev*. 13:83-105.

Harty, R.N., J. Paragas, M. Sudol, and P. Palese. 1999. A proline-rich motif within the matrix protein of vesicular stomatitis virus and rabies virus interacts with WW domains of cellular proteins: implications for viral budding. *J Virol*. 73:2921-2929.

Haseloff, J., and W.L. Gerlach. 1988. Simple RNA enzymes with new and highly specific endoribonuclease activities. *Nature*. 334:585-591.

Hilleren, P., T. McCarthy, M. Rosbash, R. Parker, and T.H. Jensen. 2001. Quality control of mRNA 3'-end processing is linked to the nuclear exosome. *Nature*. 413:538-542.

Hoffmann, E., G. Neumann, Y. Kawaoka, G. Hobom, and R.G. Webster. 2000. A DNA transfection system for generation of influenza A virus from eight plasmids. *Proc Natl Acad Sci U S A*. 97:6108-6113.

Hoffmann, E., and R.G. Webster. 2000. Unidirectional RNA polymerase I-polymerase II transcription system for the generation of influenza A virus from eight plasmids. *J Gen Virol*. 81:2843-2847.

Holz, C.L., E. Albina, C. Minet, R. Lancelot, O. Kwiatek, G. Libeau, and R. Servan de Almeida. 2012. RNA interference against animal viruses: how morbilliviruses generate extended diversity to escape small interfering RNA control. *J Virol*. 86:786-795.

Horikami, S.M., J. Curran, D. Kolakofsky, and S.A. Moyer. 1992. Complexes of Sendai virus NP-P and P-L proteins are required for defective interfering particle genome replication in vitro. *J Virol*. 66:4901-4908.

Huang, Y., Q. Tang, S.A. Nadin-Davis, S. Zhang, C.D. Hooper, P. Ming, J. Du, X. Tao, R. Hu, and G. Liang. 2010. Development of a reverse genetics system for a human rabies virus vaccine strain employed in China. *Virus Res*. 149:28-35.

Huber, H.E., J.M. McCoy, J.S. Seehra, and C.C. Richardson. 1989. Human immunodeficiency virus 1 reverse transcriptase. Template binding, processivity, strand displacement synthesis, and template switching. *J Biol Chem*. 264:4669-4678.

Hutchins, C.J., P.D. Rathjen, A.C. Forster, and R.H. Symons. 1986. Self-cleavage of plus and minus RNA transcripts of avocado sunblotch viroid. *Nucleic Acids Res*. 14:3627-3640.

Inoue, K., Y. Shoji, I. Kurane, T. Iijima, T. Sakai, and K. Morimoto. 2003. An improved method for recovering rabies virus from cloned cDNA. *J Virol Methods*. 107:229-236.

Inoue, T., F.X. Sullivan, and T.R. Cech. 1985. Intermolecular exon ligation of the rRNA precursor of Tetrahymena: oligonucleotides can function as 5' exons. *Cell*. 43:431-437.

Iseni, F., A. Barge, F. Baudin, D. Blondel, and R.W. Ruigrok. 1998. Characterization of rabies virus nucleocapsids and recombinant nucleocapsid-like structures. *J Gen Virol*. 79 (Pt 12):2909-2919.

Israsena, N., P. Supavonwong, N. Ratanasetyuth, P. Khawplod, and T. Hemachudha. 2009. Inhibition of rabies virus replication by multiple artificial microRNAs. *Antiviral Res*. 84:76-83.

Ito, N., M. Takayama-Ito, K. Yamada, J. Hosokawa, M. Sugiyama, and N. Minamoto. 2003. Improved recovery of rabies virus from cloned cDNA using a vaccinia virus-free reverse genetics system. *Microbiol Immunol*. 47:613-617.

Johnson, M.C., B.E. Simon, C.H. Kim, and J.A. Leong. 2000. Production of recombinant snakehead rhabdovirus: the NV protein is not required for viral replication. *J Virol*. 74:2343-2350.

Kelly, R.M., and P.L. Strick. 2000. Rabies as a transneuronal tracer of circuits in the central nervous system. *J Neurosci Methods*. 103:63-71.

Kennerdell, J.R., and R.W. Carthew. 1998. Use of dsRNA-mediated genetic interference to demonstrate that frizzled and frizzled 2 act in the wingless pathway. *Cell*. 95:1017-1026.

Kern, A. 2012. Assembly and Budding of Rabies Virus: The Phosphoprotein as Critical Determinant of Particle Production. *In* PhD thesis. LMU München.

Khvorova, A., A. Reynolds, and S.D. Jayasena. 2003. Functional siRNAs and miRNAs exhibit strand bias. *Cell*. 115:209-216.

Kim, M.J., and C. Kao. 2001. Factors regulating template switch in vitro by viral RNA-dependent RNA polymerases: implications for RNA-RNA recombination. *Proc Natl Acad Sci U S A*. 98:4972-4977.

Klingen, Y., K.K. Conzelmann, and S. Finke. 2008. Double-labeled rabies virus: live tracking of enveloped virus transport. *J Virol*. 82:237-245.

Kohler, A., and E. Hurt. 2007. Exporting RNA from the nucleus to the cytoplasm. *Nat Rev Mol Cell Biol*. 8:761-773.

Koser, M.L., J.P. McGettigan, G.S. Tan, M.E. Smith, H. Koprowski, B. Dietzschold, and M.J. Schnell. 2004. Rabies virus nucleoprotein as a carrier for foreign antigens. *Proc Natl Acad Sci U S A*. 101:9405-9410.

Krol, J., K. Sobczak, U. Wilczynska, M. Drath, A. Jasinska, D. Kaczynska, and W.J. Krzyzosiak. 2004. Structural features of microRNA (miRNA) precursors and their relevance to miRNA biogenesis and small interfering RNA/short hairpin RNA design. *J Biol Chem*. 279:42230-42239.

Krom, Y.D., F.J. Fallaux, I. Que, C. Lowik, and K.W. van Dijk. 2006. Efficient in vivo knock-down of estrogen receptor alpha: application of recombinant adenovirus vectors for delivery of short hairpin RNA. *BMC Biotechnol*. 6:11.

Kumar, D., C.I. An, and Y. Yokobayashi. 2009. Conditional RNA interference mediated by allosteric ribozyme. *J Am Chem Soc*. 131:13906-13907.

Kuypers, H.G., and G. Ugolini. 1990. Viruses as transneuronal tracers. *Trends Neurosci*. 13:71-75.

Lafon, M. 2005. Rabies virus receptors. *J Neurovirol*. 11:82-87.

Lafon, M. 2008. Immune evasion, a critical strategy for rabies virus. *Dev Biol (Basel)*. 131:413-419.

Lares, M.R., J.J. Rossi, and D.L. Ouellet. 2010. RNAi and small interfering RNAs in human disease therapeutic applications. *Trends Biotechnol*. 28:570-579.

Lawson, N.D., E.A. Stillman, M.A. Whitt, and J.K. Rose. 1995. Recombinant vesicular stomatitis viruses from DNA. *Proc Natl Acad Sci U S A*. 92:4477-4481.

Le Mercier, P., Y. Jacob, K. Tanner, and N. Tordo. 2002. A novel expression cassette of lyssavirus shows that the distantly related Mokola virus can rescue a defective rabies virus genome. *J Virol*. 76:2024-2027.

Lee, R.C., R.L. Feinbaum, and V. Ambros. 1993. The C. elegans heterochronic gene lin-4 encodes small RNAs with antisense complementarity to lin-14. *Cell*. 75:843-854.

Leyrer, S., W.J. Neubert, and R. Sedlmeier. 1998. Rapid and efficient recovery of Sendai virus from cDNA: factors influencing recombinant virus rescue. *J Virol Methods*. 75:47-58.

Li, B.Y., X.R. Li, X. Lan, X.P. Yin, Z.Y. Li, B. Yang, and J.X. Liu. 2011. Rescue of Newcastle disease virus from cloned cDNA using an RNA polymerase II promoter. *Arch Virol*. 156:979-986.

Li, J., J.T. Wang, and S.P. Whelan. 2006. A unique strategy for mRNA cap methylation used by vesicular stomatitis virus. *Proc Natl Acad Sci U S A*. 103:8493-8498.

Li, L., and Y. Liu. 2011. Diverse small non-coding RNAs in RNA interference pathways. *Methods Mol Biol*. 764:169-182.

Li, W.X., H. Li, R. Lu, F. Li, M. Dus, P. Atkinson, E.W. Brydon, K.L. Johnson, A. Garcia-Sastre, L.A. Ball, P. Palese, and S.W. Ding. 2004. Interferon antagonist proteins of influenza and vaccinia viruses are suppressors of RNA silencing. *Proc Natl Acad Sci U S A*. 101:1350-1355.

Lieber, A., U. Kiessling, and M. Strauss. 1989. High level gene expression in mammalian cells by a nuclear T7-phase RNA polymerase. *Nucleic Acids Res*. 17:8485-8493.

Liu, Q., and Z. Paroo. 2010. Biochemical principles of small RNA pathways. *Annu Rev Biochem*. 79:295-319.

Liu, W., Y. Liu, J. Liu, J. Zhai, and Y. Xie. 2011. Evidence for inter- and intra-clade recombinations in rabies virus. *Infect Genet Evol*. 11:1906-1912.

Lowy, D.R., E. Rands, S.K. Chattopadhyay, C.F. Garon, and G.L. Hager. 1980. Molecular cloning of infectious integrated murine leukemia virus DNA from infected mouse cells. *Proc Natl Acad Sci U S A*. 77:614-618.

Luke, G.A., P. de Felipe, A. Lukashev, S.E. Kallioinen, E.A. Bruno, and M.D. Ryan. 2008. Occurrence, function and evolutionary origins of '2A-like' sequences in virus genomes. *J Gen Virol*. 89:1036-1042.

Lund, E., S. Guttinger, A. Calado, J.E. Dahlberg, and U. Kutay. 2004. Nuclear export of microRNA precursors. *Science*. 303:95-98.

Luytjes, W., M. Krystal, M. Enami, J.D. Parvin, and P. Palese. 1989. Amplification, expression, and packaging of foreign gene by influenza virus. *Cell*. 59:1107-1113.

Macrae, I.J., K. Zhou, F. Li, A. Repic, A.N. Brooks, W.Z. Cande, P.D. Adams, and J.A. Doudna. 2006. Structural basis for double-stranded RNA processing by Dicer. *Science*. 311:195-198.

Marschalek, A., L. Drechsel, and K.K. Conzelmann. 2012. The importance of being short: the role of rabies virus phosphoprotein isoforms assessed by differential IRES translation initiation. *Eur J Cell Biol*. 91:17-23.

Marschalek, A., S. Finke, M. Schwemmle, D. Mayer, B. Heimrich, L. Stitz, and K.K. Conzelmann. 2009. Attenuation of rabies virus replication and virulence by picornavirus internal ribosome entry site elements. *J Virol*. 83:1911-1919.

Martin, A., P. Staeheli, and U. Schneider. 2006. RNA polymerase II-controlled expression of antigenomic RNA enhances the rescue efficacies of two different members of the

Mononegavirales independently of the site of viral genome replication. *J Virol*. 80:5708-5715.

Mastroyiannopoulos, N.P., J.B. Uney, and L.A. Phylactou. 2010. The application of ribozymes and DNAzymes in muscle and brain. *Molecules*. 15:5460-5472.

Mebatsion, T., and K.K. Conzelmann. 1996. Specific infection of CD4+ target cells by recombinant rabies virus pseudotypes carrying the HIV-1 envelope spike protein. *Proc Natl Acad Sci U S A*. 93:11366-11370.

Mebatsion, T., S. Finke, F. Weiland, and K.K. Conzelmann. 1997. A CXCR4/CD4 pseudotype rhabdovirus that selectively infects HIV-1 envelope protein-expressing cells. *Cell*. 90:841-847.

Mebatsion, T., M. Konig, and K.K. Conzelmann. 1996a. Budding of rabies virus particles in the absence of the spike glycoprotein. *Cell*. 84:941-951.

Mebatsion, T., M.J. Schnell, and K.K. Conzelmann. 1995. Mokola virus glycoprotein and chimeric proteins can replace rabies virus glycoprotein in the rescue of infectious defective rabies virus particles. *J Virol*. 69:1444-1451.

Mebatsion, T., M.J. Schnell, J.H. Cox, S. Finke, and K.K. Conzelmann. 1996b. Highly stable expression of a foreign gene from rabies virus vectors. *Proc Natl Acad Sci U S A*. 93:7310-7314.

Mebatsion, T., F. Weiland, and K.K. Conzelmann. 1999. Matrix protein of rabies virus is responsible for the assembly and budding of bullet-shaped particles and interacts with the transmembrane spike glycoprotein G. *J Virol*. 73:242-250.

Mirakhur, B., and R.W. Peluso. 1988. In vitro assembly of a functional nucleocapsid from the negative-stranded genome RNA of a defective interfering particle of vesicular stomatitis virus. *Proc Natl Acad Sci U S A*. 85:7511-7515.

Morimoto, K., H.D. Foley, J.P. McGettigan, M.J. Schnell, and B. Dietzschold. 2000. Reinvestigation of the role of the rabies virus glycoprotein in viral pathogenesis using a reverse genetics approach. *J Neurovirol*. 6:373-381.

Mottet-Osman, G., F. Iseni, T. Pelet, M. Wiznerowicz, D. Garcin, and L. Roux. 2007. Suppression of the Sendai virus M protein through a novel short interfering RNA approach inhibits viral particle production but does not affect viral RNA synthesis. *J Virol*. 81:2861-2868.

Neumann, G., T. Watanabe, H. Ito, S. Watanabe, H. Goto, P. Gao, M. Hughes, D.R. Perez, R. Donis, E. Hoffmann, G. Hobom, and Y. Kawaoka. 1999. Generation of influenza A viruses entirely from cloned cDNAs. *Proc Natl Acad Sci U S A*. 96:9345-9350.

Ngo, H., C. Tschudi, K. Gull, and E. Ullu. 1998. Double-stranded RNA induces mRNA degradation in Trypanosoma brucei. *Proc Natl Acad Sci U S A*. 95:14687-14692.

Niwa, H., K. Yamamura, and J. Miyazaki. 1991. Efficient selection for high-expression transfectants with a novel eukaryotic vector. *Gene*. 108:193-199.

Ogino, T., and A.K. Banerjee. 2007. Unconventional mechanism of mRNA capping by the RNA-dependent RNA polymerase of vesicular stomatitis virus. *Mol Cell*. 25:85-97.

Ong, S.T., F. Li, J. Du, Y.W. Tan, and S. Wang. 2005. Hybrid cytomegalovirus enhancer-h1 promoter-based plasmid and baculovirus vectors mediate effective RNA interference. *Hum Gene Ther*. 16:1404-1412.

Orbanz, J., and S. Finke. 2010. Generation of recombinant European bat lyssavirus type 1 and inter-genotypic compatibility of lyssavirus genotype 1 and 5 antigenome promoters. *Arch Virol*. 155:1631-1641.

Osakada, F., T. Mori, A.H. Cetin, J.H. Marshel, B. Virgen, and E.M. Callaway. 2011. New rabies virus variants for monitoring and manipulating activity and gene expression in defined neural circuits. *Neuron*. 71:617-631.

Paddison, P.J., A.A. Caudy, E. Bernstein, G.J. Hannon, and D.S. Conklin. 2002. Short hairpin RNAs (shRNAs) induce sequence-specific silencing in mammalian cells. *Genes Dev*. 16:948-958.

Paddison, P.J., A.A. Caudy, R. Sachidanandam, and G.J. Hannon. 2004. Short hairpin activated gene silencing in mammalian cells. *Methods Mol Biol*. 265:85-100.

Park, J.E., I. Heo, Y. Tian, D.K. Simanshu, H. Chang, D. Jee, D.J. Patel, and V.N. Kim. 2011. Dicer recognizes the 5' end of RNA for efficient and accurate processing. *Nature*. 475:201-205.

Park, K.H., T. Huang, F.F. Correia, and M. Krystal. 1991. Rescue of a foreign gene by Sendai virus. *Proc Natl Acad Sci U S A*. 88:5537-5541.

Paterson, R.G., C.J. Russell, and R.A. Lamb. 2000. Fusion protein of the paramyxovirus SV5: destabilizing and stabilizing mutants of fusion activation. *Virology*. 270:17-30.

Pattnaik, A.K., L.A. Ball, A. LeGrone, and G.W. Wertz. 1995. The termini of VSV DI particle RNAs are sufficient to signal RNA encapsidation, replication, and budding to generate infectious particles. *Virology*. 206:760-764.

Pattnaik, A.K., L.A. Ball, A.W. LeGrone, and G.W. Wertz. 1992. Infectious defective interfering particles of VSV from transcripts of a cDNA clone. *Cell*. 69:1011-1020.

Pattnaik, A.K., and G.W. Wertz. 1990. Replication and amplification of defective interfering particle RNAs of vesicular stomatitis virus in cells expressing viral proteins from vectors containing cloned cDNAs. *J Virol*. 64:2948-2957.

Pattnaik, A.K., and G.W. Wertz. 1991. Cells that express all five proteins of vesicular stomatitis virus from cloned cDNAs support replication, assembly, and budding of defective interfering particles. *Proc Natl Acad Sci U S A*. 88:1379-1383.

Perez, M., A. Sanchez, B. Cubitt, D. Rosario, and J.C. de la Torre. 2003. A reverse genetics system for Borna disease virus. *J Gen Virol*. 84:3099-3104.

Perrotta, A.T., and M.D. Been. 1991. A pseudoknot-like structure required for efficient self-cleavage of hepatitis delta virus RNA. *Nature*. 350:434-436.

Perrotta, A.T., and M.D. Been. 1998. A toggle duplex in hepatitis delta virus self-cleaving RNA that stabilizes an inactive and a salt-dependent pro-active ribozyme conformation. *J Mol Biol*. 279:361-373.

Perrotta, A.T., O. Nikiforova, and M.D. Been. 1999. A conserved bulged adenosine in a peripheral duplex of the antigenomic HDV self-cleaving RNA reduceskinetic trapping of inactive conformations. *Nucleic Acids Res*. 27:795-802.

Pfeffer, S., M. Zavolan, F.A. Grasser, M. Chien, J.J. Russo, J. Ju, B. John, A.J. Enright, D. Marks, C. Sander, and T. Tuschl. 2004. Identification of virus-encoded microRNAs. *Science*. 304:734-736.

Prehaud, C., N. Wolff, E. Terrien, M. Lafage, F. Megret, N. Babault, F. Cordier, G.S. Tan, E. Maitrepierre, P. Menager, D. Chopy, S. Hoos, P. England, M. Delepierre, M.J. Schnell, H. Buc, and M. Lafon. 2010. Attenuation of rabies virulence: takeover by the cytoplasmic domain of its envelope protein. *Sci Signal*. 3:ra5.

Prevosto, V., W. Graf, and G. Ugolini. 2009. Posterior parietal cortex areas MIP and LIPv receive eye position and velocity inputs via ascending preposito-thalamo-cortical pathways. *Eur J Neurosci*. 30:1151-1161.

Prody, G.A., J.T. Bakos, J.M. Buzayan, I.R. Schneider, and G. Bruening. 1986. Autolytic processing of dimeric plant virus satellite RNA. *Science*. 231:1577-1580.

Qanungo, K.R., D. Shaji, M. Mathur, and A.K. Banerjee. 2004. Two RNA polymerase complexes from vesicular stomatitis virus-infected cells that carry out transcription and replication of genome RNA. *Proc Natl Acad Sci U S A*. 101:5952-5957.

Racaniello, V.R., and D. Baltimore. 1981. Cloned poliovirus complementary DNA is infectious in mammalian cells. *Science*. 214:916-919.

Radecke, F., P. Spielhofer, H. Schneider, K. Kaelin, M. Huber, C. Dotsch, G. Christiansen, and M.A. Billeter. 1995. Rescue of measles viruses from cloned DNA. *EMBO J*. 14:5773-5784.

Rieder, M., K. Brzózka, C.K. Pfaller, J.H. Cox, L. Stitz, and K.K. Conzelmann. 2011. Genetic dissection of interferon-antagonistic functions of rabies virus phosphoprotein: inhibition of interferon regulatory factor 3 activation is important for pathogenicity. *J Virol*. 85:842-852.

Rieder, M., and K.K. Conzelmann. 2011. Interferon in rabies virus infection. *Adv Virus Res*. 79:91-114.

Rong, M., R.K. Durbin, and W.T. McAllister. 1998. Template strand switching by T7 RNA polymerase. *J Biol Chem*. 273:10253-10260.

Scherer, L.J., and J.J. Rossi. 2003. Approaches for the sequence-specific knockdown of mRNA. *Nat Biotechnol*. 21:1457-1465.

Schierup, M.H., C.H. Mordhorst, C.P. Muller, and L.S. Christensen. 2005. Evidence of recombination among early-vaccination era measles virus strains. *BMC Evol Biol*. 5:52.

Schneider, H., P. Spielhofer, K. Kaelin, C. Dotsch, F. Radecke, G. Sutter, and M.A. Billeter. 1997. Rescue of measles virus using a replication-deficient vaccinia-T7 vector. *J Virol Methods*. 64:57-64.

Schneider, L.G. 1995. Rabies virus vaccines. *Dev Biol Stand*. 84:49-54.

Schneider, U., M. Naegele, P. Staeheli, and M. Schwemmle. 2003. Active borna disease virus polymerase complex requires a distinct nucleoprotein-to-phosphoprotein ratio but no viral X protein. *J Virol*. 77:11781-11789.

Schnell, M.J., L. Buonocore, E. Boritz, H.P. Ghosh, R. Chernish, and J.K. Rose. 1998. Requirement for a non-specific glycoprotein cytoplasmic domain sequence to drive efficient budding of vesicular stomatitis virus. *EMBO J*. 17:1289-1296.

Schnell, M.J., T. Mebatsion, and K.K. Conzelmann. 1994. Infectious rabies viruses from cloned cDNA. *EMBO J*. 13:4195-4203.

Schnellhammer, C. 2009. Funktionelle Analyse des Matrixproteins des Tollwutvirus. *In* PhD thesis. LMU München.

Schwarz, D.S., G. Hutvagner, T. Du, Z. Xu, N. Aronin, and P.D. Zamore. 2003. Asymmetry in the assembly of the RNAi enzyme complex. *Cell*. 115:199-208.

Sharmeen, L., M.Y. Kuo, G. Dinter-Gottlieb, and J. Taylor. 1988. Antigenomic RNA of human hepatitis delta virus can undergo self-cleavage. *J Virol*. 62:2674-2679.

Silhavy, D., A. Molnar, A. Lucioli, G. Szittya, C. Hornyik, M. Tavazza, and J. Burgyan. 2002. A viral protein suppresses RNA silencing and binds silencing-generated, 21- to 25-nucleotide double-stranded RNAs. *EMBO J*. 21:3070-3080.

Siolas, D., C. Lerner, J. Burchard, W. Ge, P.S. Linsley, P.J. Paddison, G.J. Hannon, and M.A. Cleary. 2005. Synthetic shRNAs as potent RNAi triggers. *Nat Biotechnol*. 23:227-231.

Song, Q., Y. Cao, Q. Li, M. Gu, L. Zhong, S. Hu, H. Wan, and X. Liu. 2011. Artificial recombination may influence the evolutionary analysis of Newcastle disease virus. *J Virol*. 85:10409-10414.

Sonwane, A.A., S.S. Dahiya, M. Saini, V.K. Chaturvedi, R.P. Singh, and P.K. Gupta. 2011. Inhibition of rabies virus multiplication by siRNA delivered through adenoviral vector in vitro in BHK-21 cells and in vivo in mice. *Res Vet Sci*.

Soukup, G.A., and R.R. Breaker. 1999. Design of allosteric hammerhead ribozymes activated by ligand-induced structure stabilization. *Structure*. 7:783-791.

Spann, K.M., P.L. Collins, and M.N. Teng. 2003. Genetic recombination during coinfection of two mutants of human respiratory syncytial virus. *J Virol*. 77:11201-11211.

Starega-Roslan, J., E. Koscianska, P. Kozlowski, and W.J. Krzyzosiak. 2011. The role of the precursor structure in the biogenesis of microRNA. *Cell Mol Life Sci*. 68:2859-2871.

Sullenger, B.A., and T.R. Cech. 1994. Ribozyme-mediated repair of defective mRNA by targeted, trans-splicing. *Nature*. 371:619-622.

Superti, F., M. Derer, and H. Tsiang. 1984. Mechanism of rabies virus entry into CER cells. *J Gen Virol*. 65 (Pt 4):781-789.

Sutter, G., M. Ohlmann, and V. Erfle. 1995. Non-replicating vaccinia vector efficiently expresses bacteriophage T7 RNA polymerase. *FEBS Lett*. 371:9-12.

Tang, Y., O. Rampin, F. Giuliano, and G. Ugolini. 1999. Spinal and brain circuits to motoneurons of the bulbospongiosus muscle: retrograde transneuronal tracing with rabies virus. *J Comp Neurol*. 414:167-192.

Taniguchi, T., M. Palmieri, and C. Weissmann. 1978. A Qbeta DNA-containing hybrid plasmid giving rise to Qbeta phage formation in the bacterial host [proceedings]. *Ann Microbiol (Paris)*. 129 B:535-536.

Theriault, S., A. Groseth, G. Neumann, Y. Kawaoka, and H. Feldmann. 2004. Rescue of Ebola virus from cDNA using heterologous support proteins. *Virus Res*. 106:43-50.

Thoulouze, M.I., M. Lafage, M. Schachner, U. Hartmann, H. Cremer, and M. Lafon. 1998. The neural cell adhesion molecule is a receptor for rabies virus. *J Virol*. 72:7181-7190.

Tomar, R.S., H. Matta, and P.M. Chaudhary. 2003. Use of adeno-associated viral vector for delivery of small interfering RNA. *Oncogene*. 22:5712-5715.

Tsiang, H., P.E. Ceccaldi, and E. Lycke. 1991. Rabies virus infection and transport in human sensory dorsal root ganglia neurons. *J Gen Virol*. 72 (Pt 5):1191-1194.

Tuffereau, C., J. Benejean, D. Blondel, B. Kieffer, and A. Flamand. 1998. Low-affinity nerve-growth factor receptor (P75NTR) can serve as a receptor for rabies virus. *EMBO J*. 17:7250-7259.

Tuffereau, C., K. Schmidt, C. Langevin, F. Lafay, G. Dechant, and M. Koltzenburg. 2007. The rabies virus glycoprotein receptor p75NTR is not essential for rabies virus infection. *J Virol*. 81:13622-13630.

Tuschl, T., P.D. Zamore, R. Lehmann, D.P. Bartel, and P.A. Sharp. 1999. Targeted mRNA degradation by double-stranded RNA in vitro. *Genes Dev*. 13:3191-3197.

Ugolini, G. 1995. Specificity of rabies virus as a transneuronal tracer of motor networks: transfer from hypoglossal motoneurons to connected second-order and higher order central nervous system cell groups. *J Comp Neurol*. 356:457-480.

Ugolini, G. 2008. Use of rabies virus as a transneuronal tracer of neuronal connections: implications for the understanding of rabies pathogenesis. *Dev Biol (Basel)*. 131:493-506.

Ugolini, G. 2010. Advances in viral transneuronal tracing. *J Neurosci Methods*. 194:2-20.

Ugolini, G. 2011. Rabies virus as a transneuronal tracer of neuronal connections. *Adv Virus Res*. 79:165-202.

Uhlenbeck, O.C. 1987. A small catalytic oligoribonucleotide. *Nature*. 328:596-600.

van Tol, H., J.M. Buzayan, P.A. Feldstein, F. Eckstein, and G. Bruening. 1990. Two autolytic processing reactions of a satellite RNA proceed with inversion of configuration. *Nucleic Acids Res*. 18:1971-1975.

Vermeulen, A., L. Behlen, A. Reynolds, A. Wolfson, W.S. Marshall, J. Karpilow, and A. Khvorova. 2005. The contributions of dsRNA structure to Dicer specificity and efficiency. *RNA*. 11:674-682.

Voinnet, O. 2005. Induction and suppression of RNA silencing: insights from viral infections. *Nat Rev Genet*. 6:206-220.

Volchkov, V.E., V.A. Volchkova, E. Muhlberger, L.V. Kolesnikova, M. Weik, O. Dolnik, and H.D. Klenk. 2001. Recovery of infectious Ebola virus from complementary DNA: RNA editing of the GP gene and viral cytotoxicity. *Science*. 291:1965-1969.

Wadkins, T.S., and M.D. Been. 2002. Ribozyme activity in the genomic and antigenomic RNA strands of hepatitis delta virus. *Cell Mol Life Sci*. 59:112-125.

Wadkins, T.S., A.T. Perrotta, A.R. Ferre-D'Amare, J.A. Doudna, and M.D. Been. 1999. A nested double pseudoknot is required for self-cleavage activity of both the genomic and antigenomic hepatitis delta virus ribozymes. *RNA*. 5:720-727.

Wang, Z.W., L. Sarmento, Y. Wang, X.Q. Li, V. Dhingra, T. Tseggai, B. Jiang, and Z.F. Fu. 2005. Attenuated rabies virus activates, while pathogenic rabies virus evades, the host innate immune responses in the central nervous system. *J Virol*. 79:12554-12565.

Wargelius, A., S. Ellingsen, and A. Fjose. 1999. Double-stranded RNA induces specific developmental defects in zebrafish embryos. *Biochem Biophys Res Commun*. 263:156-161.

Wertz, G.W., V.P. Perepelitsa, and L.A. Ball. 1998. Gene rearrangement attenuates expression and lethality of a nonsegmented negative strand RNA virus. *Proc Natl Acad Sci U S A*. 95:3501-3506.

Whelan, S.P. 2008. Response to "Non-segmented negative-strand RNA virus RNA synthesis in vivo". *Virology*. 371:234-237.

Whelan, S.P., L.A. Ball, J.N. Barr, and G.T. Wertz. 1995. Efficient recovery of infectious vesicular stomatitis virus entirely from cDNA clones. *Proc Natl Acad Sci U S A*. 92:8388-8392.

Whelan, S.P., J.N. Barr, and G.W. Wertz. 2004. Transcription and replication of nonsegmented negative-strand RNA viruses. *Curr Top Microbiol Immunol*. 283:61-119.

Whelan, S.P., and G.W. Wertz. 2002. Transcription and replication initiate at separate sites on the vesicular stomatitis virus genome. *Proc Natl Acad Sci U S A*. 99:9178-9183.

WHO. 2011. Fact sheet on rabies. Vol. Fact sheet #99.

Wianny, F., and M. Zernicka-Goetz. 2000. Specific interference with gene function by double-stranded RNA in early mouse development. *Nat Cell Biol*. 2:70-75.

Wickersham, I.R., S. Finke, K.K. Conzelmann, and E.M. Callaway. 2007a. Retrograde neuronal tracing with a deletion-mutant rabies virus. *Nature Methods*. 4:47-49.

Wickersham, I.R., D.C. Lyon, R.J.O. Barnard, T. Mori, S. Finke, K.K. Conzelmann, J.A.T. Young, and E.M. Callaway. 2007b. Monosynaptic restriction of transsynaptic tracing from single, genetically targeted neurons. *Neuron*. 53:639-647.

Wiegand, M.A., S. Bossow, S. Schlecht, and W.J. Neubert. 2007. De novo synthesis of N and P proteins as a key step in Sendai virus gene expression. *J Virol*. 81:13835-13844.

Witko, S.E., C.S. Kotash, R.M. Nowak, J.E. Johnson, L.A. Boutilier, K.J. Melville, S.G. Heron, D.K. Clarke, A.S. Abramovitz, R.M. Hendry, M.S. Sidhu, S.A. Udem, and C.L. Parks. 2006. An efficient helper-virus-free method for rescue of recombinant

paramyxoviruses and rhadoviruses from a cell line suitable for vaccine development. *J Virol Methods*. 135:91-101.

Wu, X., and C.E. Rupprecht. 2008. Glycoprotein gene relocation in rabies virus. *Virus Res*. 131:95-99.

Wyatt, L.S., B. Moss, and S. Rozenblatt. 1995. Replication-deficient vaccinia virus encoding bacteriophage T7 RNA polymerase for transient gene expression in mammalian cells. *Virology*. 210:202-205.

Yi, R., Y. Qin, I.G. Macara, and B.R. Cullen. 2003. Exportin-5 mediates the nuclear export of pre-microRNAs and short hairpin RNAs. *Genes Dev*. 17:3011-3016.

Zeng, Y., and B.R. Cullen. 2005. Efficient processing of primary microRNA hairpins by Drosha requires flanking nonstructured RNA sequences. *J Biol Chem*. 280:27595-27603.

Zhang, X., W. Kong, S. Ashraf, and R. Curtiss, 3rd. 2009. A one-plasmid system to generate influenza virus in cultured chicken cells for potential use in influenza vaccine. *J Virol*. 83:9296-9303.

Zhou, H., X.G. Xia, and Z. Xu. 2005. An RNA polymerase II construct synthesizes short-hairpin RNA with a quantitative indicator and mediates highly efficient RNAi. *Nucleic Acids Res*. 33:e62.

6 Appendix

6.1 List of oligo sequences

Oligos made for this work (numerical order)

AG 8	5'-CTAGCGGTACCCGAACGGCATCAAGGTGAACTTCAAGAGAGTTCACCTTGATGCCGTTCTTTTTGGAAAGC-3'
AG 9	5'-GGCCGCTTTCCAAAAAGAACGGCATCAAGGTGAACTCTCTTGAAGTTCACCTTGATGCCGTTCGGGTACCG-3'
AG 10	5'-CTAGCGGTACCCTGATGAGGCCGAAAGGCCGAAACTCCGTAAGGAGTCCCCGAACGGCATCAAGGTGAACTTCAAGAGAGTTCACCTTGATGCCGTTCTTTTTGGAAAGC-3'
AG 11	5'-GGCCGCTTTCCAAAAAGAACGGCATCAAGGTGAACTCTCTTGAAGTTCACCTTGATGCCGTTCGGGGACTCCTTACGGAGTTTCGGCCTTTCGGCCTCATCAGGGTACCG-3'
AG 12	5'-CTAGCGAATTCAAACAACAAAGGGGCTGATGAGGCCGAAAGGCCGAAACTCCGTAAGGAGTCCCCCAAATAGAAATATAAAAG-3'
AG 13	5'-GTACCTTTTATATTTCTATTTGGGGGACTCCTTACGGAGTTTCGGCCTTTCGGCCTCATCAGCCCCTTTGTTGTTTGAATTCG-3'
AG 16	5'-CCCCGGACCGCGAGGAGGTGGAGATGCCATGCCGACCCAACACTTTTCCAAAAAGAACGGCATC-3'
AG 17	5'-GGGCCCGGGGCTAGCGGCGCCCAACATAGGGGCTGATGA-3'
AG 18	5'-GGGCCCGGGGCTAGCGGCGCCGCTAGCGGTACCCGAACG-3'
AG 19	5'-CCCGCGGCCGCCTCCCTTAGCCATCCGAG-3'
AG 24	5'-CCCGCGGCCGCTGGCTCTCCCTTAGCCATCCGAG-3'
AG 25	5'-CCCGCGGCCGCGTACCTGGCTCTCCCTTAGCCATCCGAGTGGACGACGTCCT-3'
AG 26	5'-CCCGCTCAGCGGTGGCAGCAGCCAACTCAGCTTCCTTTCGGGCTTTGTTAGCAGCCGGATCCCCGCTGGCTCTCCCTTAGCCATCCGAG-3'
AG 27	5'-GGGAAGCTTGATATCGAATTCCT-3'
AG 29	5'-GGCGCTAGCGAATTCAATCAACATAGTTCCTGATGAGGCCGAAAGGCCGAAACTCCGTAAGGAGTC-3'
AG 30	5'-GGCGCTAGCGAATTCAATCAACATAGAACCTGATGAGGCCGAAAGGCCGAAACTCCGTAAGGAGTC-3'
AG 31	5'-ATAGCTAGCCCGAAACTCCGTAAGGAGTCGAACGGCATCAAGGTGAACTTCAAGAGAGTTCACCTTGA-3'
AG 32	5'-ATAGCTAGCCCGAAACTCCGTAAGGAGTCGTTCACCTTGATGCCGTTCTTCAAGAGAGAACGGCATCA-3'
AG 33	5'-GGTCGGUCCGCGUGGUGGTGGUGUTGCCUGCCGUCCCAAGAACGGCATCAAGGTGAACTCTCTTGAA-3'
AG 34	5'-GGTCGGUCCGCGUGGUGGTGGUGUTGCCUGCCGUCCCAAGTGGACCTTGATGCCGTTCTCTCTTGAA-3'
AG 35	5'-GGGCTGCAGGGTACCGGCGCGCCTAATACGACTCACTATAGGGTTTAAACGCGTCTGATGAGGC-3'
AG 36	5'-AGGGTTTAAACGCGTCTGATGAGGCCGAAAGGCCGAAACTCCGTAAGGAGTCACGCTTAACAACCAGATC-3'
AG 37	5'-GGGCCTAGGGTTATACAGGGC-3'
AG 53	5'-ATAGCTAGCACCATGGTGAGCAAGGGCGAG-3'
AG 54	5'-TATGCGGCCGCTCAGTTATCTAGATCCGG-3'

AG 55	5'-GATCCCCGAACGGCATCAAGGTGAACTTCAAGAGAGTTCACCTTGATGCCGTTCTTTTT GGAAA-3'
AG 56	5'-AGCTTTTCCAAAAAGAACGGCATCAAGGTGAACTCTCTTGAAGTTCACCTTGATGCCGT TCGGG-3'
AG 63	5'-GGGATCGATGTTAACCATGGTGAGCAAGGGCGAG-3'
AG 64	5'-TATCCTAGGGCGCCTCAGTTATCTAGATCCGG-3'
AG 87	5'-GGGCCTAGGAAAGGCTCCCGATTTAA-3'
AG 88	5'-CCCTACGTAATGCCCGGGTGAGTCACTCGAATATGT-3'
AG 89	5'-ATACCCGGGGAAGGTAGAGGCTCTTTACTAACATGCGGCGACGTTGAGGAAAACCCA GGACCAATGAGCAAGATCTTTGTC-3'
AG 90	5'-CCCTACGTAGGAGGTTCATTT-3'
AG 93	5'-AGGGGTTTAAACGGCCGGCCCGAATTAATTCCGGTTAT-3'
AG 94	5'-ATCTGGCCGGCCTGTAGGGGTGTTACATTTTTGCTTTGCAATTGACAATGTCTGTTTTTT CTTTGATCTGGTTGTTAAGCGT-3'
AG 95	5'-AGAGGCCGGCCCCCATCAGACGCACAAAACCA-3'
AG 96	5'-ATCCACGATAATCTCAGGCTTCAAAGAGACCACCTGATTATTGACTTTGAATACAATCT TGTCGGCATGATAACAATCTGTGA-3'
AG 97	5'-CTATCCTAGGGTTATACAGGGCTTTTTCAAATCTTTGATGGCAGGGTACTTGTACTCAT ATTGATCCACGATAATCTCAGGCT-3'
AG 110	5'-AGGGTTTAAACGCGTCTGATGAGGCCGAAAGGCCGAAACTCCGTAAGGAGTCACGCT TAACAAATAAACAACAA-3'
AG 111	5'-AGGTCGGACCGCGAGGAGGT-3'
AG 131	5'-ATATGGCCGGCCATGGATGCCGACAAGATT-3'
AG 132	5'-ATATGGCCGGCCTTATGAGTCACTCGAATA-3'
AG 159	5'-ATATGGCCGGCCATGGTGAGCAAGGGCGAGG-3'
AG 160	5'-ATATGGCCGGCCTCAGTTATCTAGATCCGGT-3'
AG 162	5'-ATGAACCTCCTACGTAAGA-3'
AG 163	5'-ATATAGCGCTTATGGCCGGCCTTGAAGTAAGTCTCAGGTTG-3'
AG 164	5'-CCTTCAGCGCTCAGAATCT-3'
AG 165	5'-ATATGGCCGGCCTTATGTACTCATATTGATCCA-3'
AG 166	5'-ATATGGCCGGCCTTAGCGCTCATGCCTGACAAA-3'
AG 170	5'-ATATAGATCTGGCCGGCCGAATTCGAAGTTGAATAACAAAATGC-3'
AG 171	5'-CGCCAGATCTTTACAATTTGGACTTTCCG-3'
AG 196	5'-AGGTCGGACCGCGAGGAGGTGGAGATGCCATGCCGACCCACGCTTAACAACCAGATC -3'
AG 197	5'-ACGCTTAACAACCAGATCAAAGAAAAAACAG-3'
AG 208	5'-ATATGGGCCCAATAACCGTCCATTTACATG-3'
AG 223	5'-ATATTCGAACCATCCCAAACCGAATTAATTCCGGTTATTTTCC-3'
AG 225	5'-CTATCTCACCATGGTTGGGCG-3'
AG 226	5'-GTATAACCCTAGGAAAGGC-3'
AG 227	5'-TATTTCGAAATGGATATACACAATCCGTAG-3'
AG 259	5'-TGTAGGGGTGTTACATTTTTGCTTTGC-3'
AG 260	5'-GCAAAAATGTAACACCCCTACATTGGATGCCGACAAGATTGTATTC-3'

Oligos kindly provided

AM 9	5'-GAATTCGCTAGCATCAGACGCACAAAACCAAG-3'	A. Marschalek
AK 70	5'-TCGGGCGCCTTAGCAAGATGTATAGCG-3'	A. Kern

6.2 List of plasmids and cloning strategies

Plasmids cloned for this work (alphabetical order)	
pCAGGS-dHH-HSmm-SC1	A template-less PCR reaction with the primers AG 32 and AG 34 amplified a fragment comprising an inverse shGFP with 2 mismatches together with a shortened 5'-HHRz and 3'-HDVagRz sequences up to the *RsrII*-site (Ribozymes in direct proximity to the shGFP). The product was digested with *NheI* and *RsrII* and ligated into the equally digested vector pCAGGS-HH-shGFP-SC1.
pCAGGS-dHH-SH-SC1	A template-less PCR reaction with the primers AG 31 and AG 33 amplified an shGFP fragment with a shortened 5'-HHRz and 3'-HDVagRz sequences up to the *RsrII*-site (Ribozymes in direct proximity to the shGFP). The product was digested with *NheI* and *RsrII* and ligated into the equally digested vector pCAGGS-HH-shGFP-SC1.
pCAGGS-GFP	The eGFP-ORF was cut out from pEGFP-C3 by a digestion with *NheI* followed by Klenow fill-in and a further digestion with *XmaI*. The insert was ligated into the vector pCAGGS which was digested with *SacI* and after a Klenow fill-in further digested with *XmaI*.
pCAGGS-HH_SH_SC1	A template-less PCR reaction with the primers AG 31 and AG 33 amplified an shGFP fragment with a shortened 5'-HHRz and 3'-HDVagRz sequences up to the *RsrII*-site (Ribozymes in direct proximity to the shGFP). In a second PCR this fragment was prolonged by further HHRz sequences using the primers AG 29 and AG 33. The product was digested with *NheI* and *RsrII* and ligated into the equally digested vector pCAGGS-HH-shGFP-SC1.
pCAGGS-HH-HSmm-SC1	A template-less PCR reaction with the primers AG 32 and AG 34 amplified a fragment comprising an inverse shGFP with 2 mismatches together with a shortened 5'-HHRz and 3'-HDVagRz sequences up to the *RsrII*-site (Ribozymes in direct proximity to the shGFP). In a second PCR this fragment was prolonged by further HHRz sequences using the primers AG 30 and AG 34. The product was digested with *NheI* and *RsrII* and ligated into the equally digested vector pCAGGS-HH-shGFP-SC1.
pCAGGS-HH-shGFP-SC1	An *SacII-NheI* fragment comprising the shGFP with a 5'-HHRz and a 3'-SC1 seperated by spacer sequences was cut out from pSAD G_HH-shGFP-SC1 and ligated into the equally digested vector pCAGGS.
pCAGGS-N_eGFP	The eGFP ORF was PCR-amplified from pEGFP-C3 and prolonged by the RABV N/P gene border and adequate restriction sites using primers AG 63 and AG 64. The PCR product was digested with *ClaI* and *AvrII* and ligated into the vector pCAGGS-NPM(inv) which was digested with *BstBI* and *XbaI*.

pCAGGS-NEP(bi)M	In a PCR reaction a fragment of the RABV N gene together with the N-3'-UTR was amplified from pSAD L16. Using the primers AG 226 and AG 227 the fragment was prolonged by RABV P-5'-UTR sequences. The PCR product was digested with *SwaI* and *BstBI* and ligated into the equally digested vector pCAGGS-NEP(mono)M.
pCAGGS-NEP(mono)M	A fragment comprising the EMCV IRES and the RABV P gene up to the *NcoI*-site was PCR-amplified from pTIT-P. The primers AG 223 and AG 225 prolonged this fragment by the 5'-UTR of the RABV P gene upstream of the IRES element and adequate restriction sites. The PCR product was digested with *BstBI* and *NcoI* and ligated into the equally digested vector pCAGGS-NPM(inv).
pCAGGS-NPM(inv)	An *AvrII-SnaBI* fragment was cut out from pSAD L16 and ligated into the equally digested vector pCAGGS.
pCAGGS-T7_L16	The RABV full-length cDNA together with flanking sequences (5'-T7 promoter and 3'-HDV and T7 terminator sequences) was cut out from pSAD L16 with *PstI* and *SpeI*. This fragment was ligated into the vector pCAGGS which was digested with *NsiI* and *NheI*.
pCAGGS-T7_L16_SC	The RABV full-length cDNA together with flanking sequences (5'-T7 promoter and 3'-SC1 and T7 terminator sequences) was cut out from pSAD L16_SC with *PstI* and *SpeI*. This fragment was ligated into the vector pCAGGS which was digested with *NsiI* and *NheI*.
pCAGGS-T7_NEP(bi)EL	A 4 kb fragment was cut out of pSAD T7-HH_EP(bi)_SC by a digestion with *SwaI* followed by a partial digestion with *AsuII*. As a vector for the ligation, pCAGGS-T7_NEP(mono)EL was digested with *SwaI* and *AsuII*.
pCAGGS-T7_NEP(bi)EL_SC	A 4 kb fragment was cut out of pSAD T7-HH_EP(bi)_SC by a digestion with SwaI followed by a partial digestion with AsuII. As a vector for the ligation, pCAGGS-T7_NEP(mono)EL_SC was digested with SwaI and AsuII.
pCAGGS-T7_NEP(mono)EL	An *AsuII-RsrII* fragment was cut out from pSAD T7-HH_EL_SC and ligated into the equally digested vector pCAGGS-T7_SAD NEP(mono).
pCAGGS-T7_NEP(mono)EL_SC	An *AsuII-RsrII* fragment was cut out from pSAD T7-HH_EL_SC and ligated into the equally digested vector pCAGGS-T7_SAD NEP(mono)_SC.
pCAGGS-T7_SAD NEP(mono)_SC	A *SwaI-AflIII* fragment of the RABV full-length cDNA was cut out from pSAD T7-HH_EP(mono)_SC and ligated into the equally digested vector pCAGGS-T7_L16_SC.
pCAGGS-T7-HH_L16_SC	The RABV full-length cDNA together with flanking sequences (5'-T7 promoter and HHRz, and 3'-SC1 and T7 terminator sequences) was cut out from pSAD T7-HH_L16_SC with *PstI* and *SpeI*. This fragment was ligated into the vector pCAGGS which was digested with *NsiI* and *NheI*.
pCAGGS-T7-	A *KpnI-SpeI* fragment comprising T7 promoter, the HHRz

HH_L16_SC_T7T_pA	sequence, the RABV full-length cDNA, the SC1 and the T7 terminator sequence, was cut out from pSAD T7-HH_L16_SC and ligated into the *KpnI* and *NheI* digested vector pCAGGS.
pCAGGS-T7-HH_NEN2APEL_SC	A *PmeI-RsrII* fragment comprising the SAD NEN2APEL full-length cDNA with 5'-HHRz sequences and parts of the 3'-SC1 sequences, was cut out from pSAD T7-HH_NEN2APEL_SC and ligated into the equally digested vector pCAGGS-T7-HH_L16_SC_T7T_pA.
pCAGGS-T7-HH_NENEPEL_SC	A *PmeI-RsrII* fragment comprising the SAD NENEPEL full-length cDNA with 5'-HHRz sequences and parts of the 3'-SC1 sequences, was cut out from pSAD T7-HH_NENEPEL_SC and ligated into the equally digested vector pCAGGS-T7-HH_L16_SC_T7T_pA.
pCAGGS-T7-HH_SAD NEP(mono)	A *SacII-SwaI* fragment was cut out from pCAGGS-T7-HH_L16_SC and ligated into the equally digested vector pCAGGS-T7_SAD NEP(mono).
pCAGGS-T7-HH_SAD NEP(mono)_SC	An *AscI-RsrII* fragment was cut out from pSAD T7-HH_EP(mono)_SC and ligated into the equally digested vector pCAGGS-T7-HH_L16_SC.
pCAGGS-T7-SAD NEP(mono)	A *SwaI-AflII* fragment of the RABV full-length cDNA was cut out from pSAD T7-HH_EP(mono)_SC and ligated into the equally digested vector pCAGGS-T7_L16.
pCR3-FFluc	An *Acc65I–NotI* fragment was cut out from pCMV-RL-NP-FF and ligated into the equally digested pCR3 vector.
pCR3-FFluc-asgfpt	The firefly luciferase ORF was PCR-amplified from pCR3-FFluc and prolonged in the 3'-UTR by a GFP-tag using primers AG 59 and AG58 and digested with KpnI and NotI followed by ligation into the similarly digested vector pCR3-FFluc.
pCR3-FFluc-gfpt	The firefly luciferase ORF was PCR-amplified from pCR3-FFluc and prolonged in the 3'-UTR by a GFP-tag using primers AG 59 and AG57 and digested with KpnI and NotI followed by ligation into the similarly digested vector pCR3-FFluc.
pCR3-HH_NEP(mono)	A *PmeI-XcmI* fragment comprising the HHRz and the cDNA of the upstream part of SAD EP(mono) up to the *XcmI*-site in the P gene was cut out from pSAD T7-HH_EP(mono)_SC. The insert was ligated into the vector pCR3-P which was digested with *KpnI* and after Klenow fill-in with *XcmI*.
pCR3-HH_NPVP(bi)	A *PmeI-XcmI* fragment comprising the HHRz and the cDNA of the upstream part of SAD PVP(bi) up to the *XcmI*-site in the P gene was cut out from pSAD T7-HH_PVP(bi)_SC. The insert was ligated into the vector pCR3-P which was digested with *KpnI* and after Klenow fill-in with *XcmI*.
pCR3-T7-HH_L16_SC_T7T_pA	A *KpnI-SpeI* fragment comprising T7 promoter, the HHRz sequence, the RABV full-length cDNA, the SC1 and the T7 terminator sequence, was cut out from pSAD T7-HH_L16_SC and ligated into the *KpnI* and *XbaI* digested vector pCR3.
pCR3-T7-HH_NEN2APEL_SC	A *PmeI-Eco47III* fragment comprising the HHRz and the SAD NEN2APEL cDNA up to the *Eco47III*-site in the L gene was cut

	out from pSAD T7-HH_NEN2APEL_SC and ligated into the equally digested vector pCR3-T7-HH_L16_SC_T7T_pA.
pCR3-T7-HH_NENEPEL_SC	A *PmeI-Eco47III* fragment comprising the HHRz and the SAD NENEPEL cDNA up to the *Eco47III*-site in the L gene was cut out from pSAD T7-HH_NENEPEL_SC and ligated into the equally digested vector pCR3-T7-HH_L16_SC_T7T_pA.
pSAD dstart-EN_SC	A fragment comprising the EMCV IRES and 5'-parts of the N gene was PCR-amplified from pTIT-N and prolonged by adequate restriction sites using primers AG 93 and AG 37. The *PmeI* and *AvrII* digested product was ligated into the equally digested vector pSAD T7-HH_L16_SC. Thereby the HHRz and RABV leader sequence were deleted.
pSAD G_dHH-shGFP	Annealing of oligos AG 10 and AG 11. The oligolinker was cloned with NheI / NotI as extra transcription unit in pSAD G_DsRed
pSAD G_HH-shGFP	Annealing of oligos AG 12 and AG 13. The oligolinker was cloned with *NheI* and *Acc65I* into pSAD G_shGFP.
pSAD G_HH-shGFP-HDV	An HHRz-shGFP-HDV comprising fragment was PCR-amplified from pX8δT-HH-shGFP-HDV and prolonged by adequate restriction sites using primers AG 17 and AG 19. The PCR product was digested with *NheI* and *NotI* and ligated into the equally digested vector pSAD G_DsRed.
pSAD G_HH-shGFP-SC1	An HHRz-shGFP-SC1 comprising fragment was PCR-amplified from pX8δT-HH-shGFP-HDV, modified in the HDVagRz sequence, and prolonged by adequate restriction sites using primers AG 17 and AG 24. The PCR product was digested with *NheI* and *NotI* and ligated into the equally digested vector pSAD G_DsRed.
pSAD G_HH-shGFP-SC2	An HHRz-shGFP-SC2 comprising fragment was PCR-amplified from pX8δT-HH-shGFP-HDV, modified in the HDVagRz sequence, and prolonged by adequate restriction sites using primers AG 17 and AG 25. The PCR product was digested with *NheI* and *NotI* and ligated into the equally digested vector pSAD G_DsRed.
pSAD G_shGFP	Annealing of oligos AG 8 and AG 9. The oligolinker was cloned with *NheI* / *NotI* as extra transcription unit in pSAD G_DsRed
pSAD G_shGFP-HDV	An shGFP-HDV comprising fragment was PCR-amplified from pX8δT-shGFP-HDV and prolonged by adequate restriction sites using primers AG 18 and AG 19. The PCR product was digested with *NheI* and *NotI* and ligated into the equally digested vector pSAD G_DsRed.
pSAD G_shGFP-SC1	An shGFP-SC1 comprising fragment was PCR-amplified from pX8δT-shGFP-HDV, modified in the HDVagRz sequence, and prolonged by adequate restriction sites using primers AG 18 and AG 24. The PCR product was digested with *NheI* and *NotI* and ligated into the equally digested vector pSAD G_DsRed.
pSAD G_shGFP-SC2	An shGFP-SC2 comprising fragment was PCR-amplified from pX8δT-shGFP-HDV, modified in the HDVagRz sequence, and

	prolonged by adequate restriction sites using primers AG 18 and AG 25. The PCR product was digested with *NheI* and *NotI* and ligated into the equally digested vector pSAD G_DsRed.
pSAD GFP	The eGFP ORF from pEGFP-C3 was PCR-amplified with primers AG 53 and AG 54 and cloned with *NheI* and *NotI* into pSAD G_DsRed to replace the DsRed ORF.
pSAD GFP_SC	An *AvrII–RsrII* fragment was cut out from pSAD eGFP and ligated into the equally digested backbone of pSAD L16_SC
pSAD HHRz_GFP	A *PstI–AvrII* fragment was cut out from pSAD T7-HH_L16 and ligated into the equally digested backbone of pSAD eGFP.
pSAD HHRz_GFP_SC	An *AvrII–RsrII* fragment was cut out from pSAD eGFP and ligated into the equally digested backbone of pSAD T7-HH_L16 SC.
pSAD L16_SC	A fragment was cloned with *RsrII* and *SpeI* from pX8δT_SC into pSAD L16.
pSAD T7-HH RVL-utr-fse-eco47III_SC	A fragment from the template pSAD L16 spanning from the SnaBI site until the 5'-UTR of the L gene was PCR-amplified and prolonged by adequate restriction sites using primers AG 162 and AG 163. The PCR product was digested with *SnaBI* and *Eco47III* and ligated into the equally digested vector pSAD T7-HH_L16_SC. Thereby the 5'-third of the L gene was deleted.
pSAD T7-HH_ G_eGFP-miR23-2_SC	PCR with oligos AG 53 and AG 208 to amplify EGFP with mir23-2 in 3'-UTR from pEGFP-miR23-2. Digestion of PCR product with *NheI* / PspOMI and ligation with *NheI* and *NotI* digested vector pSAD T7-HH_eGFP_SC.
pSAD T7-HH_ G_HH-shGFP-SC1_SC	A *SnaBI-Eco47III* fragment was cut out from pSAD G_HH-shGFP-SC1 and ligated into the equally digested vector pSAD T7-HH_L16_SC.
pSAD T7-HH_ G_HH-SH-SC1_SC	An *NheI-NotI* fragment was cut out from pCAGGS-HH-SH-SC1 and ligated into the equally digested vector pSAD T7-HH_GFP_SC.
pSAD T7-HH_EL_SC	A fragment spanning the EMCV IRES and the 5'-third of the L gene was PCR-amplified from pTIT-L and prolonged by adequate restriction sites using the primers AG 93 and AG 164. The PCR product was digested with *FseI* and *Eco47III* and ligated into the equally digested vector pSAD T7-HH RVL-utr-fse-eco47III_SC.
pSAD T7-HH_EN_SC	Primers AG 36 and AG 94 were used in a template-less PCR reaction. The resulting fragment comprising HHRz and RABV leader sequences together with adequate restriction sites was digested with *PmeI* and *FseI* and ligated into the equally digested vector pSAD dstart-EN_SC.
pSAD T7-HH_EP(bi)_SC	An *SwaI-SnaBI* fragment was cut out from pCAGGS-NEP(bi)M and ligated into the equally digested vector pSAD T7-HH_L16_SC.
pSAD T7-HH_EP(mono)_SC	A fragment comprising the EMCV IRES and RABV P gene was PCR-amplified from pTIT-P and prolonged by adequate

	restriction sites using the primers AG 93 and AK 70. The product was digested with *PmeI* and *NarI*. As vector for the ligation, pSAD T7-HH_N_eGFP_dP_SC was digested with *HpaI*, followed by Klenow fill-in and further digestion with *NarI*.
pSAD T7-HH_G_dHH-HSmm-dHDV_SC	A fragment was cut out from pCAGGS-dHH-HSmm-SC1 by digestion with *RsrII*, Klenow fill-in and further digestion with *NheI*. As a vector pSAD T7-HH_GFP_SC was digested with *NotI* and after Klenow fill-in further digested with *NheI*.
pSAD T7-HH_G_dHH-HSmm-SC1_SC	An *NheI-NotI* fragment was cut out from pCAGGS-HH-HSmm-SC1 and ligated into the equally digested vector pSAD T7-HH_GFP_SC.
pSAD T7-HH_G_dHH-SH-dHDV_SC	A fragment was cut out from pCAGGS-dHH-SH-SC1 by digestion with *RsrII*, Klenow fill-in and further digestion with *NheI*. As a vector pSAD T7-HH_GFP_SC was digested with *NotI* and after Klenow fill-in further digested with *NheI*.
pSAD T7-HH_G_dHH-SH-SC1_SC	An *NheI-NotI* fragment was cut out from pCAGGS-dHH-SH-SC1 and ligated into the equally digested vector pSAD T7-HH_GFP_SC.
pSAD T7-HH_G_HH-HSmm_SC1_SC	An *NheI-NotI* fragment was cut out from pCAGGS-HH-HSmm-SC1 and ligated into the equally digested vector pSAD T7-HH_GFP_SC.
pSAD T7-HH_G_HH-HSmm-dHDV_SC	A fragment was cut out from pCAGGS-HH-HSmm-SC1 by digestion with *RsrII*, Klenow fill-in and further digestion with *NheI*. As a vector pSAD T7-HH_GFP_SC was digested with *NotI* and after Klenow fill-in further digested with *NheI*.
pSAD T7-HH_G_HH-SH-dHDV_SC	A fragment was cut out from pCAGGS-HH-SH-SC1 by digestion with *RsrII*, Klenow fill-in and further digestion with *NheI*. As a vector pSAD T7-HH_GFP_SC was digested with *NotI* and after Klenow fill-in further digested with *NheI*.
pSAD T7-HH_GFPEN_SC	The eGFP gene was PCR-amplified and prolonged by *FseI*-sites from pEGFP-C3 using primers AG 159 and AG 160. The PCR product was digested with FseI and inserted into the equally linearized vector pSAD T7-HH_EN_SC.
pSAD T7-HH_L16	A fragment between the 5'-end of the RABV full-length cDNA and the *AvrII* restriction site in the N gene was PCR-amplified and prolonged by HHrz sequences with primers AG 36 and AG 37. The PCR product was further prolonged in a second PCR with primers AG 35 and AG 37 and cloned with PstI and AvrII into pSAD L16.
pSAD T7-HH_L16_SC	A fragment between the 5'-end of the RABV full-length cDNA and the AvrII restriction site in the N gene was PCR-amplified and prolonged by HHrz sequences with primers AG 36 and AG 37. The PCR product was further prolonged in a second PCR with primers AG 35 and AG 37 and cloned with PstI and AvrII into pSAD L16_SC.
pSAD T7-HH_N(nostop)_xma_dP_SC	A fragment of the N ORF, starting with the *AvrII*-site and lacking the stop codon was PCR-amplified from pSAD L16 and prolonged by restriction sites using primers AG 87 and AG 88

	and digested with *AvrII* and *SnaBI* following ligation into the equally digested vector pSAD T7-HH_L16_SC.
pSAD T7-HH_N_eGFP_dP	An AvrII-SnaBI fragment comprising parts of the RABV N gene followed by an eGFP gene and parts of the RABV M gene, was cut out from pCAGGS-N_eGFP and ligated into the equally digested vector pSAD T7-HH_L16_SC.
pSAD T7-HH_N100(mut)ENG_eGFP_SC	A *PmeI-FseI* fragment was cut out from pSDI(+) N100(mut)-NP-FFluc and ligated into the equally digested vector pSAD T7-HH N100EN_G_eGFP_SC.
pSAD T7-HH_N100ENG_eGFP_SC	A *PmeI-FseI* fragment comprising the HHRz and leader sequences and the first 100 nts of N was cut out from pSDI(+) N100-NP-FFluc and ligated into the equally digested vector pSAD T7-HH_NEN G_eGFP_SC.
pSAD T7-HH_N100EN_SC(Fse)	The first 100 nts of the RABV N gene were PCR-amplified and prolonged by FseI-sites from pSAD L16 using primers AG 131 and AG 165. The PCR product was digested with FseI and inserted into the equally linearized vector pSAD T7-HH_EN_SC.
pSAD T7-HH_N200(mut)ENG_eGFP_SC	A *PmeI-FseI* fragment was cut out from pSDI(+) N200(mut)-NP-FFluc and ligated into the equally digested vector pSAD T7-HH N100EN_G_eGFP_SC.
pSAD T7-HH_N200ENG_eGFP_SC	A *SwaI-SwaI* fragment comprising downstream parts of the upstream N200 sequence, the EMCV IRES and upstream parts of the second N gene was cut out from pSAD T7-HH_N200EN_SC(Fse) and ligated into the SwaI-linearized vector pSAD T7-HH_eGFP_SC.
pSAD T7-HH_N200EN_SC(Fse)	The first 200 nts of the RABV N gene were PCR-amplified and prolonged by FseI-sites from pSAD L16 using primers AG 131 and AG 166. The PCR product was digested with FseI and inserted into the equally linearized vector pSAD T7-HH_EN_SC.
pSAD T7-HH_N2AP_SC	A fragment spanning the P gene and parts of the M gene until the *SnaBI*-site was PCR-amplified and prolonged by the 2A-like sequence and restriction sites using primers AG 89 and AG 90. The PCR product was digested with *XmaI* and *SnaBI* and ligated into the equally digested vector pSAD T7-HH_N(nostop)_xma_dP_SC.
pSAD T7-HH_NENG_eGFP_SC	A *SwaI-SwaI* fragment comprising downstream parts of the first N gene, the EMCV IRES and upstream parts of the second N gene was cut out from pSAD T7-HH_NEN_SC and ligated into the SwaI-linearized vector pSAD T7-HH_eGFP_SC.
pSAD T7-HH_NEN_EL_SC	A *SwaI-SwaI* fragment was cut out from pSAD T7-HH_NEN_SC and ligated into the *SwaI*-linearized vector pSAD T7-HH_EL_SC.
pSAD T7-HH_NEN_SC	The RABV N gene was PCR-amplified and prolonged by FseI-sites from pSAD L16 using primers AG 131 and AG 132. The PCR product was digested with FseI and inserted into the equally linearized vector pSAD T7-HH_EN_SC.

pSAD T7-HH_NEN2AP_SC	A *SwaI-SwaI* fragment was cut out from pSAD T7-HH_NEN_SC and ligated into the *SwaI*-linearized vector pSAD T7-HH_N2AP_SC.
pSAD T7-HH_NEN2APEL_SC	A *SnaBI-Eco47III* fragment was cut out from pSAD T7-HH_EL_SC and ligated into the equally digested vector pSAD T7-HH_NEN2AP_SC.
pSAD T7-HH_NENEP_SC	A *SwaI-SwaI* fragment was cut out from pSAD T7-HH_NEN_SC and ligated into the *SwaI*-linearized vector pSAD T7-HH_EP(mono)_SC.
pSAD T7-HH_NENEPEL_SC	A *SnaBI-Eco47III* fragment was cut out from pSAD T7-HH_EL_SC and ligated into the equally digested vector pSAD T7-HH_NENEP_SC.
pSAD T7-HH_NPVN_SC	The RABV N gene was PCR-amplified and prolonged by FseI-sites from pSAD L16 using primers AG 131 and AG 132. The PCR product was digested with FseI and inserted into the equally linearized vector pSAD T7-HH_PVN_SC.
pSAD T7-HH_PVN_SC	A fragment comprising the poliovirus IRES sequence was PCR-amplified from pCR3-RL-PV-FF and prolonged by RABV N sequences with primers AG 95 and AG 96. In a second PCR further RABV N sequences and adequate restriction sites were added using primers AG 95 and AG 97. The product was digested with *FseI* and *AvrII* and ligated into the equally digested vector pSAD T7-HH_EN_SC. Thereby the EMCV IRES was replaced by the PV IRES.
pSAD T7-HH_PVP(bi)_SC	An AvrII-SnaBI fragment was cut out from pSAD PVP(bi) and ligated into the equally digested vector pSAD T7-HH_L16_SC.
pSAD T7-HH_PVP(mono)_SC	A fragment comprising the poliovirus IRES and RABV P gene was PCR-amplified from pSAD PVP(bi) and prolonged by adequate restriction sites using the primers AM 9 and AK 70. The product was digested with *NheI*, followed by Klenow fill-in and further digestion with *NarI*. As vector for the ligation, pSAD T7-HH_N_eGFP_dP_SC was digested with *HpaI*, followed by Klenow fill-in and further digestion with *NarI*.
pSDI N100-NP-FFluc(Fse)	An *FseI*-N100-*FseI* fragment was cut out from pSAD T7-HH_N100EN_SC(Fse) and ligated into the *FseI*-linearized vector pSDI(+)-NP-FFluc.
pSDI N200-NP-FFluc(Fse)	An FseI-N200-FseI fragment was cut out from pSAD T7-HH_N200EN_SC(Fse) and ligated into the *FseI*-linearized vector pSDI(+)-NP-FFluc.
pSDI(-) HHRz_CNPL_SC	The RABV minigenome sequence from pSDI CNPL was PCR-amplified and prolonged by HHRz sequences using the primers AG 110 and AG 196. The resulting fragment was digested with *PmeI* and *RsrII* and ligated into the equally digested vector pSDI(+).
pSDI(+) HH/SC	A fragment from pSDI(+) was PCR-amplified and prolonged by HHRz and HDV sequences with primers AG 36 and AG 111 . The PCR product was further prolonged by a second PCR with primers AG 35 and AG 111 to add further HHRz sequences

	and restriction sites. The product was digested with *PstI* and *RsrII* and ligated into the equally digested vector pX8δT_SC.
pSDI(+) N100(mut)-NP-FFluc	The ATG at the leader-N gene junction was mutated to TTG in pSDI(+) N100-NP-FFluc in a mutagenesis PCR using the primers AG 259 and AG 260.
pSDI(+) N100-NP-FFluc	A fragment comprising the leader sequences and the most upstream 100 nts of the N gene was PCR-amplified and prolonged by adequate restriction sites from template pSAD L16 using the primers AG 197 and AG 165. The PCR product was digested with *Tth111I* and *FseI* and ligated into the equally digested vector pSDI(+) N200-NP-FFluc(Fse). Thereby the leader-N gene junction was restored to wild-type.
pSDI(+) N200(mut)-NP-FFluc	The ATG at the leader-N gene junction was mutated to TTG in pSDI(+) N200-NP-FFluc in a mutagenesis PCR using the primers AG 259 and AG 260.
pSDI(+) N200-NP-FFluc	A fragment comprising the leader sequences and the most upstream 200 nts of the N gene was PCR-amplified and prolonged by adequate restriction sites from template pSAD L16 using the primers AG 197 and AG 166. The PCR product was digested with *Tth111I* and *FseI* and ligated into the equally digested vector pSDI(+) N200-NP-FFluc(Fse). Thereby the leader-N gene junction was restored to wild-type.
pSDI(+)-NP-FFluc	A fragment comprising the N/P gene border and the firefly luciferase gene was PCR-amplified and prolonged with restriction sites from the template pSDI CNPL using primers AG 170 and AG 171. The PCR product was digested with *BglII* and ligated into the *BglII*-linearized vector pSDI(+) HH/SC.
pSUPER-shGFP	The oligos AG 55 and AG 56 were annealed and the oligolinker was ligated into the *BglII* and *HindIII* digested vector pSUPER.
pTre2hyg-HH_NEN2APEL_SC	A *PmeI-NotI* fragment comprising the SAD NEN2APEL full-length cDNA with 5'-HHRz sequences and with 3'-SC1 and T7 terminator sequences, was cut out from pSAD T7-HH_NEN2APEL_SC and ligated into vector pTre2Hyg which was digested with *MluI*, and after Klenow fill-in with *NotI*.
pTre2hyg-T7-HH_NEN2APEL_SC	An *AscI-NotI* fragment comprising the SAD NEN2APEL full-length cDNA with 5'-HHRz and T7 promoter sequences and 3'-SC1 and T7 terminator sequences, was cut out from pSAD T7-HH_NEN2APEL_SC and ligated into the *MluI* and *NotI* digested vector pTre2Hyg.
pTre2hyg-T7-HH_NENEPEL_SC	An *AscI-NotI* fragment comprising the SAD NENEPEL full-length cDNA with 5'-HHRz and T7 promoter sequences and 3'-SC1 and T7 terminator sequences, was cut out from pSAD T7-HH_NENEPEL_SC and ligated into the *MluI* and *NotI* digested vector pTre2Hyg.
pX8δT_SC	pX8δT was linearized with *BamHI* and used as a template in a PCR with primers AG 26 and AG 27. The PCR product was cloned with *HindIII* and *EspI* into the vector pX8δT.
pX8δT-HH-shGFP-HDV	A fragment comprising the shGFP and a 5'-HHRz together with

	a spacer sequence was PCR-amplified from pSAD G_HH-shGFP and prolonged by a 3'-spacer sequence and sequences from the HDV ribozyme using primers AG 16 and AG 17. The PCR product was digested with *XmaI* and *RsrII* and ligated into the equally digested vector pX8δT.
pX8δT-shGFP-HDV	A fragment comprising the shGFP and a 5'-HHRz together with a spacer sequence was PCR-amplified from pSAD G_ shGFP and prolonged by a 3'-spacer sequence and sequences from the HDV ribozyme using primers AG 16 and AG 18. The PCR product was digested with *XmaI* and *RsrII* and ligated into the equally digested vector pX8δT.

6.3 List of abbreviations

SI units and chemical formulas are not included.

%	per cent
α	anti-
Δ	delta-, deletion
λ	lambda, wave length
μ	micro-
A	adenine
AAV	adeno-associated virus
ABLV	australian bat lyssavirus
Amp	ampicillin
APS	ammonium persulfate
AraC	cytosine arabinoside
ATP	adenosine-triphosphate
AUG	Startcodon
BDV	Borna disease virus
bp	base pair
BSA	bovine serum albumin
°C	degree Celsius
C	Cytosine
c	centi-
C. elegans	*Caenorhabditis elegans*
CAT	chloramphenicol acetyltransferase
CCHFV	crimean-congo hemorrhagic fever virus
cDNA	complementary DNA
ChR2c	channel-rhodopsin
CNS	central nervous system
cRNP	complementary ribonucleoprotein
C-terminal	Carboxyterminal
CTP	cytosine-triphosphate
CVS	challenge virus strain
d	Day
D. rerio	*Danio rerio*
dd H_2O	double distillated water
DGCR8	microprocessor complex subunit
dHDV	defect hepatitis delta virus antigenomic ribozyme
dHH	defect hammerhead ribozyme
DI	defective interfering (particle)
DMEM	Dulbecco´s modified eagle medium
DMSO	dimethyl sulfoxide

DNA	deoxyribonucleic acid
dNTP	Deoxyribonucleotide
ds-	double strand
E	EMCV IRES
E3L	vaccinia virus protein
EBLV	european bat lyssavirus
ECL	enhanced chemiluminescence
EDTA	ethylenediaminetetraacetic acid
(e)GFP	(enhanced) green fluorescent protein
EMCV	encephalomyocarditis virus
EMCV	encephalomyocarditis virus IRES
EnvA	envelope protein A
ER	endoplasmatic reticulum
EtBr	ethidium bromide
ffu	focus forming unit
FITC	fluorescein isothiocyanate
G	Glycoprotein
G	Guanine
GCamp3, (-5)	calcium indicator
GMEM	Glasgow modified eagle medium BHK-21 1x
h	Hour
HDV	hepatitis delta virus antigenomic ribozyme „core" sequence
HDV	hepatitis delta virus
HDVagRz	hepatitis delta virus antigenomic ribozyme
HHRz	hammerhead ribozyme
hPIV3	human parainfluenza virus 3
HRP	horse radish peroxidase
HSmm	short hairpin RNA against GFP, certain construct
HSV	herpes simplex virus
IF	immuno fluorescence
IFN	Interferon
IHNV	infectious hematopoetic necrosis virus
IRES	internal ribosome entry site
IRF-3	interferon regulatory factor 3
kb	Kilobase
L	polymerase (large subunit)
LB	Luria Bertani
LCMV	lymphocytic choriomeningitis virus
le	Leader
M	Molar
M	matrix protein

m	milli-
MCMV	murine cytomegalovirus
MeV	measles virus
min	Minute
miRNA	micro RNA
MLV	murine leukemia virus
MOI	multiplicity of infection
mRNA	messenger RNA
MVA	modified vaccinia virus Ankara
N	Nucleoprotein
n	nano-
N^0	soluable N protein
nAChR	nicotinic acetylcholine receptor
NC	Nucleocapsid
NCAM	neuronal cell adhesion molecule
NDV	Newcastle disease virus
NGFR	nerve growth factor receptor
NMJ	neuromuscular junction
NNSV	non-segmented negative strand RNA virus
NP	influenza virus nucleoprotein
NPL-mix	"helper" plasmid mastermix
NS1	influenza virus non-structural protein 1
nt	Nucleotide
N-terminal	Aminoterminal
OG	gel loading dye, orange
ORF	open reading frame
^{32}P	radioactive phosphorus isotope
P	Phosphoprotein
p.i.	post infection
p.t.	post transfection
p75NTR	p75 neurotrophin receptor
PA, PB1, PB2	influenza virus polymerase
PAZ	polyubiquitin Associated Zinc finger
PBS	phosphate buffered saline
PCR	polymerase chain reaction
PEI	Polyethyleneimine
pH	potential hydrogenii
piRNA	Piwi-interacting RNA
PLB	passive lysis buffer
PML	promyelytic leukemia
Pol-I	DNA dependent RNA polymerase I

Pol-II	DNA dependent RNA polymerase II
Pol-III	DNA dependent RNA polymerase III
poly(A)	Polyadenylate
ppp	Triphosphate
pre-miRNA	precursor miRNA
pri-miRNA	primary miRNA
PV	poliovirus IRES
PV	Poliovirus
RABV	rabies virus
RISC	RNA-induced silencing complex
RNA	ribonucleic acid
RNAi	RNA interference
RNP	Ribonucleoprotein
rpm	rounds per minute
RSV	respiratory syncytial virus
RT	room temperature
SAD	Street Alabama Dufferin
SC(1/2)	hepatitis delta virus antigenomic ribozyme „supercut" (1/2)
SDS	sodium dodecylsulfate
SeV	sendai virus
SH	short hairpin RNA against GFP, certain construct
shGFP	short hairpin RNA against GFP
shRNA	short hairpin RNA
siRNA	short interfering RNA
SSC	saline-sodium citrate
sshRNA	short shRNA
SV40	simian virus 40
T	Temperature
T7-pol	T7 RNA polymerase
TAE	tris acetat-EDTA
TE	tris-EDTA
TK	thymidin kinase
tr	Trailer
TRE	Tet repressor
Tris	*Tris*(hydroxymethyl)-aminomethan
TVA	tumor virus protein A
U	Unit
U	Uracil
UTR	untranslated region
UV	Ultraviolet
v/v	volume per volume

VHSV	viral hemorrhagic septicemia virus
VP30, VP35, VP40	ebola virus proteins
vRNP	viral ribonucleoprotein
VSV	vesicular stomatitis virus
vTF7-3	vaccinia virus expressing T7-pol
vv/T7	vaccinia virus expressing T7-pol system
w/v	weight per volume
WB	Western blot
WHO	World health organization
x	Times

6.4 List of figures and tables

Figures:

Tables:

7 Acknowledgement (Danksagung)

8 Curriculum vitae

Alexander Ghanem

geb. 1977 in Freiburg i.Br.

Ausbildung

06/2007 – 11/ 2012: Promotion zum Dr. rer. nat.

An der Fakultät für Biologie der LMU München in der Arbeitsgruppe von Prof. Dr. Conzelmann (Max v. Pettenkofer-Institut) mit dem Thema:

„Innovations in rabies virus rescue - positive approaches for a negative strand RNA virus "

10/2000 – 1/2007: Studium der Biologie (Diplom):

An der Fakultät für Biologie der Albert-Ludwigs-Universität Freiburg.

Diplomarbeit in der Arbeitsgruppe von Prof. Dr. Schwemmle (Institut für Mikrobiologie und Hygiene, Freiburg).: „Charakterisierung einer peptidvermittelten Hemmung der Influenza-Viruspolymerase"

07/1997: Abitur: Am Rosensteingymnasium Heubach (BW).

Sonstige Tätigkeiten

11/2011: Fortbildung für Projektleiter und Beauftragte für Biologische Sicherheit (gem. §15 GenTSV)

08/2003 – 11/2003: Zhejiang University, Hangzhou, China

Laborpraktikum in der Gruppe von Prof. Dr. Wei-Jun Yang, Austauschstipendium der IAESTE (International Association for the Exchange of Students for Technical Experience).

08/2002 – 12/2005: Wissinfo GmbH, Freiburg

Patentrecherche, Datenbankverwaltung, Allgemeine Bürotätigkeiten als studentische Hilfskraft.

08/1997 – 09/2000: Stiftung Haus Lindenhof, Schwäbisch Gmünd (BW)

Zunächst Zivildienst, später Anstellung als Erziehungshelfer im Wohnheim für geistig Behinderte.

9 Publications and presentations

9.1 Publications

Significantly improved rescue of rabies virus from cDNA plasmids.

Alexander Ghanem, Anika Kern, Karl-Klaus Conzelmann.(2012). Eur J Cell Biol; 91(1):10-6

Reverse Genetics of Rhabdoviruses: Applications and Perspectives.

Ghanem, A. and Conzelmann, K. K. (in press). A. Bridgen, Chichester, West Sussex : John Wiley & Sons, 2012

A Radial Glia-Specific Role of RhoA in Double Cortex Formation.

Silvia Cappello, Christian R.J. Böhringer, Matteo Bergami, Karl-Klaus Conzelmann, Alexander Ghanem,Giulio Srubek Tomassy, Paola Arlotta, Marco Mainardi, Manuela Allegra, Matteo Caleo, Jolanda van Hengel, Cord Brakebusch, Magdalena Götz. (2012). Neuron; 73(5): 911-924

Rabies virus-mediated tracing of monosynaptic connections onto adult generated neurons.

Aditi Deshpande, Matteo Bergami, Alexander Ghanem, Karl-Klaus Conzelmann, Alexandra Lepier, Magdalena Götz & Benedikt Berninger. (2012). Nature Neuoscience; submitted

Peptide-mediated interference with influenza A virus polymerase.

Ghanem A, Mayer D, Chase G, Tegge W, Frank R, Kochs G, García-Sastre A, Schwemmle M.(2007). J Virol; 81(14):7801-7804.

Identification of Cellular Interaction Partners of the Influenza Virus Ribonucleoprotein Complex and Polymerase Complex Using Proteomic-Based Approaches.

Mayer D, Molawi K, Martinez-Sobrido L, Ghanem A, Thomas S, Baginsky S, Grossmann J, Garcia-Sastre A, Schwemmle M. (2006). J Proteome Res. ; 6(2):672-682.

9.2 Talks

Single infectious cDNAs of rabies virus.

21. Tagung der Gesellschaft für Virologie (GfV) (2011) Freiburg.

Single infectious cDNAs of rabies virus.

Max von Pettenkofer-Institute seminar series (2011, 2010, 2009), München

Rabies virus vectors for neuronal tracing.

SFB 870 retreat (2011) Seeon.

Single infectious RNAs of rabies virus.

14th International Negative Strand Virus Meeting (2010) Brügge, Belgien

Engineering Rabies virus as a transcription-vector for short-hairpin RNAs

Gene Center seminar series (2009), München

Improvement of rabies virus rescue system

Max von Pettenkofer-Institute seminar series (2008), München

Peptide-mediated interference with influenza A virus polymerase.

Third European Congress of Virology (2007) Nürnberg.